Independent Expert Scientific Committee
on Coal Seam Gas and Large Coal Mining Development

Australian Government
Department of the Environment

Background review

Aquifer connectivity within the Great Artesian Basin, and the Surat, Bowen and Galilee Basins

This background review was commissioned by the Department of the Environment on the advice of the Interim Independent Expert Scientific Committee on Coal Seam Gas and Coal Mining. The review was prepared by the CSIRO and revised by the Department of the Environment following peer review.

June 2014

Copyright

Enquiries concerning reproduction and rights should be addressed to:

Department of the Environment, Public Affairs
GPO Box 787 Canberra ACT 2601

Or by email to: public.affairs@environment.gov.au

This publication can be accessed at: www.iesc.environment.gov.au

Acknowledgements

This background review was commissioned by the Department of the Environment on the advice of the Interim Independent Expert Scientific Committee on Coal Seam Gas and Coal Mining. The review was prepared by CSIRO, with input from Sinclair Knight Merz Pty Ltd, Queensland University of Technology and National Centre for Groundwater Research and Training. It was revised by the Department of the Environment following peer review by Mr Doug Anderson and Dr William Glamore (University of NSW Water Research Laboratory) and relevant Queensland, New South Wales and South Australian Government departments.

Disclaimer

The views and opinions expressed in this publication are those of the authors and do not necessarily reflect those of the Australian Government or the Minister for the Environment or the Interim Independent Expert Scientific Committee on Coal Seam Gas and Coal Mining or the statutory Independent Expert Scientific Committee on Coal Seam Gas and Large Coal Mining Development (IESC).

While reasonable efforts have been made to ensure that the contents of this publication are factually correct, the Commonwealth and IESC do not accept responsibility for the accuracy or completeness of the contents, and shall not be liable for any loss or damage that may be occasioned directly or indirectly through the use of, or reliance on, the contents of this publication.

Addendum

Changes to state government departments have occurred since the finalisation of this report by the authors. The Queensland, New South Wales and South Australian Government agencies were contacted and updated information provided in September 2013; however, no guarantees can be made as to the completeness of these updates. Up-to-date information should be sourced from the relevant department.

On 1 January 2013, the Queensland Water Commission (QWC) ceased operations. The Office of Groundwater Impact Assessment (OGIA) retains the same powers as the former QWC under Chapter 3 of the *Water Act 2000* (Qld).

Contributors

The following list acknowledges the primary authors and contributors for each section of this report:

Executive Summary – Glenn Harrington[A]

Chapter 1 – Glenn Harrington[A]

Chapter 2 – Luk Peeters[A], Glenn Harrington[A], Rick Evans[B]

Chapter 3 – Stephanie Villeneuve[C], Glenn Harrington[A], Karsten Michael[A], Rick Evans[B]

Chapter 4 – John Kozuskanich[C], Rick Evans[B], Karsten Michael[A]

Chapter 5 – Chris Turnadge[A], Luk Peeters[A], Brian Smerdon[A]

Chapter 6 – Chris Turnadge[A], Luk Peeters[A], Brian Smerdon[A]

Chapter 7 – Tim Ezzy[B], Rick Evans[B], Karsten Michael[A], Malcolm Cox[D]

Chapter 8 – Stephen Parsons[B], Rick Evans[B], Malcolm Cox[D]

Chapter 9 – Glenn Harrington[A]

Chapter 10 – Glenn Harrington[A]

The authors would also like to thank Brian Smerdon[A] for useful peer review comments on a preliminary draft of this report.

[A] CSIRO Water for a Healthy Country National Research Flagship

[B] Sinclair Knight Merz Pty Ltd (now Jacobs SKM)

[C] National Centre for Groundwater Research and Training

[D] Queensland University of Technology

Contents

Summary

This background review describes the range of scientific methods that have been developed to measure and model connectivity in any hydrogeological setting, and specific knowledge of aquifer connectivity for the Great Artesian Basin (GAB), and the Surat, Bowen and Galilee (geological) Basins.

For the purposes of this review, aquifer connectivity refers to:

The groundwater interaction between aquifers that are separated by an aquitard (often termed inter-aquifer leakage) or between different parts of the same aquifer (intra-aquifer connectivity). It is dependent upon the lithology of aquitards and aquifers and their integrity and spatial continuity. Fractures, faults and open or inadequately-sealed boreholes can form preferential flow paths that also affect connectivity. The degree of connectivity and the rate of water and solute transfer between aquifers are strongly influenced by local and regional hydraulic pressure and dissolved mineral concentration gradients. As aquifer systems are dynamic, these gradients are constantly changing with time, as groundwater is recharged or removed from the system.

Key points

- Aquifer connectivity is a major determining factor in how groundwater pumping will affect other aquifers.
- There are many techniques available to investigate and evaluate aquifer connectivity that provide information at different spatial and temporal scales.
- Natural features (e.g. fractures and faults) and manmade structures (e.g. boreholes) and activities (e.g. longwall coal mining) can influence aquifer connectivity by providing preferential pathways for flow and contaminant transport.
- Few studies explicitly focus on connectivity and inter-aquifer leakage between the Great Artesian Basin (a major groundwater basin), the Surat (geological) Basin and the linked Bowen and Galilee (geological) Basins (of which the latter three have significant coal seam gas resources).
- Most existing groundwater models that claim to address aquifer connectivity via implementation of measured, site-specific hydraulic conductivity data will under-predict the magnitude of inter-aquifer leakage.
- Priorities for future work include:
  - development of an agreed methodology for determining formation-scale hydraulic conductivity of aquitards and a consistent approach for modelling inter-aquifer leakage
  - understanding dual-phase flow (i.e the flow of both gas and water within coal seams) and the conditions under which it needs to be incorporated into groundwater flow predictions
  - understanding how desorption of coal bed methane may alter the hydraulic properties of the surrounding formations.

Aquifer connectivity

Any large-scale groundwater development, including that required for coal seam gas (CSG) production and dewatering of coal mines, needs to be managed with the best available information about aquifer connectivity. This is because aquifer connectivity is a major determining factor in the way that prolonged groundwater pumping from multi-layered aquifer systems will affect aquifers other than the pumped aquifer. Potential impacts beyond the pumped aquifer can include:

- enhanced leakage of water from overlying and underlying aquifers and aquitards
- mobilisation of natural salts from overlying and underlying aquifers and aquitards, and deterioration of water quality in the pumped aquifer
- mobilisation of anthropogenic contaminants from overlying and underlying aquifers and aquitards
- changes in the nature and fluxes between surface water and groundwater systems near the ground surface
- declining water levels in shallow aquifers, leading to changes in the recharge and/or discharge rates.

Measuring and evaluating connectivity

There are many different techniques available for characterising aquifers and aquitards and evaluating connectivity. In terms of natural aquifer connectivity, assessment techniques range from laboratory and single-well-scale hydraulic tests to formation-scale investigations of environmental tracer distributions and groundwater level and pressure gradients, and regional-scale geophysical surveys. The different approaches all provide information at different spatial and temporal scales. The fundamental information requirements for understanding connectivity are largely associated with:

- geology – including lithology and structure
- groundwater hydrology – including aquifer and aquitard permeability, groundwater level and pressure gradients, and the potential influence of discrete geological and anthropogenic structures on groundwater flow.

Numerical groundwater flow and solute transport models offer a means to:

- interpret the datasets acquired from multi-disciplinary investigations, in conjunction with contemporary groundwater level and pressure monitoring data
- evaluate connectivity between and within aquifers
- use this information to predict the impacts to groundwater levels, pressure and flow, arising from activities such as coal seam gas extraction and coal mine dewatering.

Changes that can occur to connectivity

Natural (e.g. fractures and faults) and manmade (e.g. boreholes) structures can significantly influence aquifer connectivity because they can act as preferential pathways for flow and contaminant transport. In addition, they can cause changes to connectivity over time. Mechanical deformation of geological formations due to either depressurisation of aquifers by pumping, reinjection of co-produced water or hydraulic fracturing (commonly termed ‘fraccing’) can enhance fracture connectivity and thus bulk hydraulic properties of the

formation. In these instances, most of the induced fractures are propagated extensions of the natural fracture network, with characteristics determined by the geomechanical properties of the formation. Longwall coal mining also causes fracturing of strata and increased vertical connectivity above mined areas, whilst poorly-constructed wells and leaky boreholes also present a risk of accelerated inter-aquifer leakage of water and salts or contaminants.

Aquifer connectivity, expressed in terms of flux, can change from natural conditions solely by changing the hydraulic gradient. Mine dewatering, coal seam depressurisation, pumping for groundwater supply and co-produced water reinjection are all examples of how this could be achieved. Uncertainty lies in what happens to the natural system as multiple operations come online over time (cumulative impact) and after the resources have been exhausted and the infrastructure is decommissioned. This is particularly the case for the situation where aquifer connectivity has been enhanced by the creation of new preferential pathways (e.g. fractures in aquitards, leaking borehole seals, reactivated faults) that will remain in place post-production.

Aquifer connectivity in the Great Artesian Basin and the Surat, Bowen and Galilee geological Basins

Despite several decades of research and investigation in the GAB and the Surat, Bowen and Galilee geological Basins, few studies have explicitly focused on connectivity and inter-aquifer leakage. Instead the primary focus has been on quantifying rates of groundwater recharge and flow and understanding controls on water quality, at least in the GAB and Surat Basin. Work in the Bowen and Galilee Basins has traditionally involved more fundamental geological mapping and determining reservoir characteristics. In all four basins, existing data for the hydraulic properties of the aquitards is mostly derived from measurements at a very small scale compared to the thickness and horizontal extent of the formation. There is a significant body of literature, including studies from within Australia and overseas, that indicate hydraulic conductivity increases with increasing scale of measurement; this is primarily due to the presence of preferential flow paths at larger scales. Accordingly, most existing groundwater models that claim to address aquifer connectivity – via implementation of measured hydraulic conductivity data – will under-predict the magnitude of inter-aquifer leakage.

Further work

Priorities for further work include an agreed methodology for determining formation-scale hydraulic conductivity of aquitards, both under natural and highly stressed conditions. This will likely take several years of focused research to achieve; however, groundwater chemistry and environmental isotope data offers some of the greatest potential in the shorter term. For example, the use of multiple environmental tracer distributions in aquitard pore water, as recently trialled in the western GAB, provides great opportunities for assessing aquifer connectivity between the Permian coal seams that are being targeted for coal seam gas and the overlying GAB aquifers, or between Triassic and Jurassic aquifers. These isotope techniques may also be useful for the assessment of aquifer connectivity for much shallower coal mining operations, especially if coupled with geophysical techniques.

There is also a critical need to develop a consistent approach for modelling inter-aquifer leakage, especially that associated with coal seam gas development. In addition to the issues surrounding use of representative values for formation-scale hydraulic properties, there is a need to consider mechanical deformation of aquifers and aquitards and the influence of these processes on the overall connectivity. Likewise, there is a need to explore dual-phase flow (the flow of both a gas and water phase in the pores) and how desorption of

coal bed methane may alter the hydraulic properties of the surrounding formations. Regional-scale assessment of the cumulative impacts of groundwater extraction for coal seam gas and coal mining must consider these processes, which are not accounted for in traditional hydrogeological models.

Abbreviations

General abbreviations	Description
AEM	Airborne electromagnetic
APLNG	Australia Pacific Liquefied Natural Gas project
ATP	Authority to Prospect for Petroleum
AWMS	Allocating Water and Maintaining Springs project
BC	British Columbia
CO2CRC	Cooperative Centre for Greenhouse Gas Technologies
CBM	Coal bed methane
Cm	Coal Measure
CMA	Catchment management authority or area
CSIRO	Commonwealth Scientific and Industrial Research Organisation
CSG	Coal seam gas
2D	Two dimensional
3D	Three dimensional
DERM	Queensland Government Department of Environment and Resource Management (ceased operations in 2012)
DST	Drill stem tests
EIS	Environmental Impact Statement
EPBC Act	Environment Protection and Biodiversity Conservation Act 1999
FAST	Fault analysis seal technology
Fm	Formation
FRT	Flow rate testers
GA	Geoscience Australia
GAB	Great Artesian Basin
GABWRA	Great Artesian Basin Water Resource Assessment
GLNG	Gladstone Liquefied Natural Gas project
GPR	Ground penetrating radar
GSQ	Geological Survey of Queensland
GVS	Groundwater visualisation system
HSU	Hydrostratigraphic units
IAA	Immediately affected areas
IESC	Independent Expert Scientific Committee on Coal Seam Gas and Large Coal Mining Development
J-K	Jurassic-Cretaceous

General abbreviations	Description
LAA	Long-term affected areas
LHS	Left hand side
LNG	Liquefied natural gas
MDB	Murray-Darling Basin
NSW	New South Wales
OWS	Office of Water Science
PEST	Model-independent parameter estimation and uncertainty analysis
PVC	Polyvinyl chloride
QCLNG	Queensland Curtis Liquefied Natural Gas project
QDEX	Queensland Digital Exploration Reports system
QGD	Queensland Groundwater Database
QPED	Queensland Petroleum Exploration Database
QUT	Queensland University of Technology
RHS	Right hand side
SEM	Scanning electron microscopes
SI unit	International System of Units
SP	Self-potential
US EPA	United States Environmental Protection Agency
US	United States of America
USGS	United States Geological Survey
UWIR	Arrow Energy's underground water impact report
VOI	Value of information
VWP	Vibrating wire piezometers
WCM	Walloon Coal Measures
WRP	Water Resource Plan
WTP	Water Treatment Plant

Units, chemicals and symbols	Description
α, β	Compressibility
a_L, α_L	Dynamic dispersivity
α	Biot's constant, a correction factor from poroelastic theory that accounts for the efficiency with which internal pore pressure offsets the externally applied total vertical stress
bGL	Below ground level

Units, chemicals and symbols	Description
Br^-	Bromide
°C	Degree celcius
^{12}C, ^{13}C, ^{14}C	Carbon-12, Carbon-13, Carbon-14 (respectively) - isotopes
Ca	Calcium
CFC	Chlorofluorocarbons
^{36}Cl	Chlorine-36
Cl	Chlorine
Cl^-	Chloride
cm	Centimetre
CO_2	Carbon dioxide
2D	Two dimensional
3D	Three dimensional
D	Darcy (1 Darcy is approximately equal to 9.869233×10^{-13} m^2)
EC	Electrical conductivity
Eh	Reduction potential
GL	Gigalitre (1000 million litres)
^1H	Hydrogen-1 isotope, usually called protium
^2H	Hydrogen-2 isotope, usually called deuterium
^3H	Hydrogen-3 isotope, usually called tritium
H	Hydrogen
H_2O	Chemical formula for water
HCO_3	Bicarbonate
^4He	Helium-4
kg	Kilogram
kg/m^3	Kilogram per cubic metre
K_h	Horizontal hydraulic conductivity
km	Kilometre
km^2	Square kilometre
^{85}Kr	Krypton-85 (radioisotope of Krypton)
K_v	Vertical hydraulic conductivity
L	Litre (unless specified otherwise, e.g. in section 2.4 it represents ‘length’)
L/s	Litres per second
m	Metre
m^2	Square metre
M^3	Cubic metre

Units, chemicals and symbols	Description
m/d, m/day	Metre per day
m^2/d	Square metre per day
m/s	Meter per second
mA	Milliamps
Ma	Mega-annum (10^6 years)
mD	Millidarcy (1 mD is equal to 0.001 D)
m/s^2	Metre per second squared
Mg	Magnesium
mg	Milligram
mg/L	Milligram per litre
MHz	Megahertz
ML	Megalitre (1 million litres)
ML/year	Megalitre per year
mm	Millimetre
mm/yr	Millimetre per year
Na	Sodium
Na-Cl	Sodium chloride
Na-HCO_3	Sodium bicarbonate
Na(+K)-HCO_3	Sodium-potassium-bicarbonate
Na(+K)-HCO3-Cl	Sodium-potassium-bicarbonate-chlorine
n_e	Porosity
NH_3	Un-ionised ammonia
NO_2	Nitrite
NO_3	Nitrate
Nm	Nanometre
^{16}O, ^{17}O, ^{18}O	Oxygen-16, Oxygen-17, Oxygen-18 (isotopes of Oxygen)
O	Oxygen
O_2	Oxygen dioxide
σ_1, σ_2, σ_3, σ_S, σ_N, σ_{min}	Greatest (σ_1), intermediate (σ_2), least (σ_3), shear (σ_S), minimum (σ_{min}) and normal (σ_N) principal stresses (ellipse)
P	Fluid pressure
pH	pH - quantitative measure of the acidity or basicity of aqueous or other liquid solutions
PJ	Petajoules
REV	Representative Elementary Volume
^{222}Rn	Radon-222 (isotope of Radon)

Units, chemicals and symbols	Description
s, sec	Second
S	Storativity
SF_6	Sulfur hexafluoride
SO_4	Sulfate
S_s	Specific storativity
S_y	Specific yield
T	Transmissivity
Th	Thorium
µm	Micrometre (10 000 µm is equal to 1 cm)
µS/cm	Microsecond per centimetre
U	Uranium
υ	Poisson's ratio - the degree to which a rock core bulges as it shortens
V	Volume
Ω.m	Ohm-metre (metric unit for specific resistance)
%	Per cent

Formulae	Description
$q = \frac{Q}{A} = -K\frac{dh}{dz}$	Darcy's Law: q = specific discharge of water [q (m/day)] Q = volumetric flow rate [Q (m^3/day)] A = cross-sectional area [A (m^2)] K = hydraulic conductivity of the geologic media [K (m/day)] dh/dz = hydraulic gradient, where dh is the change [d] in hydraulic head [h (m)] over a distance [z (m)] along the direction of flow.
$K = \frac{k\rho g}{\mu}$	K = hydraulic conductivity k = intrinsic permeability [k (m^2) I unit) or k (D)] ρ = density g = acceleration due to gravity (1g is approximately 9.81 m/s) µ = viscosity
$Q = C(2b)^3\Delta h$	Cubic Law: Q = volumetric flow rate [Q (m^3/day)] C = a constant related to the properties of the fluid and the geometry of the fracture b = aperture of the fraction ∆h = change in hydraulic head

Formulae	Description
$v = \frac{1}{n_e} K \frac{dh}{dz}$	v = groundwater velocity n_e = effective porosity K = hydraulic conductivity of the geologic media [K (m/day)] dh/dz = hydraulic gradient, where dh is the change [d] in hydraulic head [h (m)] over a distance [z (m)] along the direction of flow.
$D_L = a_L v_z + D^*$	D_L = coefficient of longitudinal hydrodynamic dispersion a_L = the dynamic dispersivity v = groundwater velocity z = distance D* = the effective molecular diffusion coefficient
$\frac{\partial C}{\partial t} = -v_z \frac{\partial C}{\partial z} + D_L \frac{\partial^2 C}{\partial z^2}$	∂ = advection C = solute concentration t = time v = groundwater velocity z = distance D_L = coefficient of longitudinal hydrodynamic dispersion
$Pe = \frac{v_z}{D_L} L$	Pe = Peclet number v = groundwater velocity z = distance D_L = coefficient of longitudinal hydrodynamic dispersion L = length
$v = \frac{\rho g}{12\mu} (2b)^2 \frac{dh}{dz}$	v = groundwater velocity ρ = density g = acceleration due to gravity (1g is approximately 9.81 m/s) μ = viscosity b = aperture of the fraction dh/dz = hydraulic gradient, where dh is the change [d] in hydraulic head [h (m)] over a distance [z (m)] along the direction of flow.
$K = \frac{VL}{Ath}$	Hydraulic conductivity (K in L/T) from a modified version of Darcy's Law: K = hydraulic conductivity V = volume of water discharged (L^3) L = length of the sample A = cross-sectional area of the sample (L^2) t = time h = hydraulic head (L)
$\mathrm{K} = \frac{d_t^2 L}{d_c^2 t} ln\left(\frac{h_0}{h}\right)$	K = hydraulic conductivity d_t = inside diameter of the falling-head tube (L) L = length of the sample d_c = inside diameter of the sample chamber (L)

Formulae	Description
	t = time for head to go from h_o to h h_o = initial water level h = water level
$k = \frac{(2Q_e P_e \mu L)}{(P_i^2 - P_e^2)A}$	Modification of Darcy's Law: k = permeability to air (k in L^2) Q_e = exit flow rate (L^3/T) P_e = exit pressures (M/LT^2) μ = viscosity of the air (M/LT) L = length of the sample (L) P_i = entrance pressures (M/LT^2) A = cross-sectional area (L^2)
$t = -\lambda^{-1}\left(\frac{C}{C_0}\right)$	t = apparent 'age' of the groundwater C_0 = initial concentration of the radioactive tracer C = measured concentrations of the radioactive tracer λ = known decay constant for the radioactive tracer.
$[Cl]_M = x \times [Cl]_A + (1-x) \times [Cl]_B$	$[Cl]_M$ = Cl^- concentration in the mixture $[Cl]_A$ = Cl^- concentration in aquifer A $[Cl]_B$ = Cl^- concentration in aquifer B x = fraction of water from aquifer A 1-x = fraction from aquifer B
$\sigma_{min} \cong \underbrace{\frac{\upsilon}{1-\upsilon}(\sigma_{ob} - \alpha\sigma_p) + \alpha\sigma_p}_{\text{horizontal stress from the vertical stress and the poroelastic behaviour of the formation}} + \sigma_{ext}$	σ_{ob} = overburden stress (a function of depth) σ_p = pore pressure σ_{ext} = tectonic stress
$K_w = \frac{r_s^2 \rho g}{8\mu}$	K_w = hydraulic conductivity of a well r_s = radius of the well (L) ρ = density g = acceleration due to gravity μ = viscosity

Glossary

Term	Description
Adsorption	The reversible binding of molecules to a particle surface. This process can bind methane and carbon dioxide, for example, to coal particles.
Advection	The process whereby solutes are transported by the bulk mass of flowing fluid.
Alkalinity	The quantitative capacity of aqueous media to react with hydroxyl ions. The equivalent sum of the bases that are titratable with strong acid. Alkalinity is a capacity factor that represents the acid-neutralising capacity of an aqueous system.
Analytical or numerical methods	Methods based on applying mathematical solutions derived from first principles to calculate how the rock mass will behave when an excavation is made within it.
Anisotropy	The condition of having different properties in different directions.
Anthropogenic	Relating to, or resulting from, the influence of human beings on nature.
Anticline	In structural geology, an anticline is a fold that is convex up and has its oldest beds at its core.
Aperture	Hole or opening.
Aquiclude	A hydrogeologic unit which, although porous and capable of storing water, does not transmit it at rates sufficient to furnish an appreciable supply for a well or spring.
Aquifer	Rock or sediment in formation, group of formations or part of a formation, that is saturated and sufficiently permeable to transmit quantities of water to wells and springs.
Aquifer connectivity	The degree to which groundwater can transfer between two adjacent aquifers or to the surface.
Aquifer discharge	Water leaving an aquifer.
Aquifer recharge	The amount of water replenishing an aquifer over a given time period.
Aquitard	A saturated geological unit that is less permeable than an aquifer and incapable of transmitting useful quantities of water. Aquitards often form a confining layer over an artesian aquifer.
Artesian	Pertaining to a confined aquifer in which the groundwater is under positive pressure (i.e. a bore screened into the aquifer will have its water level above-ground).
Aquatic ecosystem	Any watery environment from small to large, from pond to ocean, in which plants and animals interact with the chemical and physical features of the environment.
Bore/borehole	A narrow, artificially constructed hole or cavity used to intercept, collect or store water from an aquifer, or to passively observe or collect groundwater information. Also known as a borehole, well or piezometer.
Brecciation	The formation of breccia. Breccia is a rock made up of very angular coarse fragments; may be sedimentary or may be formed by grinding or crushing along faults.

Term	Description
Casing	A tube used as a temporary or permanent lining for a bore. *Surface casing*: the pipe initially inserted into the top of the hole to prevent washouts and the erosion of softer materials during subsequent drilling. Surface casing is usually grouted in and composed of either steel, PVC-U, or composite materials. *Production casing*: a continuous string of pipe casings that are inserted into or immediately above the chosen aquifer and back up to the surface through which water and/or gas are extracted/injected.
Cataclasis	The progressive fracturing and comminution of existing rock, which results in the formation of cataclastic rock. Cataclastic rock is mainly found associated with fault zones.
Clastic sediments	Composed predominantly of broken pieces or clasts of older weathered and eroded rocks.
Clay drapes	Thin irregularly-shaped layers of low-permeability material that are often observed in different types of sedimentary deposits.
Cleats - butt cleats	Fractures that are perpendicular, or at a high angle, to the coal seam bedding planes.
Cleats - face cleats	Thin fractures that are perpendicular, or at a high angle, to the coal seam bedding planes but also orthogonal to the butt cleats.
Coal seam	Sedimentary layers consisting primarily of coal. Coal seams store both groundwater and gas and generally contain saltier groundwater than aquifers that are used for drinking water or agriculture.
Coal seam gas	A form of natural gas (generally 95-97 per cent pure methane, CH4) typically extracted from permeable coal seams at depths of 300–1000 m.
Compaction	The process by which geological strata under pressure reduce in thickness and porosity, and increase in density.
Compressibility	A parameter that determines the potential for compaction. Compressibility is typically high for soft clays, intermediate for sands, low (but variable) for coals, very low for consolidated sedimentary rocks such as sandstones and mudstone, and extremely low for competent rocks such as granites and other intrusions.
Compression	A system of forces or stresses that tends to decrease the volume or shorten a substance, or the change of volume produced by such a system of forces.
Confined aquifer	An aquifer bounded above and below by confining units of distinctly lower permeability than that of the aquifer itself. Pressure in confined aquifers is generally greater than atmospheric pressure.
Contaminant	Biological (e.g. bacterial and viral pathogens) and chemical (see Toxicants) introductions capable of producing an adverse response (effect) in a biological system, seriously injuring structure or function or producing death.
Co-produced water	The water that is pumped out of coal seams in order to extract coal seam gas. Also referred to as produced water and associated water. Over time, the volume of produced water normally decreases and the volume of produced gas increases.
Cretaceous period	A period of geologic time, 145 million to 66 million years ago.
Darcy flow equation	The equation that describes the rate and quantity of groundwater flow.

Term	Description
Depressurisation	The lowering of static groundwater levels through the partial extraction of available groundwater, usually by means of pumping from one or several groundwater bores.
Desorption	The release of a bound molecule from a host particle into a flowing medium such as a liquid or gas.
Devonian age	A period of geologic time, 419.2 million to 358.9 million years ago.
Dewatering	The lowering of static groundwater levels through complete extraction of all readily available groundwater, usually by means of pumping from one or several groundwater bores.
Diachronic nature	The study of the changes in nature over a period of time.
Diffusion	Process whereby ionic or molecular constituents move under the influence of their kinetic activity in the direction of their concentration gradient.
Dilution	Dilution is the process of making a substance less concentrated by adding water. This can lower the concentrations of ions, toxins and other substances.
Discretisation	Size of blocks and time segments for which the groundwater flow equations will be solved.
Dispersion	When water with high solute concentrations mixes with water with low solute concentrations as flow velocities in a porous medium vary, leading to a reduction of concentration at the macroscopic scale.
Dispersivity	A geometric property of a porous medium which determines the dispersion characteristics of the medium by relating the components of pore velocity to the dispersion coefficient.
Drawdown	The reduction in groundwater pressure caused by extraction of groundwater from a confined formation, or the lowering of the water-table in an unconfined aquifer.
Effective porosity	The fraction of pores that are connected to each other and contribute to flow. Materials with low or no total porosity can become very permeable if a small number of highly connected fractures are present.
Effective stress	Stress applied between the solid matrix materials of rocks and soils. The effective stress of a reservoir or coal seam is the difference between the total stress and the pore pressure. Also known as stress relief.
Electromagnetics	Relating to electromagnetism, which is a force described by electromagnetic fields, and has innumerable physical instances including the interaction of electrically charged particles and the interaction of uncharged magnetic force fields with electrical conductors.
Elliptical	Retated to, or having, the shape of an ellipse.
Equipotential line	Line along which the potential is constant.
Fault	A planar fracture or discontinuity in a volume of rock, across which there has been significant displacement along the fractures as a result of earth movement.
Flowback	The fluid that flows back, or is pumped back, to surface following hydraulic fracturing but prior to gas production.
Fracture	The separation of an object or material into two, or more, pieces under the action of stress.

Term	Description
Gamma-ray spectometry	An instrument for measuring the distribution (or spectrum) of the intensity of gamma radiation versus the energy of each photon.
Geologic stratum	A layer of sedimentary rock or soil with internally consistent characteristics that distinguish it from other layers. The 'stratum' is the fundamental unit in a stratigraphic column and forms the basis of the study of stratigraphy.
Geological layer	A layer of a given sample. An example is Earth itself. The crust is made up of many different geological layers which are made up of many different minerals/substances. The layers contain important information as to the history of the planet.
Geological window	A geologic structure formed by erosion or normal faulting on a thrust system. In such a system the rock mass (hanging wall block) that has been transported by movement along the thrust is called a nappe. When erosion or normal faulting produces a hole in the nappe where the underlying autochthonous (i.e. un-transported) rocks crop out this is called a window. Windows can be almost any size, from a couple of metres to hundreds of kilometres.
Groundwater	Water occurring naturally below ground level (whether in an aquifer or other low permeability material), or water occurring at a place below ground that has been pumped, diverted or released to that place for storage there. This does not include water held in underground tanks, pipes or other works.
Groundwater injection bore	A bore installed to facilitate the injection of liquid (for example, H_20) or gas (for example, CO_2) into an aquifer. Commonly used in Managed Aquifer Recharge schemes or groundwater remediation.
Groundwater monitoring/ observation bore	A bore installed to: determine the nature and properties of subsurface groundwater conditions; provide access to groundwater for measuring level, physical and chemical properties; permit the collection of groundwater samples; and/or to conduct aquifer tests.
Groundwater pumping/production bore	A bore installed with the primary purpose to extract groundwater for productive use from a particular hydrogeological formation.
Heterogeneity	Composition from dissimilar parts.
Hydraulic conductivity	The rate at which a fluid passes through a permeable medium.
Hydraulic fracturing	Also known as 'fracking', 'fraccing' or 'fracture simulation', is the process by which hydrocarbon (oil and gas) bearing geological formations are 'stimulated' to enhance the flow of hydrocarbons and other fluids towards the well. The process involves the injection of fluids, gas, proppant and other additives under high pressure into a geological formation to create a network of small fractures radiating outwards from the well through which the gas, and any associated water, can flow.
Hydraulic gradient	The change in hydraulic head between different locations within or between aquifers or other formations, as indicated by bores constructed in those formations.

Term	Description
Hydraulic head	The potential energy contained within groundwater as a result of elevation and pressure. It is indicated by the level to which water will rise within a bore constructed at a particular location and depth. For an unconfined aquifer, it will be largely subject to the elevation of the water table at that location. For a confined aquifer, it is a reflection of the pressure that the groundwater is subject to and will typically manifest in a bore as a water level above the top of the confined aquifer, and in some cases above ground level.
Hydraulic pressure	The total pressure that water exerts on the materials comprising the aquifer. Also known as pore pressure.
Hydrodynamic dispersion	The spreading (at the macroscopic level) of the solute front during transport resulting from both mechanical dispersion and molecular diffusion.
Hydrogeology	The area of geology that deals with the distribution and movement of groundwater in the soil and rocks of the Earth's crust (commonly in aquifers).
Hydrology	The study of the movement, distribution and quality of water on Earth and other planets, including the hydrologic cycle, water resources and environmental watershed sustainability.
Hydrostratigraphic unit	Means any soil or rock unit or zone which by virtue of its porosity or permeability, or lack thereof, has a distinct influence on the storage or movement of groundwater.
Inter-aquifer leakage	Groundwater interaction between aquifers that are separated by an aquitard.
Intra-aquifer leakage	Groundwater interaction between different parts of the same aquifer. the lateral migration of fluids and solutes within an aquifer
Intrinsic permeability	The property of a porous medium itself that expresses the ease with which gases, liquids, or other substances can pass through it.
Isotropy	The condition in which the property or properties of interest are the same in all directions.
Jurassic period	A period of geologic time, 201.3 million to 145 million years ago.
Lineaments	Linear surface expressions of subsurface fracture zones, faults and geological contacts.
Lithology	The lithology of a rock unit is a description of its physical characteristics visible at outcrop, in hand or core samples or with low magnification microscopy, such as colour, texture, grain size, or composition.
Lithostratigraphy	A sub-discipline of stratigraphy, the geological science associated with the study of strata or rock layers. Major focuses include geochronology, comparative geology, and petrology. In general a stratum will be primarily igneous or sedimentary relating to how the rock was formed.
Major unconformities	Prolonged periods of erosion without deposition of sediments
Mesozoic era	An era of geologic time, 252.2 million to 66 million years ago.
Microseismic monitoring	The monitoring of very slight tremors or quiverings of the earth's crust that are not related to an earthquake, usually from anthropogenic causes.
Mineback mapping	Observations of fractures within mining coal seams that were previously hydraulically fractured

Term	Description
Miocene	An epoch of geologic time, 23.03 million to 5.332 million years ago.
MODFLOW	A 'finite difference' numerical groundwater flow modelling code.
Molecular diffusion	The process whereby solutes are transported at the microscopic level due to variations in the solute concentrations within the fluid phases.
Overburden	Material of any nature, consolidated or unconsolidated, that overlies a deposit of useful materials such as ores or coal, especially those deposits that are mined from the surface by open-cut methods.
Palaeozoic	An era of geologic time, 541 million to 252.2 million years ago.
Peclet number	A relationship between the advective and diffusive components of solute transport expressed as the ratio of the product of the average interstitial velocity, times the characteristic length, divided by the coefficient of molecular diffusion; small values indicate diffusion dominance, large values indicate advection dominance.
Permeability	The measure of the ability of a rock, soil or sediment to yield or transmit a fluid. The magnitude of permeability depends largely on the porosity and the interconnectivity of pores and spaces in the ground.
Permeate	To spread or flow throughout.
Permien	The period of geologic time, 298.9 million to 252.2 million years ago.
Perturbation	Changes in the nature of alluvial deposits over time.
Phreatic	Matters relating to groundwater.
Physico-chemical parameters	Relating to both physical and chemical characteristics.
Pore-fluid pressure/pore pressure	See Hydraulic Pressure.
Porosity	The proportion of the volume of rock consisting of pores, usually expressed as a percentage of the total rock or soil mass.
Potentiometric surface	An imaginary surface representing the static head of groundwater and defined by the level to which water will rise in a tightly cased well.
Production well	A well drilled to produce oil or gas.
Proppant	A solid material, typically treated sand or man-made ceramic materials, designed to keep an induced hydraulic fracture open, during or following a fracturing treatment.
Quaternary	The period of geologic time, 2.500 million to zero million years ago.
Radiometrics	A measure of the natural radiation in the earth's surface, which can tell us about the distribution of certain soils and rocks.
Reinjection bores	See Groundwater injection bores.
Retardation	Retardation is a general term for processes that cause the solute front to move slower than the advective flow velocity. This can be caused by sorption, when ions or charged molecules become bound to the surface of aquifer or aquitard minerals, or reversible chemical reaction, or diffusion of solutes into pores that do not contribute to flow (adsorption).

Term	Description
Saturated zone	That part of the earth's crust beneath the regional water table in which all voids, large and small, are filled with water under pressure greater than atmospheric.
Screen	The intake portion of a bore, which contains an open area to permit the inflow of groundwater at a particular depth interval, whilst preventing sediment from entering with the water.
Sediment	A naturally occurring material that is broken down by processes of weathering and erosion, and is subsequently transported by the action of wind, water, or ice and/or by the force of gravity acting on the particle itself.
Shearing	The relative, near horizontal or low angle movement between two sections of a rock stratum or a number of strata due to failure of the rock along a shear plane.
Slug test	A particular type of aquifer test where water is quickly added (i.e. slug test or falling head) or removed (i.e. bail test or rising head) from a groundwater well and the change in hydraulic head is monitored through time, to determine the near-well aquifer characteristics.
Solute	The substance present in a solution in the smaller amount. For convenience, water is generally considered the solvent even in concentrated solutions with water molecules in the minority.
Specific storage	The amount of water that a portion of an aquifer releases as a result of changes in the hydraulic head usually through pumping.
Specific yield	A ratio indicating the volume of water that an aquifer will yield when all the water is allowed to drain out of it under the forces of gravity.
Storativity	A dimensionless ratio that relates to the volume of water that is released per unit decline in pressure head for a defined vertical thickness of the formation.
Stratigraphy	A branch of geology which studies rock layers (strata) and layering (stratification).
Subduction	The process that takes place at convergent boundaries by which one tectonic plate moves under another tectonic plate and sinks into the mantle as the plates converge.
Subsidence	Usually refers to vertical displacement of a point at or below the ground surface. However, the subsidence process actually includes both vertical and horizontal displacements. These horizontal displacements, in cases where subsidence is small, can be greater than the vertical displacement. Subsidence is usually expressed in units of millimetres (mm).
Sodium Adsorption Ratio	The ratio of sodium to calcium and magnesium in water. Water with high SAR causes dispersion of soil particles, loss of the ability of the soil to form stable aggregates and a reduction in infiltration and permeability with consequences for crop production. Water with high SAR requires treatment if it is to be suitable for irrigation.
Sorption	A physical and chemical process by which one substance becomes attached to another.
Stratification	The formation of density layers (either temperature or salinity derived) in a water body through lack of mixing. It can create favorable conditions for algal blooms and can lower dissolved oxygen levels in the bottom layers with the associated release of nutrients, metals and other substances.

Term	Description
Tension	A system of forces which stretch rocks in two opposite directions. The rocks become longer in a lateral direction and thinner in a vertical direction. One important result of tensile stress is that it creates joints or fractures in the rock. Tensile stress is rare because most subsurface stress is compressive, due to the weight of the overburden.
Tertiary	A geologic period (from 66 million to 2.588 million years ago) that is no longer recognized as a formal unit by the International Commission on Stratigraphy, but is still widely used.
Tiltmeter	An instrument designed to measure very small changes from the vertical level, either on the ground or in structures.
Toxicant	A chemical capable of producing an adverse response (effect) in a biological system at concentrations that might be encountered in the environment, seriously injuring structure or function or producing death. Examples include pesticides and heavy metals.
Triassic	The period of geologic time, 248 million to 206 million years ago.
Triaxial cell	An apparatus that applies stress to a core in three dimensions and is able to subject a sample to its original in situ stresses.
Unconfined aquifer	An aquifer which has the upper surface connected to the atmosphere.
Unconsolidated sediments/materials	Sediments or materials that are not bound or hardened by mineral cement, pressure or thermal alteration.
Vadose zone	The ‘unsaturated’ zone, extending from the top of the ground surface to the water table. In the vadose zone, the water in the soil's pores is at atmospheric pressure.
Viscosity	A measure of a fluid’s resistance to gradual deformation by shear stress or tensile stress. For liquids, it corresponds to the informal notion of ‘thickness’. For example, honey has a higher viscosity than water.
Water quality	The physical, chemical and biological attributes of water that affects its ability to sustain environmental values.
Water quantity	Water quantity describes the mass of water and/or discharge and can also include aspects of the flow regime, such as timing, frequency and duration.
Water table	The upper surface of a body of groundwater occurring in an unconfined aquifer. At the water table, pore water pressure equals atmospheric pressure.
Well	A human-made hole in the ground, generally created by drilling, to obtain water (also see bore).
Yield	The rate at which water (or other resources) can be extracted from a pumping well, typically measured in litres per second (L/s) or megalitres per day (ML/d).

1 Introduction

1.1 Background

This review is one of a number commissioned by the Department of the Environment on the advice of the Interim Independent Expert Scientific Committee on Coal Seam Gas and Coal Mining. These reviews aim to capture knowledge on the water-related impacts of coal seam gas extraction and large coal mining, but do not aim to provide detailed analysis and evaluation of methods for identifying and managing impacts, or to develop such methods.

The focus of this report is on aquifer connectivity, particularly within the Great Artesian Basin (GAB), and the Surat, Bowen and Galilee geological Basins (Figure 1), including:

- types of connectivity, its implications and measurement
- groundwater flow models, which may both rely on an understanding of aquifer connectivity, and predict the extent of connectivity between aquifers
- actions that can alter connectivity
- connectivity within the GAB, a large and high-priority groundwater resource, and within the Surat, Bowen and Galilee geological Basins, which are linked to the GAB and are highly prospective areas for coal seam gas development and/or coal mining
- knowledge gaps and recommendations.

The report provides a summary and synthesis of the relevant and available literature and the expert opinions of the authors, and focuses on issues relevant to predicting the potential impacts on water resources from coal seam gas extraction and coal mining in Australia.

1.2 Definition and relevance

The term *aquifer connectivity* can be interpreted in different ways, and in its simplest form can be considered as the:

> *'…existence of a path for flow and transport from one location to another…'*
>
> © Copyright, Rennard & Allard (2011)

For the purposes of this review, a more detailed definition has been formulated:

Aquifer connectivity is a term that describes the groundwater interaction between aquifers that are separated by an aquitard (often termed inter-aquifer leakage), or between different parts of the same aquifer (intra-aquifer connectivity). It is dependent upon the lithology of aquitards and aquifers, and their integrity and spatial continuity. Fractures, faults and open or inadequately-sealed boreholes can form preferential flow paths that also affect connectivity. The degree of connectivity and the rate of water and solute transfer between aquifers are strongly influenced by local and regional hydraulic pressure and dissolved mineral concentration gradients. As aquifer systems are dynamic, these gradients are constantly changing with time, as groundwater is recharged or removed from the system.

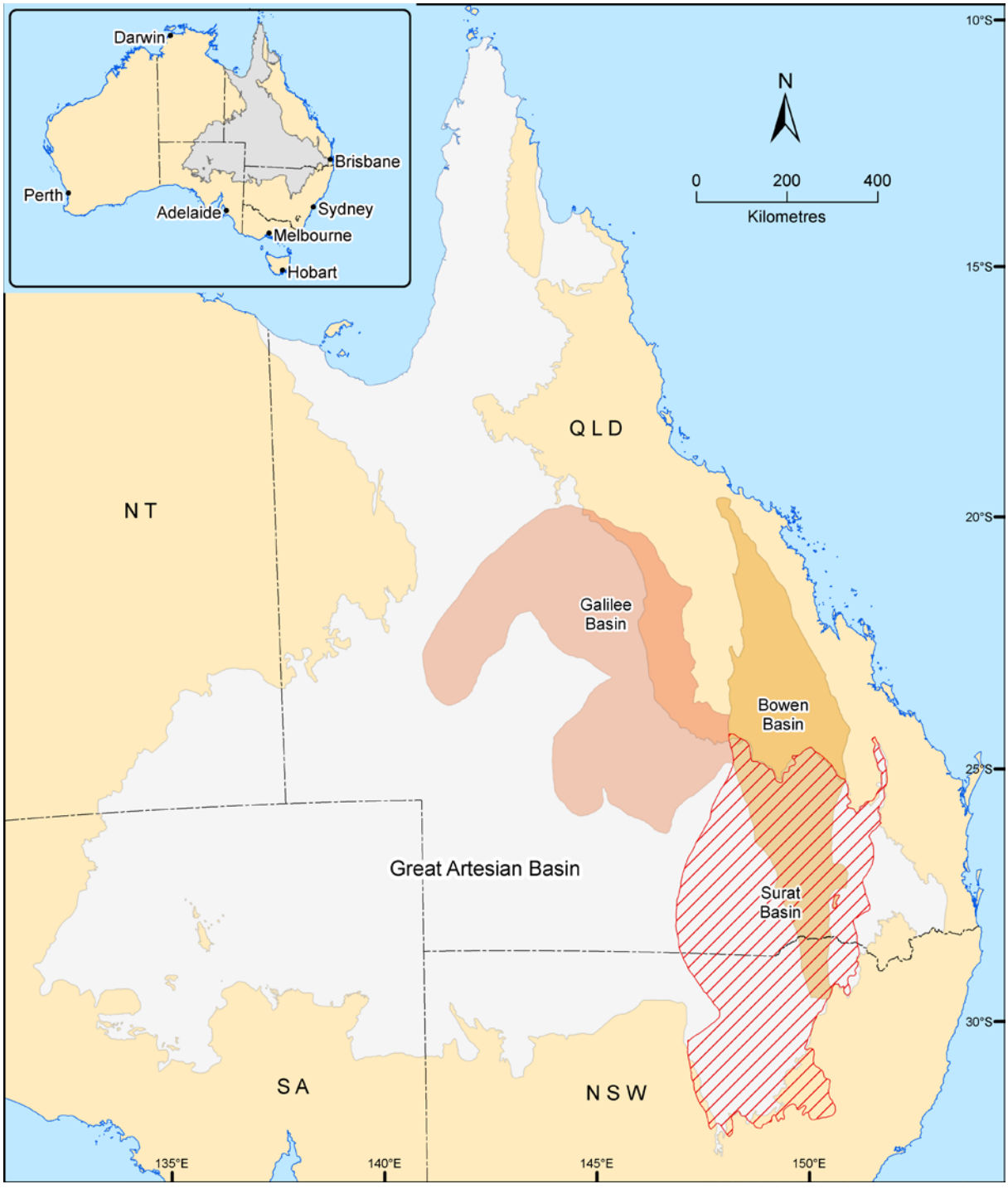

Figure 1 Location of the Great Artesian Basin, Surat Basin and underlying Bowen and Galilee Basins.

In an aquifer system under natural conditions, differences in hydraulic pressure will be present, both within aquifers and between aquifers that are separated by aquitards. These pressure differences result in flow of water and solutes within and between aquifers. When groundwater is pumped from a well it is intuitive that water pressure in the aquifer being pumped will decrease, leading to a localised increase in the rate of flow of water and its dissolved constituents towards the well. However, prolonged groundwater pumping from

multi-layered aquifer systems will also affect aquifers other than the pumped aquifer. This can result in a range of unforeseen impacts, including but not limited to the following:

- enhanced leakage of water from overlying and underlying aquifers and aquitards, resulting in the coincidental depletion of water in these resources
- mobilisation of natural salts from overlying and underlying aquifers and aquitards, resulting in the coincidental deterioration of water quality in the pumped aquifer
- mobilisation of anthropogenic contaminants from overlying and underlying aquifers and aquitards
- changes in the nature and fluxes between surface water and groundwater systems near the ground surface
- declining water levels in shallow aquifers, leading to changes in the recharge and/or discharge rates.

Thus any large-scale groundwater development, including that required for CSG production and dewatering of coal mine voids, needs to be managed with the best available information about aquifer connectivity.

1.3 Objectives and scope

The primary objective of this review is to document the range of scientific methods that have been developed to measure and model connectivity in any hydrogeological setting, and the specific knowledge of aquifer connectivity for the GAB, Surat Basin, Bowen Basin and Galilee Basin. The review captures expert knowledge from each of the primary authors and their respective organisations, as well as published material from text books and international peer-reviewed journals. However, this review does not attempt to report every publication that has mentioned aquifer connectivity. It also does not utilise nor report every investigation and dataset that is publically available for each of the four specific basins. The collection of industry and other data was out of scope for this project. Instead, the review is aimed at broad, regional-scale understandings with key examples to illustrate areas where particular data and, by inference, knowledge is either available or required in the foreseeable future. The review is relevant for aquifer connectivity in the context of both CSG and coal mining. Because the principles of groundwater flow and solute transport are independent of geology and land use, this report purposely addresses connectivity in a general sense, unless specific examples from CSG development or coal mining are available.

The summary information in this report could be useful to scientists and engineers familiarising themselves with the four specific basins reviewed in this report. The report could also provide a reference on groundwater flow and aquifer connectivity for informed, interested parties.

1.4 Outline

This report begins with a review of what is currently known about aquifer connectivity in terms of general hydrogeological and geotechnical principles (Chapter 2) and established methods for measuring and modelling fluid and solute transport within and between aquifers (Chapter 3). A particular concept introduced in these first chapters is that of spatial and temporal scales for groundwater flow and transport through different geologic media; the significant lag times that multi-layered aquifer systems may require to realise and recover from changes in groundwater pumping are explored in some detail.

A large proportion of historical research into aquifer connectivity – at least in the case of inter-aquifer leakage – has been undertaken in areas of relatively low groundwater development. Accordingly, the current scientific understanding is likely to be biased towards natural conditions. The level of understanding about connectivity in the four specific basins reviewed in this report (Chapters 5-8) can also be considered as representative of largely un-stressed (i.e. natural) systems.

Chapter 4 explores how aquifer connectivity may change as a result of prolonged groundwater extraction. The most logical change is an increase in groundwater fluxes brought about by increased hydraulic gradients (see Chapter 2 for principles of groundwater flow). However, more subtle impacts may result through reactivation of existing faults and fractures, or even brittle deformation of otherwise competent aquitards following subsidence caused by depressurisation of aquifers.

The final section of this report (Chapter 9) identifies the major knowledge gaps that present a risk to the future management of water resource impacts from CSG and coal mining. These gaps include uncertainties in the understanding of particular hydrogeological processes; limitations in the methods or tools to measure and predict the impacts of prolonged, large-scale groundwater pumping on adjacent water resources; and deficiencies in data availability for the four studied basins.

2 Aquifer connectivity

2.1 Introduction

This chapter outlines the basic concepts of hydrogeology and the fundamental equations that describe groundwater flow and solute transport in the context of aquifer connectivity. A suite of simple numerical groundwater models is also used to demonstrate the key physical processes, including the impacts of different types of connections in inter-aquifer leakage. For further background information, the reader is referred to the Glossary of terms contained herein, or the many text books available (e.g. Delleur 2007; Fetter 2001; Freeze & Cherry 1979).

Broadly speaking, groundwater flow systems can be divided into aquifers and aquitards. Aquifers are generally defined as permeable geological layers that can transmit water at a sufficient rate to sustain pumping from a well. In contrast, aquitards are low-permeability layers that retard the flow of water, and thus cannot sustain pumping from a well. Some literature also introduce the term aquiclude to represent geologic formations that preclude the flow of water, however we have reframed from using this term as there are no geological media that are completely impervious, albeit some are extremely tight. This grouping of formations based on their hydraulic properties is the hydrostratigraphy of a region. A hydrostratigraphy will always be scale-dependent as it entails a grouping based on the relative difference in hydraulic conductivity between formations. For example, at a regional scale, the alluvial deposits of the Namoi River in New South Wales (NSW) can be considered an aquifer. At a detailed local scale however, the presence of clay layers and lenses might warrant a further subdivision in aquifers and aquitards. Similarly, a coal seam will not generally be classified as an aquifer because of its low hydraulic conductivity. But at a local scale, compared to very low permeable interburden layers such as mud or claystone, a coal seam can be considered an aquifer.

Contrary to the common perception that groundwater systems are simple layer-cake organisations of geologic strata, aquifers and aquitards are seldom laterally continuous or structurally undisturbed, as is illustrated in Figure 2. For example, aquitards can pinch out or laterally transition into sediments with different hydraulic conductivity. Structural deformation, uplift, erosion and deposition can all result in the formation of faults and fractures in both aquifers and aquitards. The density and orientation of faults and fractures will ultimately affect the permeability of a geological layer, and fractures that traverse an entire aquitard will provide localised, preferential flow paths connecting two or more aquifers. Groundwater wells that have been screened over multiple aquifers or completed with faulty or inadequate casing can provide similar preferential flow paths.

Figure 2 also highlights the difference between the water table, the top of the saturated zone in an unconfined aquifer and the more generic term potentiometric surface, which is the surface expression of the level to which water would rise in a well screened in a specific aquifer. Potentiometric surface is mostly used for confined aquifers, i.e. aquifers which are fully saturated and bounded at the top and bottom by an aquitard. Unconfined aquifers on the other hand have no aquitard at the top and have a water table.

2.2 Types of aquifer connectivity

In a regional groundwater flow system, the connectivity between aquifers is controlled by the bulk hydraulic conductivity of the aquitards. Where these aquitards are uniform, massive and

laterally-extensive, the inter-aquifer leakage is diffuse. However, geological windows, faults, fractures and open wells create preferential flow paths that can provide localised but very conductive connections between aquifers. This section introduces a number of concepts relevant to understanding flow through aquifers and aquitards.

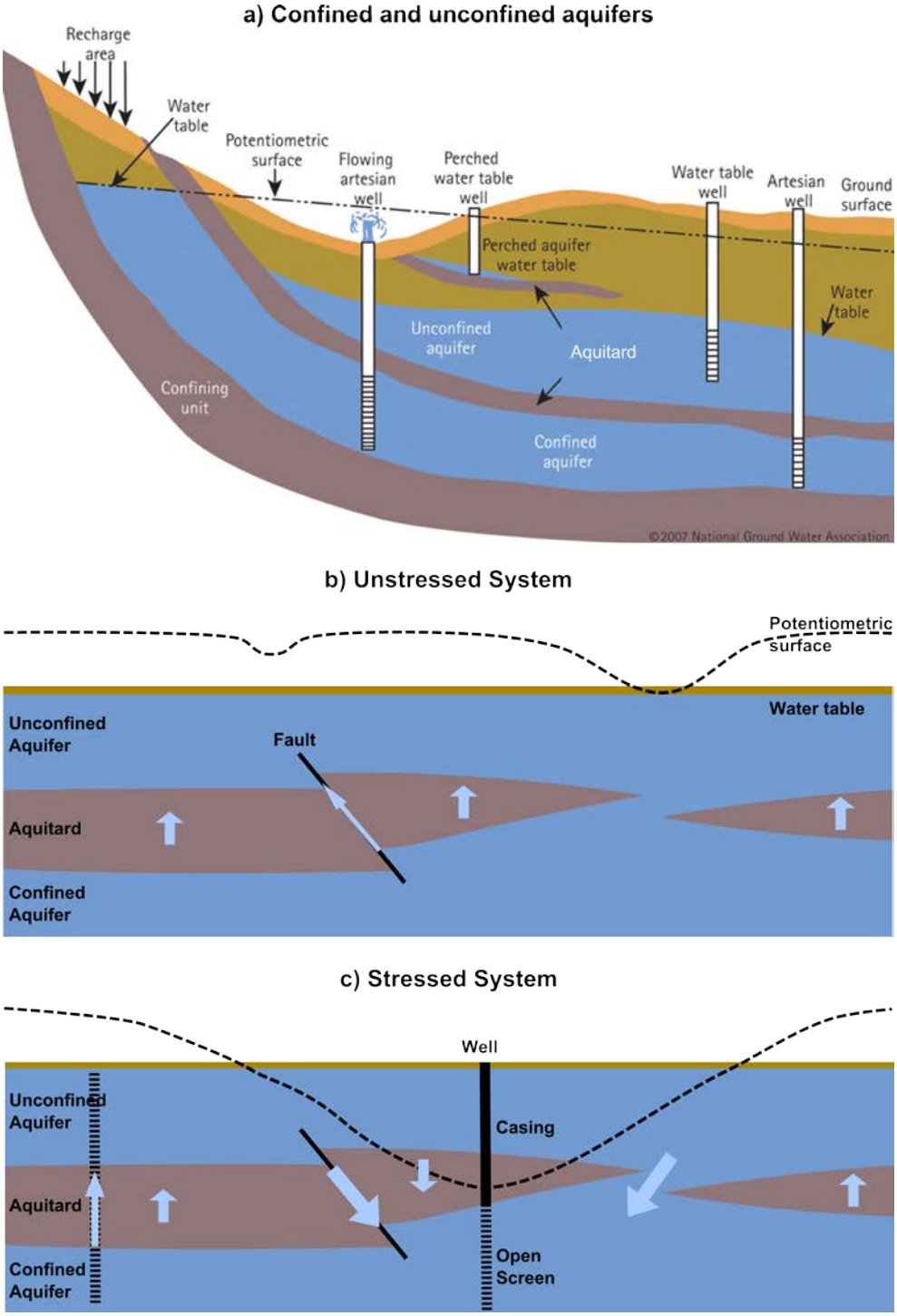

Figure 2 Schematic representation of (a) aquifer types and terminology and groundwater pressure and flow directions, under both (b) unstressed and (c) stressed conditions, in a hypothetical aquifer system, highlighting structural and stratigraphic features that affect aquifer connectivity (© Copyright, NGWA 2014).

2.2.1 Diffuse inter-aquifer leakage

One dimensional groundwater flow through porous media is governed by Darcy's Law, expressed as:

$$q = \frac{Q}{A} = -K\frac{dh}{dz}$$

where the specific discharge of water [q (m/day)] is the volumetric flow rate [Q (m^3/day)] per cross-sectional area [A (m^2)], and is equal to the product of hydraulic conductivity of the geologic media [K (m/day)] and the hydraulic gradient [dh/dz]. The hydraulic gradient is defined by the change in hydraulic head [h (m)] over a distance [z (m)] along the direction of flow. The negative sign in this equation is used to illustrate flow is in the direction of decreasing gradient. To infer the direction of flow in an aquifer, head measurements at several locations are required. While the flow direction in special cases can coincide with the dip of a geological layer, layer geometry is not sufficient to determine the flow direction in an aquifer.

The hydraulic conductivity controls the flow rate through a material and depends both on the characteristics of the fluid, such as the density (ρ) and viscosity (μ), and on the characteristics of the porous material, the intrinsic permeability (k) and acceleration due to gravity (g):

$$K = \frac{k\rho g}{\mu}$$

In hydrogeological studies, where the focus is on the flow of groundwater, density and viscosity changes are limited and hydraulic conductivity is usually considered to be independent of these variables. In studies involving oil and gas, density and viscosity changes are of greater importance and intrinsic permeability is used. The SI unit of intrinsic permeability is m^2, but a commonly used unit is the millidarcy, (mD). 1 Darcy is approximately equal to 9.869233×10^{-13} m^2.

Owing to the direction of the principal hydraulic gradient, the regional flow of groundwater in natural, unstressed systems is mainly horizontal in aquifers and mainly vertical in aquitards. The flow rate across an aquitard is generally limited, although it can be very important locally as illustrated by springs in the GAB (Love et al. 2012). The direction of flow, upwards or downwards will be determined by the local vertical hydraulic gradient (Figure 2 (b)).

In a stressed system with considerable pumping, the hydraulic gradients and flow regime change drastically (Figure 2 (c)), which in turn will result in changed flow magnitude and even flow direction. The contribution of local features, such as fractures, to flow and transport across an aquitard can change from limited under natural conditions to considerable under stressed conditions.

The intrinsic permeability, often just referred to as the permeability, depends on the porosity [n] of the medium, i.e. the ratio of the volume of voids over the total volume. In unconsolidated materials, porosity tends to increase with grain size. The larger the grain size, the larger the voids between grains. Porosity is also affected by the sorting of the sediment. Poorly sorted sediment consists of mixtures of different grain sizes. Voids between large grains can be filled with smaller grains and the porosity will decrease. The permeability of the sediment is however not controlled by the total porosity, but by the effective porosity [n_e]. This is the fraction of pores that are connected to each other and contribute to flow. In unconsolidated materials, the effective porosity is generally equal to the total porosity. In consolidated materials, many pores can be isolated from each other and notwithstanding a

high total porosity, effective porosity can be low. Materials with low or no total porosity can become very permeable if a small number of highly connected fractures are present.

Darcy's Law describes flow in steady state. To describe how flow rates change over time, changes in storage need to be taken into account through the storativity [*S*]. Storativity is the volume of water per unit aquifer surface area taken into or released from storage per unit increase or decrease in head respectively. The specific storage is the storativity per unit thickness of the aquifer (1/m). When water is added to a confined aquifer, pressure increases are accommodated by compressing water and the aquifer matrix. In an unconfined aquifer, adding water will result in raising the water table, so that a larger portion of the aquifer is saturated. Specific storage for unconfined aquifers is therefore considered to be equal to effective porosity and is often referred to as specific yield.

Table 1 gives an overview, based on values from international literature, of the range of values for porosity, hydraulic conductivity and specific storage for a variety of common aquifer and aquitard materials. A more detailed summary of values can be found in Spitz and Moreno (1996). One of the most striking aspects of this table is the huge range of hydraulic conductivities. This property can vary over up to 12 orders of magnitude from dense crystalline rock to gravel. Variation in specific storage is less, but still spans at least 4 orders of magnitude. Hydraulic conductivity generally increases with increasing porosity. The main exception is clay. Due to the random ordering of the plate-like clay minerals, clay deposits have a large proportion of very small, isolated pores. These do not contribute to flow, hence the very low hydraulic conductivity.

Table 1 Typical ranges for porosity, hydraulic conductivity and specific storage for different rock types (© Copyright, Leap 2007; based on data in Fetter 2001, Domenico & Schwartz 1990, Narashimhan & Goyal 1984, and Freeze & Cherry 1979).

Lithology	Total porosity (%)	Hydraulic conductivity (m/d)	Specific storage* (1/m)
Unconsolidated			
Gravel	25 – 40	$10 – 10^3$	$10^{-4} – 10^{-6}$
Sand	25 – 50	$0.1 – 10^2$	$10^{-3} – 10^{-5}$
Silt	35 – 50	$10^{-4} – 1$	No Data
Clay	40 – 70	$10^{-7} – 10^{-4}$	$10^{-2} – 10^{-4}$
Glacial Till	10 – 20	$10^{-7} – 0.1$	$10^{-2} – 10^{-4}$
Indurated (consolidated)			
Fractured Basalt	5 – 50	$10^{-2} – 10^3$	$10^{-4} – 10^{-5}$
Karst Limestone	5 – 50	$0.1 – 10^3$	No Data
Sandstone	5 – 30	$10^{-5} – 0.1$	$10^{-7} – 10^{-6}$
Limestone, Dolomite	0 – 20	$10^{-4} – 0.1$	$< 10^{-6}$
Shale	0 – 10	$10^{-8} – 10^{-4}$	$10^{-3} – 10^{-4}$
Fractured Crystalline Rock	0 – 10	$10^{-4} – 10$	$< 10^{-6}$
Dense Crystalline Rock	0 – 5	$10^{-9} – 10^{-5}$	$10^{-5} – 10^{-7}$

* for confined aquifer

Crystalline rock has very low porosity, which leads to very low conductivity. Fractures however will increase permeability and hydraulic conductivity to the extent that aquifers in fractured crystalline rock become productive. The effect of fractures will depend on the fracture orientation and density.

Geological deposits are seldom homogeneous and their hydraulic properties will vary from one place to another; this is known as heterogeneity. Hydraulic properties can be dependent on the direction of measurement; if a geologic medium has hydraulic conductivity equal in all directions (that is, horizontal and vertical) then it is said to be isotropic. In reality, vertical hydraulic conductivity is generally lower than horizontal hydraulic conductivity and media are anisotropic. This anisotropy is mainly due to internal layering of sediments and preferred orientation of grains. Oblong grains will generally be deposited with their long axis horizontal, resulting in resistance to flow in the vertical direction. Anisotropy can also be caused when fracture networks have a dominant direction.

Groundwater flow in aquifers is predominantly horizontal. At a contact with an aquitard with a much lower hydraulic conductivity, flow in the aquifer will decrease and the direction of flow will become more vertical. This refraction of flowlines is proportional to the ratio of the high and low conductivity. It has been shown that a difference of four orders of magnitude between aquifer and aquitard is sufficient to change flow from predominantly horizontal in the aquifer to predominantly vertical in the aquitard (Freeze and Cherry 1979).

Heterogeneity and anisotropy act on different scales. In a heterogeneous aquifer, measurements of a hydraulic property, such as porosity, on a small volume, such as a plug from a drill core, will vary greatly. By increasing the sample volume, the measurement will average the property over a larger volume and the variation in measurement values will become less (Figure 3). This means that the value will become more representative for the entire aquifer. The smallest measurement volume that will give an average, representative value for a property in a porous medium is defined as the Representative Elementary Volume (REV). It is the volume over which hydraulic properties can be defined as a mean value attributed to the centre of the volume. The size of the REV is not fixed and depends on the aquifer properties. The REV for porosity in a well-sorted, homogeneous sand will be relatively small. To measure hydraulic conductivity in fractured sediment however, a large REV will be needed as at small measurement scales the presence of a single fracture will have an enormous effect on the measured conductivity.

The mostly vertical layering of sediments also needs to be taken into account when averaging hydraulic conductivity. The average hydraulic conductivity when flow is parallel to the layering is a layer thickness-weighted arithmetic average. The overall hydraulic conductivity [K] will thus be strongly influenced by the hydraulic conductivity of the thickest layers. Average hydraulic conductivity perpendicular to the flow direction is computed as a thickness weighted harmonic average. In this case the overall conductivity will be determined by the lowest hydraulic conductivity in the layered sequence. This implies that a thin layer of low conductivity, like a clay layer, in a thick sequence of higher conductivity material, such as sand, will have very limited effect on the overall horizontal hydraulic conductivity. In the vertical direction however, the thin clay layer will dominate the average hydraulic conductivity.

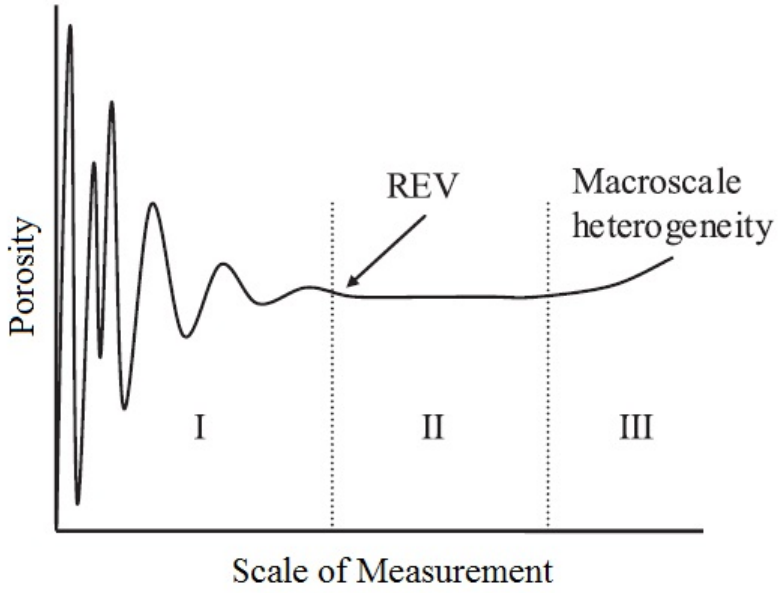

Figure 3 Concept of Representative Elementary Volume (REV): with increasing scale of measurement the hydraulic property will reach a stable, average value representative of the aquifer (© Copyright, Costanza-Robinson et al. 2011).

2.2.2 Preferential flow paths

Within and across lithological units, preferential flow paths can exist through fractures and faults or man-made features such as wells and boreholes.

In the presence of faults and fractures, describing groundwater flow with average values through a representative elementary volume is generally not valid. For the REV concept to be valid – that is, to represent hydraulic properties of a fractured aquifer with a single representative mean value - the fracture network needs to be very dense or the REV needs to be very large. To describe flow through discrete fractures at local scales, Darcy's Law can therefore no longer be used as it requires a continuous matrix.

Flow in discrete fractures can be estimated using the cubic law:

$$Q = C(2b)^3 \Delta h$$

where *C* is a constant related to the properties of the fluid and the geometry of the fracture while *b* is the aperture of the fracture. Figure 4 shows for a range of hydraulic conductivities, the thickness of porous medium that would be equivalent to a single fracture of given aperture. It illustrates that, under the same gradient, the flow through a single fracture with an aperture of 1 mm is equal to the flow through a porous medium 10 m thick layer with a hydraulic conductivity of 10^{-4} m/s.

The aperture of a fracture is controlled by the local stress-field. To allow for an open fracture, the pressure exerted by the overlying layers of sediment need to be compensated by the pressure of water in the aperture. Chapter 4 provides more detail on the different components of the stress field at depth and how groundwater pumping will affect the stress field.

Preferential flow paths are not limited to naturally occurring faults and fractures. Groundwater wells and mineral exploration boreholes can also permit rapid cross-formation flow if they are poorly constructed at the time of installation or not backfilled properly. Even wells with adequate casing and backfilling may fail after a long time due to corrosion of the casing materials or chemical alteration of the grout. Bore integrity, and whether a bore will fail within its design life, will depend on bore design, construction materials, and cementing of the annulus around the casing (DEEDI 2013; Dunnivant et al. 1997), as well as groundwater chemistry and the flow rate in the well.

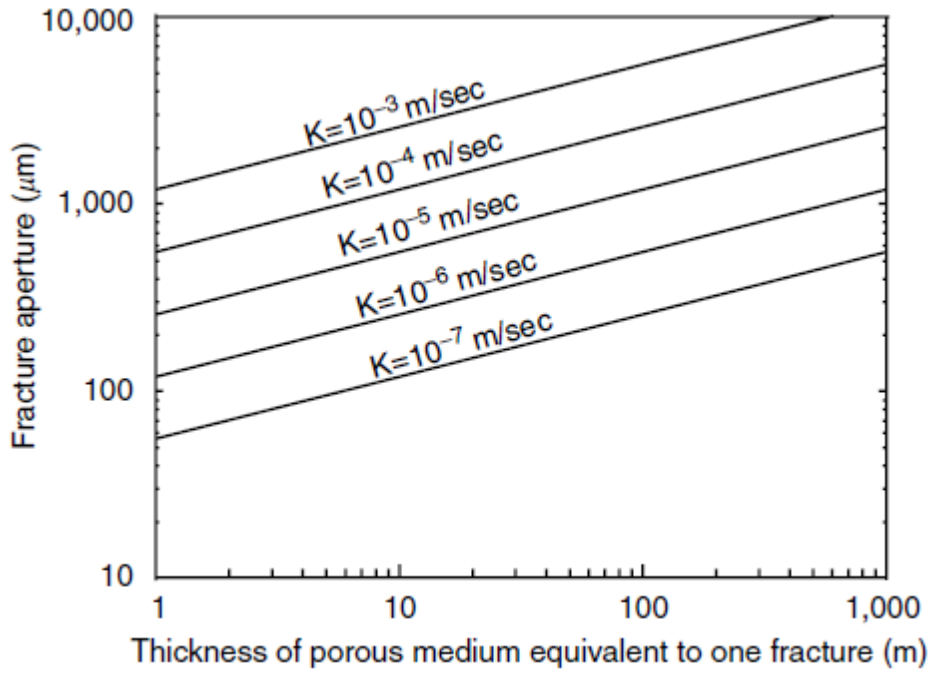

Figure 4 Comparison of aperture of a single fracture to equivalent thickness of porous media (© Copyright, de Marsily 1986; in Novakowski & Sudicky 2007).

2.3 Groundwater flow

The previous section describes the types of aquifer connectivity and the theoretical aspects of flow through an aquifer system. This section will illustrate the importance of the different kinds of connectivity through a simple numerical modelling example. Consider a multi-layered groundwater system consisting of three aquifers (layers 1, 3 and 5) and two aquitards (layers 2 and 4) with the properties listed in Table 2. Initial hydraulic heads in all aquifers and aquitards are assumed to be equal at a nominal ground surface of 500 m elevation (i.e. there is no vertical flow of water prior to pumping). Groundwater is then pumped from the lowest aquifer (layer 5) to lower the hydraulic head to just above the top of that aquifer at 205 m elevation.

This example will be used to illustrate the different aspects of groundwater flow and transport induced through pumping in a multi-layered system and how and to what extent flow and transport are influenced by different types of connectivity, including (a) a continuous aquitard, (b) a fractured aquitard, and (c) a fully-penetrating open well (Figure 5). The simulations are carried out with the analytic element method implemented in the TTIM software by Bakker (2010). The main results are summarised in Table 3.

Table 2 Hydraulic properties used for the simulation of drawdown in the multi-layered aquifer.

Name	**Elevation Top (m)**	**Elevation Base (m)**	**K (m/d)**	**Kv/Kh (-)**	**Ss (1/m)**
Layer 1	500	400	5	0.1	0.05*
Layer 2	400	350	5x10-4	0.1	10-6
Layer 3	350	250	5	0.1	10-4
Layer 4	250	200	5x10-4	0.1	10-6
Layer 5	200	100	5	0.1	10-4

* Phreatic aquifer, specific yield

Table 3 Results of the simulation of drawdown in the multi-layered aquifer.

Case	Pumping Rate (ML/yr)	Drawdown after 30 yr (m), 100m from pumping well		
		L1	L3	L5
Base Case	0.22	0.6	7.4	141.3
Fracture	0.24	1.6	38.2	124.6
Open Well	0.27	31.2	34.9	109.6

2.3.1 Continuous aquitard

In the 'base case' of laterally-continuous, undisturbed aquitards (leftmost column of graphs in Figure 5), simulated drawdown in the aquifer layers (1, 3 and 5) at a distance of 100m from the pumping well after 30 years is 0.6 m, 7.4 m and 141.3 m, respectively (Table 3). These results demonstrate that simulated drawdown in the shallowest aquifer is very small compared to that in the two deeper aquifers. It is worth noting however, that even a moderate change in water level of 0.6 m in a shallow unconfined aquifer can be enough to change the direction and/or flux of surface-groundwater interactions (for example, changing gaining streams into losing streams). For comparison, a fall in groundwater level by 0.6 m in an unconfined aquifer with a specific yield of 0.10 would be equivalent to a reduction in recharge of 60 mm/year.

It takes several years for the drawdown in the deepest aquifer (layer 5) to stabilise, however a steady state drawdown in the middle aquifer (layer 3) is not attained in the 30 year simulation period. This puts into perspective the limited value of short-term aquifer pumping tests to estimate the long-term effects of pumping.

The steady-state pumping rate from the lowest aquifer is 0.22 ML/year, of which only about eight per cent is replenished via leakage through the lower aquitard (layer 4), which implies the majority of flow to the pumping well is horizontal through the aquifer. The flow across the upper aquitard (layer 2) is very small, about one-twentieth of the flow across the lower aquitard.

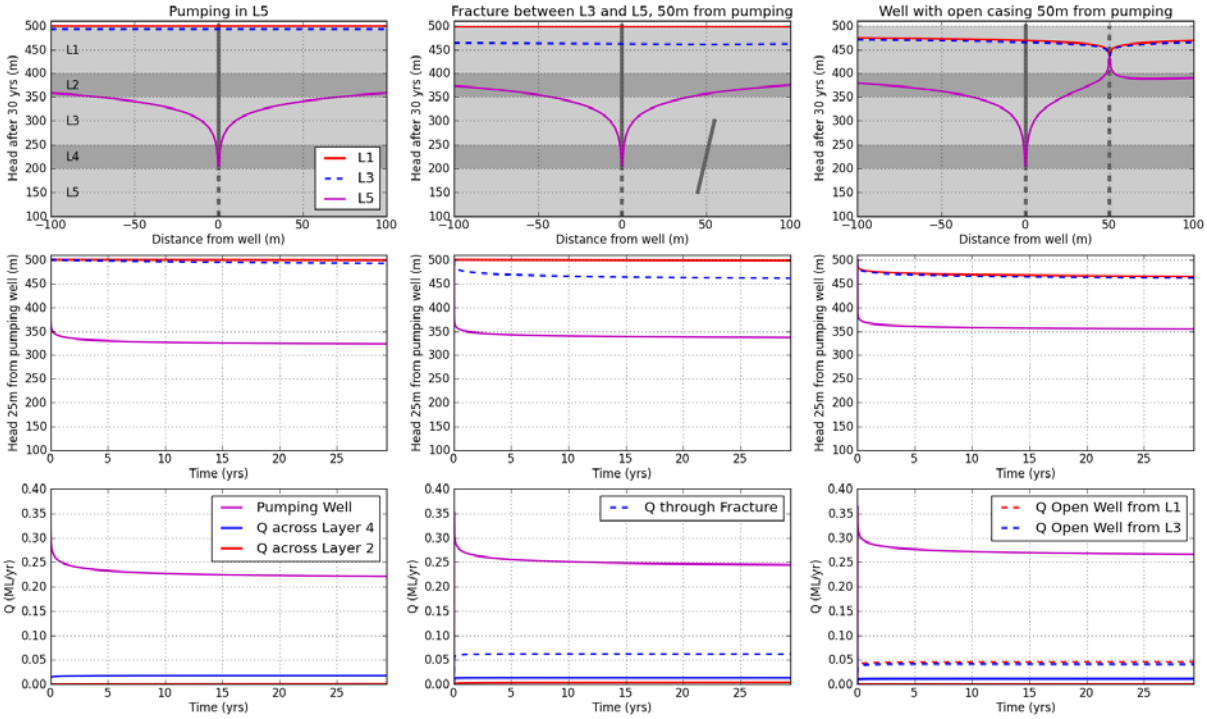

Figure 5 Simulated groundwater response in a multi-layered groundwater system caused by pumping from the deepest aquifer (layer 5). The leftmost column of graphs are for a 'base case' undisturbed aquifer system with laterally-continuous aquitards. The middle column represents the base case with a single fracture in the first aquitard (layer 2) located 50 m from the pumping well. The rightmost column represents the base case with a fully-penetrating open well located 50 m from the pumping well. The first row of graphs shows the drawdown in hydraulic head for each aquifer layer as a function of distance from the pumping well, evaluated after 30 years of pumping. The second row shows the evolution of drawdown in each aquifer through time, evaluated at 25 m from the pumping well. The third row shows the change in pumping rate required over time to maintain the hydraulic head in the lowest aquifer at 205 m.

2.3.2 Fractured aquitard

The middle column of graphs in Figure 5 represents the results of a simulation with a 1000 m long fracture in the lower aquitard, at a distance of 25 m from the pumping well. The fracture runs perpendicular to the cross-section shown. The aperture of the fracture is 0.1 mm, which corresponds to an equivalent transmissivity of about 0.4 m^2/day.

Compared to the base case, simulated drawdown at a distance of 100 m from the pumping well after 30 years is 16.7 m lower for the deepest aquifer (layer 5) and 30.8 m and 1.0 m greater for the middle aquifer (layer 3) and shallowest aquifer (layer 1), respectively.

Despite the reduction in drawdown in the deepest aquifer, pumping rates need to increase by 11 per cent to overcome the enhanced vertical leakage and maintain a hydraulic head of 205 m at the pumping well. The considerable increase in drawdown in the middle aquifer leads to greater flow across the upper aquitard (layer 2) and thus increased drawdown in the shallowest aquifer. The dashed line in the pumping rate plot represents the flow rate through the fracture, which is about five times larger than the flow through the same aquitard. Compared to the base case, flow across the deeper aquitard is lower because the vertical hydraulic gradient is less.

2.3.3 Fully-penetrating open well

The rightmost column of graphs in Figure 5 shows the results of a simulation with a full-penetrating open well with a radius of 75 mm. As the well is screened over the entire aquifer system, the simulated head is equal in all aquifers and aquitards.

Compared to the base case, simulated drawdown at a distance of 100 m from the pumping well after 30 years is 35.9 m lower for the deepest aquifer (layer 5) but 31.2 m and 34.6 m greater for the middle aquifer (layer 3) and shallowest aquifer (layer 1) respectively. The most striking feature in this simulation is the enormous increase in drawdown in the shallowest aquifer compared to the base case and fractured aquitard simulations.

Drawdown in the deepest aquifer is less than simulated for the base case and fractured aquitard, however pumping rates need to increase by 23 per cent to overcome the enhanced vertical leakage and maintain a hydraulic head of 205 m at the pumping well. The flow rate derived from the upper and middle aquifer through the well is very similar at approximately 17 per cent of the total pumped rate. While in the base case the majority of pumped water comes from horizontal flow, the open well causes a very large proportion of the pumped water to be drawn from the overlying aquifers. The more pronounced drawdown results in lower vertical gradients and thus lower flows across the aquitards.

2.4 Transport of solutes

Groundwater transports solutes along flow paths via a process known as advection. The concentration of a solute can thus be predicted by the groundwater velocity [v], which is the flow per unit cross-sectional area divided by the effective porosity [n_e]:

$$v = \frac{1}{n_e} K \frac{dh}{dz}$$

At the microscopic scale, water with high solute concentrations will mix with water with low solute concentrations as flow velocities in a porous medium vary due to the size of the pores and the flow paths around individual grains. This leads to a reduction of concentration at the macroscopic scale and is called dispersion. Dispersion acts both in a longitudinal direction, along the flow path, and in a transverse direction, perpendicular to the flow path.

A similar reduction in concentration and spread of solutes is caused by molecular diffusion, the movement of solutes from high concentration to low concentration. Although this process acts even in water that is not flowing, in groundwater transport it is indistinguishable from mechanical dispersion. Both processes are therefore usually grouped as hydrodynamic dispersion, with the coefficient of longitudinal hydrodynamic dispersion (D_L) given by:

$$D_L = a_L v_z + D^*$$

where a_L is the dynamic dispersivity and D^* the effective molecular diffusion coefficient. For small advective flow velocities, hydrodynamic dispersion will be dominated by dynamic dispersivity. In porous media with very low advective flow velocities, such as aquitards, hydrodynamic dispersion is dominated by molecular diffusion.

The value of D_L is scale-dependent. The larger the scale on which dispersion is measured, the more likely it is for the flow field to be more variable due to heterogeneity in the hydraulic properties. In their review of measured dispersivity values, Gelhar et al. (1992) showed that dispersivity indeed increases with scale, but that dispersivity can span three orders of magnitude for the same scale of measurement. Transverse dispersivity is generally at least an order of magnitude smaller than longitudinal dispersivity.

The variation of a solute concentration (*C*) with time (*t*) and distance (*z*) can be described, in this case in one dimension, with following differential equation:

$$\frac{\partial C}{\partial t} = -v_z \frac{\partial C}{\partial z} + D_L \frac{\partial^2 C}{\partial z^2}$$

where the first term of the right hand side represents change in concentration due to advection, and the second term represents change in concentration due to hydrodynamic dispersion. The Peclet number (*Pe*) is defined as the ratio of the coefficients of the advective and the dispersive term, multiplied by a length (*L*) characteristic for the problem at hand:

$$Pe = \frac{v_z}{D_L} L$$

When the Peclet number is less than one, diffusion is the dominant solute transport mechanism. Huysmans and Dassargues (2005) do show however, for a number of variants of the Peclet number, that advection can still have an important influence on transport through low-permeable materials, even if the Peclet number is much smaller than one.

Two other processes are important to describe the transport of solutes; retardation and degradation. Retardation is a general term for processes that cause the solute front to move slower than the advective flow velocity. This can be caused by sorption, when ions or charged molecules become bound to the surface of aquifer or aquitard minerals, or reversible chemical reaction, or diffusion of solutes into pores that do not contribute to flow (adsorption). After the solute front has passed, solutes are desorbed or diffuse back into the pores that contribute to flow. The total mass of solutes stays constant; however, the distribution of the solute in time and space is more spread out.

Degradation on the other hand decreases the solute mass through irreversible chemical reactions. In the case of contaminant transport, degradation reactions can have a positive effect as they reduce the concentration of contaminant. However, it is also possible that the products of the chemical degradation reactions are more toxic than the original contaminant, which would lead to exacerbation of the problem.

In the following sections we revisit the simple, multi-layered aquifer model used previously to demonstrate the impacts of different types of connectivity on groundwater flow, and focus on solute transport by advection and dispersion/diffusion through porous and fractured aquitards.

2.4.1 Continuous aquitard

Due to the low hydraulic conductivity of aquitards, advective flow velocities in these formations are generally very low and solute transport is thus diffusion dominated. Using the flow field derived from the base case simulation of a laterally-continuous aquitard (leftmost column of graphs in Figure 5), we have simulated a concentration profile through the lower aquitard, and a concentration breakthrough curve for the deepest aquifer (Figure 6). The simulation assumes there is a constant solute concentration of one (unspecified units) in the middle aquifer (layer 3), and an initial solute concentration of zero (unspecified units) in both the lower aquitard (layer 4) and deepest aquifer (layer 5). Only advection (n_e = 0.02) and hydrodynamic dispersion (α_L = 5 m, D_L = 2x10^{-6} m^2/day) are simulated, without degradation or retardation.

The simulation illustrates the long timeframes for solute transport in low-permeability aquitards. The first appearance of the solute in the deepest aquifer occurs after only about 2.5 years (Figure 6 (B)) however it takes more than 20 years for the concentration to become

equal to that in the overlying aquifer. This is very slow compared to the propagation of pressure changes, and thus drawdown; after 2.5 years, almost half of the total drawdown in the middle aquifer has occurred (Figure 5).

Aquitards can also affect the transport of solutes in aquifers through diffusive exchange and/or retardation. Such exchange can occur in either direction depending on the direction of concentration gradient: solutes may diffuse from an aquifer into an aquitard, and possibly be retarded by sorption, or they may diffuse from an aquitard into the aquifer – for example, providing a long-term source of salinity or contaminants to potable groundwater (Timms et al. 2000).

2.4.2 Fractured aquitard

Solute transport processes are the same in fractures as in porous media; however, advective velocity in a fracture is proportional to the square of its aperture, in addition to the hydraulic gradient:

$$v = \frac{\rho g}{12\mu}(2b)^2 \frac{dh}{dz}$$

Using the geometry and hydraulic head results from the fractured aquitard simulation (middle column of Figure 5) the advective flow velocity in the fracture would be more than 5000 m/day if the aperture was 0.1 mm. Even if the aperture was one-tenth of this value (i.e. 0.01 mm) the flow velocity would be 73 m/day. These simple examples demonstrate how the presence of fractures can lead to very rapid solute transport within and between aquifers. However, in practice solute transport through fractured aquitards can be severely retarded relative to advective flow (Cherry et al. 2004). This is due to a combination of the high reactive area of the fracture wall (on which sorption can occur) and the process of matrix diffusion, whereby solutes diffuse out of the fracture into the surrounding matrix due to concentration gradients.

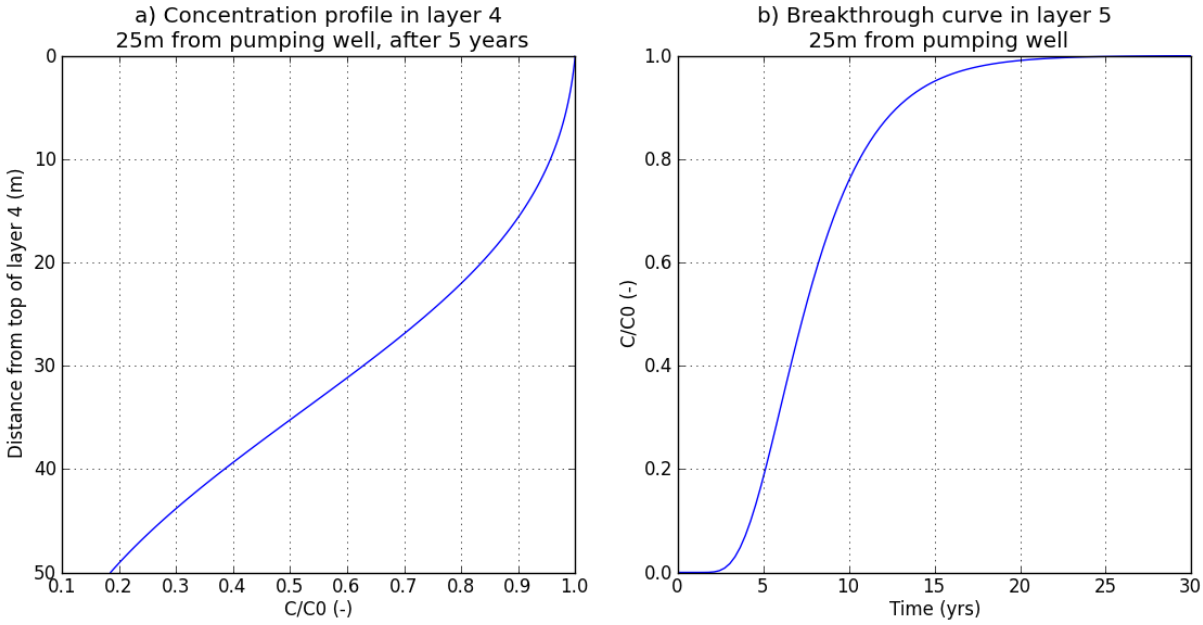

Figure 6 Simulated concentrations during pumping from the multi-layered aquifer system with a continuous aquitard. (A) vertical concentration profile across the lower aquitard, and (B) concentration breakthrough in the deepest aquifer.

2.5 Conclusions

The connectivity of aquifers is dependent upon the lithology of the aquitards, their integrity and spatial continuity. Fractures, faults and open or inadequately-sealed boreholes may form preferential flow paths between aquifers.

Stressing of aquifers through pumping will alter the magnitude and potentially the direction of hydraulic gradients and will induce greater flow across aquitards. Flow through preferential flow paths can contribute considerably to the propagation of drawdown in aquifers overlying pumped aquifers. While transport of solutes through continuous aquitards is generally slow (as it is dominated by diffusion), the presence and characteristics of preferential flow paths will be a major factor in determining inter-aquifer transport of solutes, although retardation may help to slow this transport.

3 Measurement and modelling of aquifer connectivity

3.1 Introduction

There is no single method by which aquifer connectivity can be measured or modelled. Rather, the hydraulic characterisation of the subsurface is done through measurement of properties on various time and spatial scales, from core samples in the laboratory to large scale field tests. Together these tests provide valuable and necessary information for the construction of models which may be used as predictive tools or for hypothesis testing. Additional measurements will reduce uncertainty in the predictions, but will never be able to eliminate the uncertainty. A multi-facetted approach to data collection and modelling allows those involved to build an understanding of the groundwater system of interest, target specific questions or objectives and guide the decision making process.

In a 2010 state-of-the-science report entitled *Management and Effects of Coalbed Methane Produced Water in the Western United States* (NRC 2010), the National Research Council (NRC) identified the measurement of surface water and groundwater connectivity as a major data gap and uncertainty. Geochemical, geological, geophysical, hydrological and other data are identified as key components in the necessary scientific evaluation and prediction of subsurface and subsurface-surface connectivity (NRC 2010). Riese et al. (2005) was identified by the NRC (2010) as the only study to date that sufficiently addresses connectivity with this sort of comprehensive dataset and interpretation. The NRC (2010) state that what is lacking in current practice is the testing of numerical hydrologic simulation outputs with real data (such as using age tracers to evaluate travel time predictions). They conclude that:

> *'…the ability to place more reliance in the future on outputs of models that more closely resemble natural complexities of the hydraulic conditions of [coalbed methane] basins necessitates demonstrating better convergence between existing model results and data collected and analysed from the basins.'*
>
>

The first half of this chapter will be a review of the techniques used for measuring aquifer connectivity and the second half will cover the modelling process.

3.2 Measurement

3.2.1 Aims of measurement

Before any hydrogeological investigation is undertaken, it is necessary for the parties involved (i.e. consultants, scientists, stakeholders, clients) to carefully define the problem being studied, set the objectives and determine the best type of information needed to obtain the desired end product. Every investigation is site specific and the methods used should therefore be tailored accordingly.

These decisions may be guided by the value of information (VOI) approach to reducing uncertainty in engineering solutions. In hydrogeology, for example, all predictions, such as groundwater flow rates, impact of pumping and injection, and solute transport are associated with uncertainties that arise from uncertain subsurface conditions. The VOI approach is

based on the expected decline in prediction uncertainty that may result from additional information and the associated increase in the value of a decision (Small 2004). The acceptable level of uncertainty associated with a project should be made in the planning stages of an investigation. This will lead to a choice of measurements that best suit the project objectives. It will define the regional extent of the investigation, the resolution of the data and frequency of sampling.

This also implies that hydraulic properties measured or inferred in previous projects and studies with different objectives need to be examined carefully to make sure that the values are representative and useable in the current study. Furthermore, noting the uncertainty associated with measurements, more robust interpretations and predictions will be possible when combining different types of measurements.

The following sections will describe the methods available for the measurement of hydrogeological parameters. Each section will address the scale associated with measurement type, and discuss how they can be used in interpreting aquifer connectivity.

3.2.2 Hydraulic methods

Hydraulic methods are those which are conducted in the field and record changes to hydraulic head as a result of natural or artificial stresses applied to a groundwater system. From the data collected in the field, mathematical methods may be used to estimate hydrogeological parameters, including hydraulic conductivity, storativity and leakage from adjacent aquitards. The quantification of these parameters, which cannot be measured directly, is an estimate whose accuracy depends on the methods used and the interpretation (Kresic 2007). There are three main field methods which can be used:

- single well tests, where a stress is applied to and response is recorded in the same well
- multiple well tests, where a stress is applied to one well and the response is recorded at one or more observation wells
- passive tests, where the response to natural stresses (e.g. barometric pressure, earth tides, seasonal water level fluctuations) can be recorded at multiple wells.

For the purposes of this review, the term ‘borehole’ refers to the drilled hole and the term ‘well’ refers to completed boreholes (e.g. casing, screen).

The simplest type of single well tests is the slug test, where an instantaneous change in hydraulic head is applied to a well. There are two types of slug tests:

- ‘rising head’, where a volume of water is removed from the well and the head recovery is recorded
- ‘falling head’, where a volume of water is added to the well and the head decline back to normal is recorded.

It is also common to achieve the change in hydraulic head by using a physical slug – a solid cylinder that can be lowered into the well, which causes a rapid change in hydraulic head. Air-pressurisation of a well can also be used to perform a slug test, where the increased pressure causes the water level to fall and when the pressure is released, the rising water level is recoded (Kresic 2007). Each of these methods is associated with difficulties in making the change instantaneous and recording sufficient data. Pressure transducers, which automatically record changes in water levels, are the most accurate method to monitor these tests. Slug tests are limited in their area of impact, testing only a small part of the aquifer around a borehole, and typically only provide information on hydraulic conductivity. This

being the case, these tests are more susceptible to borehole impacts caused during drilling, called skin effects. Drilling can either increase permeability (negative skin) or decrease permeability (positive skin) in the material immediately adjacent to a borehole. Slug tests can be interpreted using a number of mathematical methods which can account for the aquifer conditions (confined, unconfined), borehole skin effects and well type (screen partly or fully penetrating the aquifer) (Fetter 2001).

Single well pumping tests, which involve pumping water from a well at a constant or variable rate and monitoring the head decline and subsequent recovery in the pumped well, can be used to determine hydraulic properties. The nature of the test is longer than a slug tests and therefore impacts a larger area of the aquifer providing more representative estimates of aquifer properties. As with slug tests, mathematical methods are available to interpret the results of single well pumping tests under various conditions and can be used to identify leakage from aquitards (Fetter 2001). A variant to the single well pumping test is the constant head test where a chosen head decline is maintained by adjusting the pumping rate and this information is used to determine hydraulic properties.

Both slug tests and pumping tests, which can be performed on completed wells, can also be performed on discrete intervals of a well screen using inflatable packers. These utilise inflatable bladders to expand the packers against the sides of a borehole or well casing in order to isolate a smaller section of the hole for investigation. This allows the collection of discrete vertical data on hydraulic properties.

Single well testing methods have also been developed by the petroleum industry for determining the hydraulic properties of a geological formation during or immediately following drilling. Drill stem tests (DST) are conducted with the drilling equipment still in the hole and utilise a packer system to isolate a particular interval. The typical test sequence includes a short flow period allowing water and hydrocarbons to flow from the interval into the drill string, followed by a shut in period, which stops the flow and allows the interval to recover its original pressure. This is followed by a second, longer flow and shut in period that is comparable to a pumping and recovery test (SWS 2012). This second flow and shut in period is used to determine hydraulic properties. Flow rate testers (FRT) are another method used to obtain hydraulic properties following drilling. FRTs can be combined with geophysical logging tools (Section 3.2.5) and, similar to DSTs, can test isolated sections between inflatable packers. Results of these tests are usually used to identify high productivity zones and their thicknesses.

Single well tests are useful for obtaining hydraulic properties near the borehole (slug test) of discrete zones (DST, FRT) and for larger areas using pumping tests. These properties can be used to identify higher permeability zones that may contribute to intra-aquifer connectivity. The pumping tests, in particular, can provide information on leakage from aquitards, of interest for the interpretation of inter-aquifer connectivity as a leaky aquitard may indicate connectivity with an overlying/underlying aquifer.

Multiple well tests are those where water is pumped from one well and hydraulic head is recorded in the pumped well and one or more observation wells. These types of tests can provide more information than single well tests; in particular, they can estimate both hydraulic conductivity and storage averaged over a large aquifer volume and they can identify anisotropies in the properties. The volume being tested will depend on the distribution of observation wells and the duration of pumping. If observations are made in the overlying/underlying aquitard and aquifer (Figure 7) then possible leakage from the aquitard/aquifer to the tested aquifer may be assessed and the hydraulic properties of the aquitard may be estimated. As with single well tests, a number of mathematical methods are available for interpreting multiple well tests (Fetter 2001). Multi-well tests can be some of the

most expensive and time consuming field tests in hydrogeology; however, they can provide the most beneficial information for the identification of aquifer connectivity. Medeiros et al. (2010) used pumping tests to assess the hydraulic connectivity across low-permeability deformation bands in north-east Brazil. Well locations were selected such that the damage zone separated the pumping well from the observation wells and showed considerable connectivity across the low-permeability zones.

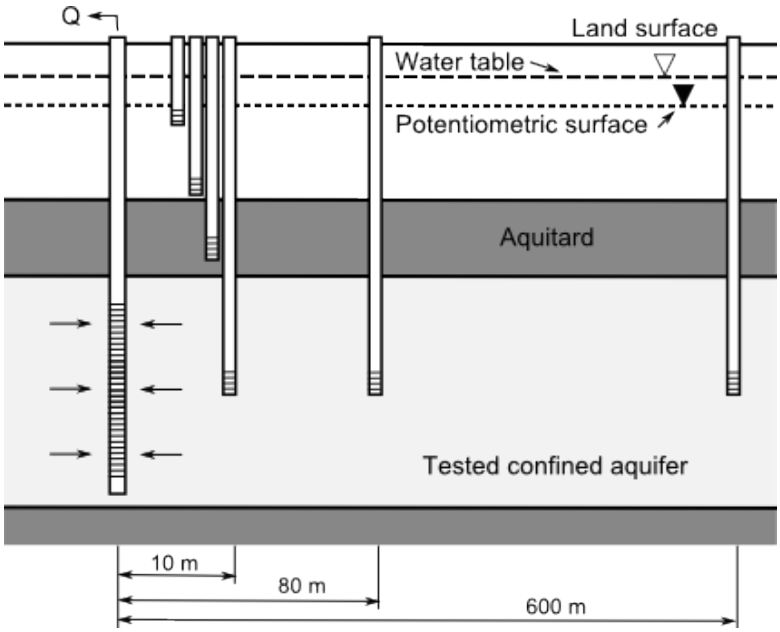

Figure 7 Pumping test example designed to determine characteristics of the tested aquifer, nature of the aquitard and possible leakage from the aquitard and overlying unconfined aquifer (© Copyright, Kresic 2007). *Q* is the flow rate of pumped water; the potentiometric surface is the surface representative of the level to which water will rise in a well cased in a confined aquifer and the water table is the water surface in unconfined aquifer.

Measuring water levels in wells is not the only method by which a hydraulic response to a stress can be monitored in the subsurface. Vibrating wire piezometers (VWP), which can measure in situ pore pressures, may be installed in a borehole and surrounded by sand, topped by a seal (bentonite) and backfilled to surface with cement. It is also possible, in soft sediments, to install these piezometers by directly pushing them into the ground. Work by Mikkelsen and Green (2003) and Contreras et al. (2007) has recommended the use of fully-grouted piezometers without the sand pack. This method of installation, which uses a bentonite and cement mixture to seal the borehole, is easier and faster. Contreras et al. (2007) tested six cement-bentonite grout mixes with different permeabilities and found that the permeability of the grout can be up to three orders of magnitude higher than the geological material without causing significant errors in the pressure measurements. Smerdon et al. (2012) used VWP to estimate the hydraulic properties of an aquitard sequence in the western margin of the GAB. They found good agreement between estimates of hydraulic conductivity and storativity determined through numerical analysis of pore pressure data and estimates inferred from environmental tracer data.

A variant of the multi-well test is the pulse interference test, where a cyclic injection of fluid is applied to one well, often in a packer isolated interval. This causes a pressure pulse (higher hydraulic head) to propagate into the subsurface and is subsequently measured at nearby wells. The propagation of the pressure pulse is highly sensitive to the hydraulic properties

between the pulsed well and the observation well. Brauchler et al. (2010) used cross-hole slug interference tests to obtain a high resolution characterisation of aquifer heterogeneity between 16 closely spaced wells.

The analysis of aquifer pumping tests can be carried out using a number of mathematical methods. The most basic methods make a series of simplifying assumptions and are only applicable to confined and homogeneous aquifers. As this is not often the case in the real world, more complex methods can account for the presence of unconfined aquifers, aquifer anisotropy, partially or fully penetrating wells, large borehole diameter, borehole skin effects and leaky aquitards. Aquifers often receive some amount of recharge from overlying or underlying aquitard units. This leakage can increase during pumping as a result of the increased hydraulic gradient between the pumped aquifer and adjacent aquitards. Over time, and as the radius of well influence increases, the volume of leakage from the aquitard may balance the pumping rate, causing the radius of influence to stop expanding (Kresic 2007).

Hantush and Jacob (1955) developed an equation that describes the flow of water towards a well in a leaky confined aquifer separated by an aquitard from an unconfined aquifer. The Hantush and Jacob solution assumes that there is no drawdown in the unconfined aquifer and that there is no water released from storage in the aquitard. Hantush (1960) later modified the solution to include storage effects in the aquitard and Neuman and Witherspoon (1969a; 1969b) presented a solution that includes both the release of storage in the aquitard and the drawdown of head in the unpumped aquifer (Freeze & Cherry 1979). For a detailed description of available mathematical methods, see Kresic (2007), Fetter (2001) or Freeze and Cherry (1979). The results of a pumping test can often be simulated equally well with different mathematical models, yielding different estimates of hydraulic properties. It is therefore essential to independently verify the assumptions and boundary conditions when interpreting pumping tests.

Passive methods for the determination of hydraulic properties of a groundwater system can also be used. In these cases, some stress that occurs naturally is recorded and the response to this stress in the subsurface is measured. Keller at el. (1989) first described a method by which the downward propagation of seasonal water level fluctuations could be used to obtain a bulk hydraulic conductivity value for a low-permeability clayey unit. Earth tides and barometric pressure changes, which are known to cause water-level fluctuations in aquifers, can be used to estimate the hydraulic properties of aquitards (Timms & Acworth 2005; van der Kamp & Gale 1983) and assess connectivity between wells (Butler et al. 2011; Burbey & Zhang 2010). These methods can be less labour intensive and less costly than the more involved field testing methods.

Potentiometric surface (or water table) mapping presents another passive method by which aquifer connectivity may be assessed. Water level information (hydraulic head) is obtained from wells screened in the aquifer of interest only. Potentiometric surface maps and water table maps can be shown as contour maps of equal water elevation. Groundwater flows from higher hydraulic head to lower hydraulic head, along the hydraulic gradient. Sudden changes in the contours, either an increase or decrease, may indicate connectivity with an overlying/underlying aquifer that has a different hydraulic head from the one being observed, as is illustrated in Figure 2.

As with all scientific methods, there are limitations associated with these hydraulic testing methods. The mathematical methods that are commonly applied to the interpretation of these tests have to make a series of simplifying assumptions. These introduce some uncertainty into the interpretation of the data. The volume of material being tested varies depending on the test (near borehole for single well slug tests to larger volumes for large-scale pumping tests), and may limit the usability of the data. There is also a well-known limitation, and

knowledge gap, associated with using field-scale tests to represent regional scale aquifer or aquitard properties (see section 3.2.3). The processes that are important on the small scale may not be important at the large scale, and processes that are important at the large scale, such as the presence of preferential flow paths (e.g. fracture, faults), may not be observed in the small scale measurements. The use of hydraulic methods in combination with other methods (e.g. geophysics, geochemical) together can provide better estimates of regional processes.

3.2.3 Laboratory methods

Laboratory methods may be used to determine the hydraulic properties of an aquifer or aquitard sample. They are conducted on small samples, often collected during drilling, and thus represent point values. The value of hydraulic conductivity from such samples may be obtained from permeameter tests. Permeameters have a chamber that holds the sample, which can vary from unconsolidated sediments to rock cores. Constant-head permeameter tests are applied to unconsolidated samples with moderate to high permeability. In these tests, a chamber provides a supply of water at a constant head (level of water does not change in the chamber) and water moves through the sample at a steady rate (Figure 8). The hydraulic conductivity (*K* in L/T) is calculated from a modified version of Darcy's law:

$$K = \frac{VL}{Ath}$$

where *V* (L^3) is the volume of water discharged in time *t* (T), *L* is the length of the sample (L), *A* is the cross-sectional area of the sample (L^2) and *h* is the hydraulic head (L) (Fetter 2001).

Falling-head permeameter tests are applied to samples with low permeability. In this test, a tube with an initial water level, h_o, is attached to the permeameter (Figure 8). After a period of time (usually days to hours) the water level is again measured, *h*, and the hydraulic conductivity (*K* in L/T) is calculated from the following:

$$\mathrm{K} = \frac{d_t^2 L}{d_c^2 t} ln\left(\frac{h_0}{h}\right)$$

where *L* is the sample length (L), *t* is the time for head to go from h_o to *h* (T), d_t is the inside diameter of the falling-head tube (L), and d_c is the inside diameter of the sample chamber (L) (Fetter 2001).

Air permeameter tests can be used on both consolidated sediments and rock samples. They measure the permeability of the sample by forcing a gas through the sample and monitoring the pressures and flow rate (ASTM 2001). This is used to calculate permeability to air (*k* in L^2; see section 2.2.1 for relationship to hydraulic conductivity) using a modification of Darcy's law:

$$k = \frac{(2Q_e P_e \mu L)}{(P_i^2 - P_e^2)A}$$

where Q_e is the exit flow rate (L^3/T), P_i and P_e are the entrance and exit pressures, respectively (M/LT^2), *L* is the length of the sample (L), *A* is the cross-sectional area (L^2), and μ is the viscosity of the air (M/LT). The permeability of a sample to air, or other gas, will result in a significant overestimation in comparison to estimates of water permeability (Klinkenberg 1941). Although permeability is a function of the porous material and is independent of fluid properties, gas slippage at pore walls allows for more gas flow as compared to liquid flow. In addition, the permeability to gas flow is related to the pressure with the largest impact occurring at low pressures and the least impact at high pressures. Called the Klinkenberg

effect, corrections can be made and laboratories often report ‘air permeability’ and ‘Klinkenberg corrected permeability’ or ‘equivalent liquid permeability’.

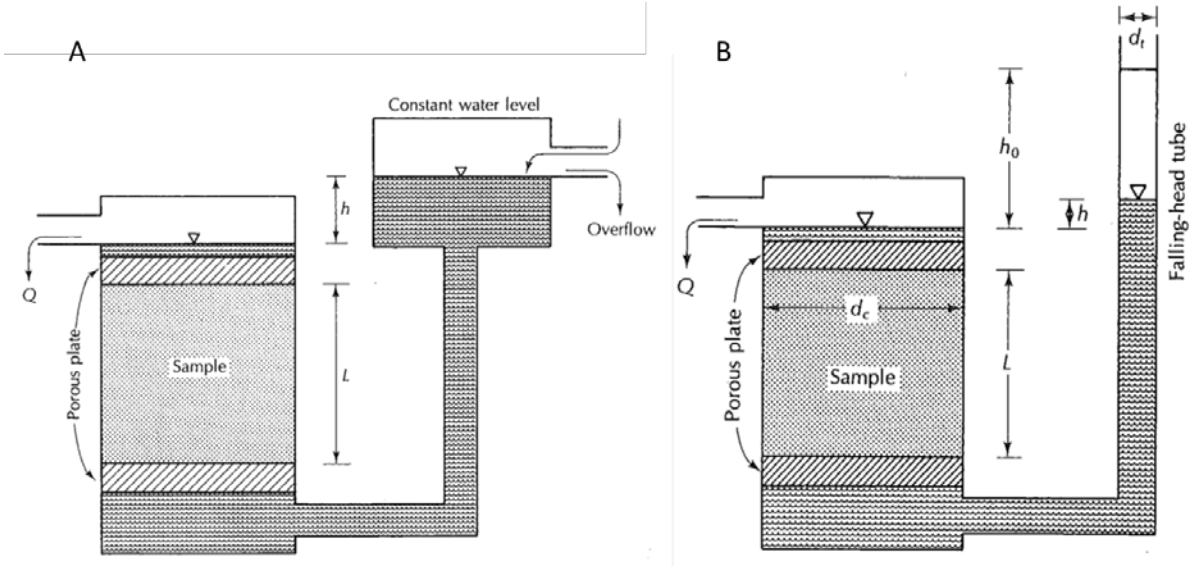

Figure 8 (A) Constant-head permeameter test and (B) falling-head permeameter test (© Copyright, Fetter 2001).

The accuracy of laboratory permeameter tests can be increased by conducting the experiments under in situ effective stresses. Effective stress is the total stress (caused by the thickness of overburden) minus the pore water pressure at a particular depth in the subsurface. Wright et al. (2002) adapted a triaxial cell, an apparatus that applies stress to a core in three dimensions and is able to subject a sample to its original in situ stresses, to measure the real hydraulic conductivity of a sample. Permeameter tests that are not conducted at in situ stresses will provide estimates of hydraulic conductivity that are too high. In addition, the drilling process can create microfractures, which may increase hydraulic conductivity, that close again when the sample is returned to its in situ stresses (Wright et al. 2002).

A further development to laboratory testing for hydraulic conductivity comes from the use of centrifuges. A centrifuge permeameter uses accelerated gravity (gravity rates many time higher than normal) to drive fluid flow through low-permeability samples. This process allows the simulation of flow over thousands of years in a much shorter timeframe (weeks to months). This advance is significant as it allows research to be conducted on very low-permeability aquitards that is not otherwise achievable on human time-scales (Timms & Hendry 2008).

Centrifuge and pressure pulse permeameters and triaxial cell apparatus are capable of measuring permeability at in situ pressure (Bouzalakos et al. 2013). These techniques (Timms et al. 2012) have been used in academic practice for many years (Nimmo & Mello 1991) and can now be routinely used by government organisations and the CSG industry in Australia (CWI 2013).

Other methods that have been developed to estimate the hydraulic permeability of porous media include high resolution X-ray tomography and mercury injection porosimetry.

Piller et al. (2009) describe a method where X-ray tomography can be used to digitally reconstruct the 3D porous system of a small sample of reservoir rock, either from drill cuttings or side wall fragments, and used to simulate pore-scale flow. The methodology developed by Piller et al. (2009) allows for the identification of the principal components and direction of hydraulic permeability for the sample. Scanning electron microscopes (SEM) can be used to image pore spaces down to the nano-scale (1 µm to 1 nm), and allow the visualisation of microstructures in fine-grained rocks such as shales (Josh et al. 2012). Mercury injection porosimetry is a standard method used in the petroleum industry to evaluate the lithologies of reservoirs and low permeability seals (aquitards). The pore volume of a sample is measured by forcing mercury into the pore spaces at increasing pressures, up to ~413 MPa (mega pascal) and can be related to sample permeability through a number of models (Olson & Grigg 2008).

Hydraulic properties that are measured in the laboratory are useful at obtaining point values, but are less suitable for characterising in situ conditions where fractures and other forms of heterogeneity exist. These heterogeneities are likely to significantly change the hydraulic conductivity measured from a core sample as compared to that occurring on a larger scale (van der Kamp 2001). It is thus important to use these methods in combination with field techniques, and even modelling, to determine if such heterogeneities exist.

Keller et al. (1988) compared the results from field (slug) tests and laboratory (falling-head permeameter) tests and found that the field determined values of hydraulic conductivity for a till in Saskatchewan, Canada, are several orders of magnitude higher than the laboratory values due to the presence of interconnected fractures. Hart et al. (2006) compared laboratory measurements of vertical hydraulic conductivity on core samples of a regional shale aquitard in Wisconsin, USA with the values of vertical hydraulic conductivity for the same unit in a regional scale numerical groundwater flow model. Calibration of their hydraulic heads in the numerical model required the vertical hydraulic conductivity (Kv) of the same shale aquitard to be higher by up to three orders of magnitude than the values estimated in the laboratory. This was attributed to the failure of the core samples to include the effects of preferential pathways present at larger scales on increasing the bulk permeability (cross-cutting fractures or even wells constructed through the shale). Bredehoeft et al. (1983) noted the same order of difference between in situ and laboratory tests with regional numerical model estimates of permeability in the shale confining layer overlying the Dakota Sandstone aquifer because of the same scale-of-measurement issues. A limitation to resolving the hydraulic properties of aquitards using regional-scale numerical models is that the resolution is inadequate for identifying the discrete features that cause this discrepancy (Feinstein et al. 2005; Neuzil 1986). In a review of hydraulic data from published studies conducted in low permeability units around the world, Neuzil (1994) concludes that permeability is not always scale dependent and that values of permeability may sometimes be lower than what is typically assumed. Chen (2000) noted that streambed hydraulic conductivity and anisotropy along or across a river channel indicated that Kh is about three to four times larges than Kv.

It is common practice for most consultants to use the results of small scale tests (e.g. laboratory tests; DSTs) as the formation-scale value of Kv for their models. Although in some cases this may be appropriate, in many cases it ignores the possible impact of preferential pathways on regional values of Kv. The end result is that these models under-predict the potential impacts of long-term pumping. There is a need for better estimates of regional Kv that account for varying hydraulic properties through upscaling and regionalisation methods. Combined with detailed borehole data, geological/geophysical models, laboratory and point scale field measurements can be used to transform data and obtain better estimates of the potential variability and uncertainty in permeability at a regional scale. This knowledge of parameter uncertainty and variability can then be considered in model uncertainty analysis.

3.2.4 Surface observations

One of the limitations to the measurement of aquifer connectivity arises from the inability to directly observe the subsurface other than at discrete points/lines (e.g. boreholes). In some cases, the aquifers and aquitards of interest may be directly observable at surface where they outcrop and along quarry walls or in the subsurface in mines. In these cases it is possible to make observations on the lithology, stratigraphy, structure, thickness and continuity of the geological material at a larger scale.

Lithology is the physical makeup of the sediments or rocks and includes the mineral composition, grain size, texture and packing. Lithology is what determines how permeable a particular unit is to groundwater flow. For example, a clay unit will be much less permeable to flow than a sand or gravel layer. Stratigraphy is the geometry and age relationship of the geologic material. It is this relationship between layers of differing lithology that give rise to layered systems of aquifers and aquitards. Structure refers to features such as fractures, faults and folds that can disturb the original stratigraphy. This is particularly important in a hydrogeological context, as structures can form barriers to flow or enhance flow. A clay unit, for example, with very low primary permeability (that based on the material properties) that is fractured, can have significant secondary permeability (that which is associated with fracture flow). A clay aquitard with fracture permeability can significantly increase inter-aquifer connectivity (section 2.3.2). Thickness and continuity refer to the measured thickness of a unit and whether it is continuous in the subsurface (does not thin or pinch out).

The biggest limitation associated with the direct observation of the geological units of interest is that they need to outcrop at surface or have been mined into at depth. As with the other measurement techniques, it is difficult to up-scale from outcrop scale observations to regional properties. In particular, observations at the surface may not extend into the subsurface. Fractures observed in outcrop may or may not occur in the subsurface, or may not be hydraulically active (carry water). The size and spacing of fractures typically decreases with depth as stresses increase, making it nearly impossible to estimate the likelihood of active fractures in the subsurface based on outcrop observations alone. It is, however, possible to extend surface observations into the subsurface by applying these techniques to core samples obtained from drilling. In the absence of surface observations, core samples are the only source of direct observation but are limited by the small scale of the sample.

3.2.5 Geophysical methods

Geophysical methods can be used to indirectly measure the nature of subsurface geological materials. It may be possible to determine the depth to the water table, salinity, location of subsurface faults, depth to basement, thickness and extent of various subsurface bodies (e.g. clay lenses, gravel beds). A contrast in physical properties is essential for geophysics to work successfully. These investigations may be carried out above the land surface (airborne), on the land surface (ground) or within the subsurface via wells and boreholes.

The most common airborne geophysical methods, electromagnetics, radiometrics and magnetics, can be used in geological mapping, mineral exploration and groundwater surveys. Increasingly, airborne electromagnetic (AEM) methods are applied in large-scale groundwater investigations, where the measured electrical conductivity of the ground can provide aquifer information (Siemon et al. 2011). This is based on the dependency of electrical conductivity on groundwater salinity and clay content of the subsurface, which can be used to interpret changes in water quality (salinity) and aquifer structure (Siemon et al. 2009). AEM surveys may be carried out by airplane or helicopter at survey specific heights and line spacing. The aircraft produces an electromagnetic field that penetrates the ground,

which induces a current in conductive materials. This then induces a secondary electromagnetic field which is measured by a receiver pulled behind the aircraft and subsequently converted to a three-dimensional map (Dent 2007). In order to make use of AEM data, it is necessary to have real measurements of conductivity from the subsurface (boreholes) against which the survey results can be calibrated (Mullen et al. 2007). The investigation depth of AEM surveys for groundwater exploration ranges from a few tens of metres in conductive ground to several hundred metres in resistive ground (Siemon et al. 2009). AEM methods are an efficient and inexpensive way to map large areas, but because the depth of investigation is limited to a few hundred metres the application of the method to deep aquifer connectivity is more limited. It may be used for cross-referencing with other geophysical methods and, in combination with other hydrogeological methods, to infer aquifer connectivity based on salinity distribution, for the identification of flow pathways, and for the partial validation of models.

Radiometrics, or airborne gamma-ray spectrometry, which measures the gamma-rays naturally emitted from rocks and weathered material at the surface, is limited to the top 30 cm of the ground surface (Wilford 2002) and is therefore not useful in interpreting aquifer connectivity.

Airborne magnetic methods rely on the anomalies that magnetic materials in the crust create in the earth's magnetic field. Sedimentary rocks are typically non-magnetic, so this method is most useful at determining the depth to basement rocks (Fetter 2001). The magnetic field is measured using a total field magnetometer, which can be mounted on an airplane or helicopter. It is also possible to obtain magnetic data at ground surface (Brodie 2002). In hydrogeology, this can be very useful at determining the bottom of a sedimentary aquifer or aquitard. Although this may not directly provide information on aquifer connectivity, this type of information helps formulate a more complete picture of the hydrogeological system of interest.

Surface geophysical methods available include electrical resistivity, electromagnetic, seismic, radar and gravity. Many of these geophysical methods involve introducing some perturbation into the subsurface and measuring the response. In electrical resistivity surveys, a direct current is introduced into the ground by two metal electrodes and the resulting voltage in the ground is measured between two additional electrodes at some distance away. It is possible to calculate the resistivity of earth materials between the electrodes based on the known current flowing through the ground and the voltage difference between the electrodes. The depth of investigation depends on the spacing of the two pairs of electrodes, the wider apart, the deeper the profile. The wide range in resistivity of earth materials (10^{-6} Ω.m for graphite to 10^{12} Ω.m for quartzite) makes it possible to identify changes in material and the variable resistivity of water (saline water is less resistive than fresh) make it possible to identify areas of fresh versus saline water (Fetter 2001). This is a cost-effective and relatively easy way of obtaining detailed geological information from the subsurface.

In electromagnetic methods a magnetic field is generated by a transmitter coil, which induces an electrical field in the earth that is subsequently measured by a passive coil. The conductivity of the ground will impact the strength with which the electrical field moves through the ground. The depth of investigation depends on the type of electromagnetic method used and varies from less than 10 m to a couple hundred metres (Fetter 2001).

Seismic methods employ an artificially produced seismic wave that may be used to determine the depth to bedrock, depth to the water table, general lithology, structural and formation boundaries. The energy source used to produce the seismic wave may vary from a sledgehammer struck on a steel plate on the ground surface, good for shallow investigations less than 15 m, to explosives that are used for investigation depths greater than 30 m. The

arrival time of the seismic wave back at surface is recorded by a line of geophones extending away from the source and recorded by a seismograph. The arrival time of the seismic wave at different distances from the source can detect the depth to various features (Fetter 2001). The investigation depth depends on the purpose of the study and the setup of the seismic survey and may focus on near-surface structures or can penetrate many hundreds of metres (Drummond 2002).

Radar methods, typically called ground penetrating radar (GPR), use repetitive pulses of electromagnetic waves transmitted into the ground at frequencies ranging from 10 to 1000 MHz. Interfaces between differing materials will cause the waves to be reflected back to surface and can be used to interpret changes in strata, depth to the water table, detect voids and cavities. The GPR system is pulled along the surface of the ground and it has antennae that both send out the signal and receive the reflected pulse. Lower frequency waves can penetrate deeper into the subsurface but at the cost of lower resolution, and higher frequency waves do not go as deep but with higher resolution, with a maximum investigation of tens of metres (Griffin & Pippett 2002). GPR is valued for its ability to produce a continuous profile of the subsurface (Fetter 2001). GPR is useful for shallow alluvium, shallow bedrock and water table imaging.

Gravity surveys are the most passive of the surface geophysical methods. They measure changes in the gravitational attraction of the earth caused by local variations in the density of the rock beneath the measurement point. Gravity measurements must be corrected for latitude, elevation, topography and tidal effects. The results, provided a strong density contrast exists, may be useful at determining the depth to bedrock and identifying subsurface features such as old river channels (Tracy & Direen 2002; Fetter 2001).

Finally, subsurface geophysical methods, generally called geophysical downhole logging, are useful in groundwater investigations because they can delineate aquifers and producing zones (high porosity and permeability). In geophysical logging the geological material surrounding a borehole can be characterised by measuring a variety of physical properties that provide information on the composition, chemistry, variability and physical properties of the material (Chopra et al. 2002). As with the measurement of hydraulic properties in boreholes, geophysical logging results are impacted by the process of drilling, which disturbs the natural environment. It is common for several complementary geophysical logs to be run together. The probes are lowered into the borehole on a cable which conveys signals from the probe back up to surface where the logging information is recorded and provide a continuous depth profile of physical properties (Fetter 2001). A summary of basic information for the most commonly used logs in hydrogeology are presented in Table 4.

Geophysical logs can be used to document the lithology of the strata and correlate it between neighbouring boreholes. They can be used to estimate hydrogeological parameters from the measured geophysical parameters (e.g. clay content, saturation, porosity) and observe geotechnical features (e.g. bedding planes, fractures). They can estimate water flux, identify saline water in the surrounding rock and measure other physico-chemical parameters of groundwater. Certain log types can also be used to calibrate airborne or surface geophysical methods (BurVal Working Group 2006). The depth of investigation into the surrounding rock is variable but typically represents the near-hole environment. The vertical depth of inspection is limited by the length of the cable supporting the probes and can go more than 1000 m deep.

Geophysical methods can be a powerful tool in hydrogeological investigations. In the context of aquifer connectivity, various methods can provide information on lithology, stratigraphy, and structure (e.g. bedrock, fractures and faults) all of which may inform an interpretation of connectivity. Information on salinity may be particularly useful - for example, a borehole

induction log that can be used to interpret groundwater salinity might be able to show vastly different salinities between two aquifers separated by an aquitard, indicating little connectivity. Conversely, if similar salinities are found, this could point to higher connectivity.

Limitations associated with all geophysical methods are the difficulties associated with interpretation. Some of the methods require complicated mathematical procedures to convert the data into useable format. In many cases, particularly for airborne or surface methods, there is little to no 'ground truthing' available to confirm interpretations. This is less of a problem with well logging where a lithological log may be produced from core or drill cuttings during drilling. Even if a feature that could increase connectivity is identified (e.g. fault, fracture), it is difficult to determine whether or not it is actually increasing the potential connectivity.

While airborne and surface geophysical methods can cover relatively large areas at low cost, subsurface methods are limited by the number of boreholes that can be drilled and require interpolation of properties between observations.

3.2.6 Geochemical methods

Geochemical methods involve sampling and analysing the groundwater for various chemical constituents and using this information to infer hydraulic properties (e.g. hydraulic conductivity) and fluxes (e.g. groundwater velocity) and interpret aquifer connectivity. These methods generally fall into one of two categories: artificial and environmental tracers. The scale of investigation varies between the two methods, where artificial tracers may be used to characterise local to intermediate connectivity on the order of tens to hundreds of metres, environmental tracers can be used to characterise regional connectivity.

Artificial tracer tests involve introducing a known tracer quantity into the subsurface and observing its arrival at other points in the flow field. Many types of tracers may be used, from a variety of salts (e.g. Cl^-, Br^-), fluorescent and non-fluorescent dyes, stable isotopes (e.g. ^2H), radioactive tracers (e.g. ^3H) and microparticles. In most cases, the chosen tracers are conservative, meaning they do not interact with the subsurface material. There are two main types of artificial tracer tests, those conducted under natural gradient conditions and those where a forced gradient is imposed. With natural gradient tests the tracer is injected at very low rates, such that the natural flow field is not disrupted. The main drawbacks to this type of test is that it can take a long time for a tracer to move through the subsurface under natural conditions and because of heterogeneity, many observation points may be needed to intercept the tracer. An alternative form of the natural tracer test is the point dilution tests, where a tracer is quickly injected into a borehole and the decrease in tracer concentration due to groundwater flow is recorded in the injection well. This type of test only provides information on the formation near the well screen (Freeze & Cherry 1979).

Forced gradient tracer tests involve actively disrupting the natural flow field. This can be done in a number of ways. Single borehole tests involve injecting water with a known concentration of tracer into a well for a given amount of time and then reversing the flow and pumping water back out again. Multiple borehole tests include divergent, convergent and injection-withdrawal tests (Figure 9 (Novakowski et al. 2006)):

- divergent tracer tests involve injecting water with a tracer into a borehole and measuring the concentration as it reaches an observation borehole(s)
- convergent tracer tests involve introducing a tracer into one or more boreholes and measuring the concentration of the tracer in another, continuously pumped, borehole
- injection-withdrawal tests use a pair of boreholes to establish a flow field between them

and then the tracer is injected into one borehole and monitored at the other.

These types of multiple borehole tests have been used extensively in research associated with the disposal of nuclear waste in Sweden. Löfgren et al. (2007) provide a comprehensive review of field tracer tests conducted at Swedish research sites from 1977 to 2007. Nordqvist et al. (2012) used large-scale (several hundred metres) multi-borehole tracer experiments to verify hydraulic connectivity that had been identified using geologic and hydraulic investigations at two sites in Sweden.

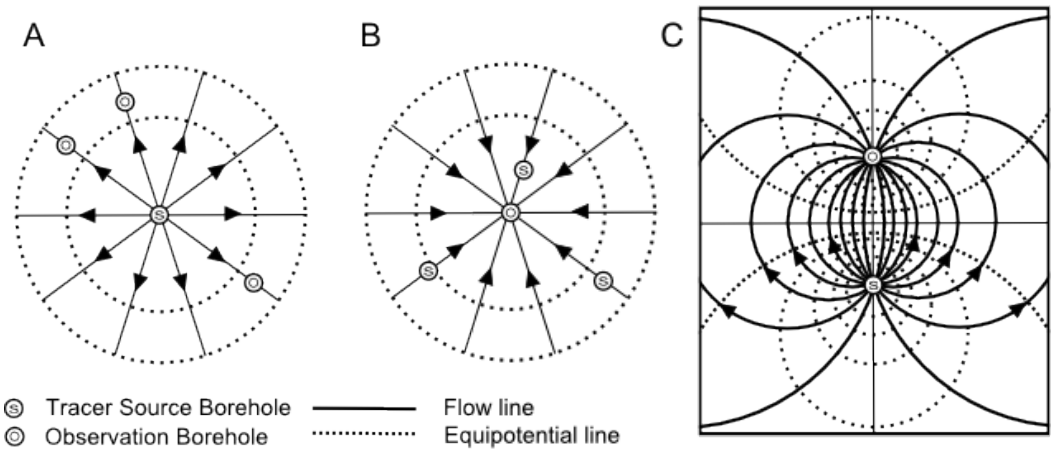

Figure 9 Plan view of flow field for a (A) divergent tracer test, (B) convergent tracer test and (C) injection-withdrawal tracer test (© Copyright, Novakowski et al. 2006). Equipotential lines are lines of equal hydraulic head.

Environmental tracers are chemicals that are already present in the subsurface. The spatial and/or temporal variability of their concentrations in groundwater is often used to determine source areas, mechanisms and rates of groundwater recharge, to estimate groundwater fluxes within and between aquifers and to provide insight to the mean residence time (or 'apparent age') of groundwater (Cook & Böhlke 2000).

Environmental tracers can provide useful insights into aquifer connectivity. For example, the profile of environmental tracers across an aquifer-aquitard-aquifer sequence can provide information on the large-scale and long-term transport behaviour across the formations. Mazurek et al. (2011) used a series of tracer profiles from nine sites in central Europe to show that transport times across a clay-rich aquitard ranged from several thousand to millions of years. Environmental tracers can be either naturally occurring or the result of some anthropogenic input, such as nuclear bomb testing, and include: radioactive tracers, accumulating tracers, event markers, stable isotopes and chemical tracers.

Table 4 Summary of geophysical logging methods used in hydrogeology. Modified from © Copyright, BurVal Working Group (2006) and *Kenyon et al. 1995.

Type	Specific log(s)	Methods	Depth of investigation	Borehole conditions	Information
Physical	Caliper	One to four arms with springs to hold ends against borehole walls	Surface	Open and cased holes with or without fluid	Borehole diameter
Acoustic	Sonic	Determine velocity of sound in rock using ultrasound generators and receivers	1-2 cm	Open holes with fluid	Lithology (porosity)
Electrical	Self-potential (SP) Resistivity	SP measures natural electrical potential between surface and borehole Constant current introduced by two electrodes; the potential measured between two other electrodes is proportional to resistivity	Up to 10 cm	Open holes with fluid	Lithology, calibration of surface geophysics, location of PVC screens
Electro-magnetic	Induction Susceptibility	Transmitter coil generates alternating magnetic field, which induces electrical eddy currents that are proportional to rock conductivity	60-350 cm	Open and PVC cased holes with or without fluid	Lithology, saline water
Nuclear	Gamma-ray Spectral gamma-ray Gamma-gamma (density) Neutron-neutron (porosity) Nuclear-magnetic-resonance*	Measures the natural gamma radiation emitted Measures the scattering of gamma or neutron between source and receptor on probe Measures the response of nuclei to a magnetic field	15-20 cm 5-10 cm 10-100 cm	Open and cased holes with or without fluid Open holes with fluid	Lithology, density, porosity, calibration of surface geophysics Porosity and permeability
Optical	Borehole camera Optical borehole televiewer	Obtain video images of borehole	Surface	Open and cased holes without water or with clear water	Casing or borehole condition, caving, slope and aspect of layers and fractures
Flow	Impeller flow meter	Water flowing through meter turns a propeller whose revolutions are recorded	Fluid in borehole	Open and cased holes with fluid	Vertical water movement in borehole

Type	Specific log(s)	Methods	Depth of investigation	Borehole conditions	Information
	Electro-magnetic flow meter Heat pulse flow meter	Water flowing through packer induces a current that can be calibrated to a flow rate Heat pulse is created and measured above or below			
Fluid	Water quality	Temperature and electrical resistivity (for salinity) probes; multi-parameter probe	Fluid in borehole	Open and cased holes with fluid	Electrical conductivity, pH, O_2, NO_3, Eh, total gas pressure

Isotopes are variants of the same element that have different masses due to a difference in the number of neutrons in the nucleus. Radioactive isotopes are not stable in the environment and decay with time, whereas stable isotopes do not decay with time (Clark & Fitz 1997). The superscript number preceding the element symbol (e.g. ^{12}C, ^{13}C, ^{14}C) in the following discussion refers to the total number of protons and neutrons in that isotope (higher number = more neutrons = heavier isotope). Radioactive isotopes can be used as tracers because their concentration in the subsurface will decrease over time according to known decay rates. The radioactive isotopes commonly used in groundwater dating (e.g. ^{14}C, ^{36}Cl) are produced in the atmosphere by the interaction of cosmic rays with various elements and deposited with precipitation or with fine particles. If the input tracer concentration is known and fairly constant then the apparent 'age' (*t*) of the groundwater can be calculated using:

$$t = -\lambda^{-1}\left(\frac{C}{C_0}\right)$$

where C_0 and C are the initial and measured concentrations and λ is the known decay constant for the radioactive tracer (Cook & Böhlke 2000). Each radioactive tracer has a different timeframe over which it can be used, based on the decay constant. For example, ^{14}C has a half-life of 5730 years and can be used to date groundwater up to about 30 000 years old (Clark & Fitz 1997), whereas ^{36}Cl has a half-life of 301 000 years and can be used to date groundwater up to a million years old (Phillips 2000). Wassenaar and Hendry (2000) used a depth profile of ^{14}C to characterise the transport of carbon and to estimate the age of groundwater through a surficial till aquitard. Their findings indicate that diffusion is the dominant transport mechanism and that the groundwater between 29 and 37 m below ground surface is between 25 000 and 31 000 years old, the approximate age of the till, indicating very low fluid flux through the aquitard.

Radiogenic isotopes, which accumulate in the subsurface due to radioactive decay, are referred to as accumulating tracers. Longer residence times of groundwater in the subsurface result in higher concentrations of radiogenic isotopes, thus this method is best applied in groundwater systems with relatively long residence times. The most commonly used accumulation tracer is Helium-4 (^4He), which is produced from the radioactive decay of Uranium (U) and Thorium (Th) in aquifer/aquitard minerals. ^4He is non-radioactive, so the concentration of this tracer increases with time. ^{222}Rn, which is also produced by the radioactive decay of U and Th, is itself radioactive, with a short half-life of 3.8 days, so it reaches an equilibrium between production and decay quickly (~30 days) and is therefore not useful for age dating older waters (Cook & Böhlke 2000). Hendry et al. (2005) measured the increase in concentration with depth of ^4He from a surficial aquitard system. Their findings indicate that the concentration of ^4He exceeded that which would occur solely from U and Th decay in the aquitard, and that some ^4He was ascending from the underlying aquitard. More recently, Gardner et al. (2012) have used ^4He measurements from the Bulldog Shale aquitard in the western GAB to understand mechanisms and quantify rates of natural upward leakage from the underlying artesian aquifer. Their work provided the first true estimates of formation-scale aquitard permeability in this part of the basin, and revealed a combination of relatively low diffuse discharge through massive sections of shale operating alongside much higher, preferential discharge (connectivity) through faults.

Event markers are a special type of environmental tracer, where the concentration in the past has been variable but well known. During the mid-20th century the atmospheric concentrations of ^3H, ^{14}C and ^{36}Cl increased dramatically due to nuclear bomb testing and have since been decreasing back to natural levels. The increasing and decreasing concentration of these tracers can lead to two possible ages for a groundwater sample. Over the same time period, the atmospheric concentrations of chlorofluorocarbons (CFCs), SF_6

and ^{85}Kr have been gradually increasing due to industrial developments and use of nuclear reactors. These tracers can be more unique, providing only one possible age for the groundwater, although CFC concentrations have also started to decrease and are prone to degradation in some geologic environments. Event marker tracers are thus limited in use to dating groundwater that has entered the subsurface since the mid-20th century (Cook & Böhlke 2000).

Stable isotopes of hydrogen and oxygen in water molecules have been used for decades in hydrologic investigations. In the context of inter-aquifer connectivity, vertical depth profiles of the stable H/O isotope ratios in aquitard pore water have been used to provide information on groundwater flow velocity, hydraulic conductivity, solute transport mechanisms and climate and geologic events (Hendry et al. 2011; Hendry & Wassenaar 2009; Hendry et al. 2004; Hendry & Wassenaar 1999; Remenda et al. 1996; Desaulniers et al. 1981). Hydrogen has two stable isotopes, ^{1}H and ^{2}H, and oxygen has three, ^{16}O, ^{17}O, and ^{18}O, each with a different abundance. The ratio of the heavy isotope to the light isotope (typically $^{2}H/^{1}H$, and $^{18}O/^{16}O$) of water is particularly sensitive to changes in temperature and humidity, and this reflects changes in climate. At decreasing temperatures, glaciation for instance, the precipitation (and thus recharge) has less of the heavy isotope. The stable isotopic ratio of water recharged during such times therefore has a distinct signature which acts as a tracer and allows the study of transport and fluid flux through aquitards.

The chemical signature of groundwater can also be used in aquifer connectivity assessments. Chloride (Cl^-), a conservative element that is highly soluble and is not involved in the geochemical reactions commonly occurring in aquifers, is particularly useful. For example, the degree of mixing between two aquifers with different chemical signatures can be estimated using Cl^- concentrations and a mass balance approach:

$$[Cl]_M = x \times [Cl]_A + (1 - x) \times [Cl]_B$$

where $[Cl]_M$, $[Cl]_A$, $[Cl]_B$ are the Cl^- concentration in the mixture, aquifer A and aquifer B, respectively, and x is the fraction of water from aquifer A, and 1-x is the fraction from aquifer B (Herczeg & Edmunds 2000). Vertical profiles of Cl^- concentration in aquitard pore water can also be used to interpret inter-aquifer leakage, mixing and historical changes in aquifer chemistry and hydraulics (Harrington et al. 2013; Hendry et al. 2000). Finally, Cl^- and other environmental tracers can be used to reveal preferential flow features such as fractures and sand layers in what are otherwise very low-permeability aquitards (Harrington et al. 2007; Hendry et al. 2004; Gerber et al. 2001).

Limitations associated with using environmental tracers to interpret aquifer connectivity arise from the fact that as groundwater moves through the subsurface it often mixes with other groundwater sources (from aquitards for instance) or interacts with the host rock itself. If these interactions are not identified and accounted for, then estimates of groundwater age, and connectivity, can be misleading. If possible, the use of multiple environmental tracers together can reduce this uncertainty. Likewise, incorporating hydraulic methods and any other methods deemed appropriate to a particular problem will increase the confidence associated with an interpretation.

3.3 Modelling

3.3.1 What is a groundwater model?

A groundwater model is a tool used to represent a simplified groundwater system, or one of its parts. This can be done in one of two ways, either physically or mathematically. Physical models are real representations of a system, such as a sand tank filled with water, and can

simulate groundwater flow and solute transport directly. Physical models, typically constructed in the laboratory, are necessarily limited in their size and represent a miniature groundwater system of limited extent. It is possible to subject a physical model to various stresses (e.g. pumping) however the difficulty associated with recreating a more complex multi-layer aquifer/aquitard system with various forms of recharge (precipitation, stream flow, inter-aquifer flow) and discharge (pumping, stream) along with possible spatial changes in properties can limit the practical use of physical models. A physical model is thus typically limited to education and demonstration purposes.

Mathematical models simulate groundwater flow indirectly by solving a series of equations that describe the physical processes and boundaries of a groundwater system. There are two ways to solve mathematical models, either analytically or numerically.

- Analytical models are an exact solution of the groundwater flow equations but they require the user to make numerous simplifying assumptions about the groundwater system, in particular the boundary conditions and that the aquifer properties need to be constant in space and time. Analytical models are available for many different hydrogeological problems and may be solved rapidly, either by hand or with a computer. If the groundwater system being modelled is too complex and the simplifying assumptions cannot be applied, then it becomes necessary to use a numerical model.
- In a numerical model, space and time are subdivided into discrete segments for each of which a solution to the groundwater flow equation is approximated. Numerical models are not subject to the same simplifying assumptions as analytical models. It is possible for the parameters of the model (coefficients of the model that describe the hydrogeological properties and boundaries of the system) to vary in space and time, allowing the user to accommodate variability in aquifer geometry, pumping, and hydraulic properties. These models are more computationally intensive and are solved by computers.

The remainder of this section will focus on numerical modelling techniques and how they may be used to interpret aquifer connectivity. The use of numerical models has grown considerably in recent years due to increased computational power, the availability of user-friendly software packages and new solution techniques. In addition, numerical models are capable of representing the groundwater system in three dimensions (if needed) and can incorporate aquifer heterogeneity allowing a more realistic representation of the system being modelled. Unless otherwise referenced, the material presented in this section is from Barnett et al. (2012), Kresic (2007) and Anderson and Woessner (1992).

3.3.2 Why model?

There are two broad types of groundwater models: groundwater flow models and solute transport models. A groundwater flow model simulates hydraulic heads and flow rates within the model and across its boundaries, whereas a solute transport model simulates the concentration of solutes and their migration in the subsurface and across model boundaries. Groundwater models can be used to measure the fluid and solute exchange between the modelled system and the surface, boreholes or other groundwater systems. They can be solved for steady-state flow conditions where the magnitude and flow of groundwater is constant with time throughout the modelled domain, or for transient flow conditions where these can change with time. In a steady-state flow simulation the hydraulic head in the model does not change with time, but can in transient simulations.

Groundwater models are generally created for one of three purposes. The first group is predictive models, which are used to forecast either natural or artificial changes to the system. Groundwater models may also be used for interpretive or descriptive purposes, which allow the user to test various assumptions, to better understand the system dynamics and identify future work. The final group of models includes those which are generic and used to analyse hypothetical groundwater systems. This group is used to study the principles of groundwater flow and solute transport without the need for site-specific data.

There is no such thing as an all-purpose model. It is crucial at the initial stages of project development that the purpose of the model be established. Why is the model being developed, what questions need to be answered, what can be learned? Can the answers to these questions be obtained through analytical models? The answers to these questions will determine the type of model that is to be produced, and the effort needed to obtain the desired results. This is the first step in in the planning stage of groundwater modelling (Section 3.3.3) (Barnett et al. 2012; Kresic 2007; Anderson & Woessner 1992).

Groundwater models vary in complexity from simple idealised groundwater systems, to intricate models incorporating many aspects of the subsurface. The level of complexity that a model will incorporate should be decided upon early in the modelling process. There are two common approaches used, one where all the available data possible is incorporated into the model (complex), and the other where the initial model design is simple and additional levels of complexity are only added as needed to test various hypotheses. Although a more complex model can simulate more processes, it requires more input data to specify the parameters of the model and higher skill-level of the modeller. If a simpler model is chosen, it does not necessarily preclude the modeller from increasing the complexity should additional data become available; however, changes in approach may involve time, computational capacity and additional analysis dependent on the type of model. For example, a conceptual model may be readily updated, a stratigraphic model may take many weeks or months to update and an existing 2D model would need to be discarded to transition to a 3D model. Likewise a 3D model may need to be rebuilt if the stratigraphy changes.

3.3.3 Groundwater modelling process

The Australian groundwater modelling guidelines (Barnett et al. 2012), commissioned by the National Water Commission, provide guidance for the development, application and use of groundwater flow and solute transport models, built upon the experience of groundwater modellers in academia and industry within the Australian context. The guidelines suggest an approach to model development that uses a series of interdependent steps with regular opportunities for feedback into earlier steps, accompanied by regular reporting and review (Figure 10).

The initial step of model development involves **planning**, which requires the modellers and stakeholders to agree on objectives and intended use of the model and the type of model to be developed. The next step is model **conceptualisation**, where all the available data and knowledge of the study area are used to identify and describe the physical features and groundwater flow of the hydrogeologic system. It is important that the conceptual model be able to explain all process occurring in the system under consideration, and it is possible that alternative conceptual models will be equally able to explain all the processes. A conceptual model is often represented pictorially in the form of a cross-section or block diagram, or through more advanced 3D visualisation software. The conceptual model should be re-visited regularly throughout model development and refinements made if necessary.

Model conceptualisation is then implemented through **model design** and **construction**. In the design stage the numerical method and modelling software is chosen as are the model

dimensions, extent, layer structure and the spatial and temporal discretisation (size of blocks and time segments for which the groundwater flow equations will be solved). Model developers are encouraged to use simpler modelling approaches where applicable – for example, 2D rather than 3D, steady-state rather than transient, and the use of analytical methods if possible. These decisions are then applied through model construction using the chosen software.

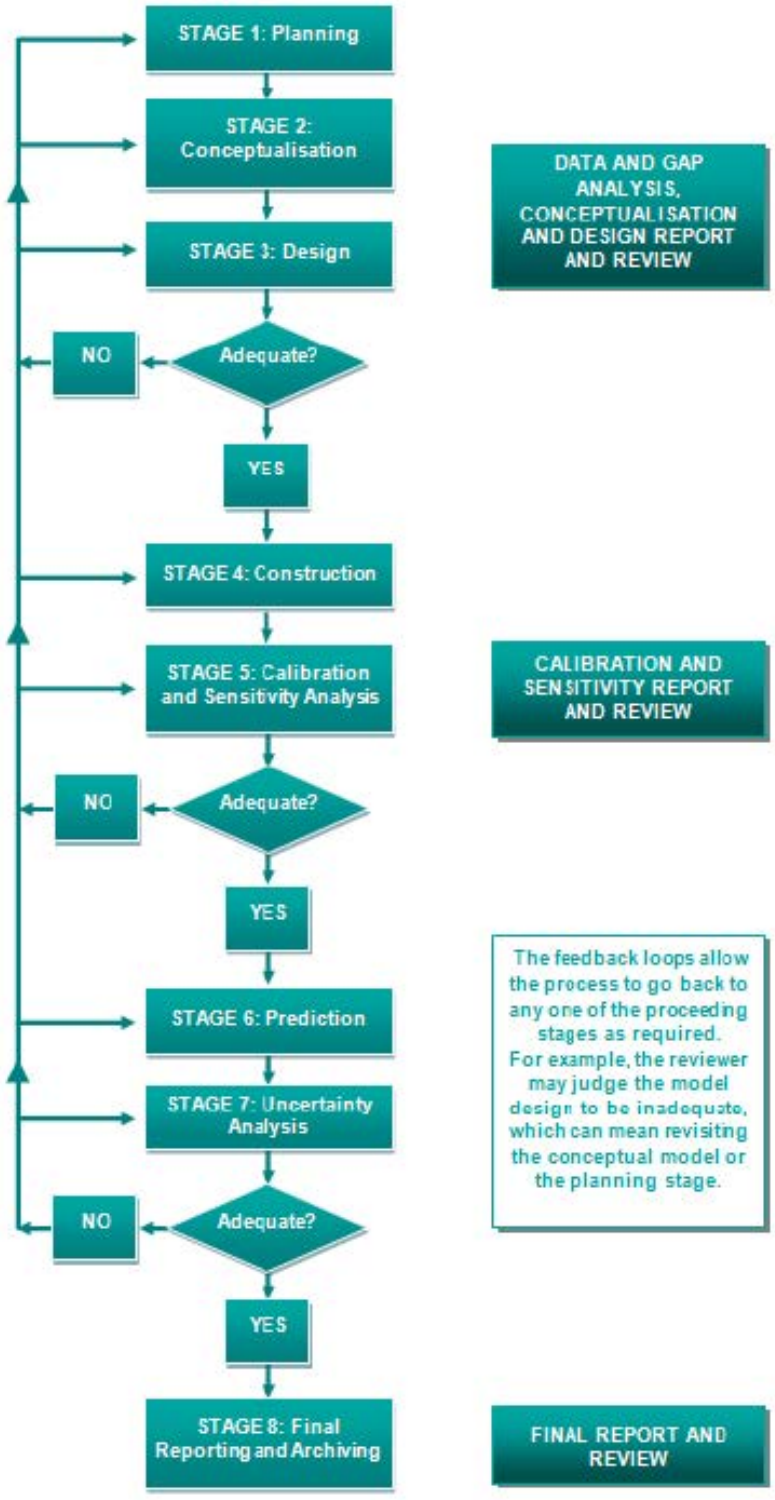

Figure 10 Groundwater modelling process (© Copyright, Barnett et al. 2012).

Once the model design has been implemented, the model may undergo **calibration** and **sensitivity analyses**. Model parameters that were implemented in the construction phase are adjusted until model simulations agree with historical data. This process can be done using a manual trial-and-error technique or through automated parameter estimation software.

Following calibration, the model may be used to make **predictions** that address the questions initially outlined in the modelling objectives (stage 1). Here it is possible to simulate the response to numerous stresses such as pumping, climate change, and solute migration, among others. Given that all modelling predictions are to some degree uncertain, it is necessary at this stage to describe the level of **uncertainty** (Section 3.3.4) and present it along with model predictions.

In addition to regular **reporting and review** throughout model development, a final report detailing the modelling process, data collection and outputs should be produced and critically reviewed by experienced peers as well as a non-technical audience. Subsequently, a post-audit should be conducted when new data becomes available.

3.3.4 Uncertainty

All groundwater models are a simplification of the natural world. In the conceptualisation and design of a model, decisions must be made on how an inherently complex system will be simplified and reproduced in the form of a numerical model. There is no single true or unique groundwater model and as such any predictions made are to some degree uncertain. It is therefore necessary, when presenting any modelling results, to include estimates of predictive uncertainty.

The uncertainty associated with predictive models stems from two main sources: field measurements and the model. The field observations that are used to constrain and calibrate the model are inherently uncertain due to the errors associated with the measurement methods. Although this error can be reduced through improved field techniques and frequency of data collection, it cannot be eliminated. Uncertainty associated with the model stems from our inability to exactly represent the complexity of the natural world in a numerical model. This uncertainty is rarely a limitation of the model itself, arising instead because the modeller is unable to provide detailed parameter values at the spatial and temporal scales that the model is able to accommodate. Additional uncertainty can arise from errors made by the model programmer, or with the modelling program itself (code errors, version).

The approaches used to conduct an uncertainty analysis can vary widely from qualitative to much more comprehensive, statistics-based, techniques. The complexity of uncertainty analysis to be conducted will depend on the risk being managed and impacts of decisions being made based on the modelling. If the risks and impacts are considered to be low, the qualitative or heuristic approach, where the prediction uncertainty is based on trial and error and the modeller's experience, may be sufficient. Where the risks and impacts are deemed to be greater, then a more detailed, robust and mathematically intensive approach becomes necessary. It is beyond the scope of this work to describe in detail these techniques, but the reader is directed to Barnett et al. (2012) and Doherty et al. (2010) for additional information.

A desirable outcome of uncertainty analyses is the identification of the features that are most responsible for the prediction uncertainty. This allows the modeller to identify data gaps or modelling methods that can best reduce the predictive uncertainty. Additionally, the uncertainty analysis allows the modeller to communicate to decision makers the probability that a particular outcome will occur. Through visual aids (figures and graphs), the modeller

should communicate that the model prediction is based on numerous model outcomes and thereby acknowledge the non-uniqueness of all models (Barnett et al. 2012).

3.3.5 Application for aquifer connectivity

Numerical groundwater modelling is a powerful tool at the disposal of hydrogeologists. It is the nature of the subsurface that we are unable to access, observe, and make measurements at every point in a groundwater system. Numerical modelling allows us to 'fill in the blanks' between observation points (e.g. boreholes), make predictions based on future scenarios (e.g. increased pumping, climate change), and test various hypotheses.

The use of numerical models when investigating aquifer connectivity can be very informative. Numerical models can be used to inversely estimate the hydraulic properties of an aquitard that separates two aquifers. Given the difficulties associated with measuring the regional hydraulic properties of aquitards, numerical models can be used to better simulate these parameters. This provides an alternative method for estimating the regional hydraulic properties of aquitards by calibrating models to comprehensive water level monitoring data. Detailed geological model data, point scale hydraulic conductivity data and up-scaling algorithms can further support these estimates by providing information on the potential bounds and spatial variability of the subsurface hydraulic properties. For example, if a large production bore is installed in a confined aquifer (below an aquitard) and observation wells are installed in the overlying aquifer, a numerical model may be able to estimate the bulk hydraulic properties of the aquitard and estimate the fluid flux across the aquitard, thereby providing information on inter-aquifer connectivity. The number of observation wells needed for such an interpretation is problem specific and depends on the spatial configuration of the existing monitoring network. With less than three observation wells however, it is not possible to make a reliable interpretation.

Hart et al. (2006) used a regional groundwater flow model to estimate the vertical hydraulic conductivity (Kv) of a shale aquitard separating a confined pumped aquifer from an overlying aquifer. They showed that the calibrated regional flow model required a Kv several orders of magnitude higher than those measured in the laboratory, indicating the presence of preferential flow pathways, either fractures or open boreholes. Likewise, numerical models may be able to estimate changes in the hydraulic properties that occur within an aquifer (intra-aquifer connectivity). This is particularly important as most aquifers/aquitards do not fit the idealised layer cake model of uniform thickness and homogeneous (uniform throughout) hydraulic properties.

Numerical models can also be a useful way of interpreting different types of data, such as environmental tracer distributions. Mazurek et al. (2011) used numerical methods to interpret the environmental tracer profiles from nine sites in central Europe and interpreted transport times across the aquitard of several thousand to millions of years.

Equally powerful, a calibrated numerical groundwater model can be used to make predictions into the future based on either natural or current conditions, or given some induced stress (e.g. large-scale aquifer pumping, carbon dioxide injection). This ability for testing future scenarios can provide information on how aquifer connectivity might be impacted (e.g. increase flux across an aquitard) by various stresses and inform management decisions on groundwater development. Noy et al. (2012) used numerical methods to simulate carbon dioxide injection into a sandstone aquifer and make predictions 3000 years into the future. They were able to estimate how much carbon dioxide could be stored per year without the pore pressure exceeding a certain limit, but also found that this would cause significant fluxes of native pore water to the sea where the sandstone crops out beneath the seabed.

Depending on the groundwater system being modelled, consideration might have to be given to the density and temperature of the water, the presence of fractures and to multi-phase flow. Groundwater flow models such as MODFLOW, which is commonly used by industry, assume that the density of water is constant and use a default value of 1000 kg/m^3, which is approximately the density of pure water at 4°C (its maximum density). The density decreases both as the temperature of the water increases and decreases from 4°C. Although this assumption is valid for near surface aquifers with low values of dissolves solids, it is not valid at greater depths (increasing temperature) or for water with high concentrations of dissolved solids, which has an increased density (Anderson & Woessner 1992). If it is not possible to assume a constant density and temperature of water for the groundwater system of interest, then it is necessary to modify the groundwater models to include these differences.

Many groundwater flow models are designed to simulate flow in porous media (flow through interconnected pore spaces) and may or may not be able to simulate flow in fractures. Fractures can significantly increase the permeability of a material, be it rock or sediments (e.g. clays), and considerably alter groundwater flow and solute transport (Chapter 2). The most common approach used to incorporate fracture permeability into numerical models is through the use of a Representative Elementary Volume (REV) as defined in section 2.2.1. Although this approach may be valid for use in regional groundwater flow models, it does not work well for solute transport models. This is because solute will move much faster along preferential pathways (e.g. fractures, faults and high conductivity lenses) than in a media with homogenized properties, thus this rapid transport is lost when using an REV. Alternatively, it is possible to represent discrete fractures in a model, but this requires excellent characterisation of the fracture network, an inherently hard task to accomplish, particularly on the regional scale.

Multi-phase flow occurs when more than one fluid phase is present in the subsurface, be it air, water or other fluid such as gas/oil. The multi-phase flow problem can arise from temperature or pressure changes in an aquifer, resulting in a phase change (e.g. pressure decrease in coal seams releases methane). The occurrence of more than one phase effectively reduces the pore space available for each of the phases to flow and retards its movement (Barnett et al. 2012). The use and development of multi-phase models is largely driven by the need to investigate the movement of contaminants in saturated and unsaturated subsurface zones (Yu et al. 2009), the subsurface sequestration of carbon dioxide (Noy et al. 2012; Bickle 2009), for engineering applications in geothermal reservoirs and for the recovery of oil and gas from hydrocarbon reservoirs (Geiger et al. 2012) and in coal bed methane development (Zarrouk & Moore 2009). Although most of the modelling codes generally used by the groundwater industry are not designed to handle multi-phase flow, codes developed by other industries that can handle phase changes and flow retardation should be considered if more than one fluid phase will be present in an aquifer (Barnett et al. 2012).

These considerations are especially relevant in the context of coal seam gas where the water quality is variable and may be high in dissolved solids and/or be at elevated temperatures due to the depths of the aquifers. In order to properly simulate the groundwater environment and interpret aquifer connectivity, it is important that these factors be considered and, if needed, incorporated into the model development and code selection. For instance, one might need to consider dual-phase flow when simulating the impacts of depressurising coal seams, as this is when both water and methane will flow into a well. Contemporary groundwater models are applicable whenever single (water only) flow is expected.

3.3.6 Limitations

Numerical groundwater models are increasingly being used in projects dealing with groundwater protection, development and remediation (Kresic 2007). It is critical that the limitations associated with modelling be recognised. As previously discussed in Section 3.3.4, the quality of the field data and the inability to determine and accurately represent field parameters in a model are two main causes of uncertainty. Even if the field data is of high quality, if the spatial and temporal distribution of the data within the study area is not uniform (generally the case) then the calibration will be not well constrained in areas with low observation density. Model outcomes in these regions will therefore have higher predictive uncertainty. Despite the availability of various mathematical interpolation methods (estimating properties between known data points; e.g. kriging) to fill in these data gaps, features could be entirely lost or created due to lack of data constraints. For example, when interpolating a surface it is possible to flatten out an existing hill or create a mound where one does not actually exist.

The conceptual model upon which the numerical model is built represents another limitation. If the conceptual model fails to incorporate all the physical features and flow processes of the groundwater system of interest, this can lead to errors in the numerical model. This is why it is important to consider more than one conceptual model, if applicable, and to keep the conceptual model flexible to changes throughout the modelling process.

Scale dependencies can also present problems. There are some parameters that are scale-dependent, which means their value changes based on the scale (size) of the model. This is particularly true for solute transport models, where the value of dispersivity (a measure of how much a solute will stray from the flow path of the groundwater) increases with the scale of the problem (Gelhar et al. 1992). It is well accepted that values of dispersivity measured in the laboratory are not applicable for analysis of field scale problems (Freeze & Cherry 1979). In cases such as these, it is up to the modeller to incorporate the scale dependencies, as the model itself cannot.

As discussed in Section 3.2, the various methods used to measure hydrologic parameters are each scale dependent, representing the area of influence of a particular method. This can become a problem when using the results from field or laboratory tests and up-scaling them for regional flow parameters where the presence of preferential flow paths (e.g. fracture and faults) may not have been observed in the smaller scale measurements. Again, it is up to the modeller to recognise the limitations of the field measurements and incorporate them accordingly. The modeller, therefore, is a potential source of error throughout the modelling process.

Despite the limitations associated with numerical modelling, it is a very useful tool so long as the limitations are recognised and documented and uncertainties are acknowledged.

3.4 Conclusions

There are many tools in the hydrogeology toolbox, from laboratory and field-scale hydraulic tests to geophysical and geochemical methods, all of which can be used to characterise the subsurface. Each of these methods provides information on a different scale and for different purposes. Where laboratory tests provide estimates of hydraulic properties for the small scale core sized sample, field hydraulic tests can provide information on a scale from tens to hundreds of metres. Airborne and surface geophysical methods are best used to interpret the geological structure of the subsurface (layering of strata, identification of faults) and salinity distribution, and can cover large areas. Borehole geophysical methods are line measurements, but they can provide quantitative information on porosity, permeability and

thickness of permeable layers. Geochemical methods can provide insights into connectivity at a range of scales, from well-to-well using artificial tracers, right up to formation and regional scales using environmental tracers. Regardless, the use of a particular method will depend on the question being asked, and how best to address it. In order to evaluate and predict aquifer connectivity, the NRC (2010) recommends the use of many different measurement methods together, which is rarely done.

Another powerful tool in the hydrogeology toolbox is numerical modelling. The nature of hydrogeology is that we cannot physically see what is happening in the subsurface. Numerical modelling gives us the opportunity to simulate what might be happening, provided we have an adequate conceptual model, and to make predictions into the future given possible scenarios. The subsurface characterisation methods described provide essential information used in the building and testing of numerical models. Although there are limitations associated with using models, primarily associated with uncertainty, the modelling method described in Section 3.3 can lead to the development of very useful models able to inform management decisions. The NRC (2010) has identified, as a major data gap, the use of independent and comprehensive data (as above) with which groundwater models for coal bed methane basins can be validated.

4 Changes in aquifer connectivity

4.1 Introduction

This chapter focuses on potential changes in aquifer connectivity resulting from coal seam gas and coal mining activities. Previous chapters have highlighted the role of aquitards in hydrogeology. Cherry et al. (2004) stress how important aquitard integrity is to protecting underlying aquifers from contamination. 'Aquifer connectivity' is synonymous with 'aquifer integrity' in the context of the vertical migration of fluids and solutes in groundwater systems, since the aquitards act as the restrictor between adjacent aquifers. Thus, as in Cherry et al. (2004), aquifer connectivity depends on the hydraulic head distribution and the hydrogeologic characteristics of the aquitard (i.e. hydraulic conductivity, porosity, thickness, etc.). Cherry et al. (2004) also include contaminant characteristics in their considerations of aquitard integrity. Aquifer connectivity could be expanded to include considerations for intra-aquifer connectivity (the lateral migration of fluids and solutes within an aquifer). The scope of this chapter is focused on considerations for changes in inter-aquifer connectivity, the vertical, both upwards and downwards, migration of fluids between adjacent aquifers, as opposed to intra-aquifer connectivity, i.e. groundwater flow within one aquifer.

The hydraulic head distribution in the subsurface and hydraulic conductivity is related by Darcy's law (Chapter 2) and, under transient conditions, storage needs to be taken into account. Thus, a change in aquifer connectivity is actually a change in the flux between aquifers, as controlled by the aquitard separating them. A change in q can be invoked by changing K, S or ∇h independently, or by modifying all at the same time.

In the first case, the effects of changing the hydraulic gradient are straightforward. For example, if water is extracted from an aquifer, the hydraulic head in the vicinity of the well decreases resulting in a hydraulic gradient which is the driving force for groundwater flow. The new hydraulic head differential between the pumped aquifer and an adjacent aquifer will directly result in a change in the flux. Because flux is a vector, both its magnitude and direction are subject to change. However, because drawdown diminishes with distance from the pumping well, so too will the induced hydraulic gradient and flux effects.

Changing aquifer connectivity by modifying the fluid (dual or multi-phase flow) and/or hydrogeologic properties in the subsurface is more complex. Quarrying, improper borehole construction and deformation due to pumping have the potential to undermine aquifer integrity by creating new preferential pathways in the subsurface (Hart et al. 2006; Botha & Cloot 2004; Cherry et al. 2004). This chapter primarily focuses on how the intrinsic permeability of aquitard materials can increase as the result of existing and new preferential pathways. This is specifically addressed in terms of mechanical deformation (Section 4.2), hydraulic fracturing and CSG operations (Section 4.3), induced seismicity and the reactivation of faults (Section 4.4), and boreholes (Section 4.5). The interplay between changing hydraulic conditions, in situ stress, mechanical deformation, fluid properties (single, dual or multi-phase) and hydrogeologic characteristics adds a level of complexity that is not generally or sufficiently addressed in current groundwater investigations.

4.2 Mechanical deformation

The Earth's crust is continually being deformed due to slow but persistent in situ stresses. Example causes for compressive (acts to reduce the volume) and tensile (acts to stretch) stresses in the natural environment include: the weight of overlying strata, the intrusion of a

magma body, cooling processes in the case of igneous rocks, and convergence, divergence and slip at plate boundaries (plate tectonics). Changes in the Australian continental-scale stress field over time are well documented in Müller et al. (2012).

The stresses acting on any point in space are vectors (having both magnitude and a direction) and can be expressed in terms of the three principal stress directions:

1. the axis of greatest principal stress σ_1
2. the axis of intermediate principal stress σ_2
3. the axis of least principal stress σ_3.

Stresses in a two-dimensional plane are expressed in terms of σ_1 and σ_3 which are perpendicular and form an ellipse (Figure 11). The three-dimensional principal stress directions are portrayed by an ellipsoid where σ_2 is perpendicular to the σ_1-σ_3 plane (Figure 11b).

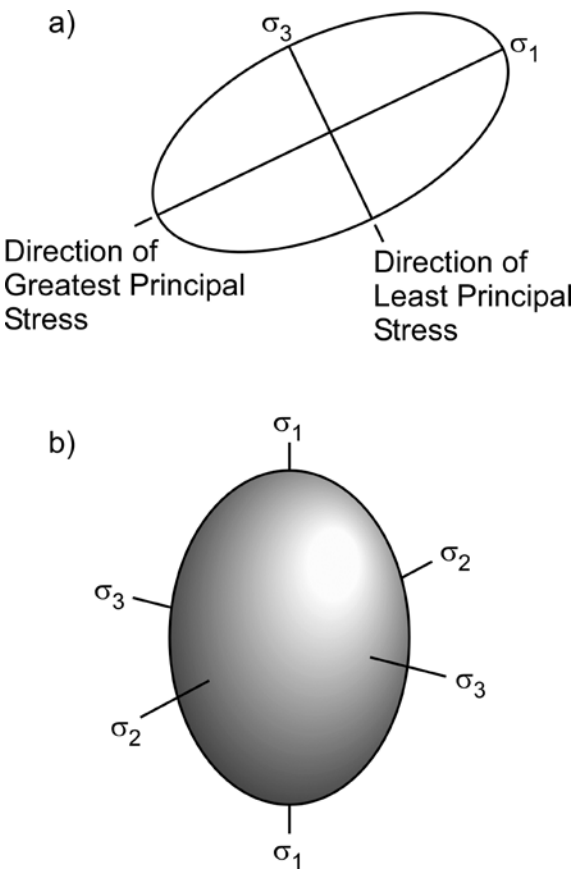

Figure 11 The (a) two-dimensional stress ellipse and (b) three-dimensional stress ellipsoid. These are visual representations of the stress tensor which show both the direction and ratios of the greatest (σ_1), intermediate (σ_2) and least (σ_3) principal stresses. Modified from © Copyright, Davis and Reynolds (1996).

The orientation of the stress ellipsoid depends on the geologic conditions and depth. In general, σ_3 tends to be vertical at shallow depths (less than ~300 m) because the contribution of the weight of the overlying geology to the total vertical stress is relatively low.

At depths greater than 300 m, the direction of σ_3 shifts towards the horizontal as the vertical stress from the overlying weight becomes significant (Nielson & Hanson 1987, as cited in US DOE (undated)). US DOE (undated) notes that the typical stress configuration in coalbed methane reservoirs is $\sigma_1 > \sigma_2 > \sigma_3$ where σ_1 is vertical and σ_2 and σ_3 are horizontal. These stresses are typically compressive and are spatially variable, particularly in the vertical direction from layer to layer (US DOE undated).

Structural deformation occurs when an applied stress exceeds the strength of the rock (i.e. the ability to resist the stress). The applied stress causes a change in the length, area or volume of the body by means of distortion (change in shape), dilation (change in size) and rotation. The ratio of the altered length, area or volume to its original value is referred to as strain. The mode of failure will be ductile (bend) or brittle (break) depending how the in situ conditions have influenced the strength properties of the rock (Davis & Reynolds 1996). Ductile deformation occurs in two forms: elastic and plastic. The difference is the former results in the rock returning to its original length once the stress is removed while the latter produces a permanent change in shape without failure or rupture. Brittle deformation occurs when fractures and faults form. Brittle rocks exhibit elastic behaviour upon the initial application of a stress and can fail suddenly without evidence of plastic deformation (Davis & Reynolds 1996). A plot of the applied differential stress versus the observed strain provides a detailed record of the deformational history. An example stress-strain diagram from a compression test is provided in Figure 12 and highlights the characteristic shape of the curve for each deformation mode and the different measures of strength (yield strength, ultimate strength and rupture strength) that can be obtained. It should be noted that the rocks are much stronger in compression than under tension (Davis & Reynolds 1996).

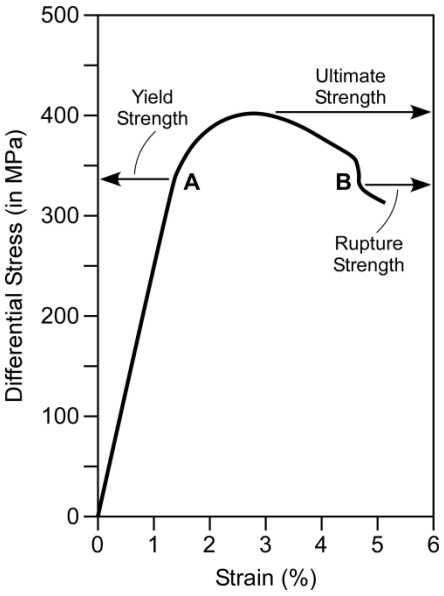

Figure 12 Hypothetical stress-strain diagram for a rock deformed under confining pressure conditions. Point A marks the onset of plastic deformation which continues along the curve until Point B, rupture. Modified from © Copyright, Davis and Reynolds (1996).

Over time, geologic structures of all scales (e.g. folds, faults, joints, microcracks between mineral grains, etc.) form in response to stresses (local to continental scale). This includes the deformation of pre-existing structures which may have formed under a different (or

palaeo) stress regime (such as a fault) or in a depositional environment, such as a bedding plane in sedimentary rock. The coincidence of the orientation of a planar structure of interest with the principal stress directions is rare. Thus, a given stress can be divided into two components: one perpendicular to the plane of interest (normal stress σ_N) and one parallel to the plane (shear stress σ_S).

The following is a brief summary of the factors that influence rock strength and ductility from Davis and Reynolds (1996):

- Lithology: strength is influenced by mineralogy, texture and the nature and orientation of mechanical heterogeneities present (i.e. fractures, layers and foliations).
- Confining pressure: yield strength, ultimate strength, rupture strength and ductility increase to greater values with increasing confining pressure. This can be offset if the pore fluids are higher pressure than they should be for a given burial depth (i.e. effective pressure = confining pressure – pore water pressure). Note: 'stress' and 'pressure' are the terms describing the intensity of force acting upon a body of solid or liquid as a function of its area, respectively. This means a deeply buried rock with high pore pressures will deform similarly to one in a shallower setting with lower confining pressures. The fluid pressure is typically scaled by Biot's constant (α, a correction factor from poroelastic theory that accounts for the efficiency with which internal pore pressure offsets the externally applied total vertical stress).
- Temperature: increasing temperature generally reduces yield strength and ultimate strength, and increases ductility.
- Strain rate: rock strength decreases during periods of prolonged stress due to eventual fatigue.
- Time: recognised as one of the least understood of all the independent variables influencing rock strength, particularly in the context of the geologic time scale.
- Pre-existing weaknesses: internal flaws and weaknesses at all scales (faults, fractures, bedding planes, joints, veins, pores, and microcracks between mineral grains) reduce rock strength. Smaller bodies of rock are typically stronger than larger bodies because they contain fewer of these weaknesses. Failure along a pre-existing plane of weakness depends on the combination of friction (dependent on the surface roughness if the normal stress is low) and normal stress (friction becomes independent of rock type when the normal stress is high).
- Size: rock strength is commonly determined experimentally on rock cores in the laboratory. As previously mentioned, the size of the sample greatly influences the measured strength because of the presence of pre-existing weaknesses. Given the inherent heterogeneity in the properties of geologic materials and the diminishing strength of increasing volumes of rock, up-scaling rock stress-strain relationships from laboratory tests to predict mechanical deformation on a larger scale remains a challenge.

Aside from these main effects, the water content and chemical reactivity of the rocks can influence their strength (Roshan & Oeser 2012; Al-Bazali et al. 2008; Heidug & Wong 1996).

The terms 'brittle' and 'ductile' are very much geared towards strain only. Models of elastic, plastic and viscous behaviour better encapsulate the full stress-strain relationship (Davis & Reynolds 1996). For the case of elastic behaviour (linear elastic deformation theory), four additional parameters are used: Young's modulus (measure of stiffness), Poisson's ratio (υ,

the degree to which a rock core bulges as it shortens), bulk modulus (resistance of an elastic solid to a change in volume) and shear modulus (resistance of an elastic solid to the shearing of planes past each other).

As cited in US DOE (undated), Gidley et al. (1989) assert the best and most reliable way to measure in situ stress is by pumping into a formation, creating a fracture, stopping the pumping, and observing the pressure at which the fracture closes. Assuming the aforementioned typical stress configuration in coal seams ($\sigma_1 > \sigma_2 > \sigma_3$ where σ_1 is vertical and σ_2 and σ_3 are horizontal), the fracture closing pressure is the minimum horizontal stress (i.e. $\sigma_{min} = \sigma_3$). The orientation of the induced fracture will be vertical (propagation occurs perpendicular to σ_3, see Section 4.3 for a more detailed explanation) and the minimum horizontal stress profile with depth can be estimated using (US DOE undated):

$$\sigma_{\text{min}} \cong \underbrace{\frac{\upsilon}{1-\upsilon}\left(\sigma_{\text{ob}} - \alpha\sigma_{\text{p}}\right) + \alpha\sigma_{\text{p}}}_{\substack{\text{horizontal stress from the vertical} \\ \text{stress and the poroelastic} \\ \text{behaviour of the formation}}} + \sigma_{\text{ext}}$$

where σ_{ob} is the overburden stress (a function of depth), σ_{p} is the pore pressure, and σ_{ext} is the tectonic stress.

Coal seam depressurisation, co-produced water reinjection, mine dewatering and rock mass removal during coal mining all have the potential to alter in situ stress from natural conditions by changing pore pressures and overburden stress in both time and space. The magnitude and timescale (including rate of change) of the pressure perturbation is an important component in predicting long-term and transient mechanical deformation, particularly in brittle confining layers. Any assessment of the effects of pumping on deformation should also include the post-production period since rock mass strength and stiffness are a function of time and the rebound of pressures back to pre-development conditions (or to the new steady-state conditions) may be prolonged and altered by any modifications to the intrinsic permeability of the strata.

Finally, Botha and Cloot (2004) call attention to their observations that aquifer deformation is regularly neglected in groundwater studies despite being recognised in the literature as far back as Meizner (1928) and Biot (1941). They observed the effects of non-linear deformation in stressed aquifers (the theory presented earlier in this section is for linear elastic deformation) and that hydraulic conductivity and specific storativity are not independent parameters as is typically assumed. Botha and Cloot (2004) conclude that following factors are the key controls on groundwater flow in stressed aquifers:

- the rate at which the aquifer is pumped
- the mechanical properties of the aquifer (Young's modulus and Poisson's ratio)
- factors controlling the isotropy of the aquifer
- linear or non-linear deformation.

Botha and Cloot (2004) attribute the general lack of consideration for deformation effects in groundwater studies to the long timeframes over which the deformations are realised and the inability to measure such small changes with current technology.

4.3 Hydraulic fracturing and coal seam gas operations

Hydraulic fracturing has become a standard method in enhancing the production/efficiency of oil and gas and geothermal wells. The first recorded case in the United States (US) was an

experimental case in Kansas in 1947 (US DOE undated) with commercial application to follow two years later in Texas. One of the concerns with hydraulic fracturing in the context of coal seam gas extraction is that the target horizons are much shallower and proximal to aquifers used as drinking water resources than conventional oil and gas wells (US EPA 2004). Coal seam gas extraction does not always involve hydraulic fracturing; of the 1844 coal seam gas wells drilled in Australia over 15 months during 2012 and 2013, only six per cent were subject to hydraulic fracturing (APPEA 2013). In Queensland, this proportion could increase to 10-40 per cent as the industry expands (DEHP 2013).

Hydraulic fracturing in the coal seam gas industry is commonly used to hydraulically connect the borehole to the coalbed and enhance methane desorption from the surface of the coalbeds. Coal is generally very weak (i.e. low Young's modulus) and fractures easily. Fractures are naturally prevalent in coal and are typically referred to as 'cleats'. The objective of hydraulic fracturing is to enlarge existing fractures or create new fractures to increase the secondary permeability. This is achieved by (US EPA 2004) pumping a thick fluid (water, foam or oil-based) into the coal seam, via a well from the surface, to induce an increase in pressure and cause:

- fractures to form/propagate once the induced pressure exceeds the ability of the coal seem to resist the stress
- proppants in the injected fluid to enter the fractures and hold the fracture open when the high fracturing pressures are released
- open fractures to provide conduits for groundwater and fracturing fluids to be extracted from the coal seam.

Two potential threats to groundwater resources due to hydraulic fracturing are recognised by US EPA (2004), which are:

- water quality impacts from hydraulic fracturing fluids being injected into aquifers or into coal seams with existing direct hydraulic connections with adjacent aquifers
- the formation of new hydraulic connections between the coal seams and aquifers.

Not all of the hydraulic fracturing fluid can be recovered by pumping post-fracturing and it has the potential to migrate post-production; however, US EPA (2004) concluded that hydraulic fluids pose little threat to water quality. This is attributed to the combined mitigating effects of high volume pumping during methane extraction, and dilution, dispersion, adsorption and (potential) biodegradation in the subsurface (US EPA 2004).

The formation of new subsurface connections is more important for the scope of this report. The US EPA (2004) and US DOE (undated) exhaustively reviewed and discussed the controls on the fractures that are created by hydraulic fracturing. The following is a brief summary of the key points:

- At depths less than 300 m, the direction of the least principal stress tends to be vertical because of the relatively low weight of the overlying geologic material. The hydraulically induced pressure forces the walls of the fracture apart in the direction of the least stress (which is vertical), resulting in the formation of a horizontal fracture. Hydraulically induced vertical fractures at shallow depths initiate from existing vertical fractures. Generally, at depths greater than 300 m (as is the case for coal seam targets in Australia), the direction of the least principal stress becomes horizontal (i.e. the weight of the overlying geologic material acting in the vertical becomes significant). Thus, the orientation of the hydraulically induced fractures tend to be vertical (i.e. the walls of the

fracture are pushed open in the horizontal direction). A vertical fracture initiated at these greater depths could propagate vertically to shallower depths and develop a horizontal component.

- The pressure will opportunistically dissipate via the path(s) of least resistance (i.e. pre-existing fractures/cleats and other structural flaws in the coalbed).
- Increased connectivity is dominated by the extension of the natural fractures, not by the creation of new fractures.
- The extent of the induced fracturing depends on the properties of adjacent strata (i.e. thickness, in situ stress differences, stress-strain characteristics), the presence of natural fractures, the type of fracturing fluid being used, the injection pressure and the target depth. High stress contrasts between strata act as a barrier to fracture propagation.
- The US EPA (2004) cites examples of sand proppant extending up to 160 m from coal seam gas bores within induced fractures and induced fracturing generally extending an additional 60 to 90 m.
- Fracture dimensions can be estimated using direct, indirect and numerical modelling methods. Direct methods include observations of fractures within mining coal seams that were previously hydraulically fractured (termed 'mineback' or 'mine-through' mapping), dye tracing, downhole camera observations, surface and downhole tiltmeters and microseismic monitoring. Indirect methods include pressure analyses and radioactive tracing. Differences between modelled hydraulic fracture geometry and mineback observations were noted in Jeffrey and Settari (1995). This was attributed to non-unique simulation interpretations that were based solely on field pressure data and the asymmetric distribution of proppants in the induced fractures.

It is important to note that while hydraulic fracturing is needed to ensure and enhance the hydraulic connection between the extraction well and the coal seam, it is not in the best interest of the operator to induce large-scale connectivity. US EPA describe these as:

> *'…financial incentives … [to reduce] expenditures on hydraulic horsepower, fracturing fluids and proppants.'*
>
> © Copyright, US EPA (2004)

Increased connectivity with adjacent units (i.e. comprised aquitard integrity) could also escalate the required amount of pumping needed to depressurise the coal seam for economic methane extraction and the costs associated with co-produced water treatment and disposal.

The permeability of coal reservoirs can also change quite significantly during production (in addition to the reduction in hydraulic conductivity resulting from the co-presence of gases with the fluid in the pore space). Pan and Connell (2012) provide a detailed review of this phenomenon and the various reservoir engineering models developed to predict the behaviour. During initial pumping it is most often observed that the permeability of the coal decreases exponentially due to the cleat compression that occurs in response to the increase in effective stress (which is the typical behaviour in fractured reservoirs). However, as methane is desorbed, the coal matrix shrinks and results in a net increase in permeability (Gray 1987a; Gray 1987b). The permeability may decrease again if carbon dioxide is used during enhanced coalbed methane recovery. The carbon dioxide adsorbs to the coal surface

causing it to swell and the cleat apertures to reduce (van Bergen et al. 2006). Thus, aquifer connectivity may be transient in this respect.

In conclusion, it is clear from the examples and theory that pre-existing weaknesses (i.e. cleats, fractures, faults, etc.), the properties of the coal, and property contrasts between the coal measures and the adjacent stratigraphic units control the connectivity created by hydraulic fracturing and permeability during production. Unfortunately, natural discrete fractures, fracture networks and the resultant flow system are often complex and heterogeneous and difficult to locate and characterise in the subsurface, particularly those relevant at different scales (Novakowski et al. 2006). This difficulty would carry forward into the ultimate determination of changes in aquifer connectivity resulting from coal seam gas and coal mining operations.

4.4 Induced seismicity and the reactivation of faults

Faults (and other pre-existing weaknesses) have previously been identified in Sections 4.2 and 4.3 as features that can reduce rock mass strength and offer a path of least resistance for the propagation of connectivity in the subsurface. Faults can become 'lubricated' by the injected water that can flow along them. The injected water increases the pore pressure in the fault, which acts to reduce the effective stress (termed stress relief), decrease the frictional resistance and can lead to slip. Failure at a fault is dependent on its orientation relative to the existing state of stress (Nicholson & Wesson 1990).

Tectonic reactivation in sedimentary basins and fold belts is on-going throughout Australia as a result of high-contrasting properties between proximal stratigraphic units and geologic structures and the effects of larger scale forces acting at the crustal plate boundaries (Müller et al. 2012). Lineaments (i.e. linear surface expressions of subsurface fracture zones, faults and geological contacts) are generally assumed to be highly permeable conduits for recharge and groundwater flow (Shaban et al. 2006; Sener et al. 2005; Krishnamurthy et al. 2000). However, Gleeson and Novakowski (2009) concluded that this is not always the case in a watershed-scale study conducted in a Precambrian crystalline rock setting. Brecciation, cataclasis and clay-rich gouge zones can contribute to permeability reduction in faults (Caine & Forster 1999; Caine et al. 1996; Goddard & Evans 1995; Evans 1988). Such conditions can result in a reduction of recharge and flow and the (sometimes anisotropic) compartmentalisation of flow systems (Bense & Person 2006; Seaton & Burbey 2005; Ferrill et al. 2004; Marler & Ge 2003).

The British Columbia (BC) Oil and Gas Commission (2012) found direct correlation between hydraulic fracturing and seismic events in the Horn River Basin located in north-east BC, Canada. The seismic activity was not found to impact shallow aquifers or the environment and only one of the measured events was large enough to be felt at ground surface.

A conference abstract by Ellsworth et al. (2012) on increased seismicity observed in the mid-continent of the US attracted wide media attention because it alluded to a relationship between these events (i.e. earthquakes) and coal seam gas and conventional oil and gas industry activities. David Hayes, Deputy Secretary of the US Department of the Interior, later released an online statement to clarify the message (Hayes 2012). Both Hayes (2012) and earlier research (Leith 2011) affirmed that the results did not suggest that hydraulic fracturing was the cause of the increased rate of earthquakes. Rather, in many cases, the increase in seismicity was shown to coincide with the injection of wastewater in deep disposal wells (which had long been known). Co-produced water from an extraction well field is often reinjected via a single or limited number of disposal wells (Hayes 2012). According to Hayes (2012), the siting of these reinjection wells tends to be in the mid-continent – Colorado, Texas, Arkansas, Oklahoma and Ohio. The largest induced earthquake (magnitude 5.3) was

observed at the Rocky Mountain Arsenal well in Colorado in 1967 following the reinjection of large volumes of wastewater from the manufacture and disposal of chemical weapons between 1962 and 1966 (Hayes 2012; Leith 2011).

Figure 13 provides worldwide localities of known induced seismicity resulting from different types of energy technologies and the measured maximum earthquake magnitude. Leith (2011) notes that induced earthquakes occur in settings with pre-existing natural faults that are capable of generating earthquakes. A positive correlation between earthquake magnitude and total volume injected has been observed in historical data; the influence of injection pressure and injection rate on earthquake magnitude is still being investigated (Hayes 2012; NRC 2012). Hayes (2012) notes that separation distances up to six miles (10 km) between the injection well and the induced earthquake have been observed. This furthers the concept that such seemingly local anthropogenic activities can have a large pressure 'footprint' in the subsurface. The three Australian cases shown in Figure 13 are from surface water reservoirs in Varragamba and Eucumbene (Guha 2001) and geothermal systems in the Cooper Basin (Majer et al. 2007)

In their evaluation entitled *Induced Seismicity Potential in Energy Technologies* (NRC 2012), NRC came to the following conclusions regarding the potential risk of induced seismicity:

- the process of hydraulically fracturing a well as presently implemented for shale gas recovery does not pose a high risk for inducing felt seismic events
- injection for disposal of waste water derived from energy technologies into the subsurface does pose a risk for induced seismicity, but very few events have been documented over the past several decades relative to the large number of disposal wells in operation
- carbon capture and storage, due to the large net volumes of injected fluids, may have the potential for inducing larger seismic events.

The risks from wastewater injection are deemed manageable through engineering controls (injection pressures and volumes can be with modified according to the capacity of the target aquifer). However, it is not known what impact a significant increase in the number of injection wells will have on induced seismicity over the long term (NRC 2012).

Apart from the induced pressure gradients and flow rates acting to change the dynamics of the flow system, subsurface connectivity could be altered at a fault by the offset of the aquifer and aquitard layers. The permeability of the fault may also change following an earthquake for reasons mentioned earlier. In addition, aquitard integrity may be decreased as the result of brittle deformation in the vicinity of the fault following displacement.

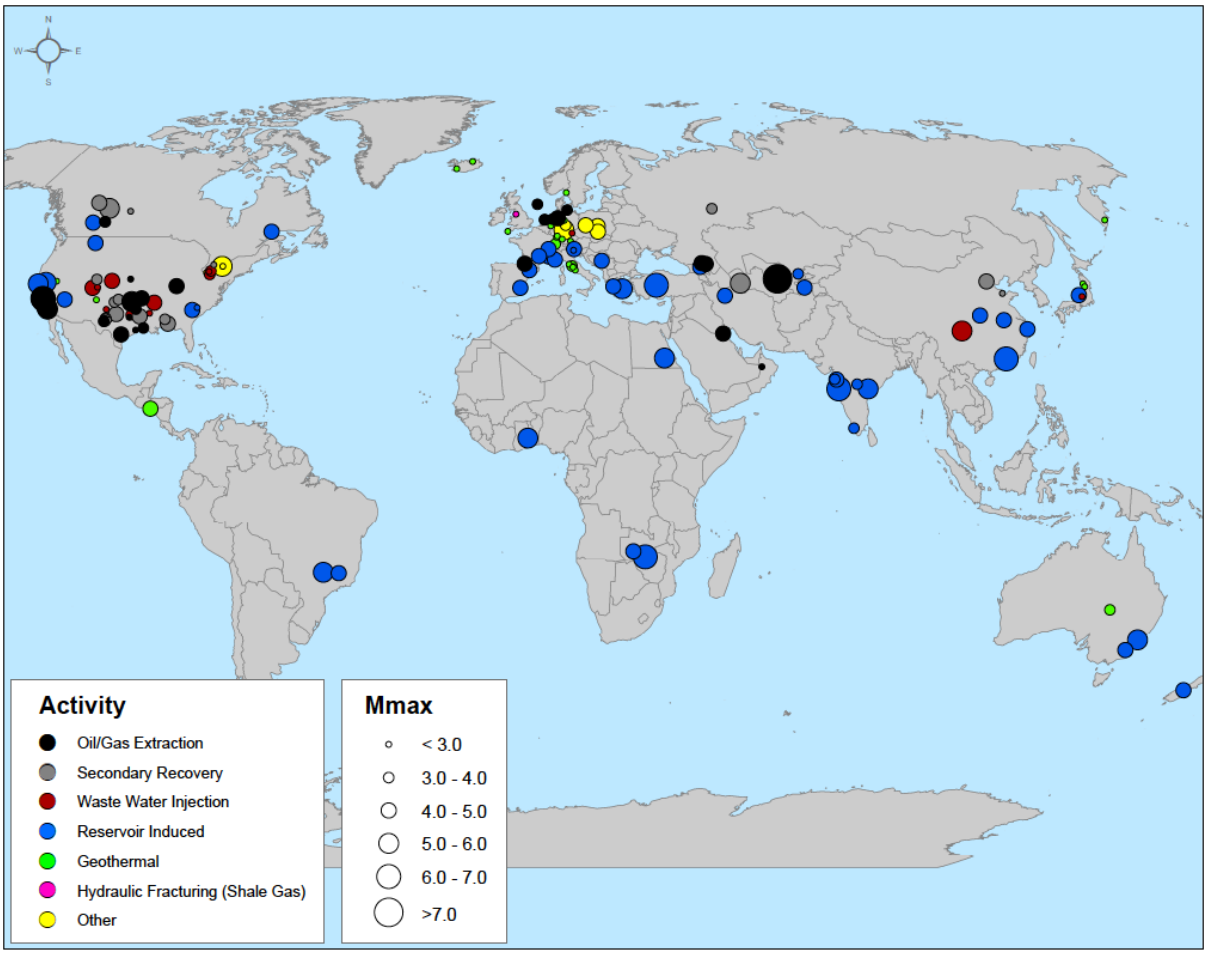

Figure 13 Locations of known or suspected induced seismicity from anthropogenic activities. The size of the symbol at each site corresponds to the measured maximum earthquake magnitude reported (© Copyright, NRC 2012).

4.5 Boreholes

Boreholes can provide a direct conduit for flow and solute transport between what may otherwise be disconnected aquifers (Chapter 2). The integrity of aquitards can be compromised by quarries, unsealed bores, abandoned bores or multi-aquifer wells (Cherry et al. 2004; Lacombe et al. 1995). All of these can provide a new pathway or create a short-circuit in the subsurface. A short-circuit refers to the case where water flows between aquifers with different hydraulic heads via the borehole or a preferential pathway associated with the construction of the borehole (fracture or void in the grout in the annular space).

The hydraulic conductivity of a well K_w is written as (Sudicky et al. 1995):

$$K_w = \frac{r_s^2 \rho g}{8\mu}$$

where r_s is the radius of the well [L]. The other terms are defined in Chapter 2 and the Abbreviations list. Consider a 10.16 cm-diameter well (i.e. four inches, typical size for a monitoring well). Using the equation, the hydraulic conductivity of the well (flow is along the axis of the well) is approximately 2.4×10^8 m/d. The hydraulic conductivity of a

15.24 cm-diameter well (six inches, typical size for a residential drinking water supply well) is approximately $5.5x10^8$ m/d. From these examples it is quite clear how many orders of magnitude greater the hydraulic conductivity of an open well can be compared to the geologic materials in which they are constructed (see Table 1). Thus, even small-diameter bores can have a significant impact on the effective vertical hydraulic conductivity of an aquitard.

Hart el al. (2006) noted that their laboratory measurements of vertical hydraulic conductivity in a shale aquitard was one to three orders of magnitude lower than the values needed for the same unit to calibrate flow in their regional-scale numerical simulations. The bulk vertical hydraulic conductivity of the shale could be increased from laboratory values to model estimates by: (i) 50 micron fractures spaced 5 km apart that extend the entire thickness of the shale, or (ii) 50 wells of 0.1 m radius through the shale and evenly spaced by 10 km. In both cases, it is clear that it only takes a few small preferential pathways to have a significant impact on permeability of an aquitard. Unfortunately, the extent and quality of data from well records (location, construction details, geology, etc.) is not always sufficient to determine their contribution to increased aquitard permeability. Rather, this is often postulated in groundwater studies but cannot be definitively distinguished from other forms of preferential pathways (Hart et al. 2006). Numerous analytical models have been developed to help estimate the influence of borehole leakage effects on pressure responses and solute transport (e.g. Celia et al. 2011; Cihan et al. 2011; Javandel et al. 1988).

Improper construction of new wells also increases the risk of reducing aquitard integrity. There is also concern about the performance of existing wells given the integrity of steel casing over time, changes in grouting technologies and previous regulations or lack thereof (Watson & Bachu 2009). Grout is used to fill and seal the annular space between the drilled hole and the well casing and to fill and ‘plug’ the well in the case of a decommissioned well. An ideal seal would be one that serves to maintain the subsurface conditions as if the well were not even there. Grout is typically a mix of cement, bentonite clay and water – the ratios of which determine its hydraulic, strength and deformation characteristics. Grouts, like aquitard materials, are not impervious by nature but can ideally be appropriately designed for the application. In practice, cement bond logs can be used to interpret the integrity of the grout seal in the annulus around the well casing during construction.

The Nebraska Grout Study (Lackey et al. 2009; Ross 2010) was the first of its kind to rigorously evaluate the performance of various grouting methods used in domestic well construction in Nebraska, US. Between 2001 and 2007, 63 observation wells located at five sites were constructed under the guidance of representatives from the Nebraska Well Drillers Association, the Nebraska Department of Health and Human Services, the Conservation and Survey Division, the Nebraska Department of Environmental Quality, and industry grout suppliers. The goal was to make the ‘ultimate well’. Wells were constructed to certain specifications using different grout mixtures. Clear PVC casing was used to allow for observations to be made from within the borehole. Video surveys of the grout were performed on a regular basis and were also used during dye tests conducted two years after well construction. In short, the tests showed that the grouts performed worse than expected in the unsaturated zone due to the formation of voids and preferential pathways (the most important place to prevent surface contamination from short-circuiting into the subsurface). In general, grouts performed as expected below the water table.

In conclusion, the drastic difference in hydraulic conductivity between wells and geologic media results in only a few, small-diameter boreholes through an aquitard being needed to significantly increase its bulk vertical hydraulic conductivity. Similarly, leaky grout seals my acts as preferential flow paths from the surface and/or between aquifers. The establishment

of best practices and regulations will help to mitigate some of the associated problems with wells needed for large-scale hydrocarbon extraction and co-produced water disposal. However, as the Nebraska Grout Study (Lackey et al. 2009) showed, grout technologies are still developing and there is a lack of data to validate their long-term performance. These issues in combination with the proposed density of coal seam gas extraction wells (and potentially co-produced water injection wells) being installed by different operators increases the uncertainty of changes in aquifer connectivity both syn- and post-production. Publically available bore integrity information, such as cement bond logs, would be useful for investigating and evaluating changes in aquifer connectivity due to leaky grout seals.

4.6 Discussion and conclusions

This chapter highlighted the significant contribution that natural (i.e. fractures and faults) and manmade (i.e. boreholes) structures can make to increasing aquifer connectivity because they can act as preferential pathways for flow and contaminant transport. An overview of mechanical deformation mechanisms and hydraulic fracturing were also provided. The hydraulic characterisation of natural fracture networks at all scales is challenging as their locations are not easy to predict. The same degree of difficulty would be incurred when assessing changes in aquifer connectivity from coal seam gas and coal mining operations since most of the induced fractures are propagated extensions of the natural fracture network.

The NRC (2010) report highlights ‘connectivity’ in this context as a major data gap and uncertainty. The research and findings summarised in this chapter support this conclusion and reiterate the same for the consideration of changes in aquifer connectivity. Part of this is due to the typical ‘model rich, data poor’ issues often faced in hydrologic studies. The lack of consideration for deformation mechanisms in groundwater modelling noted by Botha and Cloot (2004) suggests that the science might actually be ‘model poor, data poor’ in this respect.

As demonstrated, aquifer connectivity, expressed in terms of flux, can change from natural conditions solely by changing the hydraulic gradient. Mine dewatering, coal seam depressurisation and co-produced water reinjection are all examples of how this could be achieved in the given context. Uncertainty lies in what happens to the natural system as operations come online over time (i.e. cumulative impact) and after the resources have been exhausted and the infrastructure is decommissioned. This is particularly the case for the situation where aquifer connectivity has been enhanced by the creation of new preferential pathways (i.e. fractures in aquitards, leaking borehole seals, reactivated faults, etc.) that will remain in place post-production. Finally, a better understanding of the interplay between changing hydraulic conditions, in situ stress, mechanical deformation, fluid properties and hydrogeologic characteristics and the subsequent implications for changes in aquifer connectivity is needed.

5 Aquifer connectivity in the Great Artesian Basin

5.1 Introduction

The GAB is a complex hydrogeological system of aquifers and aquitards of mostly continental Jurassic and Cretaceous deposits stretching across the arid and semi-arid interior of Queensland, New South Wales, South Australia and the Northern Territory (Figure 1).

The GAB is a groundwater basin, with its boundaries defined by groundwater conditions as well as geology (Smerdon et al. 2012). It encompasses several geological basins which are generally separated from each other by major geological structures (e.g. arches, rises or ridges) (Figure 14). The most important geological basins in the GAB are the centrally-located Eromanga Basin, the Carpentaria Basin in the north and the Surat Basin in the east. The most eastern part of the GAB is the Clarence-Moreton Basin. The upper and lower stratigraphic boundaries of the GAB are major unconformities (i.e. prolonged periods of erosion without deposition of sediments).

As these basins were situated on the Eastern Plate boundary of Australia during the Mesozoic era, it is not surprising that the depositional and tectonic evolution of these basins is very similar. There are however distinct differences in the timing of subsidence, sedimentation and uplift between the basins, which are mostly due to structural features inherited from the underlying basins (CSIRO 2012a; CSIRO 2012b; CSIRO 2012c).

Traditionally, some of these older underlying basins, such as the Permien age Galilee Basin and Bowen Basin, were considered as integral parts of the GAB (Habermehl 1980), mostly because of the good hydraulic connection with some sections of the GAB. In this study, for modelling purposes, the GAB assessment has focused on aquifers of the Jurassic and Cretaceous period, which comprise the major part of the GAB and are present across the entire Basin (CSIRO 2012a; CSIRO 2012b; CSIRO 2012c). Other geological formations within the GAB, such as certain Triassic sediments may represent significant groundwater resources and are managed under the Queensland GAB Water Resource Plan (DNRM 2014a).

This chapter will describe the GAB, while chapter 7 and chapter 8 describe in detail the aquifer connectivity with and within the Galilee and Bowen Basins. The Surat Basin, an integral part of the GAB and a high potential for coal mining and coal seam gas development, will be described separately in more detail in chapter 6.

To understand aquifer connectivity in the GAB and the potential impacts of CSG development or coal mining, it is essential to have a thorough understanding on how the geological evolution of the basin affects the stratigraphy and structural geology (summarised below from CSIRO (2012a), CSIRO (2012b) and CSIRO (2012c)). After describing these, more attention will be devoted to the hydrogeological aspects related to aquifer connectivity such as the aquifer and aquitard hydraulic and geomechanical properties as well as the current understanding of recharge and hydrochemistry. An overview is also presented of current and past groundwater modelling of the GAB.

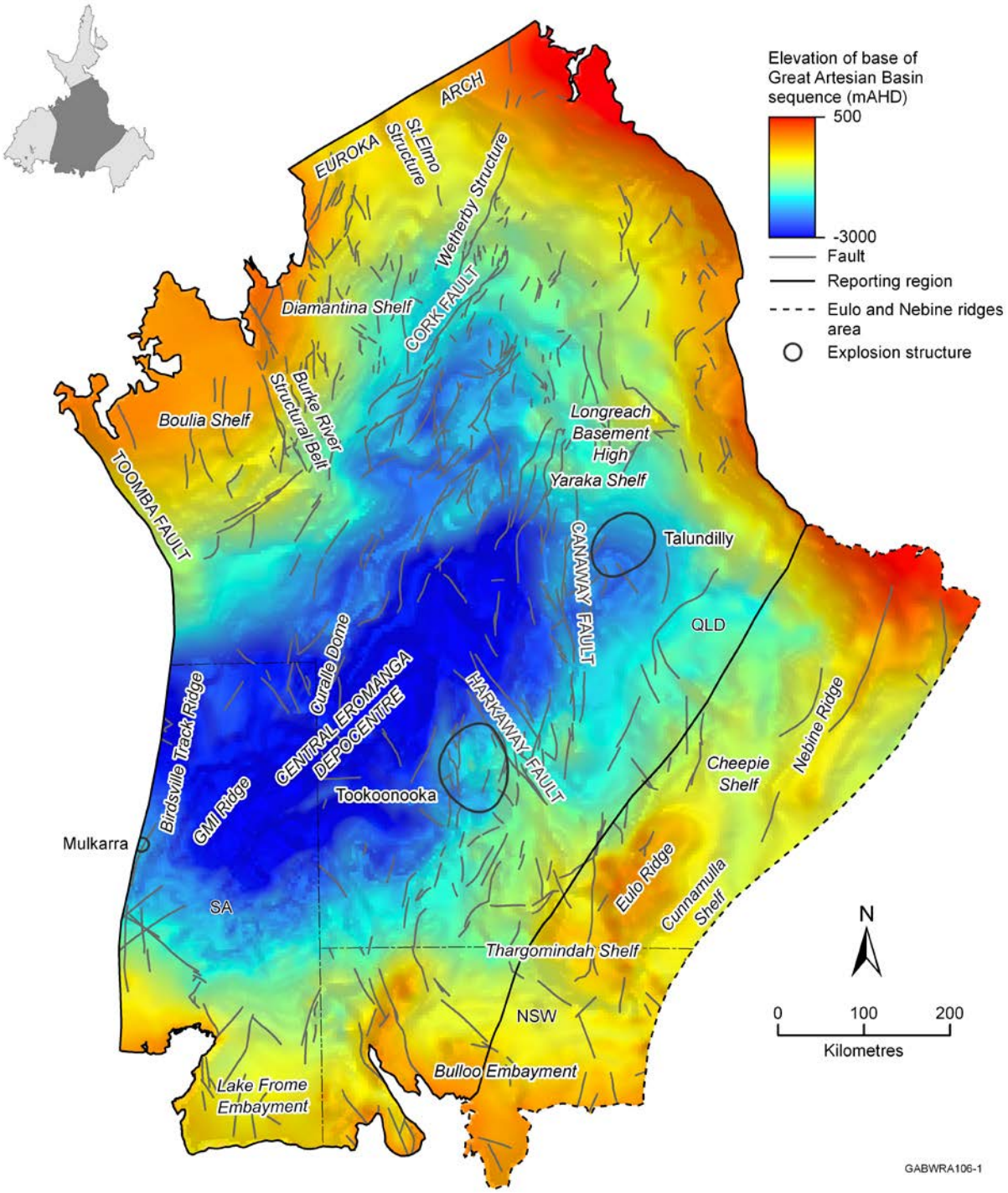

Figure 14 Structural features of the central part of the Eromanga geological Basin of the Great Artesian Basin hydrogeological system (© Copyright, CSIRO 2012b).

5.1.1 Geology

At the end of the Triassic period around 200 Ma, eastern Australia was subject to gradual and extensive erosion, which led to the development of a large area of slight topographic relief. In the early Jurassic period, intracratonic subsidence commenced in eastern Australia,

initiating sedimentation in the Clarence-Moreton, Surat and Eromanga Basins. The subsidence was linked to westward-directed subduction under eastern Australia. Subsidence, in combination with subduction, resulted in a basin with a cratonic source of mostly coarse quartzose sediments in the south-west and a volcanic source of finer sediments to the east.

A system of braided rivers that drained to inland lakes and swamps deposited relatively thin but continuous and widespread accumulations of sand-dominated sediments in the Early Jurassic. This system initiated in the east, in the Clarence-Moreton Basin and extended westwards. The sediments covering the basal unconformity are therefore diachronous (i.e. the same formation becomes younger towards the west).

During the Early Cretaceous, around 110 Ma, an extensive marine inundation occurred across eastern Australia due to a period of high subsidence. This lead to the deposition of a thick sequence of marine shales, interspersed with thin sandstone units from minor regressive cycles.

The eastern highlands started to rise about 90 Ma in the Late Cretaceous. This uplift increased the influx of erosional material across eastern Australia, which caused a relative drop in sea-level and the establishment once again of continental conditions. These consisted of a floodbasin of coal swamps and lakes, drained by a meandering fluvial system.

The Eromanga and Surat Basins became inverted in the Eocene through reactivation of pre-existing faults in the basement. Uplift and subsequent denudation in the Surat Basin was asymmetric with up to 2.5 km of denudation in the east, while this was limited to less than 1 km on the western side of the basin. Deformation during the uplift was mainly accommodated through folding in the Surat Basin, while in the Eromanga Basin the deformation led to re-activation of faults across the sediment sequence. Displacements on these faults are similar or larger than the formation thicknesses. These faults therefore can form barriers to lateral flow and thus compromise the lateral continuity of the GAB aquifers, while providing vertical pathways for flow and transport across aquitards.

Both Basins were subject to a number of denudation and weathering cycles (around 60 Ma, 30 Ma and 7 Ma) that resulted in lateritic surfaces. Compression in the Miocene reactivated several faults and culminated in the uplift of the Eastern Highlands. This created the westward tilt of the GAB and initiated the current groundwater flow patterns and artesian conditions in the GAB.

5.2 Major aquifers and aquitards

The main aquifers are situated in the Jurassic continental deposits, while the predominantly marine Cretaceous mudstones from the Rolling Downs Group form the main confining sequence for the GAB. Within the Rolling Downs Group, the permeable Winton-Mackunda Formations represent a return to continental conditions.

The hydrostratigraphy in Figure 15 is the most recent basin-wide interpretation of the lithostratigraphy in a more nuanced classification including aquifers, partial aquifers, leaky aquitards, tight aquitards and aquicludes rather than just aquifers and aquitards (CSIRO 2012b).

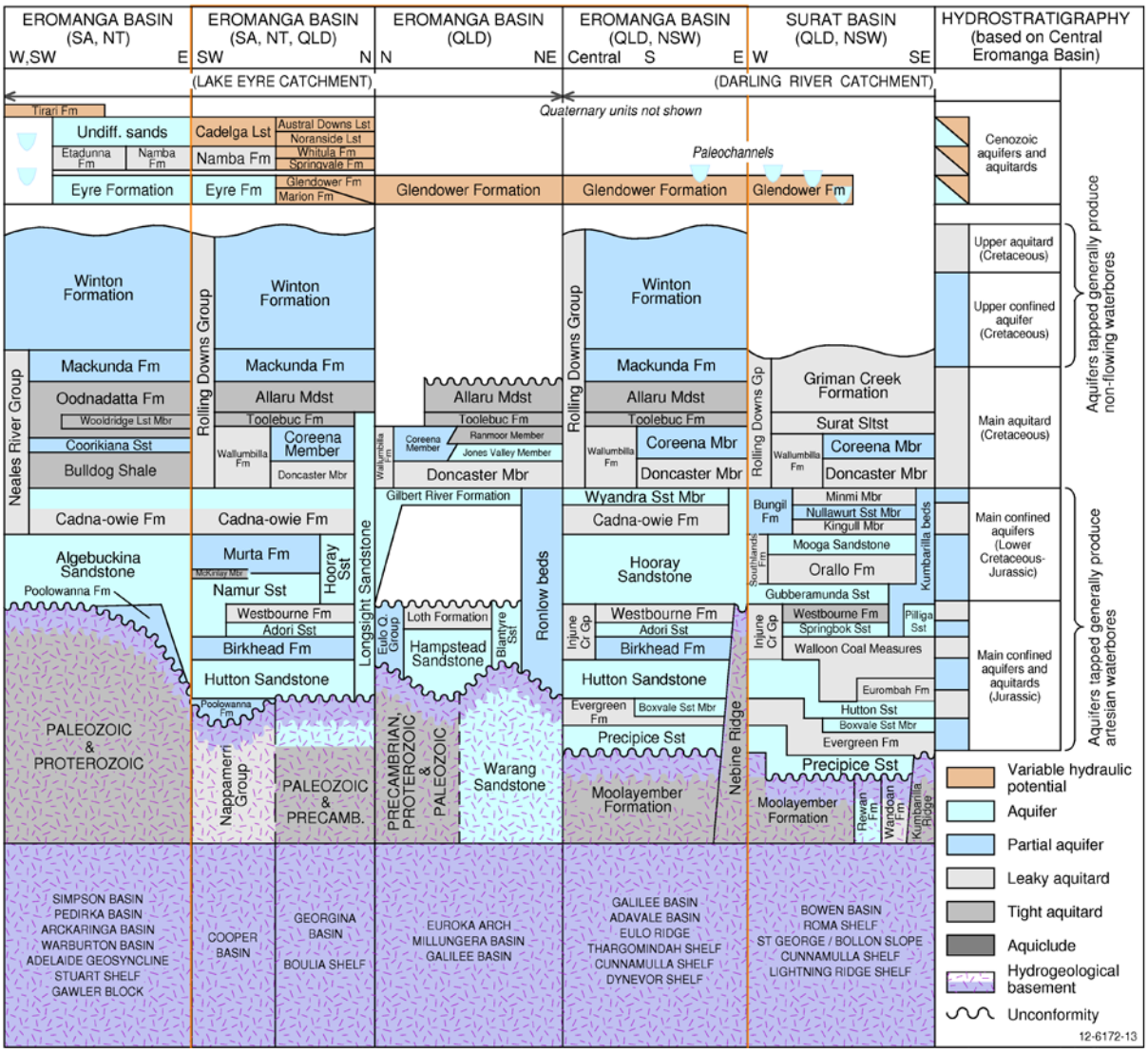

Figure 15 Lithostratigraphic table of the Eromanga and Surat Basins in the Great Artesian Basin with hydrostratigraphic interpretation (© Copyright, CSIRO 2012b).

The GAB consists of a very complex stacking of multi-layered aquifers, separated and often only partly confined by aquitards (Figure 15). The hydrogeologic characteristics of most individual aquifers are fairly uniform over large areas and they are continuous and hydraulically connected within each geological basin.

The Clematis Sandstone is traditionally seen as the deepest aquifer, although it is not strictly part of the GAB since it is Triassic in age and situated below the GAB basal unconformity. The first aquifer above the unconformity is the Precipice Sandstone. Figure 15 shows the diachronic nature of this formation; deposition started in the east in the Surat Basin and moved westwards into the central part of the Eromanga Basin. The Hutton Sandstone, separated from the Precipice Sandstone by the Evergreen Formation, is even more widespread and can also be found in the west of the Eromanga Basin. These formations do not occur in the Carpentaria Basin, where the first aquifer above the unconformity is the Hampstead Sandstone.

The Walloon Coal Measures act as a leaky aquitard in the Surat and Clarence-Moreton Basins, confining the Hutton Sandstone. In the Eromanga Basin this formation is confined by the Birkhead Formation. On top of the Birkhead Formation, the Adori Sandstone forms a minor aquifer. Its equivalent in the Surat Basin is the Springbok Formation. In both the Eromanga and Surat Basins the Westbourne Formation separates these lower aquifers from the Cadna-Owie Formation and Hooray Sandstone units that form the major aquifer system in the GAB, referred to collectively here as the Cadna-Owie-Hooray aquifers.

The Cadna-Owie-Hooray system occurs throughout the GAB, across basement highs and consists of several interconnected aquifers. Its equivalent in the Surat Basin encompasses the Gubberamunda, Mooga and Pilliga Sandstones, while in the west of the Eromanga Basin it corresponds to Algebuckina Sandstone and in the north, in the Carpentaria Basin, to the Gilbert River Formation. There is an unconformity below the Gilbert River Formation representing a hiatus in deposition in the Lower Cretaceous.

The formations of the Rolling Downs Group form the confining layer for the Cadna-Owie-Hooray aquifer system, especially the Doncaster member, the Wallumbilla and Toolebuc Formations and the Allaru Mudstone. The Mackunda and Winton formations form the shallowest aquifer system in the Eromanga Basin but are not present in the Surat Basin.

5.3 Structural properties

During the Cenozoic inversion of the Eromanga and Surat Basins, structural features and trends in the underlying basins were reactivated. This resulted in significant folding and faulting in the Eromanga Basin, while most of the deformation in the Surat Basin was accommodated through folding of the formations. The Eromanga Basin therefore is more structurally compromised than the Surat Basin.

Figure 14 showed the main structural elements in the Eromanga basin. The disruption of the sedimentary sequence in the Eromanga Basin during the 50 Ma GAB inversion is mainly manifested through vertical displacements. These can amount to 780 m on the Curalle Dome, 400 m on the Canaway Fault, up to 300 m on the Harkaway Fault and 420 m on the Cork Fault. Compared to the average thickness of the Cadna-Owie-Hooray aquifer system of about 200 m (with a maximum up to 350 m), it is clear that this episode of deformation has greatly affected fluid flow and transport. It not only affects the lateral continuity in aquifers and impedes regional groundwater flow, it also creates preferred pathways of fluid migration. The effect of these faults has been documented in numerous cases through large drops in potentiometric surface and water table near these structures and the occurrence of springs (CSIRO 2012a; CSIRO 2012b; CSIRO 2012c; Love et al. 2012).

While not tectonic in nature, polygonal faulting represents an important phenomenon compromising the integrity of especially the confining units of the Rolling Downs Group in the Eromanga Basin. Polygonal fault systems are comprised of laterally extensive arrays of extensional faults having polygonal planform geometry (Cartwright 2011). The genesis and mechanism of this kind of faulting are still not well understood, although the current thinking is that it is related to diagenetic changes in the mineralogy and pore water composition of the sediment after burial that led to dissolution of grains or alterations to mineral-fluid or mineral-mineral interactions. These changes at the grain size level can lead to shear-failure of the sediment.

Throughout the central part of the Eromanga Basin, evidence of polygonal faulting can be found as discrete, kilometre-sized basins bounded by a polygonal pattern of faulted, anticlinal ridges. The distinct polygonal planform geometry was first discovered through 3D seismic mapping (Watterson et al. 2000). The throw along the faults ranges up to 80 m and the size

of the areas bounded by the faults is between 800 m and 2 km. While the fault gouge and slip may result in fault permeability lower than the host rock, any changes in stress field or movement along the fault can create a pathway for fluid and solute migration (Cartwright 2007). Seeing the widespread occurrence and the density of these faults, this structural feature could potentially reduce the capability of the Rolling Downs Group to act as a barrier for flow and transport.

While polygonal faulting is ubiquitous throughout the central part of the Eromanga Basin, no systematic mapping of polygonal faulting has been carried out so far, nor has polygonal faulting been identified elsewhere in the GAB.

5.4 Hydraulic properties

The values of hydraulic properties, such as described in chapter 2, may be obtained from core tests, from field tests such as drill stem tests, pumping tests and slug tests, or they may be estimated independently using calibrated numerical models. The majority of hydrogeological knowledge relating to the GAB is derived from the development of potable groundwater supplies; therefore, the availability of hydraulic property data relating to the hydrogeological units of the GAB is inherently biased toward productive freshwater-bearing units. Conversely, the hydraulic properties of lower permeability layers have been relatively poorly characterised.

5.4.1 Core and field-based estimates

As discussed in chapter 3, when reviewing measurements of the hydraulic property values of aquitards (and to a lesser extent, aquifers) it should be noted that, due to inherent difficulties in obtaining measurements in situ, often such values will be exaggerated due to the effects of depressurisation from the removal of overburden pressure. Gray et al. (1963) highlighted the relationship between permeability and overburden pressure for sandstone units. More recently Gray (1987a; 1987b) has drawn attention to this phenomenon in an Australian context, with particular attention paid to coal seams by Gray (2011).

The foundation work of Habermehl (1980) on the Cadna-Owie-Hooray aquifer system of the GAB estimated the range of values for a number of hydraulic properties, based upon field studies undertaken by the Bureau of Mineral Resources, Geology and Geophysics from 1971 to 1979 (Table 5).

Table 5 Estimated hydraulic properties of the Cadna-Owie-Hooray aquifers of the Great Artesian Basin (from © Copyright, Habermehl 1980).

Property	Units	Minimum	Maximum
intrinsic permeability	mD	10's	1000's
porosity	%	10	30
horizontal hydraulic conductivity	m/d	0.1	10
vertical hydraulic conductivity	m/d	10-4	10-1
transmissivity	m2/d	1	2000
storativity	unitless	10-5	10-4

Field-based estimates of hydraulic property values for the Cadna-Owie-Hooray aquifer from subsequent geological reports and from environmental assessments for proposed mines are summarised (after Welsh 2006) in Table 6. It may be seen that storativity and porosity values

are within the ranges estimated by Habermehl (1980). Ranges of observed hydraulic conductivities and transmissivities are broader than estimated, but are consistent in terms of orders of magnitude.

Table 6 Estimated hydraulic properties of the Cadna-Owie-Hooray aquifers of the Great Artesian Basin from field tests (© Copyright, Welsh 2006).

Reference	K_h (m/d)	T (m^2/d)	S	n_e
Audibert (1976)	0.02 - 82	0.1 - 2295	mean = $2.5x10^{-4}$	mean = 0.21
RUST PPK (1994)	1 - 13.1	-	mean = $2.7x10^{-4}$	-
Berry & Armstrong (1995)	1.6 - 18.5	5 - 380	-	-
Armstrong & Berry (1997)	0.5 - 22	0.1 - 3200	-	-

K_h= horizontal hydraulic conductivity, T=transmissivity, S=storativity, n_e=porosity.

As part of the GAB Water Resource Assessment (GABWRA) (CSIRO 2012a; CSIRO 2012b; CSIRO 2012c), measurements of porosity and permeability recorded in databases maintained by the state governments of Queensland and South Australia were collated and summarised. The results for the Central Eromanga region of the GABWRA are summarised in Table 7 (CSIRO 2012b). Data scarcity in both the Western Eromanga and Carpentaria regions precluded the creation of similar summaries for those regions (CSIRO 2012a; CSIRO 2012c). Mean porosity values are reasonably consistent, with no apparent trend with depth. Mean permeability values range from 96 mD in the Cadna-Owie Formation up to 813 mD in the Adori Formation.

Table 7 Porosity and permeability measurements for various Great Artesian Basin units (© Copyright, CSIRO 2012b).

Unit	Porosity		Horizontal permeability		
	n	mean (%)	n	mean (mD)	equivalent K_h* (m/d)
Cadna-Owie Formation	405	15	331	96	0.09
Hooray Sandstone	4438	16	4222	131	0.12
Westbourne Formation	951	14	896	105	0.10
Adori Formation	64	22	71	813	0.77
Birkhead Formation	1578	14	1348	130	0.12
Hutton Sandstone	2928	17	2687	452	0.43

K_h=horizontal hydraulic conductivity; * K_h equivalents are provided for comparison purposes only and are calculated from mean permeability values using the equation defined in chapter 2 and using values of g=9.8 m/s^2, ρ=997.0479 kg/m^3, and μ=8.91x10^{-4} kg/[m.s], the latter two of which assume fresh groundwater with a temperature of 25^{o}C.

The GABWRA project (CSIRO 2012b) also described the spatial variability of horizontal permeability for the Cadna-Owie Formation, the Hooray Sandstone, the Birkhead Formation and the Hutton Sandstone. The permeability of each of these units essentially follows a common spatial trend: high values are observed close to the recharge beds in the east and permeabilities decrease with depth toward the Eromanga Basin depocentre.

A similar summary of permeability and porosity measurements in the Queensland region of the Eromanga Basin was presented by Bradshaw et al. (2010) and is provided in Table 8. The sample sizes used by Bradshaw et al. (2010) to calculate mean porosities and median permeabilities differ significantly from those used by CSIRO (2012b), although mean porosity values are reasonably consistent. Median permeabilities are orders of magnitude smaller than those reported by CSIRO (2012b) but this may be due to the different statistical measure and/or datasets used in the analyses.

Table 8 Porosity and permeability measurements for various Great Artesian Basin units (© Copyright, Bradshaw et al. 2010).

Unit	**Porosity**		**Horizontal permeability**		
	n	**mean (%)**	**n**	**median (mD)**	**equivalent K_h* (m/d)**
Wyandra Sandstone	42	21.8	222	0.4	3.8×10^{-4}
Hooray Sandstone	1984	17	1834	4.5	4.3×10^{-3}
Adori Sandstone	82	19.8	78	403	0.38
Hutton Sandstone	1984	17	2321	91	0.086
Lower Poolowanna Formation	525	12	489	6.4	6.1×10^{-3}

K_h=horizontal hydraulic conductivity; * K_h equivalents are provided for comparison purposes only and are calculated from mean permeability values using the equation defined in chapter 2 and using values of g=9.8 m/s^2, ρ=997.0479 kg/m^3, and μ=8.91x10^{-4} kg/[m.s], the latter two of which assume fresh groundwater with a temperature of 25^{o}C.

5.4.2 Model-based estimates

As discussed in chapter 3, estimates of hydraulic properties obtained from inverse models assume a correct choice of conceptual model and are therefore inherently subject to uncertainty. Since models are always imperfect representations of reality, inaccuracies in estimated values may be due to compensatory effects, such as accounting for misrepresentations of model stresses such as recharge and discharge or other conceptual model choices (Doherty & Welter 2010).

Since the late 1970s, groundwater models have been developed to represent various parts of the GAB. A summary of these models was provided in Smith and Welsh (2011). In early models such as GABSIM (Ungemach 1975) and GABHYD (Seidel 1978) parameter values were specified, based upon available hydrogeological observations. Alternatively, the parameterisation of numerical models may be based upon the calibration of model outputs to observations; for example, hydraulic head measurements. The development of two basin-scale groundwater flow models, GABFLOW (Welsh 2000) and GABTRAN (Welsh 2006), used this method of estimating spatially distributed hydraulic property values.

GABFLOW, a single layer steady state flow model, used horizontal hydraulic conductivity values for the Cadna-Owie layer ranging from $1x10^{-3}$ to 40 m/d and transmissivity values ranging from 0.03 to 10033 m^2/d. GABTRAN, a transient flow model, used horizontal hydraulic conductivities of 0.1 to 20 m/d, transmissivities of up to 22629 m^2/d, specific storage values of $7x10^{-6}$ to $7x10^{-3}$ and specific yield values of $8x10^{-6}$ to 0.155.

5.5 Geomechanical properties

A range of geomechanical properties for GAB aquifers and aquitards are of relevance to assessing the potential for induced mechanical deformation, fracturing and seismicity. Such properties may include geological unit permeabilities; shale volume data for aquitard seals; the location, type and throw of faults; horizontal and vertical stress directions and magnitudes; and the volumetric rates of fluid extraction involved in mining operations. Borehole leakage presents an additional hazard of intensive drilling operations. Currently, there are no published syntheses of geomechanical properties in the GAB, nor published studies of the potential for induced geomechanical stresses resulting from mining operations.

5.5.1 Properties relating to induced geomechanical stresses

Pressure and permeability data are available from the CSIRO PressurePlot database and from relevant state government databases such as the Queensland Petroleum Exploration Database[1] (DNRM 2014b) and the South Australian Resources Information Geoserver (SARIG 2014). As described in section 5.3, permeability data for the GAB were recently summarised by GABWRA (CSIRO 2012a; CSIRO 2012b; CSIRO 2012c), as were temperature data. The clay composition of GAB aquitards is poorly characterised, particularly spatially. The locations of significant faults in the GAB have been well-documented and have also been summarised recently by GABWRA (CSIRO 2012a; CSIRO 2012b; CSIRO 2012c) from foundation works by the Geological Survey of Queensland (GSQ). Fault types and throw information may also be obtained from Geological Survey of Queensland Bulletins. Horizontal stress directions at a continental scale may be obtained from the Australian Stress Map (Hillis et al. 1998). Horizontal stress over much of the GAB area is in a northeast-southwest orientation, while the southwest region of the GAB features an east-west orientation. Vertical stress magnitudes are a function of depth (Mildren et al. 2002) and may be estimated from borelog data. Finally, local estimates of future rates of fluid extractions by CSG operations may be obtained from relevant Environmental Impact Statements (EIS). Maximum total extraction rates have been projected at approximately 10 ML/d (Gladstone LNG), 140 ML/d (Arrow), 170 ML/d (Australia Pacific LNG), and 200 ML/d (Queensland Curtis LNG) (SWS 2011).

Future syntheses of such data may subsequently be used in quantitative assessments of the potential for geomechanical effects induced by mining operations, such as the fault analysis seal technology (FAST) methodology of Mildren et al. (2002). Similarly, such data may be used to develop numerical geomechanical and/or hydrogeological models, which may be used to predict the effects of mining activities such as aquifer/aquitard depressurisation. In summary, the potential for induced mechanical deformation, fracturing, and seismicity would need to be assessed on a case-by-case basis. This cannot currently be addressed without improved characterisation of geomechanical properties at a local scale.

[1] Queensland Petroleum Exploration Database is managed by the Geological Survey of Queensland, which is part of the Department of Natural Resources and Mines.

5.5.2 Borehole leakage

Boreholes and well construction can significantly affect the connectivity between boreholes (see section 4.5). Borehole leakage in the GAB was investigated by Habermehl (2009). Geophysical logs were acquired from 68 bores in Queensland and from 31 bores in New South Wales. Inter-aquifer leakage was observed in 22 bores while the possibility of leakage was proposed for another 41 bores.

5.6 Groundwater recharge, flow and discharge

5.6.1 Groundwater recharge

Recharge to GAB aquifers occurs predominantly via preferred pathways, such as highly porous interbeds, rock fractures, solution cavities and root cavities (Kellett et al. 2003). Other mechanisms include diffuse recharge through the aquifer matrix and by localised leakage below perennial or ephemeral rivers. Due to significant historical use of the Cadna-Owie-Hooray aquifers, the research relating to recharge processes tends to be focussed on this particular aquifer system. The currently accepted extent of the Cadna-Owie-Hooray aquifer recharge areas was defined by Habermehl and Lau (1997). Recharge occurs primarily in intake beds located along its eastern margin, where aquifer unit outcrops or subcrops occur. Quantitative studies of aquifer recharge in the Eromanga Basin are limited to McMahon et al. (2002), who estimated diffuse recharge at 0.1 to 2 mm/yr, preferential pathway recharge of up to 20 mm/yr, and recharge from leakage below rivers and creeks at 45 to 80 mm/yr. Field investigations of recharge in the Carpentaria Basins have not been undertaken. Recharge on the western margin of the GAB was studied by Love et al. (2000), who used hydrochemistry and isotope studies to estimate a diffuse recharge rate of 0.16 ± 0.08 mm/yr.

The mechanisms, spatial extent and rates of recharge in the western GAB have recently been revised in volume 2 of the report produced by the Allocating Water and Maintaining Springs in the GAB project (AWMS; Wohling et al. 2012). Diffuse recharge was found to be effectively zero along the western margin, with estimates ranging from 0.01 to 1.8 mm/yr and a mean value of 0.15 mm/yr. The significance of ephemeral river recharge and mountain block recharge at isolated locations was identified. Ephemeral river recharge, which had been first proposed by Matthews (1997), was estimated at 380-850 mm/yr for the Finke River and 17-92 mm/yr for the Plenty River (Wohling et al. 2012). These recharge events are however very episodic and associated with major flood events. Mountain block recharge in the Peake and Dennison Ranges was estimated to provide a significant component (10-15 per cent) of groundwater discharge to nearby springs; however, mountain block recharge was not believed to contribute significantly to the broader flow system.

Estimations of recharge using calibrated numerical models are limited to that of Welsh (2006). A single layer groundwater flow model, GABTRAN, was calibrated to observations of hydraulic head, which had been corrected for density effects. Model calibrated resulted in recharge rates of up to 33 mm/yr, with an average of 2.4 mm/yr. Locations of highest rates correlated with the recharge beds of highest elevation in the Great Dividing Range east of Hughenden, Queensland. This was consistent with the work of DNRM (2005), who identified leakage occurring to GAB aquifers from Porcupine Creek north of Hughenden, though the flux was not quantified.

5.6.2 Groundwater flow

Habermehl (1980) characterised groundwater in the Cadna-Owie-Hooray aquifers of the GAB as flowing primarily from the recharge areas of the east-northeast to discharge features

located along the southern margin. In ensuing publications, this interpretation has been further clarified. Radke et al. (2000) used outputs from the GABFLOW model (Welsh 2000) in combination with observed hydrochemical trends to produce a map of groundwater flow directions that is generally consistent with that of Habermehl (1980). Exceptions included northward flow directions in the southwest of the GAB and an apparent groundwater divide west of the Eulo-Nebine Ridge. Recent work by GABWRA (CSIRO 2012a; CSIRO 2012b; CSIRO 2012c) has identified the importance of (a) impermeable faults and (b) correcting measured hydraulic heads to account for density effects when interpolating potentiometric surfaces. For the central part of the Eromanga Basin, faults that are believed to act as barriers to flow were identified according to the magnitude of vertical displacement around the fault. The potentiometric surface developed from hydraulic head observations is shown in Figure 16 for the pre-development period of 1900 to 1920, including the influence of impermeable faults.

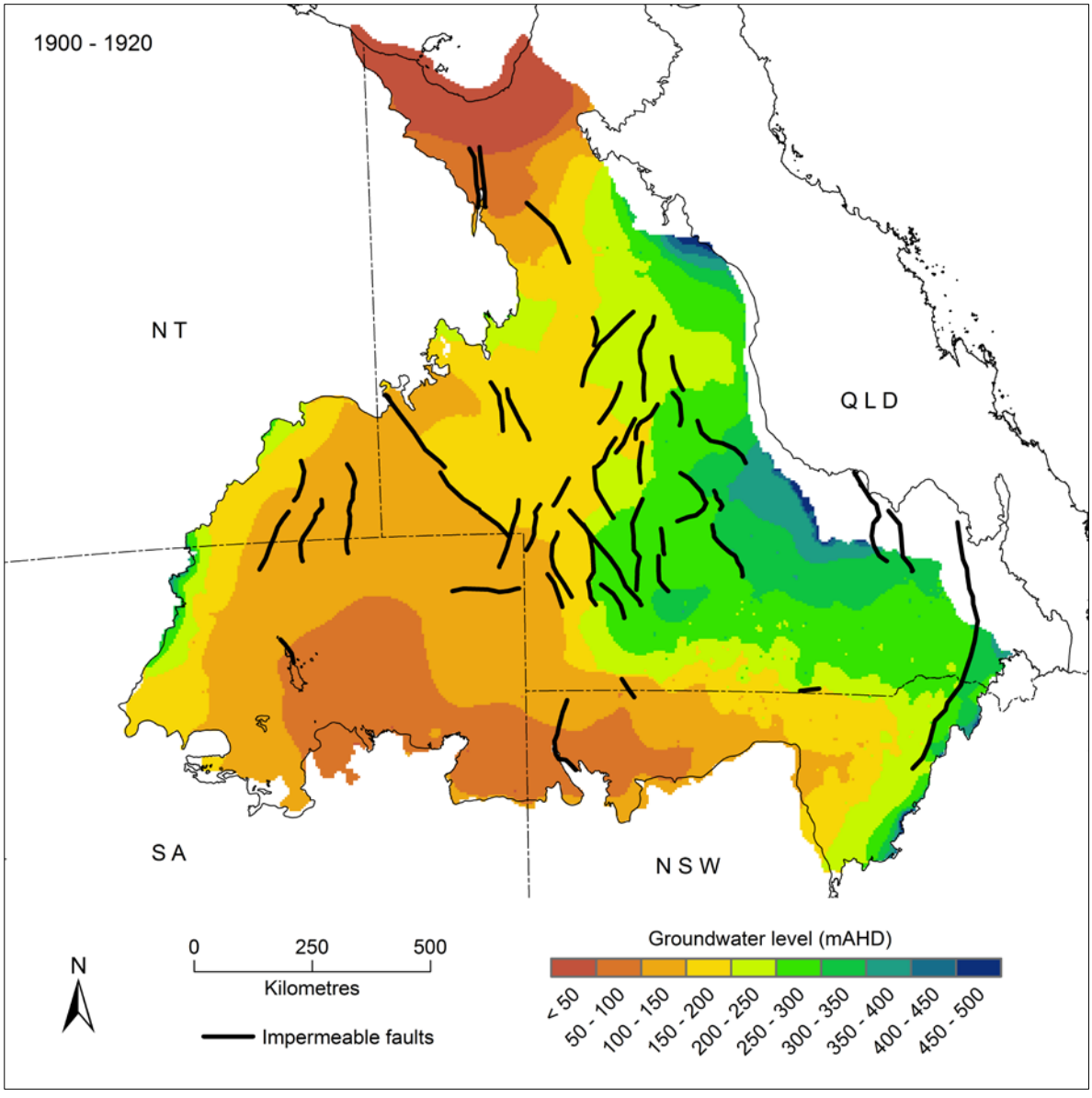

Figure 16 Interpolated potentiometric surface - Great Artesian Basin, 1900 to 1920; including the effects of impermeable faults (© Copyright, CSIRO 2012a; CSIRO 2012b; CSIRO 2012c).

Past characterisations (e.g. Habermehl 1980) of the Cadna-Owie-Hooray aquifers have assumed a steady-state flow system, in which recharge inputs are equal to discharge outputs. Wohling et al. (2012) demonstrated that a groundwater system as large as the GAB is more likely to feature transient flow conditions, in which modern day discharge rates exceed current recharge rates and greatly exceed estimates of historical recharge.

From analyses of discharge spring hydrochemistry in the western GAB, Crossey et al. (2012) concluded that faults play a significant role in the mixing of western GAB groundwaters. Hydrochemical modelling predicted that groundwater flow across major faults in the GAB is characterised by abrupt - rather than continuous - changes in chemistry. The authors also suggested that groundwater flow in the GAB should be conceptualised as a number of discrete flow systems defined by major faults, rather than as a simple continuous flow system.

5.6.3 Groundwater discharge

The discharge of artesian groundwater may occur as diffuse discharge through confining layers or as preferential flow via features such as faults and fractures. Although rates of diffuse discharge may be relatively low (i.e. in the order of millimetres per year), the process may occur over a considerable spatial extent; therefore, the total volumetric discharge may be significant. A field-based study by Woods (1990) estimated diffuse groundwater discharge from the Cadna-Owie-Hooray aquifers in the west of the Eromanga Basin at 0.5 to 4.5 mm/yr. A more recent field study by Costelloe et al. (2008) estimated rates of approximately 35 to 80 mm/yr where salt crusting had formed at the ground surface and rates of less than 1 mm/yr where salt crusting was absent. Through calibration of the GABTRAN groundwater flow model, Welsh (2006) estimated rates of diffuse discharge in the west of the Eromanga Basin at 0.4 to 0.9 mm/yr. Most recently, contributors to the AWMS project (Harrington et al. 2012; Wolaver 2012) have identified the importance of preferential flow mechanisms to groundwater discharge and to flow dynamics in the Cadna-Owie-Hooray aquifers of the west of the Eromanga Basin.

Harrington et al. (2012) used a combination of physical and environmental tracer techniques to quantify diffuse discharge from the Cadna-Owie-Hooray aquifers in the west of the Eromanga Basin. The authors estimated the vertical hydraulic conductivity of diffuse flow though confining shale aquitards at 4.0×10^{-14} to 1.2×10^{-13} m/s, which is equivalent to a discharge flux of 3×10^{-4} mm/yr. Conversely, the vertical hydraulic conductivity of fractures and faults in the confining layers was estimated to be orders of magnitude higher: at least 10^{-9} to 10^{-8} m/s.

In a study of the Dalhousie Springs complex in South Australia, Wolaver (2012) confirmed that discharge to the springs occurs via a major regional fault, as first proposed by Krieg (1989). In this region, the Cadna-Owie-Hooray aquifer system is confined by the overlying Bulldog Shale. The author suggested that, in addition to erosion of the Bulldog Shale in the vicinity of the springs due to tectonic uplift, groundwater discharge occurs via fractures associated with faults in the McHills-Dalhousie Ridge anticline that underlies the springs.

5.7 Hydrochemistry and isotopes

The majority of hydrogeological knowledge relating to the GAB has come from the development of potable groundwater supplies. Therefore, the availability of hydrochemical information relating to the hydrogeological units of the GAB is inherently biased toward productive freshwater-bearing units. Conversely, the hydrochemistry of confining aquitard layers is relatively poorly characterised.

5.7.1 Hydrochemical studies

GABWRA (CSIRO 2012a; CSIRO 2012b; CSIRO 2012c) summarised key works such as Herczeg et al. (1991) and Radke et al. (2000) to provide an up-to-date synopsis of the hydrochemistry (including isotopic studies) of the Lower Cretaceous-Jurassic aquifers of the GAB. Groundwater of the Lower Cretaceous-Jurassic aquifers typically features salinities of 500 to 1500 mg/L total dissolved solids and pH values of 7.5 to 8.5. Groundwater chemistry is typically of sodium-bicarbonate-chloride type, with these ions representing more than 90 per cent of the total ionic strength in most regions of the GAB. In contrast, groundwater in the southwest of the central part of the Eromanga Basin is of sodium-chloride-sulfate type, with sodium adsorption ratios and pH levels both decreasing with proximity to the discharge regions on the western margin. Concentrations of calcium, magnesium and sulfate ions typically decrease downgradient of recharge areas. Conversely, concentrations of bicarbonate and sodium increase along flowpaths, resulting in elevated alkalinities and sodium adsorption ratios, respectively. A number of mechanisms for hydrochemical alteration along flowpaths have been posited. These include changes in the rates and hydrochemical composition of recharge over time; groundwater interactions with aquifer materials, such as cation exchange of calcium and magnesium ions for sodium ions; and mixing with deeper groundwater and/or aquitard leakage of higher salinities. High fluoride concentrations of up to 10 mg/L have been observed in many parts of the GAB and have been attributed to water-rock interactions involving igneous basement strata.

5.7.2 Isotopic studies

Over the last 40 years, numerous studies using stable and radioactive isotopes have been undertaken in order to identify the origins, ages and dynamics of groundwater in the Lower Cretaceous-Jurassic GAB aquifers. A broad range of isotope tracers have been used to measure increasing groundwater ages downgradient of recharge beds (e.g. Mahara et al. 2009; Love et al. 2000; Radke et al. 2000; Bethke et al. 1999; Herczeg et al. 1991; Torgersen et al. 1991; Bentley et al. 1986; Calf & Habermehl 1984; Airey et al. 1983). The results of such studies have enabled the estimation of groundwater travel times and groundwater flow rates. These may subsequently be compared with travel times calculated independently from hydrogeological characteristics or by numerical groundwater models. Large-scale studies of stable isotope ratios for deuterium and oxygen-18 indicate that artesian GAB groundwater is meteoric (rather than connate or magmatic) in origin and have confirmed the role of aquifer subcrop and outcrop locations as recharge zones (Airey et al. 1979). Other isotope concentrations and fractions that confirm the existence of modern recharge areas have been observed in studies using carbon radioisotopes (Airey et al. 1983; Calf & Habermehl 1984). Based upon spatial distributions of chloride, alkalinity, calcium, and delta-carbon-13, carbon-14, and chlorine-36, Radke et al. (2000) hypothesised the existence of a bimodal flow system, in which older groundwater moves one order of magnitude more slowly in deeper regions of the GAB than the younger water of an overlying flow system. Relatively unradiogenic strontium-87/86 ratios have also been observed; these have been interpreted as being a result of water-rock interaction involving igneous basement rocks (Collerson et al. 1988).

5.8 Groundwater modelling

Modelling of the entire GAB groundwater flow system began with models by Ungemach (1975; GABSIM) and Seidel (1978; GABHYD), followed many years later by Welsh (2000; GABFLOW), Welsh (2006; GABTRAN). These models represented only the Lower Cretaceous-Jurassic sandstone aquifers using a single layer discretisation. Modelling of subsections of the GAB began with models of the Olympic Dam borefield (e.g. GAB95 (Berry & Armstrong 1995) and GABROX (AGC 1984)) and of the dewatering impacts of the

Ernest Henry mine (AGC - Woodward Clyde 1995; RUST PPK 1995). More recently, local- to regional-scale models have been developed for mining projects such as Prominent Hill, Mount Margaret and the Olympic Dam expansion (SKM 2010; BHP Billiton 2009; AGE 2007).

As part of recent GABWRA work, Smith and Welsh (2011) reviewed all available and existing groundwater models that represented the GAB to varying extents (horizontally and vertically). Aspects of this review are collated into Table 9. It may be seen that these models feature a wide range of spatial model extents, ranging from small local-scale models of around 5 km^2 in size, to models that represent the entire GAB. Vertical complexity is also variable, though most models represent less than ten relevant hydrogeological layers. None of these models simulated the effects of preferential pathway flow, multiphase flow or geomechanical processes.

Table 9 Summary of hydrogeological models of the Great Artesian Basin (© Copyright, Smith and Welsh 2011).

Model name	Reference	Purpose	Basins	Areal extent (km^2 x 1000)	Layers	Software
Cannington-Osbourne	WMC (2010)	borefield production	Eromanga Basin, Carpentaria Basin	107	1	MODFLOW
EHM regional model	AGC - Woodward Clyde (1995)	mine dewatering	Eromanga Basin, Carpentaria Basin	147	1	MODFLOW
EHM sub-regional	AGE (2010)	mine dewatering	Carpentaria Basin	5	2	MODFLOW
EHM underground mining	Itasca Denver (2011)	mine dewatering	Carpentaria Basin	5	33	MINEDW
GAB95	Berry and Armstrong (1995)	borefield production	unknown	unknown	4	MODFLOW
GABFLOW	Welsh (2000)	water resources	All	1539	10	MODFLOW
GABHYD	Seidel (1978)	water resources	All	1539	1	MODFLOW
GABROX	AGC (1984)	borefield production	unsourced			
GABSIM	Ungemach (1975)	water resources	All	1539	1	MODFLOW
GABTRAN	Welsh (2006)	water resources	All	1539	1	MODFLOW
Mount Margaret project	AGE (1999)	mine dewatering	Carpentaria Basin	5	2	MODFLOW

Model name	Reference	Purpose	Basins	Areal extent (km^2 x 1000)	Layers	Software
Olympic Dam dewatering	BHP Billiton (2009)	mine dewatering	Eromanga Basin	26	8	FEFLOW
Olympic Dam ODEX5	Berry (2005)	borefield production	Eromanga Basin	196	4	MODFLOW
Prominent Hill PH5	SKM (2010)	borefield production, mine dewatering	Eromanga Basin	13	6	MODFLOW

5.9 Aquifer connectivity

From the research presented in the preceding sections, it can be seen that studies of aquifer connectivity in the GAB are relatively few. The hydraulic connection between two aquifers separated by an aquitard will be a function of the hydraulic properties of each of the units, particularly the confining unit. Historically, the GAB was conceptualised as a binary layered system of aquifers and confining beds. A recent reclassification of the hydrostratigraphy of the GAB by GABWRA (CSIRO 2012a; CSIRO 2012b; CSIRO 2012c) has expanded the definition of confining unit to include three aquitard types of varying hydraulic conductivity: leaky aquitards, tight aquitards and aquicludes. Distinctions are also now made between aquifers and partial aquifers. The classification of a given hydrogeological unit is also spatially dependent. This revision was motivated by various observations of aquifer connectivity throughout the GAB. Anomalous decreases in potentiometric pressure that are coincident with major displacement faults have been observed in the northeast of the Eromanga Basin. The Eromanga Basin depocentre features widespread faulting and displacement of aquifers. As described in section 5.2, polygonal faulting has been observed in the Rolling Downs Group aquitard throughout the deeper regions of the central part of the Eromanga Basin. In summary, significant tectonic disruption of the Eromanga Basin has compromised the sealing capacity of (what were traditionally viewed as) confining beds in many parts of the Basin.

The connectivity between hydrogeological units may also be inferred from the vertical hydraulic gradient between them. As described in section 5.5, in a deep basin such as the GAB hydraulic heads need to be corrected to account for the confounding effects of varying groundwater densities. The GABWRA project produced pressure elevation plots in which pressure differences between coincident bores or piezometers (i.e. one sited in the watertable aquifer, the other sited in the Cadna-Owie-Hooray aquifers) were compared. Differences were calculated for three study areas in the GAB (Figure 17(a)) and are presented in Figure 17(b) below.

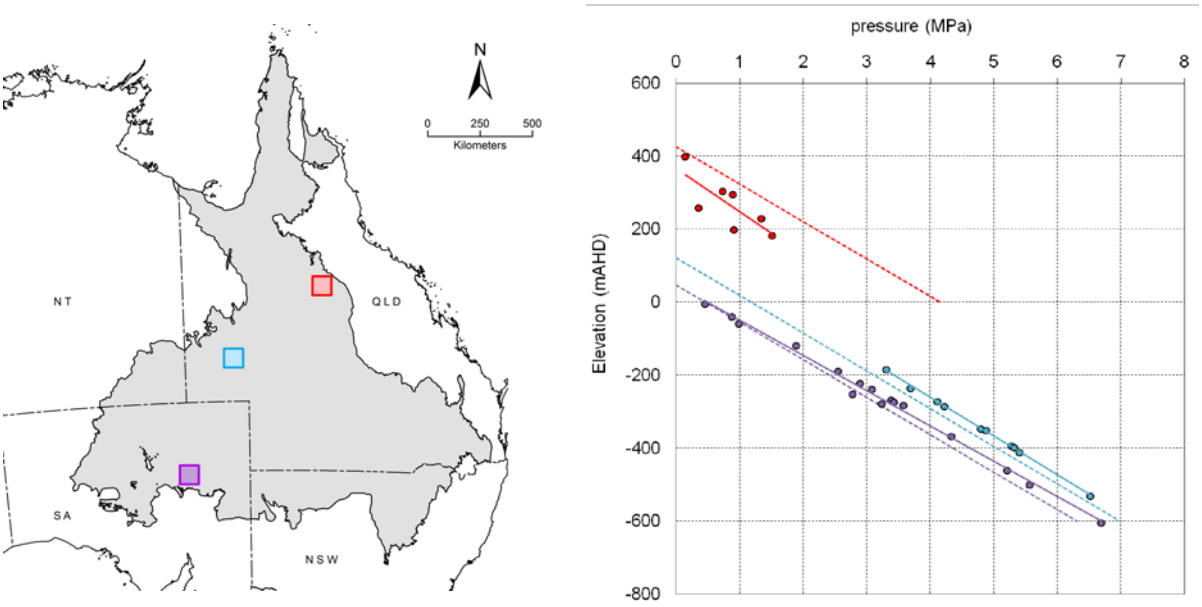

Figure 17 (a) Left-hand side map shows locations of pressure-elevation studies in the Eromanga Basin and (b) right-hand side graph shows pressure-elevation plots for locations indicated (© Copyright, CSIRO 2012b).

Dashed lines represent the hydrostatic gradients for each study area and solid lines represent the observed trend in vertical flow. Trend lines derived from observed data that plot below the hydrostatic gradient indicate downward pressure gradients. This is true for the red data series, which was observed in a recharge area on the eastern margin of the Basin. Conversely, trend lines that plot above the hydrostatic gradient indicate upward pressure gradients. This is true for the remaining data series, which were observed in the west (blue) and south (purple) of the Basin.

Currently, there have been no significant studies of stress-induced connectivity in the GAB. Similarly, studies of aquifer connectivity using hydrochemical or isotopic methods are limited. Borehole leakage in the GAB was identified in a limited study by Habermehl (2009). Recent studies of groundwater discharge in the GAB represent some of the most relevant research relating to aquifer connectivity to-date. Various discharge studies have identified the role of faults and fractures as preferential paths for groundwater flow (Crossey et al. 2012; Wolaver 2012). Other studies have quantified the rate of diffuse vertical leakage from GAB aquifers which, although often infinitesimal, can occur over broad areas and thereby constitute a significant component of groundwater fluxes (Harrington et al. 2012).

5.10 Knowledge gaps

The following knowledge gaps relating to aquifer connectivity in the GAB have been identified in this review:

- Currently available measurements of hydraulic properties are sufficient for a general characterisation of GAB hydrogeological units. However, in order to address regional or local-scale groundwater management issues, location-specific hydrogeological characterisation would be required. In comparison to aquifers, the hydraulic properties of aquitards have been relatively poorly characterised and summaries of the hydraulic properties of aquitard units are not currently available. For example, the summaries of

geological unit permeabilities by CSIRO (2012b) and Bradshaw et al. (2010) presented here focus predominantly on the properties of aquifer (mostly sandstone) units.

- In comparison to differences in hydraulic properties between hydrogeological units, the variability of properties within units is poorly characterised. In the past, this has contributed to a simplified conceptualisation of vertical connectivity in the GAB, involving lateral flow through aquifers that are confined by aquitard units. The recent reconceptualisation of the GABWRA (CSIRO 2012a; CSIRO 2012b; CSIRO 2012c) has expanded the classification of aquitard units to account for the variability of hydraulic properties. For the purposes of addressing groundwater management issues, such variability would need to be characterised at a regional or local scale.
- In-depth studies of the geomechanical properties of GAB units have not been undertaken. Consequently, the potential for changes in hydraulic properties due to changes in stress regimes has not been studied in the GAB. National-scale datasets of horizontal stress directions and magnitudes are available; however, for the purposes of addressing groundwater management issues, regional- or local-scale studies of the stress regimes associated with major faults and fractures in the GAB would need to be undertaken.
- Other than Habermehl (2009), no other published studies have investigated the occurrence of borehole leakage in the GAB. A broader knowledge of past incidents would assist the minimisation of future occurrences through a greater understanding of casing and/or grout interactions with surrounding media.
- Field-based studies of diffuse recharge are limited in the Eromanga Basin, and have not been undertaken in the Carpentaria Basin; this represents a significant knowledge gap, since rates of recharge may vary considerably with latitude. Although localised recharge from rivers and creeks has been identified along the eastern margin of the Eromanga and Carpentaria Basins, rates of recharge (as well as the spatial variability and temporal dynamics thereof) have not been estimated. The quantification of recharge rates is of high importance, since the hydraulic gradients produced by recharge influxes are the primary driver of groundwater flow in the GAB. The robustness of predictions produced numerical models used to guide decision making in the GAB are heavily dependent upon accurate quantification of recharge fluxes.
- Studies of GAB hydrochemistry and isotopes have historically focused upon characterising horizontal groundwater flow and mixing in aquifers. The use of similar tools to identify and quantify aquifer connectivity has rarely been undertaken. In comparison to GAB aquifers, the hydrochemistry of aquitards is relatively poorly characterised.
- Numerical models of groundwater flow in the GAB have historically focused on single-phase flow; consequently, no published studies of multi-phase flow modelling currently exist. This type of modelling would be particularly pertinent to future impact assessments involving mixed-phase flow (e.g. water and gas) in the GAB. Similarly, geomechanical modelling of the potential effects induced by changes in stress fields in the GAB (e.g. due to fluid and gas extraction or injection) is not publicly available. This type of modelling could assist impact assessments in the vicinity of tectonic stress features such as faults and fractures.
- Measurements of vertical hydraulic head gradients are currently limited to those of

CSIRO (2012b) presented in Section 5.9. The availability of vertical head gradient data is restricted to locations where wells that are sited in different aquifers are located in close proximity. Mapping of vertical gradients at a basinal-scale has not been undertaken. Where available, vertical hydraulic head gradient data provide valuable first-order insights into aquifer connectivity.

6 Aquifer connectivity in the Surat Basin

6.1 Major aquifer and aquitard stratigraphy

The Surat Basin is a geological basin, and forms part of the GAB (Figure 1). An outline of the major geological evolution and hydrostratigraphy of the Surat Basin is included in the general description of the GAB in Chapter 5. From the hydrostratigraphic sequence presented in Figure 15 it is clear however that there are some distinct differences between the Surat Basin and other geological basins of the GAB.

Figure 18 shows a more detailed lithostratigraphic table of the Surat Basin and neighbouring geological basins (CSIRO 2012c). At least five fining upwards sequences are described in the Surat Basin. The base of each sequence mostly consists of coarse quartzose sandstones deposited in braided rivers. These sediments form the main aquifers in the Surat Basin. Braided rivers grade into meandering rivers, floodplains and lacustrine environments in which finer grained material is deposited and coal can be formed. These formations generally form aquitards, although they can act locally as aquifers, due to presence of sandstone or even conglomerate members.

The first Jurassic aquifer above the unconformity that marks the bottom of the Surat Basin is the Precipice Sandstone. Beneath this unconformity the Moolayember Formation acts as an aquitard and separates the Surat Basin from the permeable Clematis Sandstone and Rewan and Bandanna Formations in the Bowen Basin. The Precipice Sandstone is considered the start of a supersequence (Hoffmann et al. 2009) and is deposited by a braided fluvial system. With increased subsidence, this system evolved into a system with meandering streams and deltas in which the finer grained material of the Evergreen Formation was deposited. The Evergreen Formation is therefore considered to be a leaky aquitard. The Boxvale Sandstone Member of this formation is considered an aquifer as it is a well-sorted, fine- to medium-grained sandstone, representing either a shoreline or lacustrine environment (Hoffmann et al. 2009).

The Hutton Sandstone marks the onset of a second sequence in the Surat Basin and is classified as an aquifer. It represents a sudden drop in erosional base level and a return to a more fluvial environment with meandering streams. This again grades into a fluvial, swampy and even lacustrine depositional environment with the sedimentation of the Eurombah Formation and Walloon Coal Measures. Both the Walloon Coal Measures and the Eurombah Formation are considered leaky aquitards because they are dominated by low-permeable sediments such as coal, siltstone and mudstone. There are however several sandstone and even conglomerate beds present in the Eurombah Formation. It should be noted that the Eurombah Formation interfingers with both the Hutton Sandstone and the Walloon Coal Measures.

On top of the Walloon Coal Measures, a third fining upwards sequence is recognised on seismic profiles (Hoffmann et al. 2009), which consists of the permeable Springbok Sandstone that grades into the coastal plain deposits of the Westbourne Formation. Due to its fine-grained nature and dominance of coal, mudstone and siltstone, this formation is classified as a tight aquitard. The Springbok Sandstone lies unconformably on the Walloon

Coal Measures and has an erosional base. This implies that locally the Springbok Sandstone can be in direct contact with sandstone layers or coal seams of the Walloon Coal Measures.

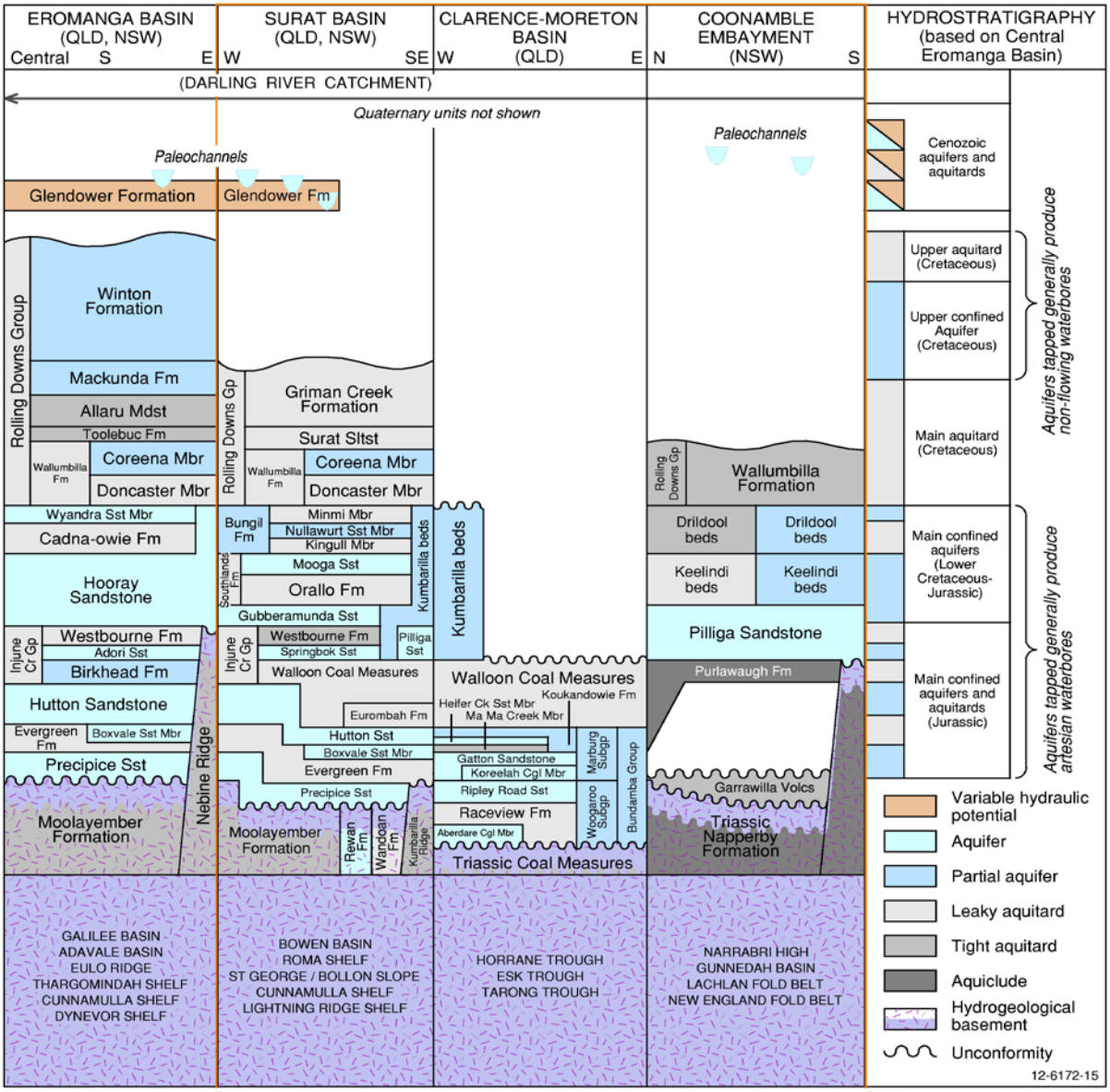

Figure 18 Lithostratigraphic table of Surat and surrounding basins with hydrostratigraphic interpretation (© Copyright, CSIRO 2012c).

The sedimentation of the Westbourne Formation is followed by deposition of the Gubberamunda Sandstone. These fluvial deposits again form an aquifer that is confined by a finer-grained deposit, the Orallo Formation. These sediments were deposited in a fluvio-lacustrine environment, which implies that while they act as low-permeable layer on a regional scale, local aquifers can be present in sandstone members.

The final Jurassic sequence in the Surat Basin is formed by the coarse sediments of the Mooga Sandstone, considered an aquifer, covered and confined by the Bungil Formation. The Gubberamunda to Bungil succession in the Surat Basin is equivalent to the Cadna-

Owie-Hooray deposits in the Eromanga Basin. In both basins, these Late Jurassic deposits are covered by the marine Cretaceous mudstones of the Rolling Downs Group. These include the Doncaster Member, Wallumbilla Formation, Surat Siltstone and Griman Creek Formation, all considered leaky aquitards. Only the Coreena Member is classified as a partial aquifer.

The Clarence-Moreton Basin is located east of the Surat Basin, separated by the Kumbarilla Ridge. A clear lithostratigraphic correlation exists between both basins (Figure 18) and the sedimentary sequence can be considered continuous across the Ridge. The Woogaroo Subgroup is equivalent to the Precipice Sandstone and the Hutton Sandstone corresponds to the Koukandowie Formation in the Marburg Subgroup. The Walloon Coal Measures are present in both basins. The Kumbarilla Beds are equivalent to and connected with the Hutton, Gubberamunda and Mooga Sandstone Aquifers. The Rolling Downs Group is not present in the Clarence-Moreton Basin; the Jurassic deposits are instead covered by Tertiary Volcanics, mostly basalts, and the Tertiary Condamine Alluvium. The latter unconformably overlies the Walloon Coal Measures. The Condamine Alluvium is up to 150 m thick and contains coarse sediments, especially near the base of the formation, making it an important unconfined aquifer that supports agriculture in the Condamine Valley (CSIRO 2008b).

Stratigraphic data for the Surat Basin have been summarised by the Queensland University of Technology to produce 3D geological models for the Queensland Water Commission[2] (Hawke et al. 2011) and for Arrow Energy (James et al. 2011).

6.2 Structural properties

The Surat Basin inherited most of its structural features from the underlying basins, especially its main depocentre, the Mimosa Syncline, which is situated above the Bowen Basin (Figure 19). In the Eromanga Basin, post-depositional tectonics activated and propagated several pre-existing faults, which resulted in faults that affect the entire sedimentary sequence. This was less so for the Surat Basin, where re-activation of pre-existing faults was mostly accommodated by deformation through folding rather than faulting. This is illustrated by the two fault systems that delineate the Roma Shelf: the Hutton-Wallumbilla Fault and the Merivale and Abroath Faults. Displacements of the Surat Basin basement on these faults is up to 1000 m, but displacement within the Surat sequence rarely exceeds 100 m. Some faults however do affect the entire sequence, such as the Moonie-Goondiwindi Fault, although its displacement is also limited to about 100 m.

AGE (2007) in Golder Associates (2009) do point out that the uplift and folding above deeper structural features have induced small-scale fracturing and faulting of the sedimentary layers, which can compromise the integrity of the aquitards and enhance connectivity between aquifers. The displacement along faults in the Surat appears to laterally isolate portions of the Surat Basin (Golder Associates 2009).

6.3 Hydraulic properties

The values of hydraulic properties, such as described in chapter 2, may be obtained from core tests, from field tests such as drill stem tests, pumping tests or slug tests, or they may be estimated independently using calibrated numerical models. The majority of hydrogeological knowledge relating to the Surat Basin is derived from the development of

[2] As of January 2013 the Queensland Water Commission (QWC) is now known as the Office of Groundwater Impact Assessment (OGIA). OGIA is an independent entity established under the *Water Act 2000* (Qld).

potable groundwater supplies. Therefore the availability of hydraulic property data relating to the hydrogeological units of the Surat Basin is inherently biased toward productive freshwater-bearing units. The hydraulic properties of lower permeability layers have been relatively poorly characterised, although recent coal seam gas development in the basin has prompted enhanced study of all GAB units.

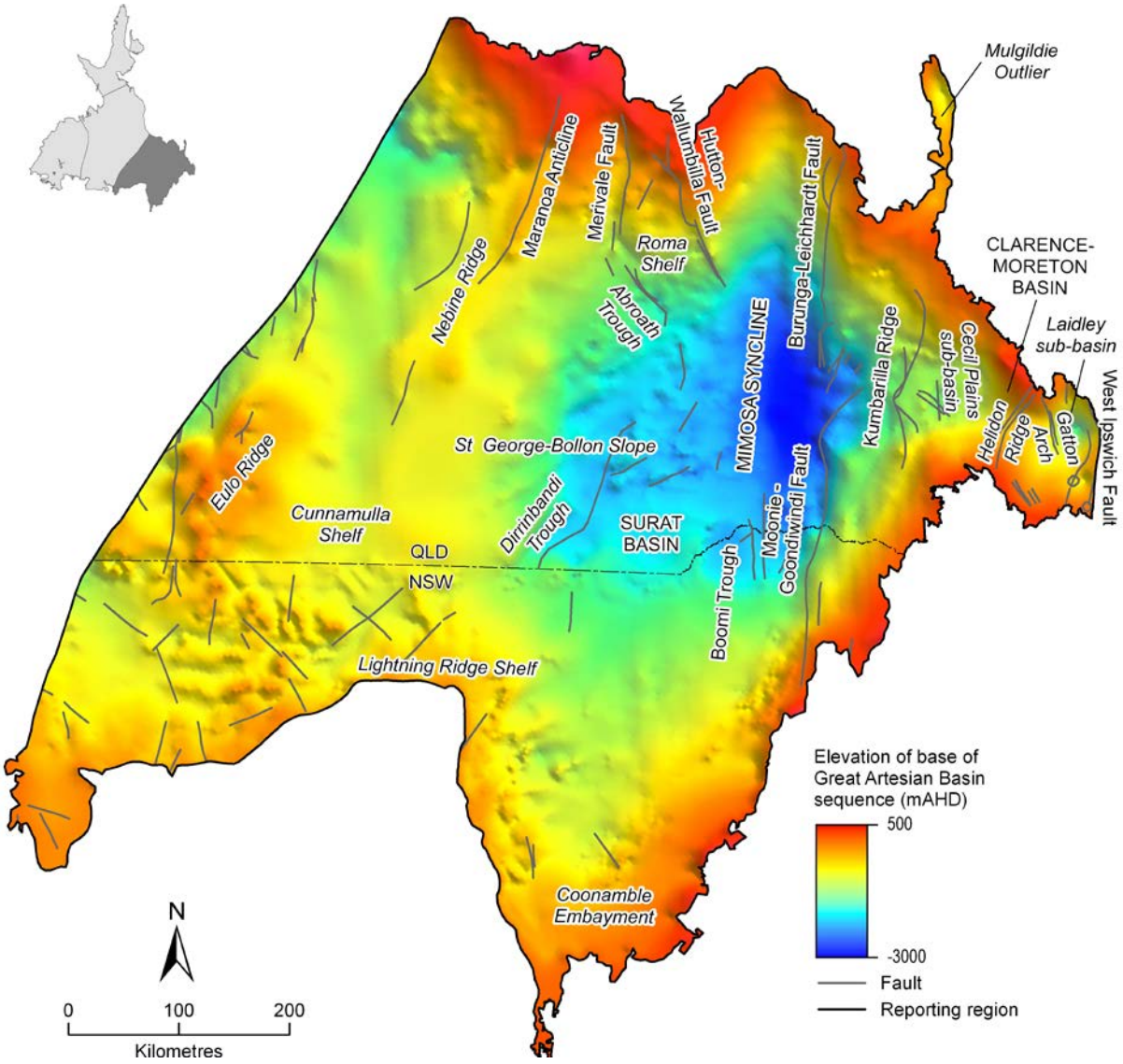

Figure 19 Structural elements of the Surat and Clarence-Moreton Basins at the base of the Surat sequence (© Copyright, CSIRO 2012c).

6.3.1 Core and field-based estimates

As discussed in chapter 3, when reviewing measurements of the hydraulic property values of confining layers (and to a lesser extent, aquifer layers), it should be remembered that, due to

the inability to obtain measurements in situ, often such values will be exaggerated due to the effects of depressurisation from the removal of overburden pressure.

As discussed in chapter 5, Habermehl (1980) estimated ranges of values for a number of hydraulic properties on the Cadna-Owie-Hooray aquifer system; these ranges are also appropriate for the Surat Basin. Recently, the GAB Water Resource Assessment (GABWRA) (CSIRO 2012c) collated and summarised measurements of porosity and permeability recorded in the Queensland Petroleum Exploration Database (Table 10).

Table 10 Porosity and permeability measurements for various Surat Basin units (© Copyright, CSIRO 2012c).

Unit	**Porosity**		**Horizontal permeability**		
	n	**mean (%)**	**n**	**mean (mD)**	**equivalent K_h* (m/d)**
Wallumbilla Formation[#]	33	30	17	71	0.07
Mooga Sandstone	35	28	29	728	0.69
Gubberamunda Sandstone	38	28	23	1051	1.00
Westbourne Formation	24	26	21	630	0.60
Walloon Coal Measures	118	18	95	67	0.06
Hutton Sandstone	333	22	426	426	0.40
Evergreen Formation	766	15	624	87	0.08
Precipice Sandstone	3172	16	2799	320	0.30

K_h=horizontal hydraulic conductivity; *hydraulic conductivity equivalents are provided for comparison purposes only and are calculated from mean permeability values using the equation defined in chapter 2 and using values of g=9.8 m/s^2, ρ=997.0479 kg/m^3, and μ=8.91x10^{-4} kg/[m.s], the latter two of which assume a fresh groundwater temperature of 25^{o}C; [#]also includes hydrostratigraphic equivalents and its component Doncaster and Coreena Members.

Mean porosity values appear to decrease with depth, from 30 per cent in the Wallumbilla Formation to 15 per cent in the Evergreen Formation. Mean permeability values range from 67 mD in the Walloon Coal Measures up to 1051 mD in the productive Gubberamunda Formation.

GABWRA (CSIRO 2012c) also described the spatial variability of horizontal permeability for the Hooray Sandstone, the Hutton Sandstone, the Evergreen Formation and the Precipice Sandstone. The sparseness of vertical permeability observations precluded interpretation. Similarly, due to the paucity of horizontal permeability observations, interpretations were limited to the north of the Surat Basin. Spatial distributions of permeability are not consistent between units and are attributed to differences in depositional sources and histories.

A similar summary of permeability and porosity measurements for aquifer units of the Surat Basin was presented by Bradshaw et al. (2010) and is provided in Table 11.

Table 11 Porosity and permeability measurements for various Great Artesian Basin units (© Copyright, Bradshaw et al. 2010).

Unit	Porosity		Horizontal permeability		
	n	mean (%)	n	median (mD)	equivalent K_h* (m/d)
Hutton Sandstone	2649	17.6	2451	98	$9.3x10^{-2}$
Boxvale Member	475	15.7	426	7.1	$6.7x10^{-3}$
Evergreen Formation	32	14.9	32	5.4	$5.1x10^{-3}$
Precipice Sandstone	1654	16.8	1519	13	$1.2x10^{-2}$

Note: K_h=horizontal hydraulic conductivity; *hydraulic conductivity equivalents are provided for comparison purposes only and are calculated from mean permeability values using the equation defined in chapter 2 and using values of g=9.8 m/s^2, ρ=997.0479 kg/m^3, and μ=$8.91x10^{-4}$ kg/[m.s], the latter two of which assume a fresh groundwater temperature of 25^{o}C.

The sample sizes used to calculate mean porosities and median permeabilities differ significantly from those used by CSIRO (2012c). Mean porosity values for the Evergreen Formation and Precipice Sandstone are comparable to those reported by CSIRO (2012c), while the reported mean porosity of the Hutton Sandstone is approximately four per cent lower. Median permeabilities are orders of magnitude smaller than those reported by CSIRO (2012c); however, this may be due to the different statistical measure and/or datasets used in the analyses.

The Queensland State Government administers two databases containing data relating to hydraulic properties: the Queensland Groundwater Database (QGD), managed by the Department of Environment and Heritage Protection, and the Queensland Petroleum Exploration Database (QPED) (DNRM 2014c), managed by the Geological Survey of Queensland. These data sources (available upon request) contain field-based measurements of unit thickness, permeability, porosity, hydraulic conductivity, transmissivity and storativity. The Queensland Water Commission developed a groundwater flow model (QWC 2012a; QWC 2012c) in order to independently estimate the effects of CSG production. This work summarised more than 13 000 drill stem test records from the Queensland Petroleum Exploration Database and more than 1000 pumping test records from the Queensland Groundwater Database (Table 12). As of January 2013, this represented the most up-to-date and publically available synthesis of Queensland Groundwater Database and Queensland Petroleum Exploration Database hydraulic conductivity data.

Higher median and maximum hydraulic conductivities are associated with unconsolidated alluvial media, and with aquifer units such as the Gubberamunda, Hutton and Precipice Sandstone units. Conversely, lower median and maximum hydraulic conductivities are associated with the Westbourne Formation, Walloon Aquitards, and Evergreen Formation.

Table 12 Horizontal hydraulic conductivity (m/d) measurements for various units of the Surat Basin (© Copyright, QWC 2012a).

Unit	n	minimum	median	maximum
Alluvium	101	0.14	8.60	1500
Main Range Volcanics	14	0.02	0.54	6.8
Rolling Downs Group	61	$4.40x10^{-4}$	0.03	1.0
Bungil/Mooga Sandstone	290	$2.80x10^{-5}$	0.04	5.4
Orallo Formation	78	$9.30x10^{-5}$	0.30	5.9
Gubberamunda Sandstone	154	$3.70x10^{-3}$	0.85	33
Westbourne Formation	140	$1.90x10^{-5}$	0.01	4.6
Springbok Sandstone	55	$1.70x10^{-6}$	$4.10x10^{-3}$	4.1
Walloon Aquitards	123	$2.60x10^{-6}$	0.01	1.5
Walloon Productive Coal	217	$8.30x10^{-5}$	0.08	2.2
Hutton Sandstone	1427	$8.30x10^{-6}$	0.05	13
Evergreen Formation	1113	$4.30x10^{-6}$	$3.40x10^{-3}$	6.9
Precipice Sandstone	1745	$2.60x10^{-6}$	0.02	23

6.3.2 Model-based estimates

As discussed in chapter 3, estimates of hydraulic properties obtained from inverse models assume a correct choice of conceptual model and are therefore inherently subject to uncertainty. Since models are always imperfect representations of reality, inaccuracies in estimated values may be due to compensatory effects, such as accounting for misrepresentations of model stresses such as recharge and discharge (Doherty & Welter 2010).

Since the late 1970s, groundwater models have been developed to represent various parts of the Surat Basin. A summary including these models was provided in Smith and Welsh (2011). Parameterisation of such models is often based upon the calibration of model outputs to observations of hydraulic heads. A summary of hydraulic property values estimated through model calibration is presented in Tables 13, 14 and 15. The majority of the models simulate alluvial aquifer systems and do not represent consolidated GAB units; therefore the relevance of these models to future aquifer connectivity studies is minimal.

As part of environmental assessment requirements, four hydrogeological models of the Surat Basin have been created by each of Australia Pacific Liquified Natural Gas (LNG), Arrow Energy, Gladstone LNG and Queensland Curtis LNG. Each of the models represents the majority of the stratigraphic layers of the GAB in the Surat Basin. The following tables summarise the horizontal and vertical hydraulic conductivity values ascribed to each hydrogeological unit by each of the four numerical models. Each model was based upon hydraulic property values derived from exploration activities, Queensland government databases, various literature sources and subsequently adjusted through model calibration to hydraulic head observations and estimated aquifer fluxes (Coffey 2012; WorleyParsons 2010a; Golder Associates 2009; MatrixPlus 2009).

Table 13 Summary of hydrogeological models of the Surat Basin (© Copyright, Smith & Welsh 2011).

Model name	Reference(s)	Relevant unit(s)	K_h (m/d)	K_v (m/d)	S_s (/m)	S_y
Dumaresq Border Rivers	Chen (2003), Welsh (2008)	Alluvium (unconfined)	$5.8x10^{-3}$ - 7.8	$8.6x10^{-7}$ - $4.8x10^{-5}$	-	$6.6x10^{-3}$ - 0.05
		Alluvium (confined)	0.5 - 100	-	$8.6x10^{-7}$ - 10^{-3}	-
Lower Gwydir	Bilge (2002)	Alluvium	0.01 - 70	not reported	10^{-5} - 10^{-3}	0.05 - 0.35
Lower Macquarie	Bilge (2007)	Alluvium	0.01 - 20	10^{-5} - 0.01	-	0.09 - 0.23
		Pilliga Sandstone	0.01 - 10	10^{-5} - $6.0x10^{-3}$	10^{-4} - 10^{-6}	
Lower Namoi	Merrick (2001)	not reported	-	-	-	-
Moree	Hopkins (1996)	not reported	-	-	-	-
Narrabri Coal Project	Aquaterra (2009)	Alluvium	0.3 - 5	$5.0x10^{-4}$ - $5.0x10^{-3}$	$5.0x10^{-6}$	0.1
		Pilliga Sandstone	$4.0x10^{-3}$ - 0.3	$1.5x10^{-5}$ - $2.0x10^{-3}$	$5.0x10^{-6}$	0.1
		Purlawaugh Formation	$4.0x10^{-3}$ - 0.02	$6.0x10^{-6}$ - $1.0x10^{-3}$	$5.0x10^{-6}$	10^{-3}
Upper Condamine	Barnett & Muller (2008)	Alluvium	0.01 - 12	10^{-3} - 1	$5.0x10^{-6}$	0.04 - 0.06

Note: K_h=horizontal hydraulic conductivity, K_v=vertical hydraulic conductivity, S_s=specific storage, S_y=specific yield.

The Australia Pacific LNG model uses a specific storage value of $4x10^{-6}$ /m for all modelled layers (WorleyParsons 2010b). The Arrow Energy model uses a specific storage value of $5x10^{-6}$ /m for all modelled layers except subunits of the Walloon Coal Measures ($1x10^{-6}$ to $5x10^{-6}$ /m; SWS 2011). The Gladstone LNG model uses a wide range of specific storage values, ranging from $8x10^{-6}$ /m for the Hutton and Precipice Sandstone units, to $1x10^{-4}$ /m for the Cainozic and Alluvium units (MatrixPlus 2009). The Queensland Curtis LNG model uses a storativity value of $5x10^{-4}$ for all units above the Gubberamunda Sandstone and a value of $5x10^{-5}$ for all units below, inclusive (Golder Associates 2009).

6.4 Geomechanical properties

A range of geomechanical properties of Surat Basin aquifers and aquitards are of relevance to assessing the potential for induced mechanical deformation, fracturing and seismicity. Such properties may include geological unit permeabilities, Poisson's Ratio and Young's Modulus; shale volume data for aquitard seals; the location, type and throw of faults; horizontal and vertical stress directions and magnitudes; and the volumetric rates of fluid extraction involved in mining operations. Borehole leakage presents an additional hazard of intensive drilling operations. Currently, there are no published syntheses of geomechanical properties in the Surat Basin, nor published studies of the potential for induced geomechanical stresses resulting from mining operations.

Table 14 Horizontal hydraulic conductivity (m/d) values for various Surat Basin units used by coal seam gas models (© Copyright, USQ 2011; also SWS 2011; WorleyParsons 2010b; Golder Associates 2009; MatrixPlus 2009).

Unit	Australia Pacific LNG	Arrow	Gladstone LNG	Queensland Curtis LNG
Cainozic and Alluvium	0.22 to 5	5	0.31	$3.6x10^{-3}$ to $3.6x10^{-2}$
Rolling Downs Group	0.05	10^{-3}	0.027	$3.6x10^{-3}$ to $3.6x10^{-2}$
Bungil Formation	0.12	10^{-3}	0.022	$3.6x10^{-3}$ to $3.6x10^{-2}$
Mooga Sandstone	0.12	0.5	0.117	$3.6x10^{-3}$ to $3.6x10^{-2}$
Orallo Formation	0.12	0.1	0.25	$3.6x10^{-3}$ to $3.6x10^{-2}$
Gubberamunda Sandstone	0.31	0.5	0.49	0.036 to 0.36
Westbourne Formation	$5.6x10^{-3}$	10^{-3}	$2.6x10^{-3}$	10^{-4} to 10^{-3}
Springbok Sandstone	0.28	0.5	0.12	1.25
Walloon Coal Measures	$1.5x10^{-4}$ to 0.14	10^{-3} to 0.05	$1.1x10^{-3}$ to $4x10^{-3}$	$5.0x10^{-4}$ to 1.36
Eurombah Formation	$6.2x10^{-4}$	0.05	$1.1x10^{-3}$	$2.5x10^{-4}$ to $2.5x10^{-3}$
Upper Hutton Sandstone	2.4	0.1	0.13	0.01 - 0.1
Lower Hutton Sandstone	0.12	0.1	0.13	0.01 - 0.1
Evergreen Formation	$6.5x10^{-4}$	10^{-3}	$3.0x10^{-3}$	10^{-4} - 0.01
Precipice Sandstone	3.1	1	0.21	0.38 - 3.8

Table 15 Vertical hydraulic conductivity (m/d) values for various Surat Basin units used by coal seam gas models (© Copyright, USQ 2011; also SWS 2011; WorleyParsons 2010b; Golder Associates 2009; MatrixPlus 2009).

Unit	Australia Pacific LNG	Arrow	Gladstone LNG	Queensland Curtis LNG
Cainozic and Alluvium	$7.3x10^{-3}$ to 0.167	0.5	0.031	$7.2x10^{-4}$ to $7.2x10^{-3}$
Rolling Downs Group	$1.67x10^{-4}$	10^{-5}	$2.7x10^{-4}$	$7.2x10^{-4}$ to $7.2x10^{-3}$
Bungil Sandstone	$4.0x10^{-3}$	10^{-5}	$2.2x10^{-3}$	$7.2x10^{-4}$ to $7.2x10^{-3}$
Mooga Sandstone	$4.0x10^{-3}$	0.05	0.0117	$7.2x10^{-4}$ to $7.2x10^{-3}$
Orallo Formation	$4.0x10^{-3}$	$2.0x10^{-3}$	$2.5x10^{-5}$	$7.2x10^{-4}$ to $7.2x10^{-3}$
Gubberamunda Sandstone	0.0103	0.05	0.049	$7.2x10^{-4}$ to $7.2x10^{-3}$
Westbourne Formation	$1.87x10^{-5}$	10^{-5}	$2.6x10^{-5}$	$2.0x10^{-6}$ to $2.0x10^{-5}$
Springbok Sandstone	$9.33x10^{-3}$	0.05	0.012	0.025
Walloon Coal Measures	$5.0x10^{-7}$ to $4.67x10^{-3}$	10^{-5} to 10^{-3}	$1.5x10^{-6}$ to $4.0x10^{-4}$	$5.0x10^{-7}$ to 0.453
Eurombah Formation	$2.07x10^{-6}$	10^{-3}	$1.1x10^{-5}$	$5.0x10^{-7}$ to $5.0x10^{-6}$
Upper Hutton Sandstone	0.08	$2.0x10^{-3}$	0.013	$1.4x10^{-3}$ to $1.4x10^{-2}$
Lower Hutton Sandstone	$4.0x10^{-3}$	$2.0x10^{-3}$	0.013	$1.4x10^{-3}$ to $1.4x10^{-2}$
Evergreen Formation	$2.17x10^{-6}$	10^{-5}	0.013	$1.4x10^{-3}$ to $1.4x10^{-2}$
Precipice Sandstone	0.103	0.1	$3.0x10^{-5}$	$2.0x10^{-6}$ to $2.0x10^{-4}$

6.4.1 Properties relating to induced geomechanical stresses

Pressure and permeability data are available from the CSIRO PressurePlot database (CSIRO 2007) and from relevant state government databases such as Queensland Petroleum Exploration Database (DNRM 2014c) and the South Australian Resources Information Geoserver (SARIG 2014). As described in section 6.3, permeability data for the Surat Basin were recently summarised by GABWRA (CSIRO 2012c), as were temperature data. The clay composition of Surat Basin aquitards is poorly characterised, particularly spatially. The locations of significant faults in the Surat Basin have been well-documented and have also been summarised recently by GABWRA (CSIRO 2012c) from foundation works by the Geological Survey of Queensland, such as Quarantotto (1989). Fault types and throw information may also be obtained from Geological Survey of Queensland Bulletins. Horizontal stress directions at a continental scale may be obtained from the Australian Stress

Map (Hillis et al. 1998). Horizontal stress over much of the Surat Basin is in a northeast-southwest orientation. Vertical stress magnitudes are a function of depth (Mildren et al. 2002) and may be estimated from borelog data. Finally, local estimates of future rates of fluid extractions by CSG operations may be obtained from relevant Environmental Impact Statements. Maximum total extraction rates have been projected at approximately 10 ML/d (Gladstone LNG), 140 ML/d (Arrow), 170 ML/d (Australia Pacific LNG) and 200 ML/d (Queensland Curtis LNG) (SWS 2011). Alternatively, the CSG water production forecasting model developed by Klohn Crippen Berger (2011) for DERM[3] (Qld) could be used to provide a local-scale estimate.

As part of Environmental Impact Statement reporting for the Australia Pacific LNG project, WorleyParsons (2010a) used a simplified qualitative method to estimate the hazard of land subsidence caused by aquifer compression. Using projected drawdowns from a numerical model, the authors estimated that the potential for compaction was less than half a metre across the Surat Basin region, which may be considered significant in the context of a broad area of relatively flat topography. The likelihood of subsidence being propagated to the land surface was estimated to be low, due to the incompressibility of aquifer units between the surface and the Walloon Coal Measures.

Hodgkinson and Grigorescu (2012) summarised a number of available datasets that are relevant to the potential for carbon sequestration in the Surat Basin. These included the Queensland Petroleum Exploration Database and Queensland Groundwater Database, the seismic survey database maintained by the Queensland Geological Survey, and the data available from the CSIRO PressurePlot database. The authors state that the upper Precipice Sandstone and the Evergreen Formation have shown suitable seal rock characteristics essential in the early stages of carbon dioxide injection into the aquifer. They state that there are currently no suitable pressure tests in wells in the Walloon Subgroup and the Hutton Sandstone to reliably assess possible reservoir or seal characteristics.

Varma et al. (2011) reviewed the currently available literature relating to groundwater and other natural resources in four geological basins including the Surat Basin. The authors concluded that insufficient petrophysical and geomechanical data currently exist in the public domain for use in fault reactivation and seal deformation modelling, with the exception of horizontal stress data (Hillis and Reynolds 2003; Hillis et al. 1999; Hillis et al. 1998). In particular, the authors noted the lack of publicly available shale volume and fault throw data.

Future syntheses of such data may subsequently be used in quantitative assessments of the potential for geomechanical effects induced by mining operations, such as the FAST methodology of Mildren et al. (2002). Similarly, such data may be used to develop numerical geomechanical and/or hydrogeological models which may be used to predict the effects of mining activities such as aquifer/aquitard depressurisation. In summary, the potential for induced mechanical deformation, fracturing, and seismicity would need to be assessed on a case-by-case basis. This cannot currently be addressed without improved characterisation of geomechanical properties at a local scale.

6.4.2 Borehole leakage

Although the borehole leakage study of Habermehl (2009) mentioned in previous section also included bores in the Surat Basin, to date no study exists on borehole leakage specifically for the Surat Basin.

[3] In April 2012 the Queensland Department of Environment and Heritage Protection was established, replacing the former Department of Environment and Resource Management (DERM).

6.5 Groundwater recharge, flow and discharge

6.5.1 Groundwater recharge

Recharge to GAB aquifers in the Surat Basin is believed to predominantly occur via preferred pathways such as highly porous interbeds, rock fractures, solution cavities and root cavities (Kellett et al. 2003). Other mechanisms include diffuse recharge through the aquifer matrix and by localised leakage below perennial or ephemeral rivers. The currently accepted extent of the Cadna-Owie-Hooray recharge areas was defined by Habermehl and Lau (1997). Recharge occurs primarily in intake beds located along its eastern and southern margin, where aquifer unit outcrops or subcrops occur. Barclay (2001) identified the Jurassic-Cretaceous (J-K) aquifers as receiving the majority of current-day recharge to the GAB (up to 51 per cent), compared to the Hutton Sandstone (13 per cent) and Adori Sandstone (4 per cent). For this reason, and due to significant historical use of the artesian Cadna-Owie-Hooray aquifers of the GAB, the research relating to recharge processes in the Surat Basin tends to be focused on this particular aquifer system.

Mechanisms, extents and rates of recharge in the GAB were reviewed by Herczeg and Love (2007). Rates of recharge in the eastern intake beds of the Surat Basin have been studied by Kellett et al. (2003), McMahon et al. (2002), Radke et al. (2000) and Wolfgang (2000). Wolfgang (2000) estimated a recharge area of 453 - 35 000 km^2 with corresponding diffuse recharge rates of 2 - 51.2 mm/yr and a logarithmic mean of 6 mm/yr. Radke et al. (2000) estimated diffuse recharge rates of 0.2 - 1.1 mm/yr. McMahon et al. (2002) estimated diffuse recharge rates of 0.1 to 2 mm/yr and preferential pathway rates of up to 20 mm/yr. Leakage below rivers and creeks was estimated to provide 45 to 80 mm/yr of recharge. Kellett et al. (2003) estimated rates of preferred pathway recharge between 0.5 and 28 mm/year. Rates of diffuse recharge were estimated to be between 0.3 and 2.4 mm/year. Recharge from localised river leakage was estimated as being up to 30 mm/year. Leakage from the Macquarie and Castlereagh rivers into the Pilliga Sandstone was supported by isotopic evidence.

DNRM (2005) identified leakage occurring to Surat Basin aquifers from a number of sources: the Warrego River northeat of Augethella; the Nive River southeast of Tambo; the Maranoa River north of Mitchell; and the Weir River/Western Creek west of Toowoomba. Estimations of recharge using numerical models are limited to that of Welsh (2006), who used the GABTRAN model to estimate rates of up to 33 mm/yr, with an average of 2.4 mm/yr.

6.5.2 Groundwater flow

Habermehl (1980) characterised groundwater in the Cadna-Owie Hooray aquifers of the Surat Basin as flowing primarily from the recharge areas of the north and east toward the Eulo and Nebine ridges that separate the Surat and Eromanga basins. More recent work by Radke et al. (2000) based on modelling by Welsh (2000) did not significantly revise this interpretation. Recently, GABWRA (CSIRO 2012c) highlighted the influence of impermeable faults on groundwater flow, particularly the Hutton-Wallumbilla and Merivale faults in the north, and the Burunga-Leichardt and Moonie faults in the east. Faults that are believed to act as barriers to flow were identified according to the magnitude of vertical displacement around the fault. These faults were then included in a potentiometric surface developed from hydraulic head observations for the period 1900-1920 (Figure 20).

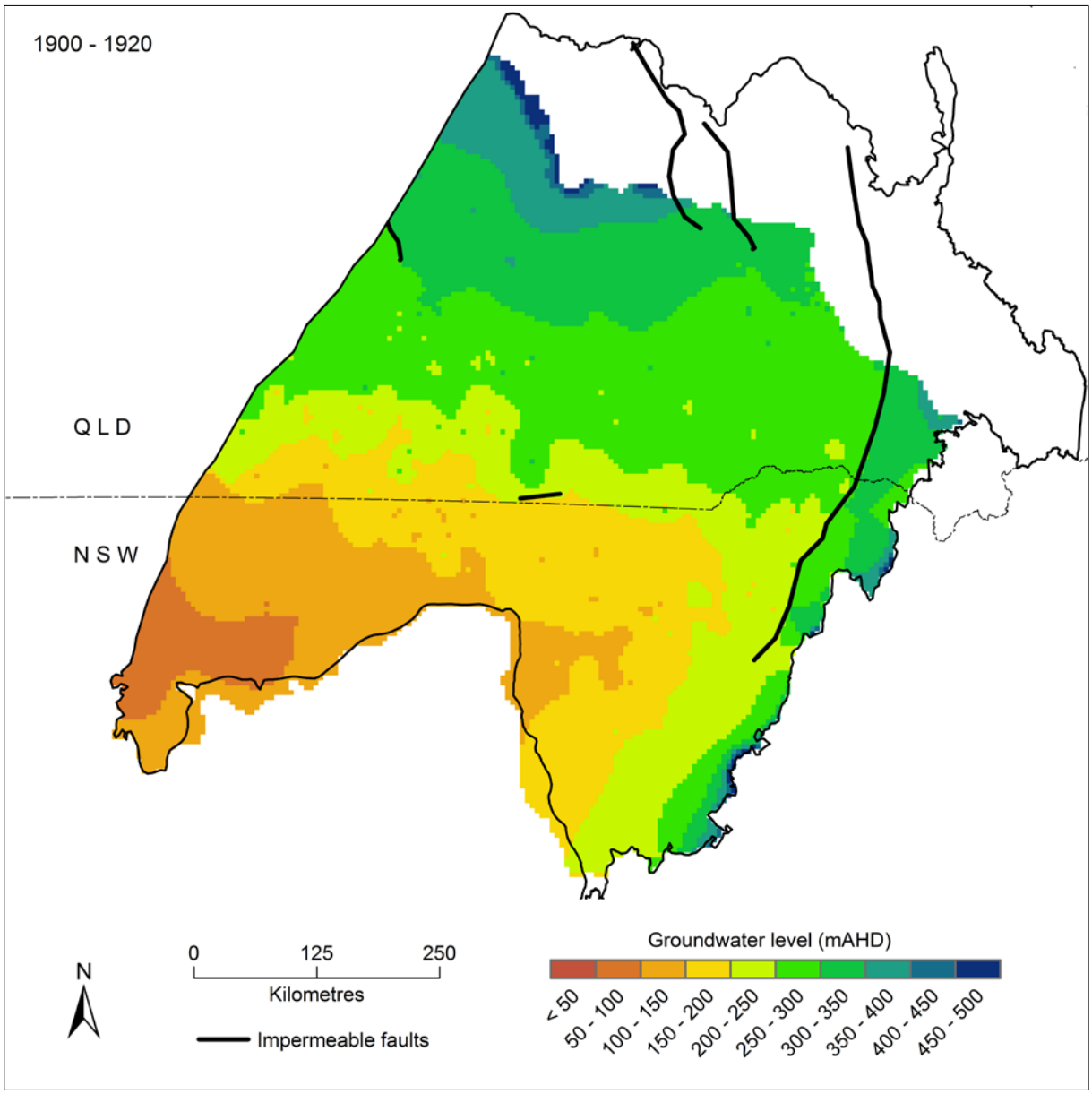

Figure 20 Interpolated potentiometric surface for the Surat Basin for the period 1900-1920, including the effects of impermeable faults (© Copyright, CSIRO 2012c).

Hodgkinson et al. (2010) interpolated potentiometric surfaces for multiple GAB units from data obtained from the Queensland Groundwater Database and Queensland Petroleum Exploration Database (hydrogeological databases) and from the CSIRO PressurePlot pressure database. The authors observed that in the southeast and east of the Surat Basin, groundwater systems behave as discrete aquifers with independent flow regimes. In the Precipice Sandstone, inter-basin flow from the Surat Basin into the Clarence-Moreton Basin was identified. In the Hutton Sandstone, the opposite relationship was observed, with groundwater flowing from the Clarence-Moreton Basin into the Surat Basin.

6.5.3 Groundwater discharge

The discharge of artesian groundwater may occur as diffuse discharge through confining layers or via preferential pathways such as faults and fractures. Although rates of diffuse discharge may be relatively low (i.e. in the order of millimetres per year), the process may occur over a considerable spatial extent; therefore the total volumetric discharge may be significant. GABWRA (CSIRO 2012c) provided a first-order estimate of diffuse discharge for the Surat Basin of 90 GL/yr, based upon hydraulic gradients between the potentiometric surface of the Cadna-Owie-Hooray aquifers and the regional water table. In the Surat Basin, 643 groundwater-fed springs have been identified, of which 52 per cent are currently active. The majority of springs are associated with geologic faults (CSIRO 2012c). Habermehl (1982) estimated the volumetric rate of groundwater discharged to springs in the Surat Basin at 14 000 ML/yr.

6.6 Hydrochemistry and isotopes

The majority of hydrogeological knowledge relating to the Surat Basin has come from the development of potable groundwater supplies. Therefore the availability of hydrochemical information relating to the hydrogeological units of the Surat Basin is inherently biased toward productive freshwater-bearing units. Conversely, the hydrochemistry of confining aquitard layers is relatively poorly characterised.

6.6.1 Hydrochemical studies

GABWRA (CSIRO 2012c) provided an up-to-date summary of the hydrochemistry (including isotopic studies) of the Lower Cretaceous-Jurassic aquifers of the Surat Basin. Groundwater generally contains 500 to 1500 mg/L total dissolved solids and features a pH of 7.5 to 8. The hydrochemical composition typically evolves from low salinity and slightly acid groundwater in recharge zones, to calcium-magnesium-bicarbonate-chloride-type groundwater, to sodium-bicarbonate-chloride-type groundwater toward discharge zones. The dissolution of silicate and carbonate minerals due to the presence of carbon dioxide in recharge zones can lead to elevated alkalinity levels and increased sodium, calcium and magnesium concentrations. Cation exchange reactions can lead to elevated sodium concentrations, which in turn can result in increased sodium adsorption ratios. Increases in chloride concentration may be due to mixing with saline aquitards or with deeper groundwater of relatively higher salinity. Local-scale characterisation of GAB unit hydrochemistry in the Surat Basin has been undertaken by each of the four CSG mining operations as part of EIS requirements (see Coffey 2012; WorleyParsons 2010a; WorleyParsons 2010b; QGC 2009; URS 2009a; URS 2009b). Analysis of the spatial variability of the hydrochemistry of the Walloon Coal Measures has also recently been undertaken by WorleyParsons (2010b).

6.6.2 Isotopic studies

As discussed in chapter 5, isotopic studies of groundwater have been undertaken in the Eromanga Basin, including those of Mahara et al. (2009), Torgerson et al. (1991), Bentley et al. (1986), Airey et al. (1983), and among others. The eastward extent of each of these studies lies to the west of the Eulo-Nebine Ridge, and therefore outside of the Surat Basin. No significant studies using groundwater isotopes have been published for the Surat Basin. Recently, CSG development in the Surat Basin has driven new interest in applied groundwater isotope studies, particularly to characterise interactions between the Walloon Coal Measures and confining units. A review of various isotope measurements undertaken to-date in the Surat Basin has recently been undertaken by Geoscience Australia; the results of this review are yet to be published.

6.7 Groundwater modelling

Modelling of the Surat Basin began with basin-scale models by Ungemach (1975; GABSIM) and Seidel (1978; GABHYD), followed many years later by the work of Welsh (2000; 2006). Each of these models sought to represent only the Lower Cretaceous-Jurassic sandstone aquifers using single layer models. Modelling of subsections of the Surat Basin began with water resource models of the Lower Namoi (Merrick 2001) and Moree (Hopkins 1996). More recently, multi-layered regional-scale models of CSG impacts have been developed as part of Environmental Impact Statement requirements (SWS 2011; WorleyParsons 2010a; Golder Associates 2009; MatrixPlus 2009). There are currently no publicly available reservoir models or CO_2 sequestration models for the Surat Basin. Smith and Welsh (2011) summarised the details of a number of past hydrogeological models of the Surat Basin and this information is collated in Table 16. The QWC has developed a 3D geologic model for the Surat Basin (QWC 2012c).

These models feature a wide range of spatial model extents, ranging from small local-scale models of around 5 km^2 extent, to basin-scale models that cover the entirety of the GAB. Vertical complexity is also variable, with more recent (post-2000) models representing multiple (>10) hydrogeological layers. None of these models simulated the effects of preferential pathway flow, multiphase flow or geomechanical processes.

6.8 Aquifer connectivity

From the research presented in the preceding sections, it can be seen that studies of aquifer connectivity in the Surat Basin are relatively few. The hydraulic connection between two aquifers separated by an aquitard will be a function of the hydraulic properties of each of the units, particularly the confining unit.

Hitchon and Hays (1971) applied a simplified conceptualisation of groundwater flow system to the Surat Basin in order to assess the economic viability of developing the hydrocarbon resources of the Basin. The authors combined existing and unpublished pressure measurements from drill-stem tests and standing water level measurements to create pressure-depth plots and thereby develop two vertical cross-sections of the Basin. Along a 450 mile-long north-south-oriented cross-section the authors interpret upward vertical groundwater flows occurring to the Middle and Upper Jurassic units from underlying Permian and Triassic units. Similar interpretation of upward vertical flow is also presented for a 225 mile-long east-west-oriented cross-section, with some downward flows from the Middle and Upper Jurassic units. Hitchon and Hays (1971) also suggested that the low relative permeability of confining units alone is not sufficient to significantly retard vertical flow where a hydraulic gradient exists.

Historically, the Surat Basin was conceptualised as a binary layered system of aquifers and confining beds. A recent reclassification of the hydrostratigraphy of the Surat Basin by GABWRA (CSIRO 2012c) has expanded the definition of confining unit to include three aquitard types of varying hydraulic conductivity: leaky aquitards, tight aquitards and aquicludes. Distinctions are also now made between aquifers and partial aquifers. The classification of a given hydrogeological unit is also spatially dependent and has been applied across the GAB, including the Surat Basin.

Table 16 Summary of hydrogeological models of the Surat Basin (© Copyright, Smith & Welsh 2011; SWS 2012; USQ 2011).

Model name	Reference	Purpose	Areal extent (km^2 x 1000)	Layers	Software
Australia Pacific LNG project	WorleyParsons (2010b)	CSG extraction	173	23	FEFLOW
Arrow Surat Gas	SWS (2011)	CSG extraction	123	15	MODFLOW
Dumaresq Border Rivers	Chen (2003)	water resources	5	2	MODFLOW
GABFLOW	Welsh (2000)	water resources	1539	1	MODFLOW
GABHYD	Seidel (1978)	water resources	1539	1	custom
GABSIM	Ungemach (1975)	water resources	1539	1	custom
GABTRAN	Welsh (2006)	water resources	1539	1	MODFLOW
Gladstone LNG project	Matrixplus (2009)	CSG extraction	153	19	FEFLOW
Lower Gwydir	Bilge (2002)	water resources	5	2	MODFLOW
Lower Macquarie	Bilge (2007)	water resources	4	4	MODFLOW
Lower Namoi	Merrick (2001)	water resources	5	3	MODFLOW
Moree	Hopkins (1996)	water resources	unsourced		
Namoi Water Study	SWS (2012)	water resources	30	18	MODFLOW
Narrabri Coal Stage 2	Aquaterra (2009)	mine dewatering	2	11	MODFLOW
Queensland Curtis LNG project	Golder Associates (2009)	CSG extraction	17	18	MODFLOW
QWC Surat CMA	QWC (2012a)	water resources	363	19	MODFLOW
Upper Condamine	Barnett and Muller (2008)	water resources	3	3	MODFLOW

The connectivity between hydrogeological units may also be inferred from the vertical hydraulic gradient between them. As described in section 5.5, in a deep basin such as the Surat Basin, hydraulic heads need to be corrected to remove the effects of varying groundwater densities and temperatures. The GABWRA project produced pressure elevation plots in which pressure differences between coincident bores or piezometers (i.e. one sited in the watertable aquifer, the other sited in the Cadna-Owie-Hooray aquifers) were compared.

Differences were calculated for three study areas of the Surat Basin (Figure 21(a)) and are presented in Figure 21(b). Dashed lines represent the hydrostatic gradients for each study area and solid lines represent the observed trend in vertical flow. Trend lines derived from observed data that plot above the hydrostatic gradient indicate upward pressure gradients. This is true for the two data series depicted, which were located in the west (red) and centre (blue) of the Basin.

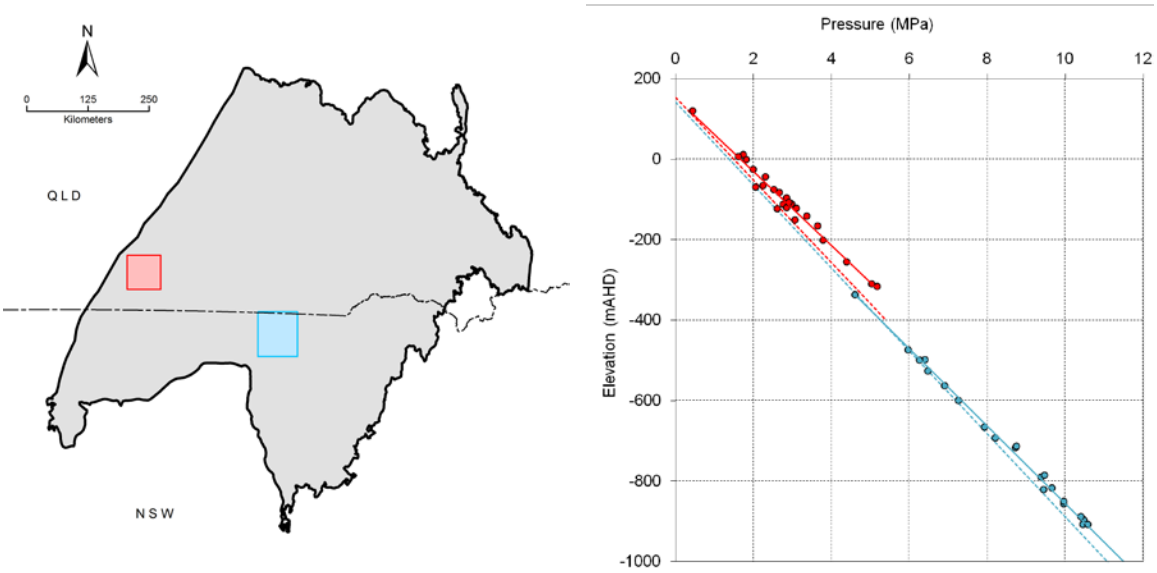

Figure 21 (a) Left-hand side map shows locations of pressure-elevation studies in the Surat Basin and (b) right-hand side graph shows pressure-elevation plots for locations indicated (© Copyright, CSIRO 2012c).

Hodgkinson et al. (2009) performed similar analyses for the eastern Surat Basin, focusing on the Hutton Sandstone, Evergreen Formation, and Precipice Sandstone. Their results suggested that the Evergreen Formation serves as an effective seal over much of the study area; however, hydraulic connection between the two sandstone units via the Evergreen Formation is hypothesised to occur in parts of the Basin.

In a recent review of coal seam water chemistry, WorleyParsons (2010b) summarised the results of Hodgkinson et al. (2010) when discussing indicators of inter-aquifer flow. Potential connectivity between the Hutton and Precipice Sandstone units in the central region of the Surat Basin was inferred from pressure data and potentiometric head measurements. The authors suggested that the Evergreen Formation may not be an effective seal in this region, which is consistent with its characterisation as a leaky aquitard by GABWRA (CSIRO 2012c).

Based upon comparisons of water levels and hydrochemistry, Hillier (2010) concluded that the Walloon Coal Measures and Alluvium of the Condamine River are currently hydraulically connected. The author presented hydrographs from bores sited in each formation and highlighted correlations in gradually decreasing water levels over time. Hillier also stated that a negative hydraulic gradient exists between the Condamine Alluvium and the Walloon Coal Measures. Similarly, the author proposed that elevated salinities in the Condamine Alluvium indicate input of lower quality groundwater from the underlying Walloon Coal Measures.

Currently, there have been no significant studies of stress-induced connectivity in the Surat Basin. Similarly, no significant studies of diffuse leakage from aquifers in the Surat Basin have been undertaken. Borehole leakage in the Surat Basin was identified in a limited study by Habermehl (2009). Studies of groundwater discharge in the Surat Basin have identified the role of faults and fractures as preferential paths for vertical groundwater flow (Habermehl 1982).

6.9 Knowledge gaps

Knowledge gaps relating to aquifer connectivity in the Surat Basin are similar to those identified for the GAB in chapter 5, due to consistencies in depositional history and stratigraphy between the two basins. Exceptions include improved hydraulic and hydrochemical characterisation of certain aquitards, due to their relevance (as hydrocarbon seals) to mining operations. Knowledge gaps for the Surat Basin identified in this review include:

- Currently available measurements of hydraulic properties are sufficient for a general characterisation of Surat Basin hydrogeological units; however, in order to address specific issues, local-scale characterisation would be required. In comparison to differences in hydraulic properties between hydrogeological units, the variability of properties within units is poorly characterised. The exception to this is distinctions between sub-units of the Walloon Coal Measures provided in data compilation by QWC (2012a) and utilised in multi-layer models, such as the Australia Pacific LNG model (WorleyParsons 2010b). Poor past characterisation of hydraulic properties within hydrogeological units has contributed to a simplified conceptualisation of vertical connectivity in the Surat Basin, involving lateral flow through aquifers that are confined by aquitard units. The recent reconceptualisation of the GABWRA (CSIRO 2012c) has expanded the classification of aquitard units to account for the variability of hydraulic properties. For the purposes of addressing groundwater management issues, such variability would need to be characterised at a regional or local scale.
- In-depth studies of the geomechanical properties of Surat Basin units have not been undertaken. Consequently, the potential for changes in hydraulic properties due to changes in stress regimes has not been studied in the Surat Basin. National-scale datasets of horizontal stress directions and magnitudes are available; however, for the purposes of addressing groundwater management issues, regional- or local-scale studies of the stress regimes associated with major faults and fractures in the Surat Basin would need to be undertaken.
- Other than Habermehl (2009), no other published studies have investigated the occurrence of borehole leakage in the Surat Basin. A broader knowledge of past incidents would assist the minimisation of future occurrences through a greater understanding of casing and/or grout interactions with surrounding media.
- Recharge studies in the Surat Basin are currently limited to those of Kellett et al. (2003) and McMahon et al. (2002). Due to variations in geology and vegetation cover, recharge rates are expected to vary spatially. Additional field-based estimates of recharge rates in the Surat Basin would enable the characterisation of such variability. The quantification of recharge rates is of high importance, since the hydraulic gradients produced by recharge influxes are the primary driver of groundwater flow in the Surat Basin. The robustness of predictions produced numerical models used to guide decision-making in

the Surat Basin are heavily dependent upon accurate quantification of recharge fluxes.

- Studies of Surat Basin hydrochemistry have historically focused upon characterising horizontal groundwater flow and mixing in aquifers. The use of hydrochemical analyses to identify and quantify aquifer connectivity has rarely been undertaken. In comparison to Surat Basin aquifers, and with the recent exception of the Walloon Coal Measures, the hydrochemistry of aquitards is relatively poorly characterised. No significant studies of groundwater processes using isotopes have been undertaken.
- Numerical models of groundwater flow in the Surat Basin have historically focused on single-phase flow; consequently, no published studies of multi-phase flow modelling currently exist. This type of modelling would be particularly pertinent to future impact assessments involving mixed-phase flow (e.g. water and gas) in the Surat Basin. Similarly, geomechanical modelling of the potential effects induced by changes in stress fields in the Surat Basin (e.g. due to fluid and gas extraction or injection) is not publicly available. This type of modelling could assist impact assessments in the vicinity of tectonic stress features such as faults and fractures.
- Measurements of vertical hydraulic head gradients are currently limited to those of CSIRO (2012b) (for the Cadna-Owie-Hooray aquifers) and Hodgkinson et al. (2009) (for the Hutton, Evergreen and Precipice units) presented in Section 6.8. The availability of vertical head gradient data is restricted to locations where wells that are sited in different aquifers are located in close proximity. Mapping of vertical gradients at a basinal-scale has not been undertaken. Where available, vertical hydraulic head gradient data provide valuable first-order insights into aquifer connectivity.

7 Aquifer connectivity in the Bowen Basin

7.1 Major aquifer and aquitard stratigraphy

7.1.1 Basin geology

The Bowen Basin is a geological basin forming the northern part of the Bowen-Gunnedah-Sydney Basin system (Figure 1 and Figure 22). The Basin transitions into the congruent Gunnedah Basin in northern NSW. The Basin outcrops to the north near Collinsville (20°S) through to latitude 25°S. South of 25°S, the Bowen Basin is unconformably overlain by the Surat Basin (DME 1997). The interpreted boundary limits of the Bowen Basin have been generally consistent over the years (e.g. Bureau of Rural Sciences and Geological Survey of Queensland interpretations), particularly in the outcropping northern areas of the Basin.

The Bowen Basin is comprised of Permian to Middle Triassic clastic sediments, limestone, andesite, basalt and coal deposited in continental and marine depositional environments (Day et al. 1983). The Basin has a maximum thickness of 10 000 m within two major north-south trending depositional troughs: the Taroom Trough to the east and the Denison Trough to the west (Brakel et al. 2009; Geoscience Australia 2008; SRK 2008; Cadman et al. 1998). Figure 22 shows the locations of the major geological structures within the Basin. The Comet Ridge/Platform and Collinsville Shelf separate the two major troughs. The Nebine Ridge and Springsure Shelf border the Denison Trough to the west and the Auburn Arch borders the Taroom Trough to the east (Hodgkinson 2008 in QWC 2012a). Along its eastern border, the Bowen Basin is bound by a series of north-south thrust faults including the Chinchilla-Goondiwindi, Moonie and Leichardt-Burunga Fault zones (Cadman et al. 1998). These faults have up to 2000 m of displacement (QWC 2012a). The western margins of the basin are vaguely defined owing to subtle thinning and inter-fingering with sediments from the Galilee Basin (QWC 2012a; WorleyParsons 2010).

The Basin has not been subjected to significant metamorphism, although burial metamorphism may have occurred in deeper parts of the Basin (Day et al. 1983). The relationship between potential burial metamorphism and permeability has not been researched. There are small Early Cretaceous granodiorite plutons in the north (Day et al. 1983). The northern outcropping regions of the Basin are covered with irregular Tertiary and Quaternary deposits. Tertiary basalts cover a significant portion of the western Basin.

Table 17 summarises the geological evolution of the Bowen Basin in context of the dominant tectonic regimes, depositional environments and major structural elements such as faults.

Over 100 hydrocarbon accumulations have been discovered in the Bowen Basin within non-marine Permian and Middle Triassic sediments (Geoscience Australia 2008). Most accumulations have been detected beneath anticlinal closures as well as fault rollovers (Geoscience Australia 2008). The Bowen Basin also has vast coal resources, with major open cut and underground coal mines in the north of the Basin. Coal reserves have been estimated at up to 20 billion tonnes of Permian-age coal (Mallett et al. 1995). The Bowen Basin is also a target area for coal seam gas, with large volumes of thermally mature methane gas contained at shallow depths within the vast Late Permian coal deposits (SRK 2008).

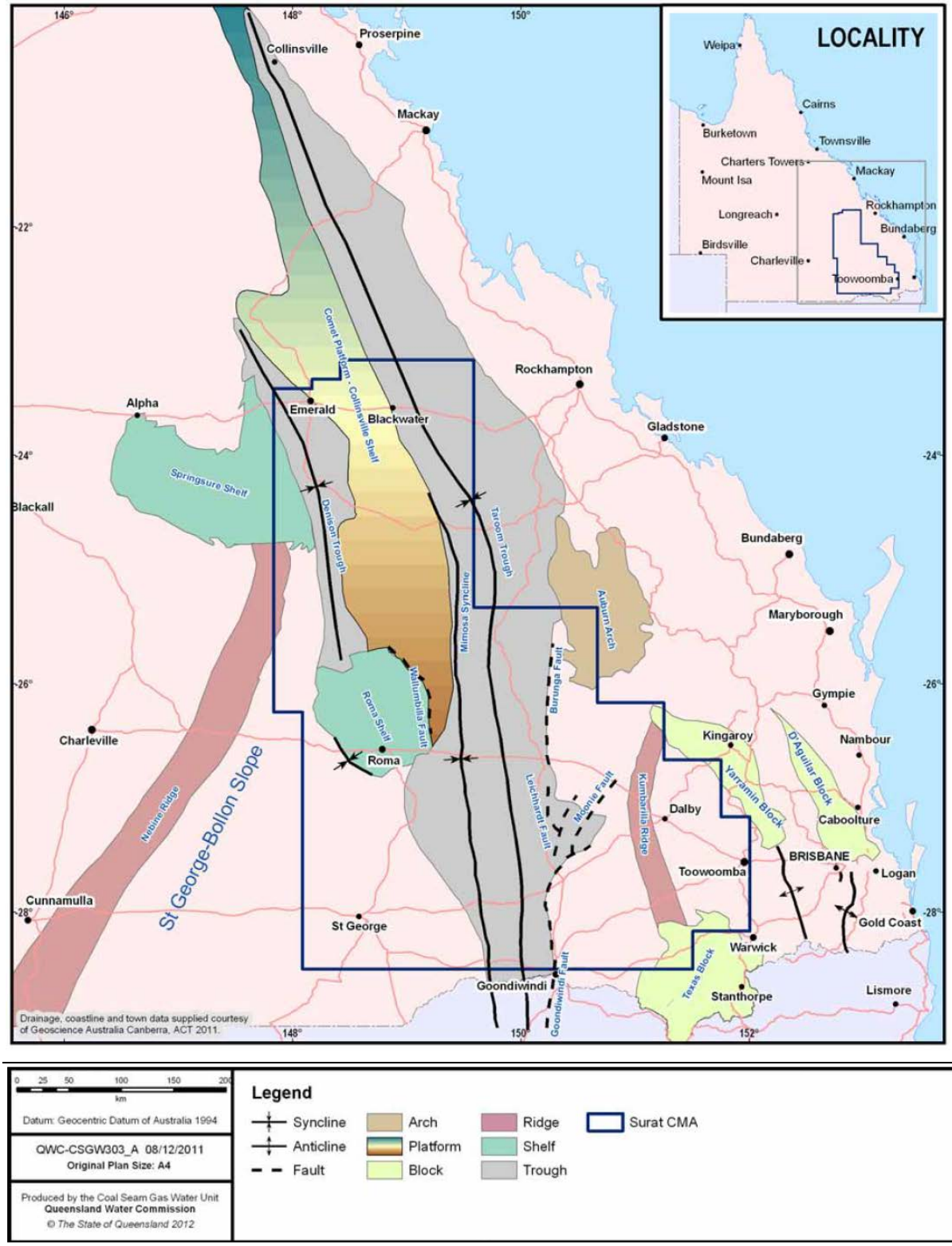

Figure 22 Major geological structures within the Bowen Basin (and Surat Basin) and the margins of the Queensland-extent of the Basin (© Copyright, QWC 2012a).

Table 17 Summary of geological evolution of the Bowen Basin.

Geological Age	Tectonic Regime	Dominant depositional environment	Structural Elements	References
Early Permian	Continent-ocean plate convergence led to a north-south trending back-arc basin west of the Camboon Volcanic Arc	Shallow marine deposition on west margin of basin within half-graben structures (e.g. Denison Trough) and andesite/volcaniclastics laid down on east margin of basin	Back-arc extension on western margin produced series of half-grabens (e.g. Denison and Taroom Troughs)	DME 1997 Day et al. 1983 Draper 1985 Fielding et al. 1990b Brakel et al. 2009
Mid to Late Permian	Subduction and extension cease and thermal relaxation and subsidence allowed incursion of sea over the arc and westward across the basin	Shallow marine delta (west and north edges of basin), infilling of the sea and transitioning into peat-forming coastal swamps (deposited extensive coal seams), wetlands and fluvial systems. Initial deposition of volcanolithic alluvial sediments of Rewan Group	Compressive deformation related to the arc resulted in shedding of volcanolithic sediments from uplifted areas to east	Fielding et al. 1990a DME 1997 Brakel et al. 2009
Early to Late Triassic	Subduction resumes to the east causing prolonged compression in central Queensland. Thrust induced loading of the foreland caused rapid subsidence in the adjacent Taroom Trough	Early Triassic terrestrial deposition of Rewan Group. Quartzose sandstones of Middle Triassic Clematis Group were sourced from the uplifted western craton. The Middle Triassic Moolayember Formation deposited in a marginal marine or tidal-flat environment	Major compressive deformation during Middle to Late Triassic resulted in regional uplift, folding and erosion. Evidence of strike-slip faulting to accommodate compressional forces	Fielding et al. 1990b DME 1997 Brakel et al. 2009

7.1.2 Stratigraphy

The representative stratigraphic column for the Bowen Basin is summarised in Table 18 and a representative west-east cross-section through the Taroom Trough is shown in Figure 23. The nature and age of the basement beneath the basin has only been inferred from exposed rocks outside of the basin and deep seismic survey acquired by Geoscience Australia (CSIRO 2008a). Apart from the margins of the Bowen Basin, the basin has not been full penetrated by exploration drilling to date. Interpretation of the regional deep seismic survey suggests that the underlying rocks are derived from the Lachlan orogen (Korsch et al. 1998 cited in CSIRO 2008a). The basement consists of the Timbury Hills Formation, Kuttung Formation, Roma Granites, Auburn Complex, Yarraman Complex and Texas High Granite (Exon 1976). The oldest formation in the Bowen Basin is the Early Permian Back Creek Group and equivalents, which is predominantly made up of fine-grained deposits of marine origin.

Extensive coal deposits accumulated in swampy terrestrial environments in the mid to late Permian. In the north of the Basin, the coal seams are present within the Moranbah Coal Measures, Fort Cooper Coal Measures and Rangal Coal Measures. In the south of the exposed Basin, the coal seams are present within the Bandanna Formation and the Baralaba Coal Measures. Coal seams throughout the Basin typically split and coalesce at the mine site scale (e.g. over 10 km along strike). Individual coal seams usually vary in thickness from one to 10 m, and coal interburden is typically fine-grained comprising mudstone, siltstone and sandstone.

The Early Triassic Rewan Formation has a maximum encountered thickness of over 1360 m and is comprised predominantly of fine-grained alluvial sediments laid down during late-stage basin subsidence (Exon 1976). The Rewan Group includes the Arcadia Formation overlying the Sagittarius Sandstone. The Arcadia Formation is characterised by thick sequences of red-brown mudstone (Exon 1976).

The Clematis Group is made up of quartzose sandstone, siltstone and mudstone deposited in higher energy fluvial environments (e.g. braided river and meandering river systems) and lower energy floodplains (Cadman et al. 1998 and Olgers 1970 cited in DNRM 2005). The unit is thickest (2000 m) proximal to the source in the north and thins to about 300 m southwest of Wandoan (Exon 1976). The Clematis Group is exposed and outcrops on either side of the Mimosa Syncline within the Taroom Trough. The unit has an obvious northwest-southeast offset where it coincides with the Jellinbah Thrust Belt, southeast of Blackwater.

The Moolayember Formation mainly consists of fine-grained siltstone and mudstone laid down in terrestrial and shallow marine environments (WorleyParsons 2010; Cadman et al 1998). The unit outcrops along the axis of the Mimosa Syncline and provides a 0.3 to 1.5 km buffer between the underlying Clematis Group directly to the north, west and east, and the overlying Precipice Sandstone to the south. The boundary between the Moolayember Formation and the unconformably overlying Precipice Sandstone of the Surat Basin is marked by a transition from fine to medium-grained lithic sublabile sandstones, siltstones and shales to porous fine to very coarse-grained quartzose sandstones (DME 1997). Where the Evergreen Formation of the Surat Basin directly overlies the Moolayember Formation, the boundary is difficult to pick on lithological grounds because of very similar rock types (DME 1997).

Cretaceous gabbros and granodiorite intrusions occur throughout the Basin (see CSIRO 2008a) and Tertiary basalts cover a significant portion of the western Basin stretching from approximately Moranbah in the north to Rolleston in the south.

Table 18 Summary of the Bowen Basin regional stratigraphy.

Geological age	Stratigraphic unit	Lithological description	Thickness	Depositional environment
Quaternary	Recent alluvial deposits	Sand, silt, gravel, clay	0 to 90 m	Alluvial
Tertiary	Tertiary alluvium	Silts, clay, sand and gravel	Up to 100 m	Alluvial and fluvial
	Fresh and weathered basalt	Olivine basalt flows, rare basalt plugs and sills, interbedded with and overlying Tertiary sediments	0 to 250 m	Volcanic
Triassic	Moolayember Formation	Mudstones, siltstones, sandstones, carbonaceous shale, coal, conglomerate and minor tuff and limestone	0 to 1500 m	Dominantly fluvial-lacustrine environment, although includes deltaic and shallow marine transition environments
	Clematis Group	Quartzose sandstone, siltstone and mudstone	0 to 2000 m	Fluvial (braided and meandering) and floodplain
	Rewan Formation	Mudstone, siltstone and labile sandstone	0 to 1360 m	Alluvial and lacustrine
Mid to Late Permian	In the north of the basin, the coal seams are within the Moranbah Coal Measures, Fort Cooper Coal Measures and Rangal Coal Measures. In the south of the basin the seams are within the Bandanna Formation and the Baralaba Coal Measures	Shale, siltstone, mudstone, tuff, coal, sandstone	0 to 600 m	Coal deposits accumulated in swamp environments on an extensive coastal plain and alluvial plain
Early Permian	Back Creek Group	Siltstone, carbonaceous shale, mudstone, clayey sandstone	0 to 600 m	Marine shelf deposits during period of slow basin subsidence

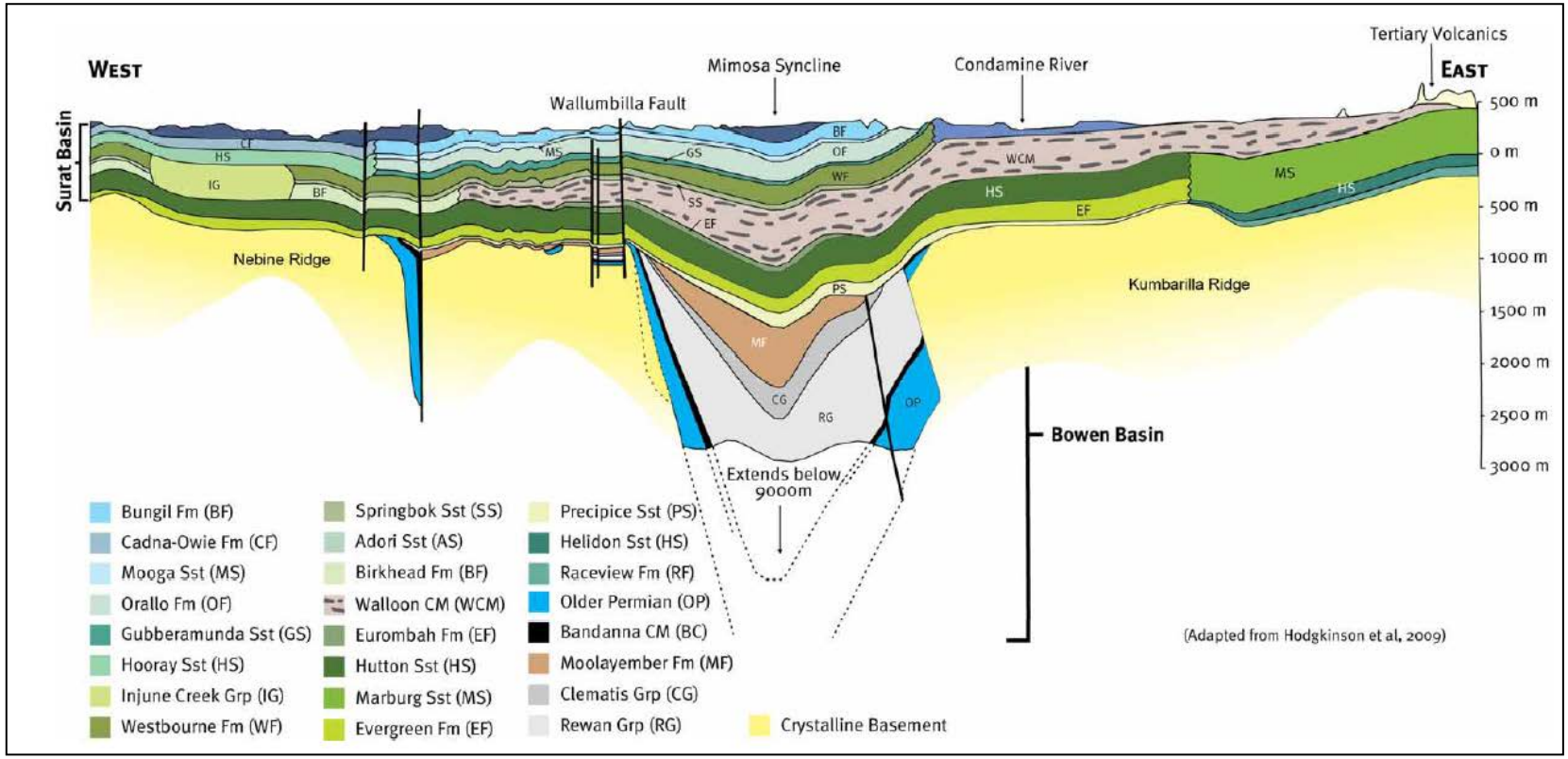

Figure 23 Schematic west-east cross-section across the southern regions of the Bowen Basin where it is overlain by the Surat Basin. Bowen Basin units present below depths of 1500 m within the Mimosa Syncline are shown by units MF, CG, RG and OP (© Copyright, QWC 2012a).

7.1.3 Basin structure

As described in SRK (2009) and CSIRO (2008a), the tectonic history of the Bowen Basin is complex and spans across a number of geological periods. According to CSIRO (2008a) the deformational style of the basin varies from northeast to southwest with the amount of crustal shortening, proximity to basement, presence of varying stratigraphy and presence of older basement structures. CSIRO (2008a) has summarised the major structural characterisation of the Bowen Basin and identified five major structural zones (see Figure 24 and Figure 25):

- Gogango Fold Belt: deforms the eastern margin of the basin and consists of moderate open folding and east-over-west thrust faults that shear the western limb of some of the folds. A moderate amount of crustal shortening has occurred during the formation of this fold belt throughout a high strain regime.
- Dingo Fold Belt: lies directly to the east of the Jellinbah Thrust Belt in central basin. The rocks are folded into tight upright northwest trending folds producing dips of 50 to 80°. A moderate amount of crustal shortening has occurred during the formation of this fold belt throughout a high strain regime.
- Jellinbah Thrust Belt: a north-west trending zone (follows the synclinal axis of the Basin) of complex thin-skinned thrust faulting, in a zone that is up to 80 km wide (and directly west of the Dingo Fold Belt). Majority of the faults dip at low angles to the east, commonly targeting weak coal seams as exit points. It has been noted that in addition to the northwest trending faults, there are a group of faults in the northern part of the Basin that trend north-south, consistent with the faulting associated with the Denison Trough. CSIRO have postulated that this orientation of faulting is potentially indicating Early Permian rift structures at depth.
- Denison Trough: Crustal shortening focused along large (10-100 km long) north-south thrust faults that dip at moderate angles to both the east and the west. Most of the thrust faults have hanging wall anticlines. Seismic interpretation shows that the thrust faults are reactivated (inversion) Early Permian growth faults. There are also a number of smaller north-south normal faults present at depth in the Denison Trough, with offset of Early Permian sediments and basement.
- Springsure Shelf: Minimal crustal shortening associated with a series of reactivated basement faults. The faults are up to 100 km long and record a considerable Pre-Permian strike-slip component. These faults are covered by a veneer of Permian sediments.

Each zone is parallel to the axis of the Basin and transitions from high strain features in the east (Gogango Fold Belt and Dingo Fold Belt) to low strain features in the west (Denison Trough and Springsure Shelf). Compressional deformation in the Basin is primarily related to the protracted Hunter-Bowen shortening event in the Late Triassic, with subsequent influence from later tectonic events reactivating these structures.

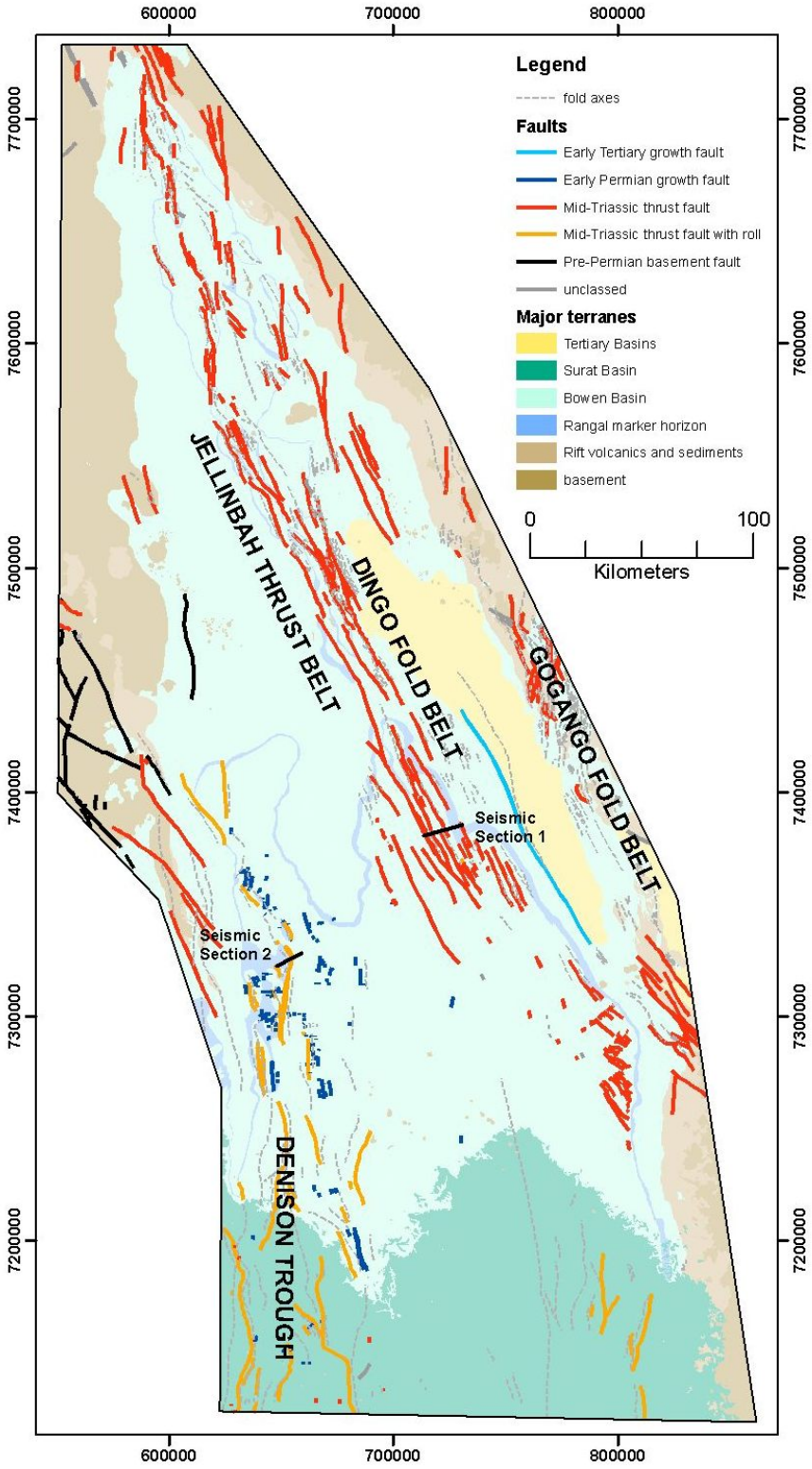

Figure 24 Major structural elements of the Bowen Basin (© Copyright, CSIRO 2008a).

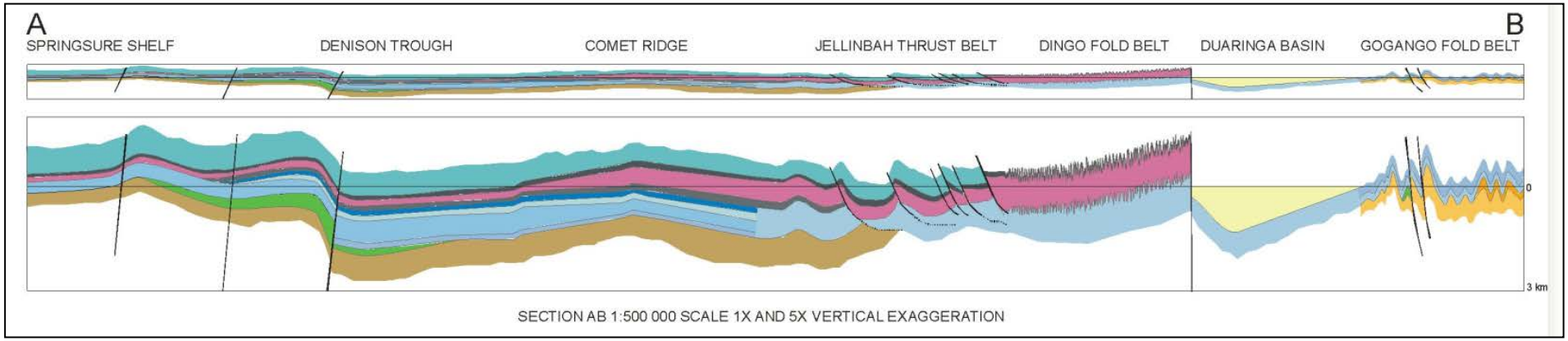

Figure 25 Representative west-east cross section through the central part of the Bowen Basin, showing the presence of the five major structural elements of the Bowen Basin (© Copyright, CSIRO 2008a).

7.1.4 Hydrostratigraphy

The region-wide hydrostratigraphy of the Bowen Basin has been summarised recently by WorleyParsons (2010) and QWC (2012a), with a focus on major aquifers and aquitards that influence basin-wide and inter-basin regional groundwater flow processes. From a regional perspective, both QWC and WorleyParsons identified one major aquifer system (the sandstones of the Clematis Group) separated by two main aquitard systems (the Moolayember Formation and the Rewan Group) and a series of water-bearing units in deep, isolated and confined reservoirs (e.g. Late Permian coal measures and sandstones within the Back Creek Group). While these regionally-extensive major hydrostratigraphic units (HSUs) typically span hundreds of kilometres and can be hundreds to thousands of metres thick, they can be locally discontinuous or absent.

Table 19 provides a summary of both the regionally-extensive major HSUs of the Bowen Basin.

Within the Bowen Basin there are also other minor, local-scale aquifers and aquitards that are not regionally-extensive, due to their irregular and limited occurrence. However, during hydrostratigraphic model development for the Bowen Basin, these minor, local-scale permeable and non-permeable units should not be ignored. These units have the potential to be impacted as a result of coal mining and CSG activities and although they are not regionally important (i.e. as major basin-wide aquifers for water supply), they can be relevant and significant at the local scale (i.e. for domestic and stock water supply or as sources for local groundwater dependent ecosystems). Herein, localised HSUs will be referred to as ‘minor’ aquifers or aquitards (as opposed to the regionally-extensive major HSUs described above).

Table 19 Summary of Bowen Basin regional hydrostratigraphy.

Hydrostra-tigraphic Unit	Description	Reference	Major HSU	Minor HSU	Predominant occurrence	Hydrogeological role
Triassic Moolayembe r Formation	Major aquitard	WorleyParsons 2010 QWC 2012a	✓		Pinches out on western margins of Basin	Major aquitard. Responsible for artesian conditions in the underlying Clematis Group sandstones
Triassic Clematis Group	Major aquifer	WorleyParsons 2010 QWC 2012a	✓		Widespread unit across the Basin. Artesian in northern Basin. Most abstraction at outcrop	Major aquifer of the Bowen Basin
Triassic Rewan Group	Major aquitard	WorleyParsons 2010 QWC 2012a Cadman et al. 1998	✓		Widespread unit across the Basin	Major aquitard of the Bowen Basin and it is recognised as the basal confining layer of the GAB
Permian Coal Measures	Water-bearing units* within aquitard interbeds	BMA 2008 BMA 2009a BMA 2009b Ensham 2006 WorleyParsons 2010 QWC 2012a	✓		Extensive coal measures across the Basin	Target coal seams for both coal mining and CSG abstraction
Deep Reservoirs	Water-bearing units* within aquitard interbeds	WorleyParsons 2010 QWC 2012a	✓		Present at significant depths within the Basin	Limited data available on the groundwater conditions within the deeper Permian sediments

Note: * Water-bearing unit' is considered here as a saturated and moderately permeable unit that can yield water to wells or springs, but not at an economic quantit, and/or suitable water quality.

7.1.5 Description of aquifers

7.1.5.1 Regional-scale aquifer

Clematis group sandstones

Sandstones of the Clematis Group (including previously referenced Clematis Sandstone in the Denison Trough and Showgrounds Sandstone in the Taroom Trough) form the major

confined aquifer within the Bowen Basin with good aquifer yields and good water quality (QWC 2012a). The Clematis Group aquifer is predominantly comprised of quartzose sandstone interbedded with siltstone and mudstone and has been described as highly heterogeneous with rapid lateral and vertical variations in texture and hydraulic properties (Cadman et al. 1998; Olgers 1970). Recharge enters this aquifer in exposed outcrop near the northern margin of the Mimosa Syncline (Radke et al. 2000).

The Clematis Group sandstones are artesian in the northern Bowen Basin with groundwater levels between 10 m to 60 m above ground surface (QWC 2012a). This is the only HSU within the Bowen Basin that is known to be artesian. Bores within the Clematis Group sandstones have shown declining trends over recent decades, in the order of 5m (QWC 2012a). Given the limited development of this aquifer, this slow and steady decline may indicate that long-term storage depletion may not become noticeable for decades to centuries.

DNRM (2005) summarised the Clematis Group aquifer as follows:

- A reliable source of good quality water.
- Yields are generally small, being less than 1.0 L/s, with high yields being rare. These low yields are a potential constraint on future water demand and availability.
- Groundwater extraction occurs dominantly in the north of the Mimosa Syncline (in the Mimosa Management Area) close to outcrop areas. The aquifer is 500 m to 1500 m deep in these areas.
- Further to the south (in the Surat Management Areas) the Clematis Group aquifer is encountered at much greater depths and is not useful as a supply source, despite the good quality of the groundwater.
- Groundwater is dominantly used for stock and domestic purposes, plus town supply for Woorabinda and Bauhinia.
- Springs rise from the Clematis Sandstone in the Expedition Range. They are ‘recharge area’ springs and the majority fall within Crown Reserves, with the high value springs lying within the Blackdown Tablelands National Park.
- The Clematis Sandstones contribute baseflow to Mimosa Creek, Conciliation Creek, Clematis Creek, Dyllingo Creek and Claude River.

7.1.5.2 Regional scale water-bearing units

The major water-bearing units in the Bowen Basin have been described by WorleyParsons (2010) and QWC (2012a) as deep reservoirs of confined and isolated groundwater of generally poor quality. These water-bearing units include:

- Rewan Group Basal Sands
- Late Permian Coal Measures
- Sandstones within the Back Creek Group.

The Rewan Group Basal Sands contain porewater of poor quality and are confined by the overlying mudstones of the Rewan Group. There is limited data available on the groundwater conditions within the deeper Permian sediments below the coal measures, such as the Back Creek Group; however, these formations are believed to be fine-grained, cemented and have

very limited permeability (QWC 2012a). Water quality is poor with very high salinities in some places.

The extensive distribution of Permian coal measures throughout the Bowen Basin and northern Surat Basin is shown in Figure 26. Representative hydrostratigraphic sequences associated with each major productive, water-bearing coal measure are also shown in Figure 26. The Moranbah Coal Measures (light green) are the target coal seam for both coal mining and CSG abstraction in the northern Bowen Basin. Figure 26 shows that the Rangal Coal Measures and the Fort Cooper Coal Measures separate the Moranbah Coal Measures from the minor aquifers of the Isaac River alluvium and Tertiary basalt. In the southern parts of the exposed Bowen Basin, the Bandanna Coal Measures (dark blue) in the west and the Baralaba Coal Measures (maroon) in the east, are separated from the overlying major GAB aquifers (Precipice and Clematis) by the tight Rewan and Moolayember Formations. The major coal unit in the Surat Basin is the Walloon Coal Measures (light blue).

The Coal Measures are highly heterogeneous and comprise interbedded coal, mudstone, siltstone and minor clayey sandstone (QWC 2012a; BMA 2009a; BMA 2009b; BMA 2008). The Bandanna Formation outcrops in the transition zone between the exposed Bowen Basin and the overlying Surat Basin. The outcrop area constitutes the primary recharge zone for the formation (QWC 2012a). The Baralaba Coal Measures outcrop along the Dawson River in the south-east of the Bowen Basin and the Moranbah Coal Measures subcrop south of Moranbah (BMA 2009a; BMA 2009b).

The Bandanna Formation coals are the only sediments with any appreciable permeability within predominantly low permeability interbeds of fine-grained sandstone and siltstone (QWC 2012a). The coal seams split and coalesce and cannot be correlated over any significant distance. These seams are often thin (less than 2 m) and total coal thickness is generally less than 10 m (QWC 2012a). It is likely that the permeability of the coals of the Bandanna Formation within the deepest areas of the Bowen Basin in the Taroom Trough is so low that there is very limited groundwater flow (QWC 2012a).

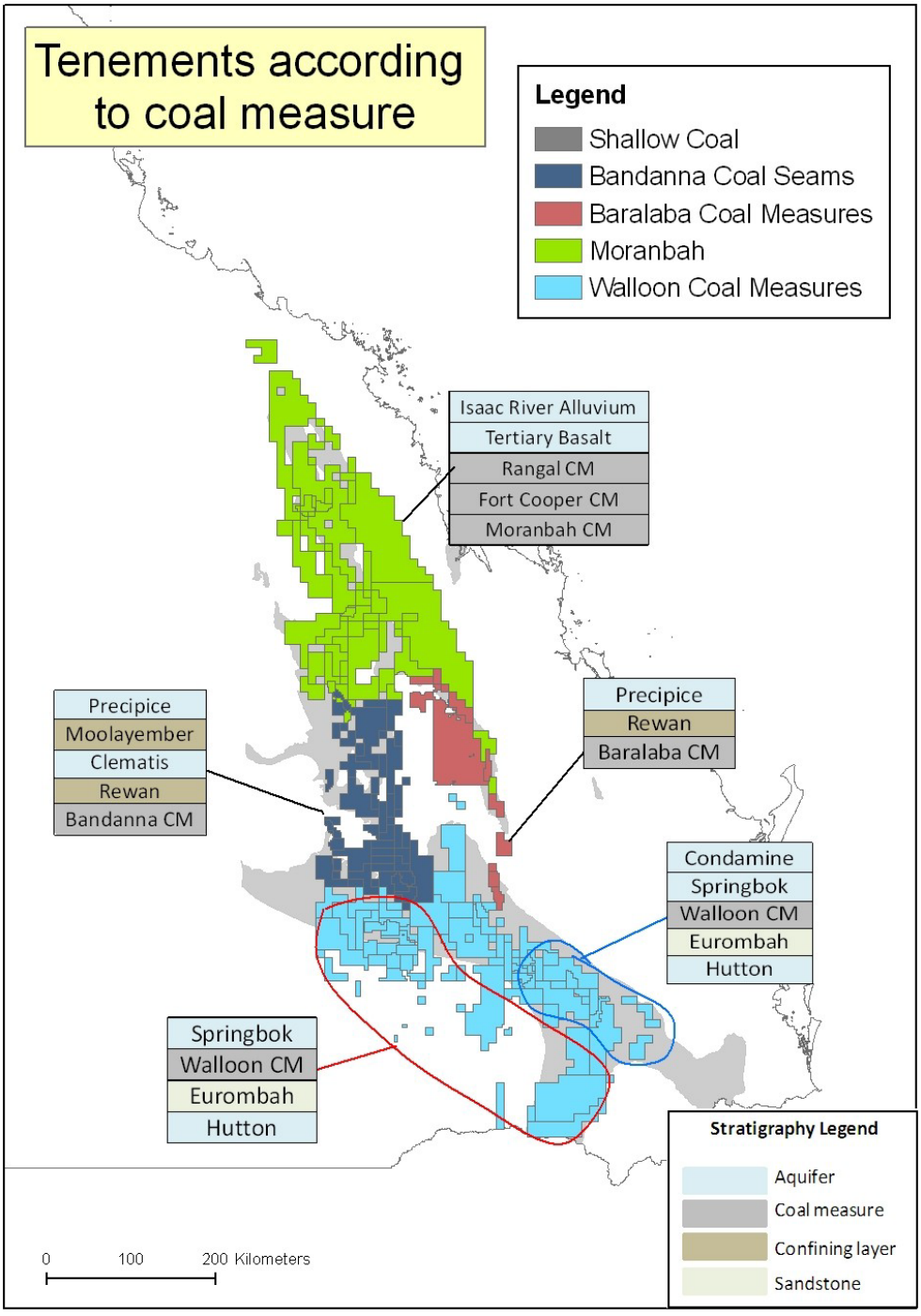

Figure 26 Typical stratigraphic sequences at each of the major Permian Coal Seam water-bearing units in areas of CSG production (© Copyright, CWIMI 2008).

7.1.6 Description of aquitards

7.1.6.1 Regional-scale aquitards

The Moolayember formation

The Moolayember Formation is the shallowest major HSU within the Bowen Basin and is a major aquitard of the GAB. It predominantly comprises low permeability mudstone, shale and siltstone to a thickness of over 1500 m (Habermehl 1980). This aquitard is responsible for generating artesian conditions in the underlying Clematis Group sandstones and separates the sandstones from overlying aquifers of the Surat Basin (QWC 2012a). The formation is a poor producer of groundwater, with predominantly poor water quality. While the yields are comparable to the Clematis Group sandstones (< 1.0 L/s; DNRM 2005), supplies are unreliable and generally only suitable for stock watering. QWC (2012a) estimated that 433 ML/annum is abstracted from the Moolayember Formation for stock and domestic purposes.

On the western margin of the Basin, the Moolayember Formation pinches out and there is hydraulic connection between the Clematis Group sandstones and the Precipice Sandstone (WorleyParsons 2010). Within part of this western area, the underlying Clematis and Rewan Groups are also eroded and the underlying Bandana Formation is in direct contact with the Precipice Sandstone in the vicinity of the Spring Gully Gas Fields (QWC 2012a).

The Rewan Group

The Rewan Group is considered to be a major aquitard of the Bowen Basin and it is recognised as the basal confining layer of the GAB. The Rewan Group separates the overlying Clematis Group sandstones from the underlying Permian coal measures and deep isolated reservoirs (WorleyParsons 2010). The Rewan Group consists of interbedded shale, mudstone, siltstone and lithic sandstone with minor amounts of conglomerate (Radke et al. 2000). The upper section is mostly shale and is considered to be a seal for the basal Rewan Group sandstones (Hennig et al. 2006). Silicification and clay alteration has significantly reduced the porosity and permeability in this formation (Cadman et al. 1998 cited within QWC 2012a) and no significant aquifers exist. The maximum encountered thickness of 1363 m in the Bowen Basin (DME 1997) may increase up to a suspected maximum thickness of 3500 m (WorleyParsons 2010).

Groundwater level data reviewed by Santos (2009) suggest little or no response to seasonal influence of wet and dry seasonal cycles (WorleyParsons 2010). QWC (2012a) estimated that 185 ML/annum is abstracted from the Rewan Group for stock and domestic purposes.

7.1.7 Cumulative management of aquifers in the Surat and Bowen Basins

Coal seam gas production involves pumping large quantities of groundwater from buried coal formations to reduce groundwater pressure and release the gas that is attached to the coal (QWC 2012a). In the Surat and southern Bowen Basins, rapid expansion of coal seam gas production is proposed, involving multiple developers across many adjacent tenements. In response to these proposals, the Surat Cumulative Management Area (Surat CMA) was established on 18 March 2011, the management of which is overseen by the Office of Groundwater Impact Assessment (OGIA). The Surat CMA is focused on coal seam gas produced from the Walloon Coal Measures of the Surat Basin and the Bandanna Formation of the Bowen Basin. It does not include CSG abstracted from the Moranbah Coal Measures in the northern Bowen Basin. Figure 27 shows the boundaries of the Surat CMA in context of the southern bounds of the Bowen Basin.

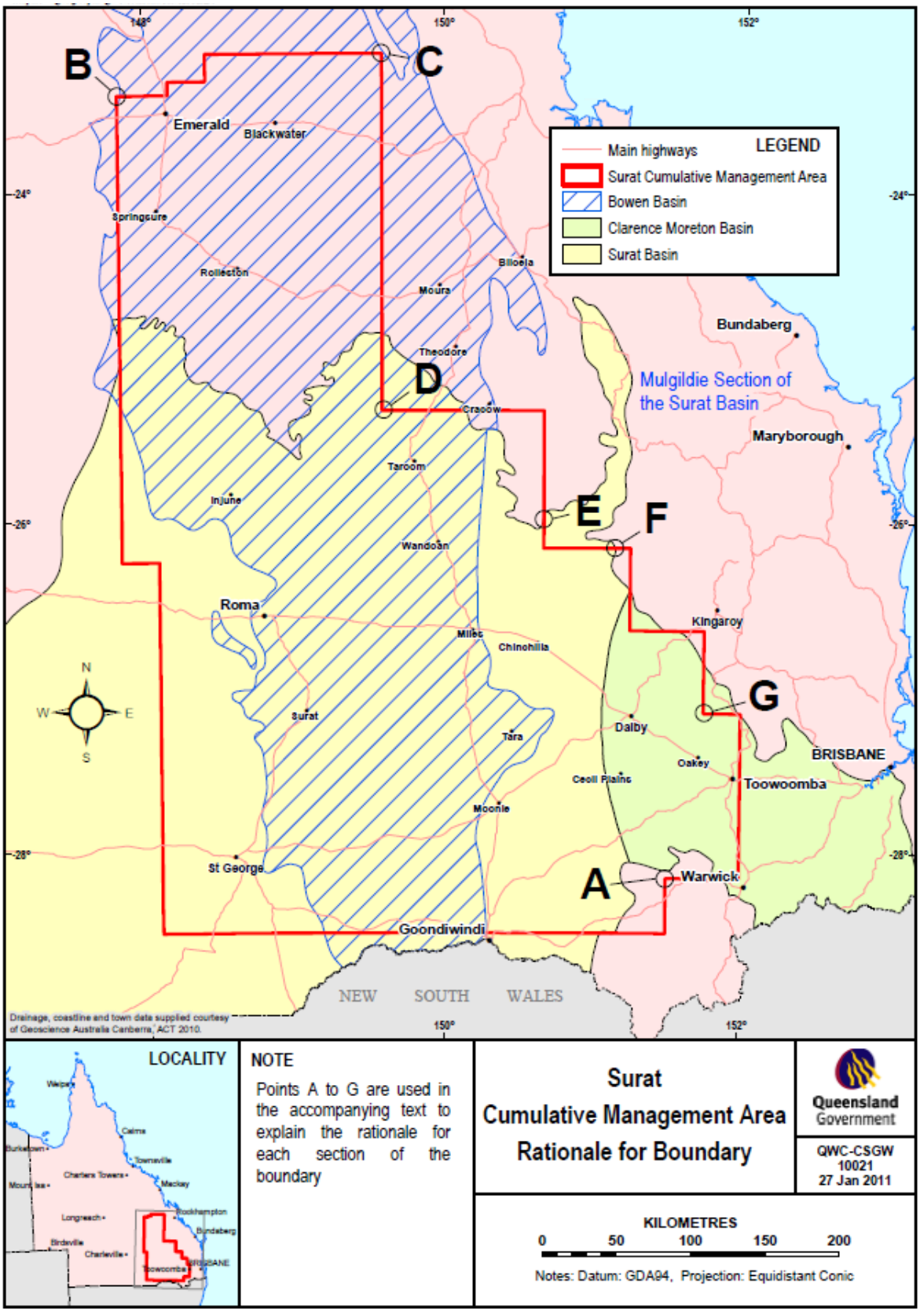

Figure 27 Bounds of the Surat Cumulative Management Area including aquifers and aquitards of the southern Bowen Basin (© Copyright, QWC 2012a).

7.2 Hydraulic properties

7.2.1 Horizontal and vertical hydraulic conductivity measurements

QWC (2012c) estimated hydraulic parameter data for the Surat CMA groundwater model HSUs (including the major HSUs within the Bowen Basin) based on three main sources:

- Queensland Petroleum Exploration Database: a total of 9639 estimates of horizontal and/or vertical hydraulic conductivity obtained from Drill Stem Testing (DST) were extracted from the database
- Queensland Groundwater Database (QGD): transmissivity estimates from 2783 pumping tests and 61 estimates of storativity
- CSG companies.

Estimates of horizontal hydraulic conductivity (Kh) for the Moolayember Formation aquitard, the Clematis Group Sandstone aquifer, the Rewan Group aquitard, the Bandanna Formation water-bearing unit and the deeper reservoirs are summarised in Table 20. Equivalent estimates of vertical hydraulic conductivity (Kv) for the same units are summarised in Table 21.

Figure 28 provides a statistical summary of hydraulic conductivity (K) data available for the Surat and Bowen Basins. The provided ranges and means are plausible, but since it combines data from different tests, the Figure 28 needs to be interpreted with care. Figure 28 does show that the median horizontal hydraulic conductivity for the Clematis Group sandstone aquifer is equivalent to the overlying Precipice Sandstone aquifer of the Surat Basin (see chapter 6). The median horizontal hydraulic conductivity for the Clematis Group is also one to two orders of magnitude higher than the horizontal hydraulic conductivities for the Moolayember Formation, the Rewan Group and the Bandanna Formation.

Table 20 Summary of Kh estimates collated for Bowen Basin HSUs within the Surat CMA (© Copyright, QWC 2012b).

HSU	Number of tests / estimates	Horizontal hydraulic conductivity (m/day)		
		Minimum	Maximum	Median
Moolayember Formation (Aquitard)	416	$8.31x10^{-6}$	$1.03x10^{1}$	$1.6x10^{-3}$
Clematis Group Sandstones and equivalents (Aquifer)	1950	$8.31x10^{-6}$	$5.46x10^{1}$	$2.7x10^{-2}$
Rewan Group (Aquitard)	822	$8.31x10^{-6}$	$1.86x10^{0}$	$3.6x10^{-4}$
Bandanna Formation – Coal producing formation	261	$8.31x10^{-6}$	$7.84x10^{0}$	$1.0x10^{-3}$
Deeper Reservoirs (e.g. Back Creek Group)	393	$8.31x10^{-6}$	$1.91x10^{0}$	$1.5x10^{-3}$

Table 21 Summary of Kv estimates collated for Bowen Basin HSUs within the Surat CMA (© Coypright, QWC 2012b).

HSU	Number of tests / estimates	Horizontal hydraulic conductivity (m/day)		
		Minimum	Maximum	Median
Moolayember Formation (Aquitard)	199	$9.32x10^{-6}$	$9.06x10^{0}$	$1.3x10^{-3}$
Clematis Group Sandstones and equivalents (Aquifer)	570	$8.31x10^{-6}$	$1.15x10^{1}$	$1.2x10^{-2}$
Rewan Group (Aquitard)	252	$8.31x10^{-6}$	$4.50x10^{-1}$	$1.9x10^{-4}$
Bandanna Formation – Coal producing formation	70	$8.31x10^{-6}$	$1.26x10^{0}$	$5.6x10^{-4}$
Deeper Reservoirs (e.g. Back Creek Group)	18	$4.16x10^{-5}$	$1.12x10^{-1}$	$3.2x10^{-4}$

The estimates in Table 20, Table 21 and Figure 28 are likely to be biased, in that they are test wells and bores that have been drilled to target productive horizons for either CSG production or groundwater. These holes were intended to find the most permeable and productive parts of the heterogeneous aquifers, aquitards or coal seams, at the shallowest and most accessible depths. Given the significant thicknesses of the actual HSUs in the Bowen Basin (e.g. thousands of metres in the Taroom Trough) it is likely that deeper parts of the Basin are under-represented in the dataset. It is also likely that hydraulic conductivity will reduce with depth, as the aquifer/aquitard material is compacted and fracture and fissure apertures close up and diminish (QWC 2012c). The Queensland Carbon Gas Storage Initiative (QCGI 2009) describes a tendency for the permeability of the Walloon Coal Measures to reduce with depth of burial (QWC 2012c). This permeability reduction phenomenon is likely to occur in the equivalent Late Permian coal measures of the Bowen Basin. For these reasons, it is plausible that the bulk Kh values for the HSUs may actually be a lot lower than the values summarised in Table 20, Table 21 and Figure 28.

Additionally, the testing methods used to obtain the horizontal hydraulic conductivity and vertical hydraulic conductivity parameters (i.e. pumping tests, core tests, drill stem tests) only provide a localised indication of aquifer properties. They are not representative of the bulk aquifer properties of the HSUs and should not be considered as such. The vertical hydraulic conductivity estimates in particular are unlikely to reflect the regional properties of the aquitards, as the tests would not have been completed for a sufficient period of time to generate vertical flow at the scale of the HSU, and as such the regional bulk vertical hydraulic conductivity values may be greater than what the local-scale tests indicate. It has to be noted that horizontal hydraulic conductivity estimates from such short tests can have great uncertainty as well.

Field testing at the local scale also ignores the influence of regional-scale faults, fractures, facies changes and leaky bores, all of which can greatly influence regional horizontal hydraulic conductivity and vertical hydraulic conductivity values.

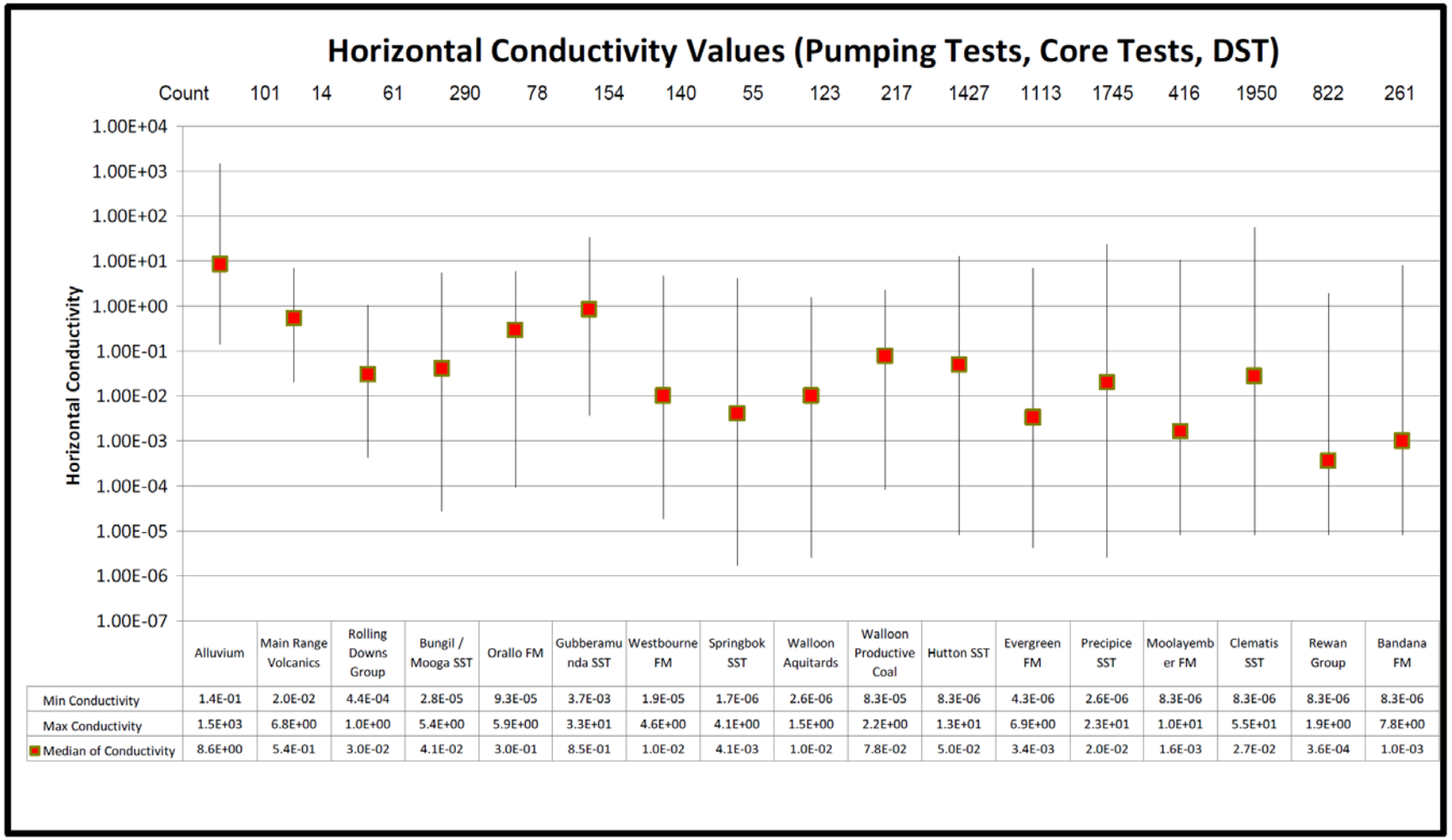

	Alluvium	Main Range Volcanics	Rolling Downs Group	Bungil / Mooga SST	Orallo FM	Gubberamunda SST	Westbourne FM	Springbok SST	Walloon Aquitards	Walloon Productive Coal	Hutton SST	Evergreen FM	Precipice SST	Moolayember FM	Clematis SST	Rewan Group	Bandana FM
Count	101	14	61	290	78	154	140	55	123	217	1427	1113	1745	416	1950	822	261
Min Conductivity	1.4E-01	2.0E-02	4.4E-04	2.8E-05	9.3E-05	3.7E-03	1.9E-05	1.7E-06	2.6E-06	8.3E-05	8.3E-06	4.3E-06	2.6E-06	8.3E-06	8.3E-06	8.3E-06	8.3E-06
Max Conductivity	1.5E+03	6.8E+00	1.0E+00	5.4E+00	5.9E+00	3.3E+01	4.6E+00	4.1E+00	1.5E+00	2.2E+00	1.3E+01	6.9E+00	2.3E+01	1.0E+01	5.5E+01	1.9E+00	7.8E+00
Median of Conductivity	8.6E+00	5.4E-01	3.0E-02	4.1E-02	3.0E-01	8.5E-01	1.0E-02	4.1E-03	1.0E-02	7.8E-02	5.0E-02	3.4E-03	2.0E-02	1.6E-03	2.7E-02	3.6E-04	1.0E-03

Figure 28 Statistical summary of measured horizontal hydraulic conductivity (Kh) values (in m/day) for all HSUs in the Surat CMA, including the Moolayember Formation aquitard, the Clematis Group Sandstone aquifer, the Rewan Group aquitard and the Bandanna Formation (© Copyright, QWC 2012a).

7.2.2 Model-derived horizontal and vertical hydraulic conductivity estimates

QWC (QWC 2012a; QWC 2012c) developed a 19-layer MODFLOW numerical groundwater model to determine the cumulative impacts of CSG abstraction on aquifers within the Surat and Bowen Basins. The model was calibrated by adjusting hydraulic conductivity values to groundwater head data using the parameter estimation software package PEST (i.e. model-independent parameter estimation and uncertainty analysis). Calibrated horizontal and vertical hydraulic conductivity values were obtained for the five major regionally-extensive HSUs within the Bowen Basin. Of those five HSUs, it was noted that calibration performance was poor for the Moolayember Formation due to various reasons including spatial heterogeneity of aquifer properties and the use of point scale estimates of hydraulic conductivity, and should therefore be given a lower level of confidence (QWC 2012c). Table 22 summarises the calibrated horizontal hydraulic conductivity values for the Bowen Basin HSUs and Table 23 summarises the calibrated vertical hydraulic conductivity values.

Table 22 Summary of calibrated horizontal hydraulic conductivity (Kh) values for Bowen Basin HSUs within the Surat CMA (© Copyright, QWC 2012c)

HSU	Model layer	Horizontal hydraulic conductivity (m/day)		
		Minimum	Average	Maximum
Moolayember Formation (Aquitard)	15	$3.7x10^{-06}$	$1.4x10^{-03}$	$1.4x10^{+00}$
Clematis Group Sandstones and equivalents (Aquifer)	16	$6x10^{-04}$	$2.0x10^{-01}$	$5.0x10^{+00}$
Rewan Group (Aquitard)	17	$1.0x10^{-04}$	$5.4x10^{-02}$	$1.4x10^{+00}$
Bandanna Formation – Coal producing formation	18	$1.0x10^{-05}$	$3.2x10^{-02}$	$1.0x10^{+00}$
Deeper Reservoirs (e.g. Back Creek Group)	19	$5.0x10^{-07}$	$8.5x10^{-06}$	$5.0x10^{-03}$

Table 23 Summary of calibrated vertical hydraulic conductivity (Kv) values for Bowen Basin HSUs within the Surat CMA (© Copyright, QWC 2012c).

HSU	Model layer	Vertical hydraulic conductivity (m/day)		
		Minimum	Average	Maximum
Moolayember Formation (Aquitard)	15	$3.6x10^{-07}$	$1.3x10^{-04}$	$1.1x10^{-01}$
Clematis Group Sandstones and equivalents (Aquifer)	16	$1.0x10^{-04}$	$2.7x10^{-02}$	$6.9x10^{-01}$
Rewan Group (Aquitard)	17	$1.0x10^{-07}$	$9.7x10^{-05}$	$1.1x10^{-01}$
Bandanna Formation – Coal producing formation	18	$2.0x10^{-09}$	$6.4x10^{-06}$	$2.0x10^{-04}$
Deeper Reservoirs (e.g. Back Creek Group)	19	$5.0x10^{-08}$	$8.5x10^{-07}$	$5.0x10^{-04}$

7.2.3 Model-derived specific storage estimates

With the exception of the Bandanna Formation, the other regionally-extensive HSUs (Moolayember Formation, the Clematis Group sandstones, the Rewan Group and the deeper reservoirs) were all calibrated to a specific storage value of $5.0x10^{-05}$ m^{-1} (QWC 2012c). The Bandanna Formation varied between $1.0x10^{-7}$ and $3.4x10^{-05}$ m^{-1} (QWC 2012c).

7.3 Structural properties

7.3.1 Major structural features

Because of the strong compressional regime present in the Bowen Basin during the Triassic, there are many instances where individual formations have been truncated, offset or eroded, and where a number of formations that would not otherwise be in contact (due to large vertical separation) are now in contact. From a connectivity perspective, the structural fabric of the Basin is a significant factor. As discussed previously, CSIRO (2008a) have summarised the major structural characterisation of the Bowen Basin and identified five major structural zones:

- Gogango Fold Belt: deforms the eastern margin of the Basin and consists of moderate open folding and east-over-west thrust faults.
- Dingo Fold Belt: lies directly to the east of the Jellinbah Thrust Belt in the central Basin. The rocks are folded into tight upright northwest trending folds producing dips of 50 to 80°.
- Jellinbah Thrust Belt: north-west trending zone (follows the synclinal axis of the Basin) of complex thin-skinned thrust faulting, in a zone that is up to 80 km wide (and directly west of the Dingo Fold Belt). Majority of the faults dip at low angles to the east, commonly targeting weak coal seams as exit points.
- Denison Trough: crustal shortening focused along large (10-100 km long) north-south thrust faults that dip at moderate angles to both the east and the west.
- Springsure Shelf: minimal crustal shortening associated with a series of reactivated basement faults. The faults are up to 100 km long and record a considerable Pre-Permian strike-slip component. These faults are covered by a veneer of Permian sediments.

7.3.2 Relationships between structural features and aquifer connectivity

The influence of regional structural features on groundwater flow processes in the Bowen Basin is not well understood. With regards to the Surat CMA, there are contrasting perspectives about the overall influence of major faults in the Surat and Bowen Basins on regional groundwater flowpaths. Some of the views include:

- the faults are likely to reduce hydraulic connection (Golder Associates 2009)
- the faults are unlikely to present barriers to horizontal groundwater flow in the Surat Basin (Hodgkinson et al. 2010).

There does not appear to be any hydrogeological evidence at this stage to prove or disprove whether structural features have enhanced or diminished aquifer connectivity in the Bowen Basin. The lack of evidence and understanding is mainly attributed to:

- the significant depth to HSUs in the Basin makes groundwater exploration and

development difficult

- the limited use of groundwater within the Basin and the generally low yields of the aquifers. Without significant pumping stresses on the aquifers to date, there has been no means of identifying positive or negative hydraulic flow behaviour caused by structural features.

Theoretically, structural features such as faults, fractures and dykes can provide pathways for groundwater movement between aquifers; however, they can also serve as hydraulic barriers, where mineralisation can create a seal and limit groundwater flow across the structures (Hennig 2005 cited in QWC 2012a). High-strain structural features in the east of the Basin (e.g. Jellinbah Thrust Belt and Dingo Fold Belt) consist of tight, upright folding within Permian units and complex series of thrust faults including instances where low permeability HSUs (e.g. Rewan Group) are thrust up onto water-bearing units (e.g. the Baralaba Coal Measures) (CSIRO 2008a) and vice versa. These faults have created significant unit offset e.g. the Bandanna Formation has been fully displaced in the Jellinbah Thrust Belt (QWC 2012a).

Where these structural features have imposed localised changes to bedding continuity or have emplaced previously disconnected HSUs in direct contact, then there will be inevitable alteration to local groundwater flowpaths and aquifer connectivity. What influence these localised alterations have on regional, Basin-wide groundwater dynamics is still unknown. Where faults and fractures occur repeatedly in a complex series, it is likely that the aquifer can become compartmentalised and aquifer connectivity can be diminished.

Based on current knowledge and understanding of regional groundwater flowpaths, QWC (2012a) acknowledged the uncertainty on structural controls in the Bowen Basin and concluded:

- any influence of the fault structures on regional groundwater flow, either as pathways or barriers, is likely to be restricted to the Bowen Basin where there is the most offset and is unlikely to materially influence a majority of the (overlying) GAB aquifers in the Surat Basin
- any regional effect of faults on groundwater flow over long periods of time should be reflected in current observed water levels which are used in calibrating the regional groundwater flow model
- further targeted research is required to assess the influence of regional structures on groundwater flow in and around areas of CSG development.

7.4 Geomechanical properties

A review of the hydrogeology literature associated with the Bowen Basin did not identify any references (of significance) regarding geomechanical properties of formations in the Bowen Basin. This information may be present in engineering or petroleum literature, which was outside the scope of this review. CSIRO (2008a) and SRK (2009) provide insights into the tectonic regimes that existed in the Permian and Triassic geological periods and the subsequent zones of high and low strain during the development of the Basin. These reports did not contain information on current in situ stresses, relative stress magnitudes or stress contrasts within/between units. It is apparent that CSG companies are currently collecting geomechanical information; however, this information is generally not publicly available.

7.5 Geochemistry

7.5.1 Major ion chemistry and salinity

The Fitzroy Basin is a major water resource plan (WRP) area in Queensland and extends across most of the exposed northern Bowen Basin. The DNRM groundwater database (GWDB) contains more than 13 000 subartesian water quality samples collected from 4780 bores in the Fitzroy Basin spanning across a period of 50 years (DERM 2011). Approximately 75 per cent of the samples have been taken from shallow bores (less than 30 m) and 25 per cent (3300) are from deeper bores. Multi-variate analyses of the entire water quality database identified two main hydrochemical sequences. The first, designated the 'alluvial sequence' occurs in surface waters and alluvial aquifers. Their cations are moderately balanced and dominated by bicarbonate (HCO_3), except in the highest salinity range where sodium chloride (Na-Cl) begins to dominate (DERM 2011). The second sequence, the 'sodic sequence', is dominated by sodium chloride, although bicarbonate may be high at the lowest salinities (DERM 2011). The sodic sequence is compositionally similar to marine water and is associated with deep and occasionally shallow groundwater that is in contact with older sedimentary rocks (DERM 2011).

Figure 29 shows the hydrochemical provinces established by DERM (2011) within the Fitzroy Basin Water Resource Plan (WRP) area. Of significance for the Bowen Basin hydrochemistry are the provinces delineated in red representing saline, sodium chloride, sodic sequences:

- provinces 31 and 35 in the vicinity of Emerald and Rolleston, which are deep samples taken from within the coal measures of the Bandanna Formation
- province 34 which stretches from Moranbah through Baralaba and down to Moura, which are deep samples taken from within Rangal, Fort Cooper and Moranbah Coal Measures in the north and the Baralaba Coal Measures in the south-east.

Out of interest, Province 32 in the vicinity of Wandoan is also classified as a saline sodic sequence and is underlain by the Walloon Coal Measures of the Surat Basin. Table 24 summarises the salinity and major ion statistics for each of the major coal measure zones identified above. The 50th percentile electrical conductivity (EC) value for the Bandanna Formation is 3150 µS/cm (near Emerald) and 9375 µS/cm (near Rolleston). The 50th percentile electrical conductivity (EC) value for the Moranbah Coal Measures and the Baralaba Coal Measures is 6100 µS/cm. These saline sequences demonstrate the poor groundwater quality of the coal seams in the Bowen Basin.

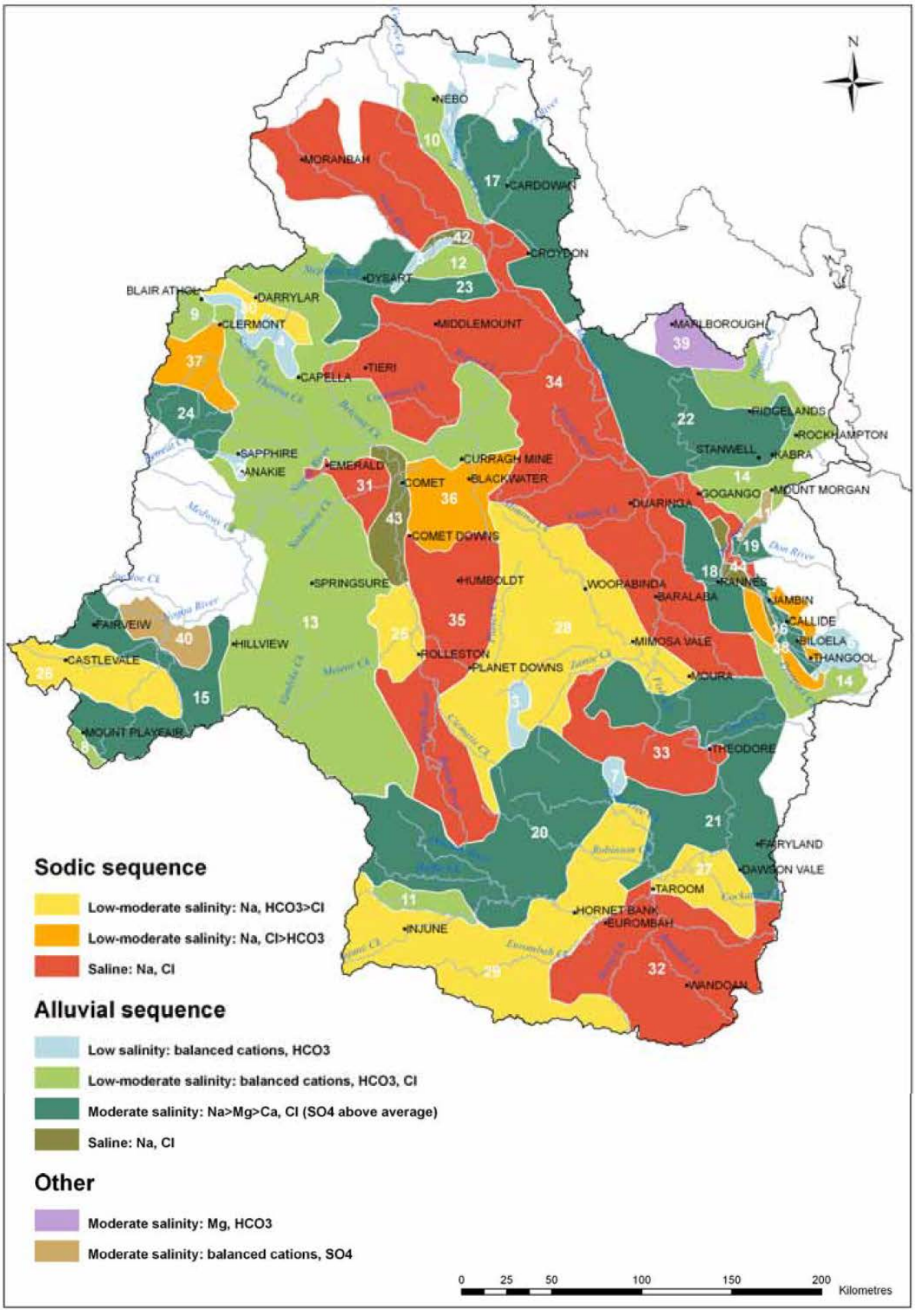

Figure 29 The dominant hydrochemical provinces within the Fitzroy Basin (© Copyright, DERM 2011).

Table 24 Summary of salinity and major ion statistics for each of the major 'deep' hydrochemical provinces associated with the Late Permian coal measures in the Bowen Basin (© Copyright, DERM 2011).

Hydrochem zone	Coal measures	Percentile	EC (uS/cm)	pH	Major Ions (mg/L)					
					Ca	Mg	Na	Cl	SO_4	HCO_3
31	Bandanna Fm	20th	2151	7.70	9	14	375	414	0	412
		50th	3150	7.95	27	28	589	554	10	683
		80th	3540	8.20	70	106	734	954	64	763
34	Moranbah CM and Baralaba CM	20th	3419	7.40	46	35	480	753	25	188
		50th	6100	7.80	145	115	1100	1900	138	330
		80th	16000	8.03	442	491	2565	5905	398	650
35	Bandanna Fm	20th	4103	7.37	33	45	465	1079	0	126
		50th	9375	7.60	146	204	1750	3316	20	268
		80th	13604	8.01	366	226	2555	5368	122	376

WorleyParsons (2010) conducted a literature review of the spatial attributes of coal seam water chemistry in the Bowen and Surat Basins. Their major findings for the Bowen Basin were as follows:

- The major HSUs of the Bowen Basin (e.g. Clematis Group sandstones and the Moolayember Formation) display similar hydrochemical characteristics to the overlying GAB units and for this reason are thought to be somehow connected (Habermehl 1980).
- The Moolayember Formation has been established as Na-Cl-HCO_3 type groundwater (Santos 2009). Samples collected from the Formation were generally found to be elevated in manganese and with low pH at several locations and with EC values of approximately 2000 µS/cm in the upper horizons (Santos 2009).
- The Clematis Group sandstones and equivalents (based on only eight bores) had EC values between 131 and 900 µS/cm, with one outlier of 1980 µS/cm. The salinities within the Clematis Sandstone increase from north to south, which is suspected to be a function of proximity to nearby outcropping recharge areas. There is insufficient data to determine spatial variations in chemical composition (Hennig et al. 2006).
- The hydrochemistry of the Clematis Group sandstones is stable over time with only minor fluctuations in major ion concentrations. The geochemical signature may be overprinted to some extent by the diffusion of Na and Cl ions (as well as other soluble ions) from overlying or underlying aquitards with marginal marine depositional histories (Radke et al. 2000).
- The Rewan Group has very limited hydrochemical data; however, groundwater quality is generally considered to be poor with elevated salinity on the order of 25 000 µS/cm (Santos 2009). The groundwater is generally a Na-Cl dominant type with elevated potassium and sulphate when compared to the other aquifers (Santos 2009).

- Groundwater in the isolated, deep reservoirs displays different hydraulic characteristics and hydrochemistry from the overlying HSUs. Groundwater quality in the isolated, deep reservoirs is variable but generally of a much poorer quality than the overlying Clematis Group. The Late Permian coal seams in the area under review by Santos (2009) yielded EC values up to 19 000 µS/cm. Salinity within the coal seams was generally observed to increase from north to south. Electrical conductivity values within the Back Creek Group were found to range from 2800 µS/cm to 30 000 µS/cm (Santos 2009).

7.5.2 Isotope studies and hydrogeological implications

Environmental isotope studies in the region have focused on recharge mechanisms and residence times in the overlying GAB aquifers (GABCC 1998). Although limited data is available for the deeper aquifer and aquitards of the Bowen Basin, it can be assumed that water movement is slow and that aquifers have very long residence times. For this reason, it can be expected that the system will have significant lag times associated with responses to stresses, and significant recovery times should impacts occur.

7.6 Regional groundwater flow trends

There is not enough current spatial and temporal groundwater monitoring data for HSUs across the Bowen Basin to interpret regional groundwater flow patterns. Conceptually, groundwater flow should flow from the outcropping recharge zones to the south and south-west along the direction of dip in the Basin (WorleyParsons 2010). Table 25 summarises the very limited number of DNRM and CSG groundwater monitoring locations for the major HSUs within the Surat CMA. This table highlights that there are only 33 groundwater level and quality monitoring sites for the five major Bowen Basin HSUs in the Surat CMA (data obtained from QWC 2012d). The Clematis Group sandstones comprise approximately half of the current network. Additional monitoring sites will be installed by CSG operators as the industry expands in this Basin. The significant depth of the HSUs within the Taroom and Denison Troughs precludes the practicality of installing more monitoring sites in the buried, down-gradient extents of the Bowen Basin. Most of the current sites are situated along the outcropping areas in the exposed parts of the Basin.

Table 25 Existing and proposed groundwater monitoring sites for the Bowen Basin HSUs within the Surat CMA (© Copyright, QWC 2012d).

HSU	Existing DNRM groundwater monitoring sites	Existing CSG operator groundwater monitoring sites	Total existing groundwater monitoring sites
Moolayember Fm	2	0	2
Clematis Group sandstones	7	8	15
Rewan Group	4	0	4
Bandanna Fm	0	3	3
Deep Reservoirs	9	0	9

A review of the literature did not identify any references regarding the connectivity of the northern Bowen Basin aquifers and water-bearing units and their equivalents in the southern Bowen Basin.

7.7 Recharge

7.7.1 Surat CMA

The commonly accepted theory for recharge into the GAB aquifers is via rainfall recharge along the outcrop areas proximal to the Great Dividing Range (see Kellet et al. 2003; Habermehl 2002; Habermehl 1980). Collectively these outcrop recharge areas are often referred to as the GAB intake beds (QWC 2012a; QWC 2012c). QWC (2012a) summarise the main recharge process for the Surat CMA as:

> *'Recharge occurs predominantly by rainfall, either by direct infiltration into the outcrop areas, or indirectly via leakage from streams or overlying aquifers. It has been identified (Kellett et al. 2003) that direct rainfall or diffuse recharge rates are generally small, generally less than 2.5 mm per year. However, recharge rates through preferred pathway flow during high intensity rainfall events, and localised recharge from stream or aquifer leakage can be up to 30 mm per year.'*
>
>

QWC (2012a), QWC (2012b) and QWC (2012c) identified that there is some disagreement regarding which aquifers comprise intake beds. Habermehl (2002) listed the main intake beds as the Hooray, Hutton, Precipice and Clematis sandstone aquifers and their equivalent formations. Kellet et al. (2003) only describe the Hooray and Hutton sandstones and suggest that recharge through other outcropping units is minimal. These differing theories have significant implications for recharge into the major aquifer of the Bowen Basin - the Clematis Group sandstones. Using the original Kellet et al. (2003) chloride mass balance calculations for recharge rates through the Hooray and Hutton sandstones, QWC (2012a) estimated that the Clematis Group sandstones have an outcrop area of just over 5000 km^2 and receive approximately 29 000 ML/year of recharge at a recharge rate of 5.8 mm/year.

Calibrated recharge rates for the 19 layer, Surat CMA, MODFLOW model (QWC 2012c) indicate that far less annual recharge reports to the Clematis Group sandstones than the Kellet-based estimate of 29 000 ML/annum rate. The model predicts that only 2540 ML/year of net watertable recharge reports to the Clematis Group aquifer. Table 26 summarises the calibrated recharge values for all five of the major Bowen Basin HSUs within the Surat CMA. The net recharge values listed in the table take account of modelled water table recharge, subtracting modelled discharge to local shallow groundwater systems and adding in net inflow from adjacent layers (QWC 2012c). As can be seen from the table, very little recharge enters the two major aquitards (Moolayember Formation and Rewan Group) or the water-bearing Bandanna Formation coal seams. No water table recharge is predicted to occur to the deeper reservoirs beneath the Bandanna Formation as these do not outcrop. The Clematis Group aquifer accounts for 79 per cent of the calibrated recharge flux into the Bowen Basin in the Surat CMA area.

Table 26 Summary of calibrated recharge values for Bowen Basin HSUs in the Surat CMA groundwater model (© Copyright, QWC 2012c).

HSU	Model layer	Net recharge (ML/annum)
Moolayember Formation	15	445
Clematis Group sandstones	16	2,540
Rewan Group	17	115
Bandanna Formation	18	130
Other Deep Reservoirs	19	0

7.7.2 Northern Bowen Basin

The Clematis Group, Rewan Group and Moolayember Formation also subcrop/outcrop within the axis of the syncline that extends up through the northern extents of the elongated Bowen Basin. No information was available regarding recharge rates into the northern intake beds of these HSUs. The Arrow Energy underground water impact report (UWIR) assessment for the northern Bowen Basin (Arrow Energy 2011) adopted recharge rates as a percentage of rainfall. The Arrow UWIR groundwater model used a recharge value of 0.5 per cent of annual rainfall. Across the model area of approximately 150 km^2, this was translated into 226.5 ML/day (or 82 670 ML/year) of recharge. This recharge rate in the northern Bowen Basin is an order of magnitude higher than the recharge rate predicted for the southern Bowen Basin by the QWC groundwater model. The presence of Quaternary alluvial aquifers, Tertiary unconsolidated aquifers and Tertiary basalt aquifers in the northern Bowen Basin are a possible explanation for this much higher recharge rate.

7.8 Groundwater modelling

7.8.1 Surat CMA modelling

A major groundwater modelling exercise was undertaken by QWC (2012a; 2012c) to determine the cumulative impacts of CSG extraction within the Surat and Bowen Basins on aquifers within those two Basins. Figure 30 shows a west-east cross-sectional conceptual model of the northern extents of the Surat CMA. Figure 30 also shows the hydrostratigraphic relationship between the Surat Basin HSUs (shown in various shades of green) and the underlying Bowen Basin HSUs (shown in various shades of grey). The conceptual model reflects the shallow nature of the Bowen Basin HSUs in their northern outcropping area. Further to the south, these same HSUs will be buried by thousands of metres of Surat Basin sediments.

QWC (2012c) developed a numerical groundwater flow model using the MODFLOW code. The model domain overlays the entire Surat CMA area and includes 19 layers to represent the full GAB sequence and the CSG producing Bandanna Formation in the Bowen Basin (QWC 2012c). The Bowen Basin is represented by Layers 15 to 19 of the model: the Moolayember Formation, Clematis Group sandstones, Rewan Group, Bandanna Formation and deep Permian reservoirs. The primary purpose of the model is to predict groundwater level changes in aquifers within the Surat CMA in response to proposed extraction of CSG water by the four major CSG proponents operating in the two Basins.

Model predictions were scrutinised to identify impacts using the following criteria:

- *significant drawdown:* 5 m drawdown for consolidated aquifers (such as sandstone) and

2 m drawdown for unconsolidated aquifers (such as alluvial sands)

- *immediately affected areas (IAA):* those aquifers that register a significant drawdown impact in the short-term (i.e. 0-3 years)
- *long-term affected areas (LAA):* those aquifers that register a significant drawdown impact beyond the short-term IAA. The LAA is more aligned with the expected delayed responses in the Bowen Basin HSUs.

It should be noted that the Surat CMA groundwater model did not include the northern Bowen Basin and therefore the impacts of CSG abstraction from the Moranbah Coal Measures have not been considered.

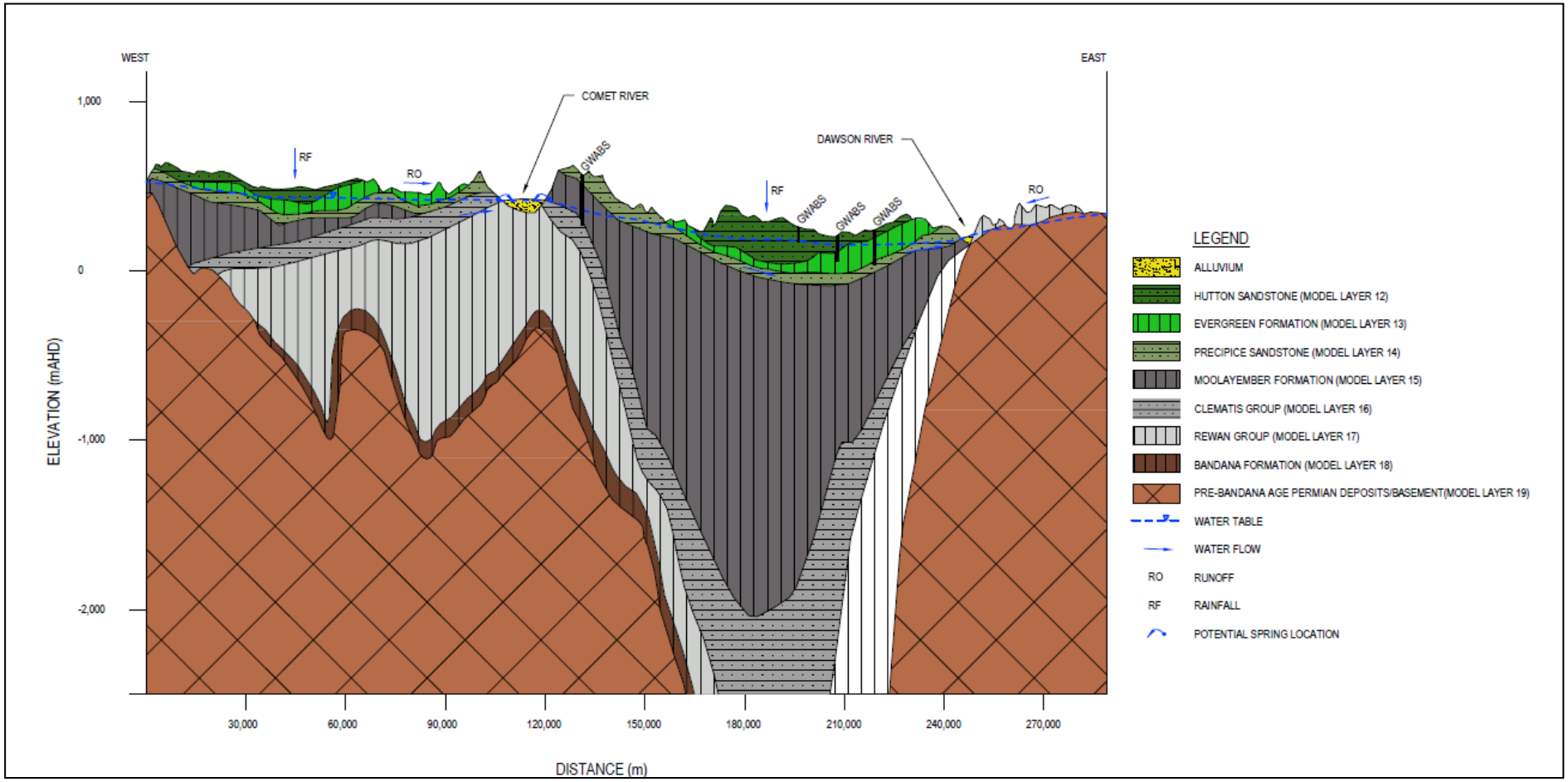

Figure 30 Conceptual Model of the Surat CMA in the northern Bowen Basin area (© Copyright, QWC 2012c).

Model predictions have shown that the Walloon Coal Measures (Surat Basin) and the Bandanna Formation (Bowen Basin) (see Figure 31) were the only IAAs, as would be expected given that they are the productive coal seams. The LAAs that were predicted to be significant include: the Walloon Coal Measures (Surat Basin), the Bandanna Formation (Bowen Basin), the Springbok Formation (Surat Basin) and the Hutton Sandstone (Surat Basin).

There are localised and discrete LAAs for the Precipice Sandstone (Surat Basin) and Clematis Sandstone (Bowen Basin) (see Figure 32). Regarding the Bowen Basin, this means that major LAAs appear to be limited to the coal seams themselves, and areas of the Clematis Sandstone that are locally impacted due to high levels of vertical connectivity. As described in Section 7.1.6.1 Regional-scale acqitards, the Moolayember Formation pinches out near Injune and there is hydraulic connection between the Clematis Group sandstones and the Precipice Sandstone (WorleyParsons 2010). Within part of this western area, the underlying Clematis and Rewan Groups are also eroded and the underlying Bandana Formation is in direct contact with the Precipice Sandstone in the vicinity of the Spring Gully Gas Fields (QWC 2012a). This enhanced connectivity may explain the elongated and enlarged drawdown predicted in the Clematis Sandstone in the Injune area.

QWC (2012c) summarise the specific impacts to the Bowen Basin HSUs as follows:

- Bandanna Formation*:* the target CSG formation in the Bowen Basin. In most of the area the long-term impact is expected to be less than 200 m. Impacts in the Bandanna Formation are also greater in areas where the coal formation is deep. The impact in these areas is expected to be up to 1000 m. However in areas where private bores tap the formation the impacts are expected to be much smaller. It is expected that impacts will not exceed 5 m in any bore.
- Clematis Sandstone*:* there are small areas where an impact of up to 2 m is simulated. Near Moonie there are very small areas of local impact where conventional petroleum and gas is currently being produced directly from the formation.

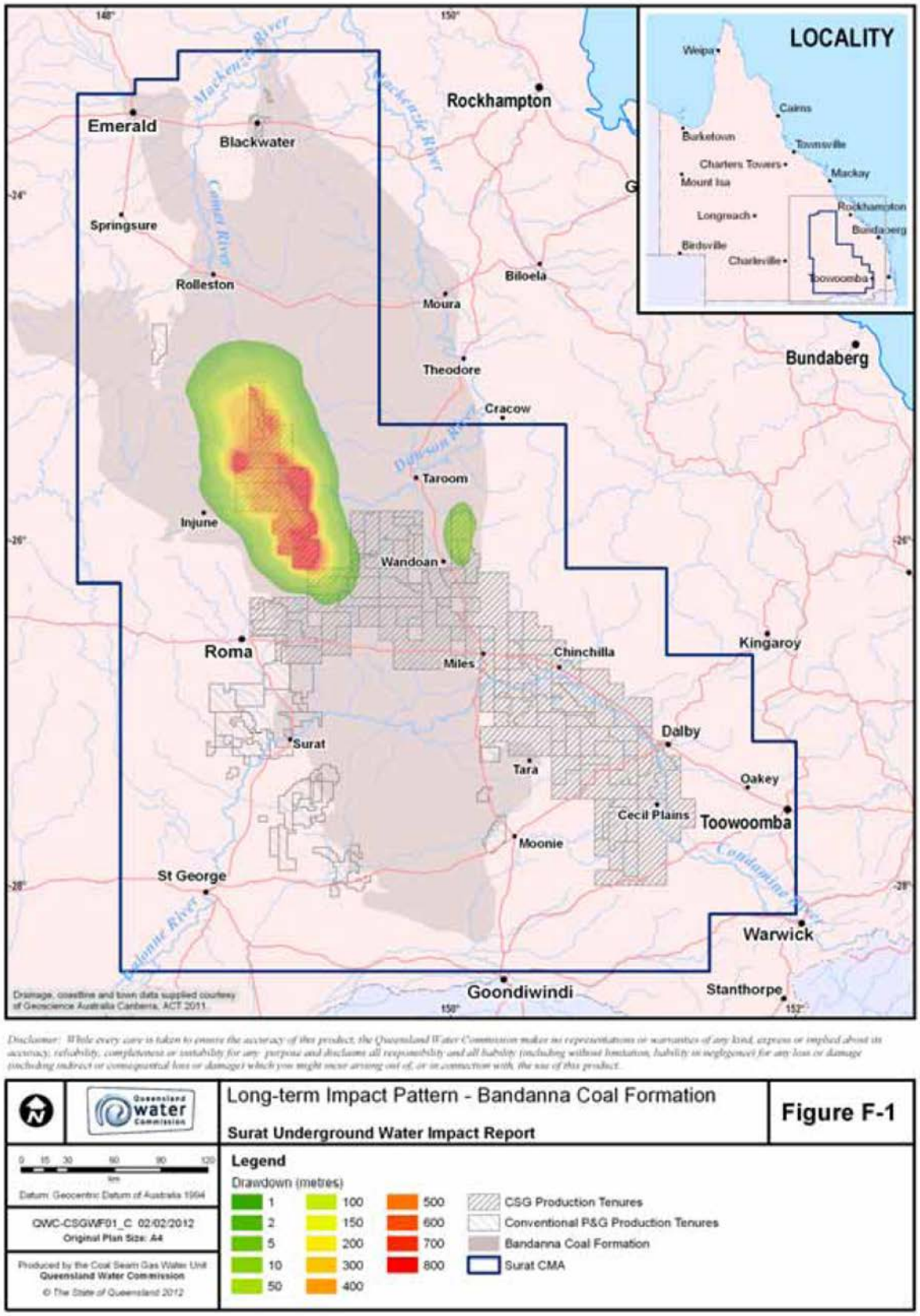

Figure 31 Long-term (LAA) drawdown predictions for the Bandanna Formation within the Surat CMA (© Copyright, QWC 2012c).

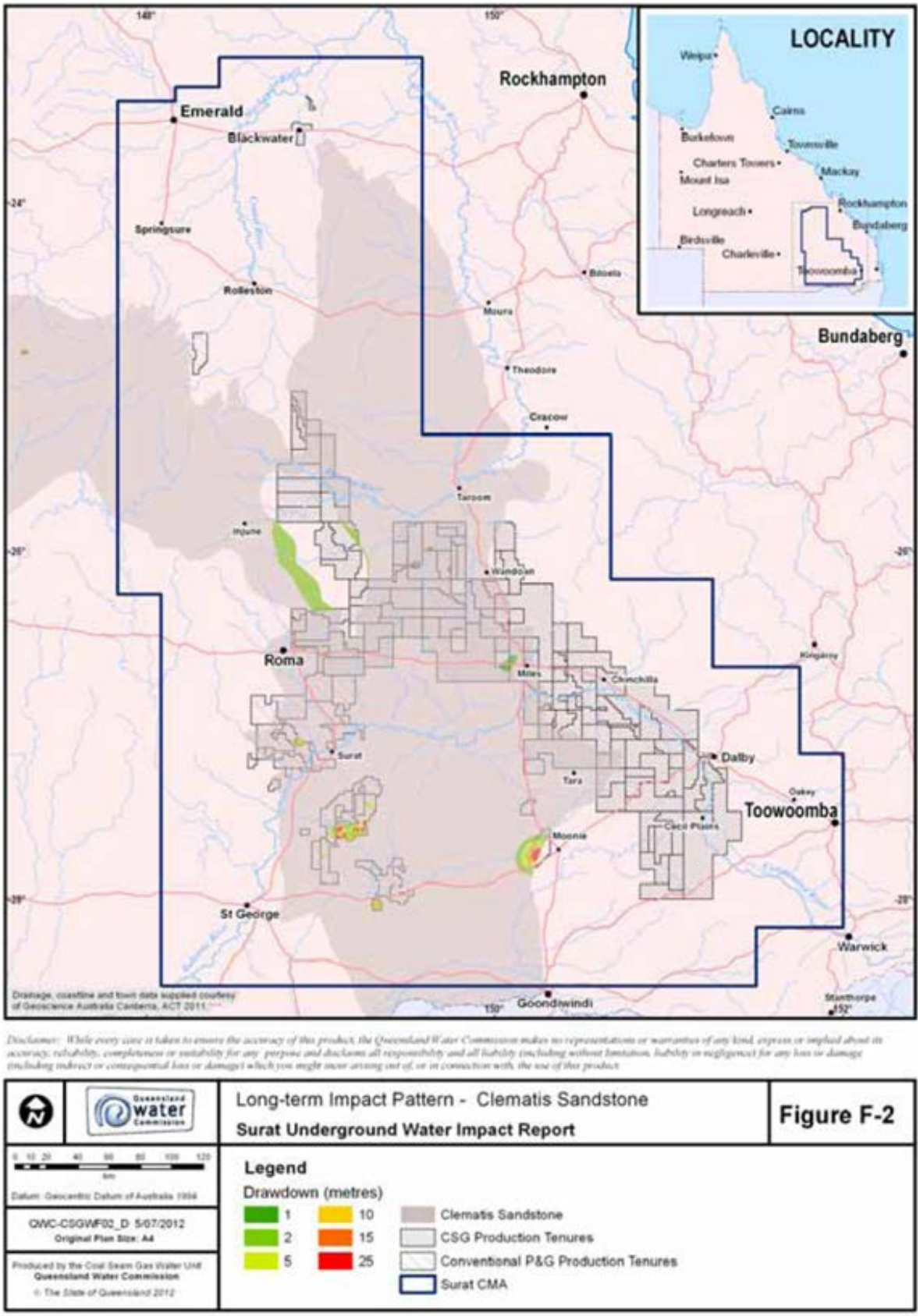

Figure 32 Long-term (LAA) drawdown predictions for the Clematis Group aquifer within the Surat CMA (© Copyright, QWC 2012c).

7.8.2 Visualisation of Surat CMA groundwater model

QWC developed a 3D geological model (QWC 2012c) and the Queensland University of Technology (QUT) produced a 3D visualisation of the Surat CMA groundwater modelling predictions (Hawke et al. 2011). The model domain is around 660 x 550 km and includes the Surat Basin and underlying southern Bowen Basin (see Figure 27 Basin map). The 3D model was built using Groundwater Visualisation System (GVS) with data supplied by QWC. The solid geology is from the QWC groundwater model. Data from 26 388 bores were included in the visualisation. Simulation data of water levels and pressures from steady state conditions (year 1995) to the year 2305 were imported into the GVS 3D model and can be displayed as time series animation (see Figure 33 and Figure 34 for example outputs).

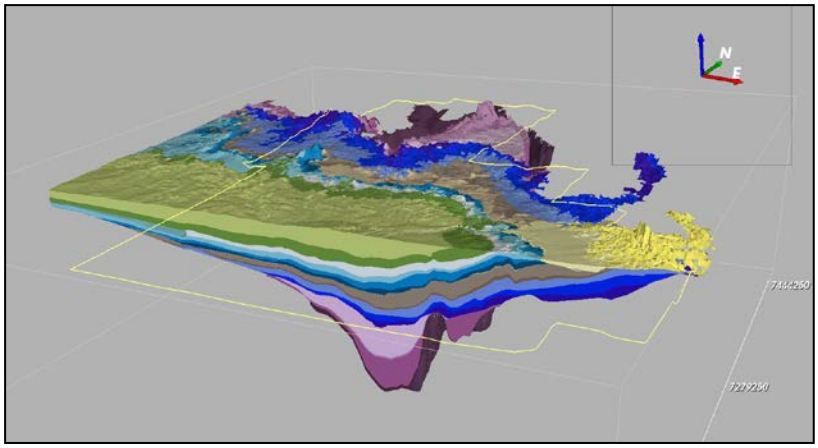

Figure 33 Oblique view of GVS 3D visualisation of Surat CMA model domain (including southern Bowen Basin) with cross-section displayed. Outline of the CMA is shown in yellow.

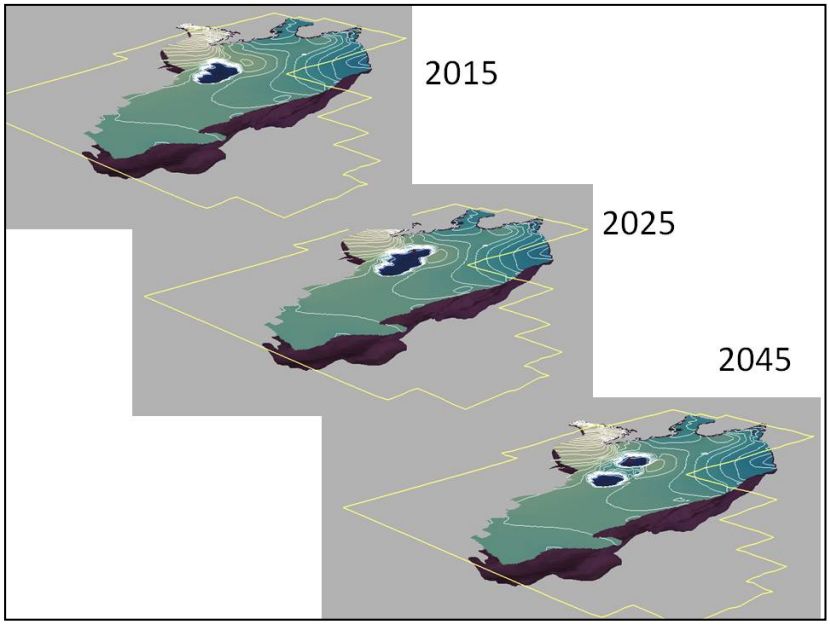

Figure 34 Oblique view of Bandanna Formation with simulated piezometric surface at the years 2015, 2025 and 2045.

7.9 Aquifer connectivity

Coal mining has been a constant occurrence in the Bowen Basin for over one hundred years. Over time, shallow open-pit mining operations have evolved into deeper underground mines and large-scale CSG fields. To date, the potential for connectivity between coal seams and overlying aquifers has usually been assessed at the local scale of the mining operation, and not at the cumulative basin-scale.

In the south of the Basin, the significant vertical thickness of the low permeability Rewan Group is relied upon as a regional hydraulic seal between the coal seams in the Bandanna Formation and the overlying Clematis Group sandstones. The effectiveness of this seal has not been field-validated, although groundwater modelling by QWC (2012c) seemed to support its role as a significant barrier to vertical flow (with exceptions as described in Section 7.8). This modelling does not account for faults or other structural features to enhance preferential flow through the Rewan Group aquitard (e.g. Brown (1981) attributed hydrocarbon occurrences within the Clematis Group to fault-induced hydraulic pathways across the Rewan Group seal). The modelling predictions will only be as reliable as the quality of the physical data and knowledge that are used to construct and constrain the model. As discussed in Section 7.2.1, the catalogue of horizontal and vertical hydraulic conductivity estimates for the major HSUs needs to be continually revised and improved as longer-term stress testing becomes available. The regional vertical hydraulic conductivity values should ideally be based on regional field tests that have been completed for a sufficient period of time to generate vertical flow at the scale of the HSU. Longer-term field testing will also enable better understanding of the influence of regional-scale faults, fractures, facies changes and leaky bores on regional vertical hydraulic conductivity values. QWC (2012a; 2012c) have acknowledged these uncertainties and have adopted an adaptive management approach to the Surat CMA.

The significant vertical thickness of the low permeability Moolayember Formation provides another hydraulic barrier between the coal seams and the overlying sandstone aquifers of the GAB. However, the Moolayember Formation is not a continuous geological unit across the Basin and for this reason the upper HSUs (Rewan Group, Clematis Sandstone and the Moolayember Formation) of the Bowen Basin are considered to be in hydraulic connection at a regional scale with the aquifers of the Surat Basin. This connection is reflected by the similar groundwater chemistries of these Bowen Basin HSUs and the overlying GAB aquifers (Hennig 2005). The mechanisms and timescales for these interactions are poorly understood.

Bradshaw et al. (2009) have conducted significant research on the potential for carbon geostorage across a number of basins in Queensland, including the Bowen Basin. They concluded that the presence of thrust fault systems in the eastern parts of the Taroom Trough and extensive faulting in the northern Basin compromised the potential integrity of seals (i.e. Moolayember Formation and basal Snake Creek Mudstone) and made these areas unsuitable for carbon dioxide (CO_2) storage.

The heterogeneity within each of the major Bowen Basin HSUs is acknowledged in the published geology and hydrogeology literature. As mentioned in Section 7.1.4, grouping these regionally-extensive geological units into hydrostratigraphic units (HSUs) simplifies the process of analysing the interconnectivity of aquifers and aquitards at the Basin-scale and also allows the potential for cumulative impacts to be considered. These HSUs can be readily and conveniently used within groundwater models to represent packages of sediment that span hundreds of kilometres and can be hundreds to thousands of metres thick. In reality, within a given HSU, there are countless facies changes (both horizontally and vertically) from fine-grained units (e.g. mudstones and shales) to coarser-grained units (e.g.

sandstones). There are also complex Basin-wide erosion events that can remove large sections of a sedimentary profile and other zones that are altered post-deposition (e.g. cementation). Hydrogeological 'expert knowledge' is used to account for all of these geological parameters when defining the over-riding hydraulic functioning of a given HSU. Given that the geological 'unknowns' in such a massive basin are far greater than the geological 'knowns', targeted ongoing groundwater investigations and monitoring of all of the major HSUs must continue to be undertaken to provide valuable data and information on how the actual bulk aquifers and aquitards behave under natural or developed conditions.

A known example of geological control on interconnectivity in the Bowen Basin is discussed in Sections 7.1.6.1 and 7.8. Significant erosion of the Clematis Group and Rewan Group in a narrow area where the Moolayember Formation pinches out has led to direct hydraulic connection between the Bandanna Formation and the Precipice Sandstone in the near vicinity of the Spring Gully gas field. The groundwater quality of the Late Permian coal seams (i.e. Moranbah Coal Measures, Bandanna Formation and Baralaba Coal Measures) is generally very poor and has been characterised by DERM (2011) as being saline. Draper and Boreham (2006) have noted that coal seam waters abstracted from CSG operations in the Fairview and Spring Gully fields show a wide range of salinity values and ionic compositions, which may reflect the influx of water to the coal seams from shallower depths (i.e. the Precipice Sandstone).

The groundwater flowpaths within and between HSUs in the Bowen Basin are poorly understood and are based on a very limited spatial and temporal monitoring record. It is generally accepted that the deeper reservoirs beneath the Rewan Group aquitard are considered to have very low permeability, negligible yields and are not considered to be at risk of being impacted by depressurisation of overlying coal seams.

As summarised in Section 7.1.3, the Bowen Basin has undergone major periods of crustal shortening and basin strain during the Triassic period. These tectonic pressures have led to major folding, faulting and fracturing of HSUs within the Basin, to the point that the Bandanna Formation has been fully displaced in the Jellinbah Thrust Belt (QWC 2012a). The influence that these major structural changes have on enhancing or reducing connectivity between the Late Permian coal seams and the overlying aquifers (including the Clematis Group sandstones and other overlying GAB aquifers) is unknown at this stage. As described in Section 7.3.2, the QWC (2012a) have concluded that fault structures in the Bowen Basin may influence regional groundwater flow within the Basin, either as pathways or barriers; however, these influences are not likely to extend to the overlying GAB aquifers in the Surat Basin. Further study and targeted monitoring is required to validate this assumption.

Groundwater modelling (MODFLOW) by the QWC (2012c) has indicated that the Clematis Group aquifer will have long-term drawdown impacts in discrete areas as a direct result of depressurisation of the Bandanna Formation. It is unlikely that the groundwater model has captured the influence of the many structural elements across the Basin. QWC (2012c) acknowledged that the potential effect of faults and other structural features on the development of impacts from CSG abstraction is poorly understood, and have recommended further work be undertaken to understand the impacts faults may have on groundwater flow within the Surat CMA.

In the north of the Basin, the connectivity between the coal seams (the Moranbah Coal Measures, Fort Cooper Coal Measures and Rangal Coal Measures) and the overlying alluvial and Tertiary basalt aquifers is poorly understood. No cumulative Basin-scale assessment of interconnectivity has been conducted. Additionally, the role that the Moolayember Formation, Rewan Group and Clematis Group sandstones play in the north of the Basin is unknown.

7.10 Knowledge gaps

The following key knowledge gaps have been identified in this review:

- A significant portion of the southern Bowen Basin is deeply buried by the Surat Basin sediments (particularly in the Taroom Trough and Denison Trough) making these HSUs relatively inaccessible for groundwater monitoring and hydraulic testing purposes. It is widely believed that hydraulic conductivity will reduce with depth in the Basin, as the aquifer/aquitard material is compacted and fracture and fissure apertures close up and diminish (QWC 2012c). Further targeted testing in higher risk areas is needed to validate these assumptions.
- The interconnectivity of coal seams, aquifers and aquitards in the northern Bowen Basin has not been studied or modelled at a regional, cumulative scale. Additionally, the connectivity of the northern Bowen Basin aquifers and water-bearing units and their equivalents in the southern Bowen Basin has only been addressed at a qualitative level.
- The role that the Moolayember Formation, Rewan Group and Clematis Group sandstones play with regards to interconnectivity in the north of the Basin is unknown. The Clematis Group sandstones are believed to be under artesian pressures. No information was found regarding recharge rates into the northern intake beds of these HSUs.
- The mechanisms and timescales for the interactions between the Rewan Group, Clematis Sandstone and the Moolayember Formation and the overlying aquifers of the GAB are poorly understood. Groundwater geochemistry signatures suggest some degree of interconnection between the HSUs.
- It is widely accepted that the two major aquitards in the Bowen Basin (the Rewan Group and the Moolayember Formation) will provide an adequate regional hydraulic seal between the deeper Late Permian coal seams and overlying aquifers. Given that these aquitards are up to 1500 m thick suggests that they should provide significant resistance to vertical flow. Uncertainty remains with regards to:
    - Have these units have been compromised by structural deformation to enhance vertical hydraulic conductivity?
    - Are there are any other major erosion features or pinch outs, as observed east of Injune, to enhance interconnectivity with overlying aquifers?
- Given the significant thicknesses of the actual HSUs in the Bowen Basin (e.g. thousands of metres in the Taroom Trough) it is likely that most of these units will be buried at far greater depths than the depths of the test bores, which are typically drilled in accessible parts of the Basin. It is expected that the hydraulic conductivity will reduce with depth, as the aquifer/aquitard material is compacted and fracture and fissure apertures close up. This could result in a reduction of bulk horizontal hydraulic conductivity values for HSUs, as compared to the current catalogue of expected values.
- The majority of the testing methods used to obtain the horizontal hydraulic conductivity and vertical hydraulic conductivity parameters (i.e. pumping tests, core tests, drill stem tests) only provide a very localised indication of aquifer properties (with the exception of larger pumping tests). They are not likely to be representative of the bulk aquifer properties of the HSUs and should not be considered as such. The vertical hydraulic

conductivity estimates in particular are unlikely to reflect the regional properties of the aquitards, as the tests would not have been completed for a sufficient period of time to generate vertical flow at the scale of the HSU, and as such the regional bulk vertical hydraulic conductivity values may be greater than what the local-scale tests indicate.

- Field hydraulic testing at the local scale also ignores the influence of regional-scale faults, fractures, facies changes and leaky bores, all of which can greatly influence regional vertical hydraulic conductivity values.
- The hydraulic behaviour of faults is poorly understood in the Basin. Further targeted research is required to assess the influence of major regional structures on groundwater flow and interconnectivity. Given the size and depth of the Basin, research may need to be retrospective once groundwater level anomalies are detected.
- Currently, the geomechanical properties of the individual HSUs within the Bowen Basin are not described within the hydrogeology and geology literature.
- There is some disagreement regarding which aquifers comprise recharge intake beds. Habermehl (2002) listed the main intake beds as the Hooray, Hutton, Precipice and Clematis sandstone aquifers and their equivalent formations. Kellet et al. (2003) only describe the Hooray and Hutton Sandstones and suggest that recharge through other outcropping units is minimal. Groundwater modelling (MODFLOW) by QWC (2012c) has followed the Kellet et al. (2003) approach.
- There is not enough spatial and temporal groundwater monitoring data for HSUs across the Bowen Basin to confidently interpret regional groundwater flow patterns. Conceptually, groundwater flow should flow from the outcropping recharge zones to the south and south-west along the direction of dip in the Basin (WorleyParsons 2010; GABCC 1998).
- There are only 33 groundwater level and quality monitoring sites for the five major Bowen Basin HSUs in the Surat CMA. The Clematis Group sandstones comprise approximately half of the current network. The significant depth of the HSUs within the Taroom and Denison Troughs precludes the practicality of installing more monitoring sites in the buried, down-gradient extents of the Bowen Basin. Most of the current sites are situated along the outcropping areas in the exposed parts of the Bowen Basin.
- There is very little understanding of the vertical hydraulic gradients across the major HSUs in the southern and northern parts of the Bowen Basin.

8 Aquifer connectivity in the Galilee Basin

The Galilee Basin is a geological basin located in central-western Queensland covering approximately 247 000 km^2 (Figure 1). It extends around 700 km from Charleville in the south to near Charters Towers in the north, and from east to west around 550 km, from east of Emerald to Julia Creek in the northwest. The Galilee Basin is a geologically and hydrogeological diverse sedimentary basin, most of which is buried and outcropping only along the eastern boundary of the Basin. The buried portion is overlain by strata of the Eromanga Basin, a geological basin that forms part of the GAB. Details of the geology and hydrogeology of the Galilee Basin are further described in Section 8.1.1.

Compared to the other sedimentary basins described in this report, the Galilee Basin remains relatively unexplored with respect to conventional petroleum, CSG main previous constraints (Holland et al. 2008). However, successful exploration and production of CSG in the nearby Bowen and Surat Basins, along with plans for major transport links, have renewed interest in the Galilee Basin and exploration activity has increased significantly in recent years. The following history of exploration in the Basin is summarised from RLMS (2009):

- Petroleum exploration in the Galilee Basin began around 1959 and continued to the mid-1970s. This phase of exploration was focussed on the deep sandstone reservoirs of the Galilee Basin with wells up to 2000 m deep.
- Early seismic exploration occurred in the 1960s and 1970s, mainly by various exploration companies and some by the Bureau of Mineral Resources.
- There was a lull in exploration in the mid to late 1970s, followed by a second phase of exploration in the 1980s including seismic and well drilling. This phase was generally focused on shallower targets with wells penetrating around 500 m. Thirty-one wells, and a further five stratigraphic bores were installed by the Queensland government in this phase, however no economic hydrocarbon discoveries were made.
- Stratigraphic drilling by the Department of Mines/Geological Survey of Queensland occurred during 1970s. Two deep stratigraphic tests east of Aramac were completed in 1974. Further drilling occurred in 1989 and 1990 to examine the stratigraphic relationship between the Aramac Coal Measures and the Jochmus Formation.
- There was high interest in 18 areas made available for Authority to Prospect (ATP) by the Department of Mines and Energy in 2008. Altogether a total of 67 applications by 11 companies for the 18 areas available were received. Petroleum exploration leases now almost cover the entire Basin, but the most active exploration is occurring in the northern region. Much of the eastern half of the Basin is also covered by coal leases. There is significant overlap between coal and petroleum tenures.
- On the margins of the Galilee Basin there are some areas under application for geothermal exploration. These tenures are located where hot granites are inferred to lie close to the surface.

- The area is also of interest for potential geosequestration: in 2008 the Cooperative Centre for Greenhouse Gas Technologies (CO2CRC) completed a regional study in the Galilee Basin looking for suitable areas for long-term CO_2 storage (Rawsthorn et al. 2009 and Marsh et al. 2008).
- At the time of writing (early 2013), there had been no commercial extraction of petroleum or coal from the Galilee Basin.

For this review, data from the early petroleum exploration phases has been sourced from the various Hawkins papers (e.g. Hawkins & Green 1993; Jackson et al. 1981; Hawkins 1978), Marsh et al. (2008) and Rawsthorn et al. (2009).

8.1 Major aquifer and aquitard stratigraphy

8.1.1 Geological summary

The Galilee Basin is a sedimentary basin deposited during the Late Carboniferous to Middle Triassic period. The architecture of the Basin is largely controlled by overlying/underlying basins and basement topography, as shown in Figure 35. The eastern third of the Basin is underlain by the Drummond Basin (late Devonian to early Carboniferous age) and in the south by the Adavale Basin (mainly Devonian age). Figure 35 also shows the key basement features, including the Mt Isa Inlier in the north-west, the Lolworth-Ravenswood Block in the north and the Maneroo Platform in the south. These basement rocks are predominantly early Palaeozoic in age. The Maneroo Platform formed a barrier between the eastern and western parts of the Basin during much of its depositional history. The Galilee Basin is overlain by the Eromanga Basin (Jurassic-Cretaceous age), which is formally part of the GAB. Note that the GAB is a hydrogeologically based grouping and is not based on stratigraphy or geological evolution. Down-warping of the Eromonga Basin (up to 1200 m thick over the Galilee Basin) imposed a regional south-westerly tilt on the sedimentary sequence (Jackson et al. 1981). The relationship between the Galilee and Eromanga Basins is important, as the Eromanga Basin comprises significant regional aquifers.

The Galilee Basin is roughly ‘kidney-shaped’ and descriptions of the Basin commonly subdivides these two ‘lobes’, with the Northern Galilee Basin approximately divided from the South by the 24°S line of latitude (refer Figure 35). There are three main centres of deposition in the Galilee Basin. In the northern Basin there is the Koburra Trough in the east (which contains the oldest formations) and the Lovelle Depression in the west (which is the more distal part of the basin where deposition began much later and several formations are missing). The Koburra Trough contains up to 3000 m of sediments, whereas the Lovelle Depression around 730 m of sediments (Jackson et al. 1981). Note that the Aramac Depression, shown in Figure 35, is a smaller depositional centre within the Koburra Trough. The Koburra Trough and Lovelle Depression are separated by the Maneroo Platform. The Powell Depression is the main depositional feature in the southern half of the Basin, with a thickness of up to 1400 m (RPS 2012 in AGL 2012).

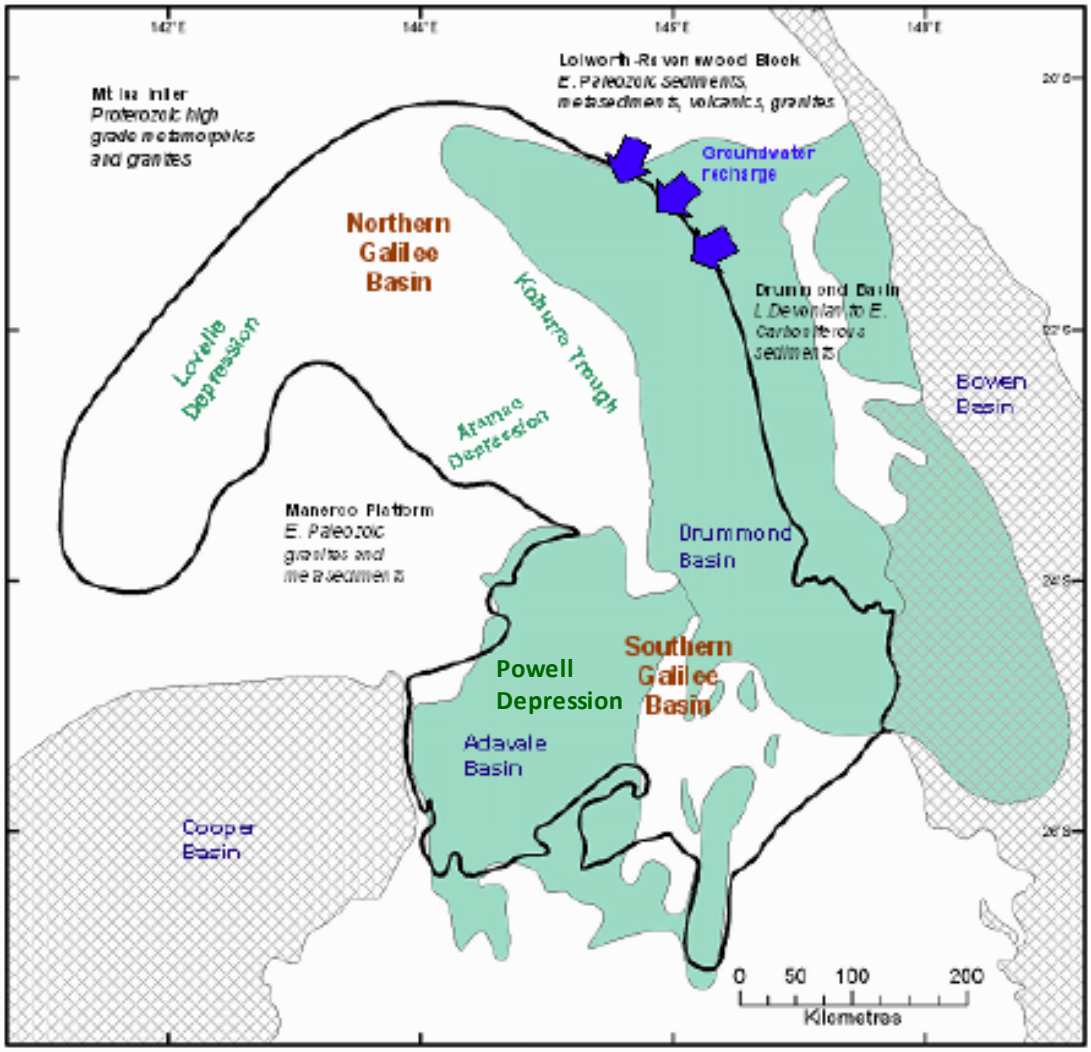

Figure 35 The Galilee Basin and its subdivisions (brown and green labels), provenances/basement (black labels), contemporaneous basins (hatched areas) and underlying basins (blue and green areas) (© Copyright, Marsh et al. 2008).

A simplified stratigraphy of the Northern Galilee Basin is presented in Figure 36. This figure shows that the formation of the Galilee Basin commenced in the Late Carboniferous and in its early depositional stages was confined to the Koburra Trough in the east. By the Early Permian, sedimentation was continuous to the west, from the Koburra Trough across the northern end of the Maneroo Platform and into the Lovelle Depression. There are two major unconformities in the Galilee Basin (shown as 'wavy' lines in Figure 36):

- Permian unconformity – an erosional event occurred at the end of the Early Permian after which sedimentation continued until the Middle Triassic (Hawkins & Green 1993). This erosional event was interpreted as a period of non-deposition and/or gentle uplift before the accumulation of widespread fluvial and coal deposits of the Betts Creek Beds and related deposits started (Allen & Fielding 2007a; Evans 1980).
- Basal Jurassic unconformity – marks the transition from the Galilee Basin sediments to the Eromanga Basin sediments. This period corresponds to a period of non-deposition

and erosion (of the Moolayember Formation). This unconformity is of importance when considering potential connectivity between Galilee Basin coal seams and the major artesian aquifers in the lower Eromanga Basin.

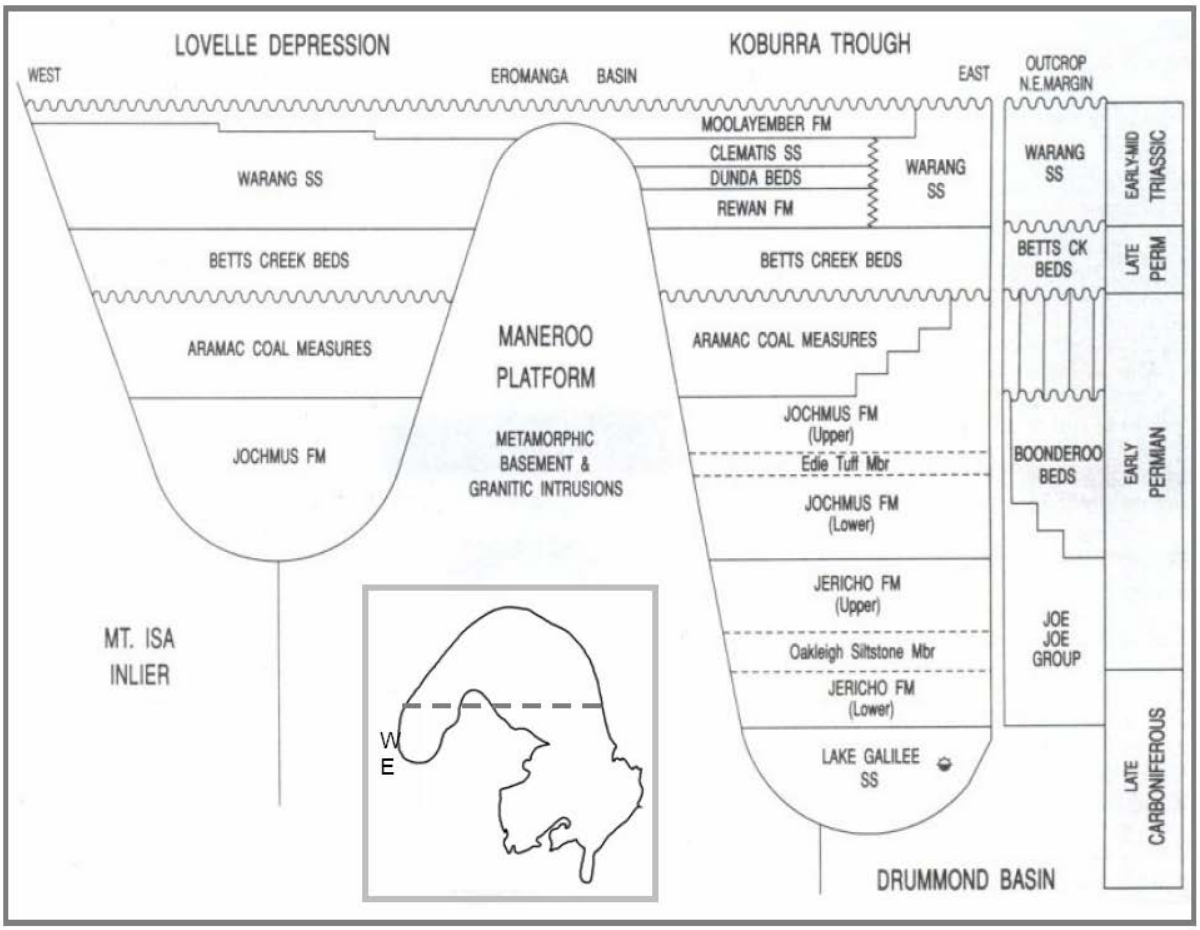

Figure 36 Simplified stratigraphic relationships in the Northern Galilee Basin (© Copyright, Marsh et al. 2008).

Marsh et al. (2008) suggests that the Southern Galilee Basin appears to have been largely ignored in the literature and requires considerably more study. Unlike the Koburra Trough, they note that it has no apparent Late Carboniferous sediments, a condensed or absent Permian section and sporadic Triassic section.

The Galilee Basin sediments were mainly deposited in a fluvio-lacustrine environment (i.e. by rivers and lakes), resulting in channel sands, floodplain siltstones and coals, lacustrine shales, alluvial fan deposits and some glacial deposits. The two major unconformities in the Galilee Basin divide the infilling of the Basin into two depositional episodes:

- Late Carboniferous-Early Permian - during this period the climate varied from glacial in the Late Carboniferous and early 'Early Pemian' to warm and humid in the late Early Permian. This episode is characterised by the sediments of the Joe Joe Group, which consists of the Lake Galilee Sandstone at its base, the Jericho Formation, the Jochmus Formation and the Aramac Coal Measures in the Koburra Trough; there are also the

Jochmus Formation and Aramac Coal Measures correlatives in the Lovelle Depression (Hawkins 1978).

- Late Permian-Middle Triassic – the climate varied during this period from warm and humid in the Late Permian to more temperate in the Triassic. This episode started during the Upper Permian when the Betts Creek Beds were deposited across the entire Basin (Allen & Fielding 2007b) and during the Triassic when there was deposition of the Rewan Group, the Clematis Group and the Moolayember Formation in the Koburra Trough. The Warang Sandstone is an Early to Middle Triassic unit found mainly in the northern half of the Basin, including parts of the Lovelle Depression. It is contemporaneous with the Moolayember Formation, Clematis Sandstone, Dundas Beds and Rewan Formation but is comprised mainly of sandstone. Due to its lithology and interfingering with the entire Jurassic sequence, Marsh et al. (2008) recognised the potential liability this unit posed to storing CO_2 in the Clematis Sandstone. There are similar implications for this unit to 'connect' Permian units and the overlying Eromanga basin under CSG depressurisation or coal dewatering. Marsh et al. (2008) also recommended that the relationship of the Warang Sandstone and the remaining Triassic sequence was an area requiring further investigation.

Figure 37 and Figure 38 present stratigraphic cross sections through the Galilee Basin. These sections help in understanding the relationship between the Galilee, GAB and Eromanga Basins. The blue units are the late Permian coal measures, which contain the coal/carbonaceous material which are the target for CSG or coal development. The east to west cross section (Figure 38 B-B') illustrates how these units rise steeply and outcrop on the eastern margins of the Basin.

The underlying grey coloured units are the early Permian age sediments. The green layers mark the beginning of the Triassic formations. The red dashed line indicates the boundary between the Galilee Basin and the Eromanga Basin, which as described above represents a major unconformity. The cross sections show that a thick sequence of the Moolayember Formation commonly separates the formations targeted by extractive industries (Betts Creek Beds and Aramac Coal Measures) from the overlying aquifers of the Eromanga Basin. However, there are locations where the Moolayember Formation thins significantly or is absent, such that in some areas there is (effective) contact between the Permian Coal measures and the Hutton Sandstone (via the Clematis Sandstone).

Marsh et al. (2008) note difficulty in correlating Galilee Basin stratigraphy from the well studied outcrop areas to the central areas of the Basin. In particular they note nomenclature problems in attempts to correlate the units of the Clematis and Colinlea Sandstone in the centre of the Basin with formations named in outcrop areas in the northern margin of the Basin and the Springsure Shelf.

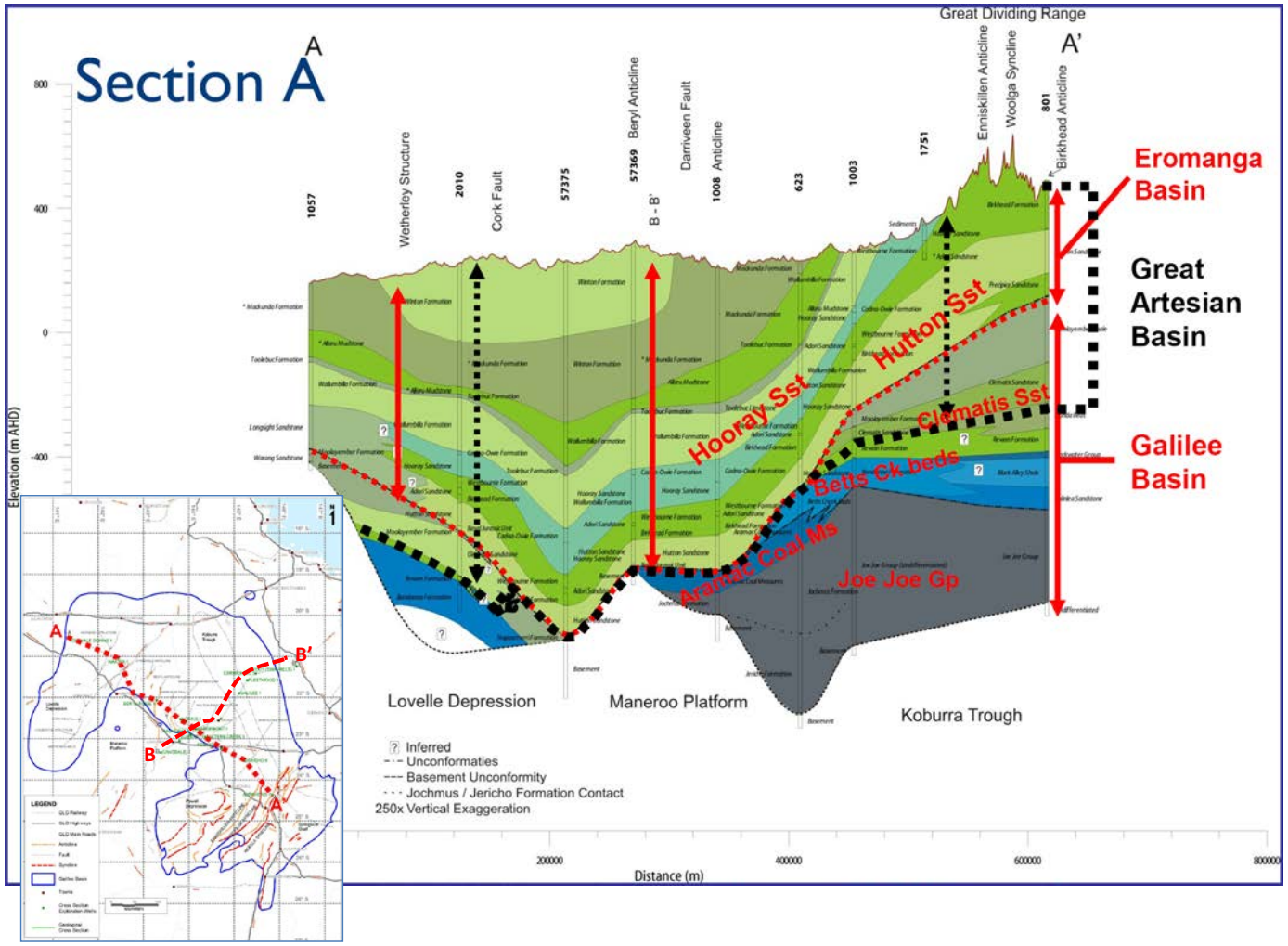

Figure 37 North to south stratigraphic cross section of the Galilee Basin (© Copyright, RPS 2012). Note. Moolayember and Clematis group are no longer formally part of the GAB.

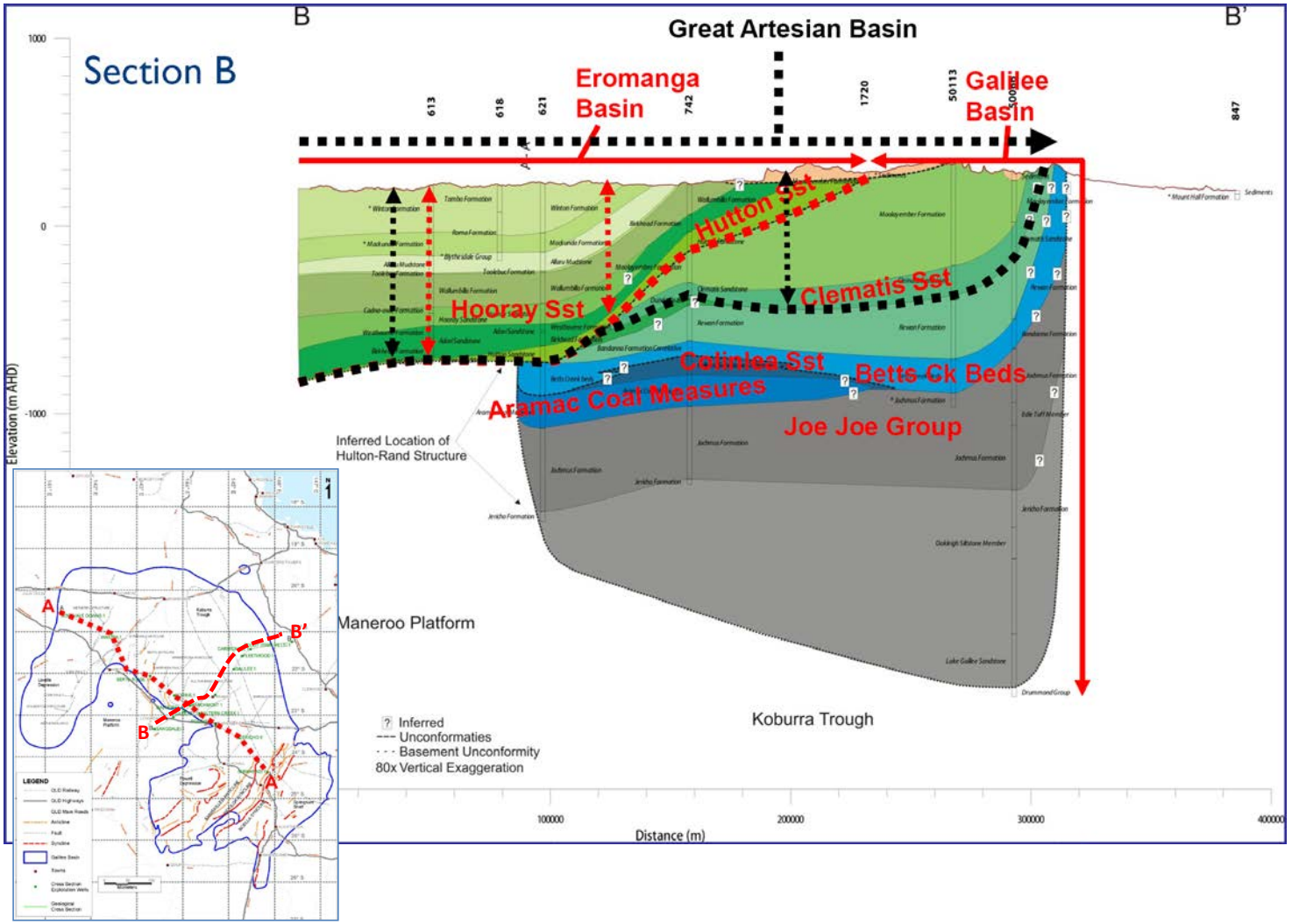

Figure 38 East to west stratigraphic cross section of the Galilee Basin (© Copyright, RPS 2012). Note that Moolayember and Clematis group are no longer formally part of the GAB.

8.1.2 Hydrostratigraphy

A simplified hydrostratigraphy of the Galilee Basin is presented in Figure 39 (after Moya 2011). Essentially, the hydrostratigraphy indicates the tendency of stratigraphic units to act as aquifers or aquitards. This is based mainly on the lithology of the unit, with formations predominantly comprised of sandstones assigned as aquifers and formations comprised of fine grain sediments (siltstones and shales) assigned as aquitards.

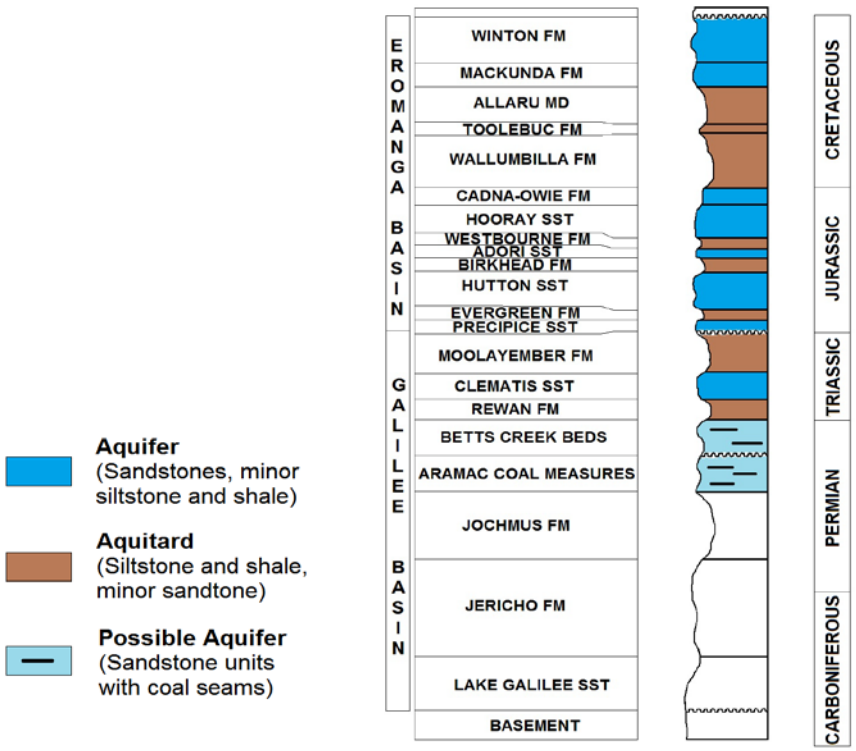

Figure 39 Simplified hydrostratigraphy in the Galilee and Eromanga Basin (© Copyright, Moya 2011)

Figure 39 does not indicate the hydrostratigraphy of the lower units of the Galilee Basin (the Lake Galilee Sandstone and the Joe Joe Group Formations). Marsh et al. (2008) provide some indication of the hydrostratigraphic nature of these formations:

- Lake Galilee Sandstone – even though this formation has a sandstone lithology, quartz cementation has reduced the porosity and permeability to virtually zero, hence this unit can be considered an aquitard. Marsh et al. (2008) cites porosities of 2 to 10 per cent and permeability from 0 to 7 mD (average of 0.9 mD, which is approximately 0.001 m/day).
- Jericho Formation – this formation is predominantly comprised of siltstone and mudstone and is considered to act as an aquitard.
- Jochmus Formation – this formation is comprised of sandstone in the upper and lower parts, with a middle part composed of tuff with minor mudstones and siltstone. Marsh et al. (2008) considered that the sandstones within the Jochmus Formation appear to be more porous and permeable than the formations below, but suggests there may be a high proportion of clay present (related to volcanic activity during deposition) but likely to

be less in the Lovelle Depression. Permeabilities for this unit cited in Marsh et al. (2008) of 0 to 1634 mD (approximately zero to 1.6 m/day) are not indicative of an aquifer from a typical water resource perspective, but indicate higher permeability than in underlying aquitards.

The Permian coal measures (Betts Creek Beds and Aramac Coal Measures) represent aquifers of poor to moderate permeability based on the sandstone layers within these units.

The Rewan Formation is considered to be an aquitard – it is comprised of interbedded sandstone, mudstone and siltstone, however the sandstone is predominantly labile and has an abundance of clay and silt, and hence poor permeability (Moya 2011). Marsh et al. (2008) cited a range of permeabilities for the Rewan Formation, from 0 to 472 mD and an average of 143 mD (which is approximately 0.1 m/day), which is not indicative of an aquitard (i.e. hydraulic conductivity is too high); however, as discussed later in this chapter, the Marsh et al. (2008) dataset was very small.

The overlying Clematis Sandstone is the most significant aquifer within the Galilee Basin (Figure 37, Figure 38). It consists of quartzose sandstone with minor siltstone and mudstone. The Clematis Sandstone is a useful aquifer and is present below much of the Eromanga Basin in the central GAB. There are some users tapping this aquifer in the Galilee Basin, predominantly in the east, where the aquifer is shallower.

The contemporaneous Warang Sandstone (which as noted earlier spans the whole Triassic sequence) has a wide range of permeabilities, but as shown in data in Section 8.2, it has a median permeability of around 100 mD (approximately 0.1 m/day) but 10 per cent of values were over 1000 mD (approximately 1.0 m/day), indicating the significant aquifer potential of this unit.

The Moolayember Formation is considered to be an aquitard, and is considered highly prospective as a sealing unit for potential carbon dioxide storage in the Galilee Basin (Marsh et al. 2008). It consists of mudstone with minor siltstone and sandstone (Scott et al. 1995). Marsh et al. (2008) cited a range of permeabilities for the Moolayember Formation, from 0 to 503 mD and an average of 81 mD (approximately 0.1 m/day), which is not indicative of an aquitard (i.e. hydraulic conductivity is too high); however (again), as discussed later in this chapter, the Marsh et al. (2008) dataset was very small.

The Galilee Basin sequence ends with the Moolayember Formation and after a period of compression and erosion, deposition started again in the Early Jurassic with the basal units of the Eromanga Basin. As shown in Figure 39, the Eromanga Basin comprises some significant aquifers. These can be divided into the deeper Jurassic units and the shallower Cretaceous units. The main Jurassic aquifers include the Hutton Sandstone, Cadna-owie Formation and Hooray Sandstone. The main Cretaceous aquifers are the Winton and Mackunda Formations, which include unconfined to confined aquifers.

8.2 Hydraulic properties

There has been some determination of hydraulic properties of formations in the Galilee Basin, but given the size of the Basin compared to other more studied and developed basins (e.g. the Surat), the dataset is small. The following sections describe various sources of hydraulic property data. The largest and most important dataset is that presented in Section 8.2.1, which is a compilation of data (collected over a number of decades) from petroleum and coal exploration drilling. The remaining sections present results from individual investigations related to a specific part of the Basin.

8.2.1 Regional datasets

Marsh et al. (2008) presents a compilation of permeability and porosity data for part of the Galilee Basin. This is comprised of a Northern Galilee dataset compiled by Peter Hawkins (Geological Survey of Queensland) and supplemented by Marsh et al. (2008) with some data from the Southern Galilee Basin. Marsh et al. 2008 noted that the dataset has the potential to be extended so that it covers the entire Galilee Basin. The Hawkins dataset is not specifically referenced in Marsh et al. (2008) and review of the Hawkins references provided in Marsh et al. (2008) did not identify the original Northern Galilee dataset. Hence, the original source of the Hawkins dataset is not certain.

The dataset from Marsh et al. (2008) is presented in Figure 40 (porosity versus horizontal permeability) and Figure 41 (porosity versus depth and permeability versus depth). The data exhibits a wide spread of values within and between formations. There is some trend apparent between porosity and depth, albeit with large uncertainty, and even larger uncertainty in the permeability versus depth relationship.

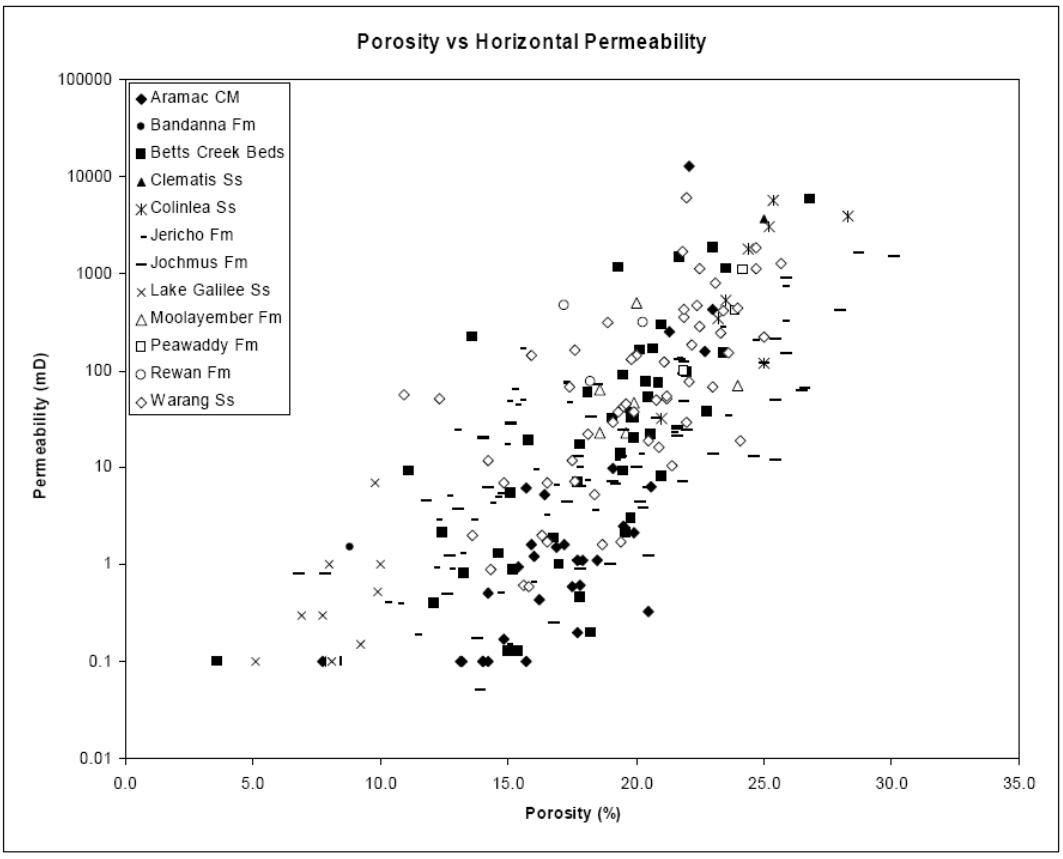

Figure 40 Porosity versus permeability for Galilee Basin sedimentary rocks by formation (© Copyright, Marsh et al. 2008).

Marsh et al. (2008) also present a summary of porosity and permeability for key formations in the Galilee Basin, along with other key properties, which is replicated in Figure 42. A generalised observation from these datasets is that the Triassic and Late Permian formations obtain a maximum permeability of around 10 000 mD (approximately 10 m/day), whereas the maximum permeability for the Early Permian rocks is around an order of magnitude lower (approximately 1 m/day).

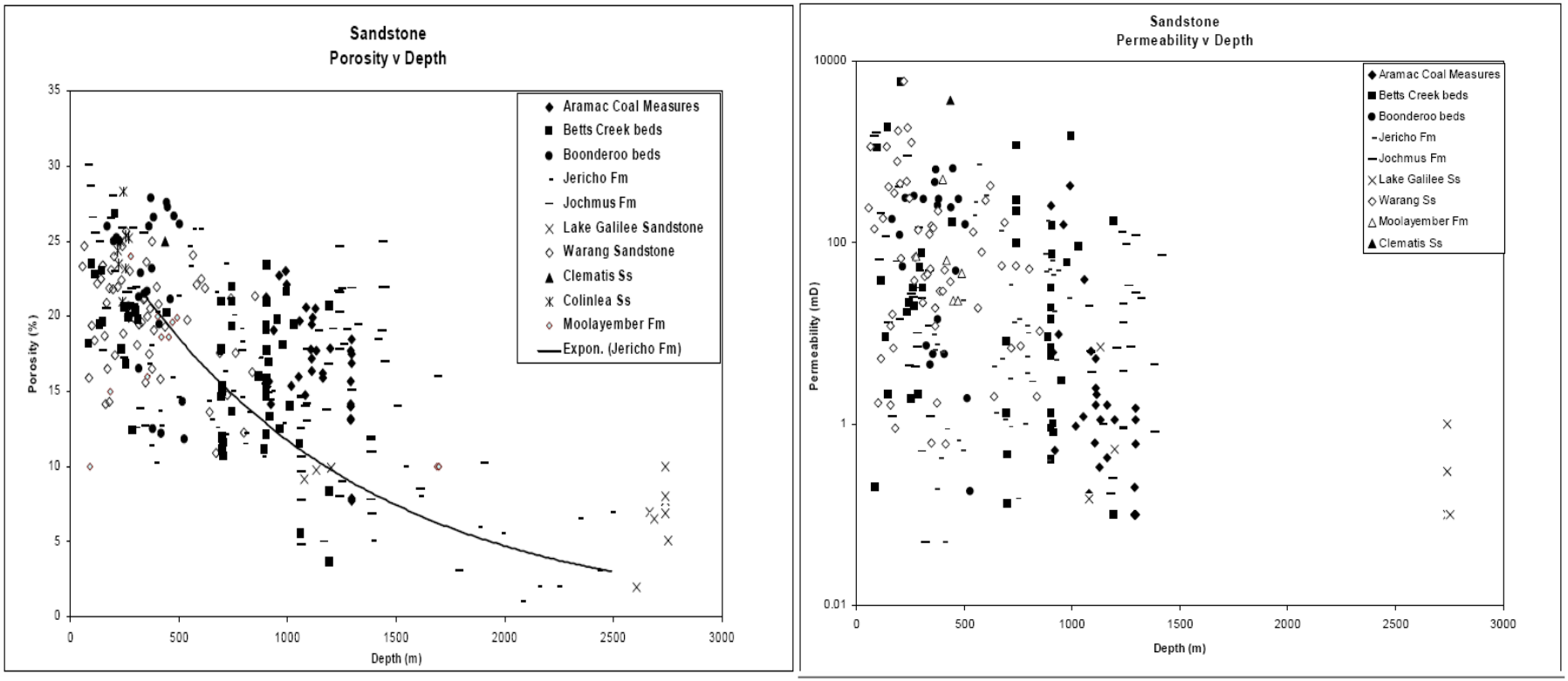

Figure 41 Porosity versus depth (LHS) and permeability versus depth (RHS) for sedimentary rocks in the Galilee Basin (© Copyright, Marsh et al. 2008).

There is no indication of how the Marsh et al. (2008) permeability dataset was collected. It is important to know the method behind the permeability data because the method impacts the result. For example, laboratory determined permeability tests (as the bulk of data for the Galilee Basin appears to be) generally underestimate permeability compared to field tests, as rock defects (i.e. fractures, bedding planes, etc) are usually not captured in laboratory permeability tests. This difference will tend to be more pronounced in low permeability formations, where low density rock defects (i.e. widely spaced) dominate the contribution to overall rock mass permeability.

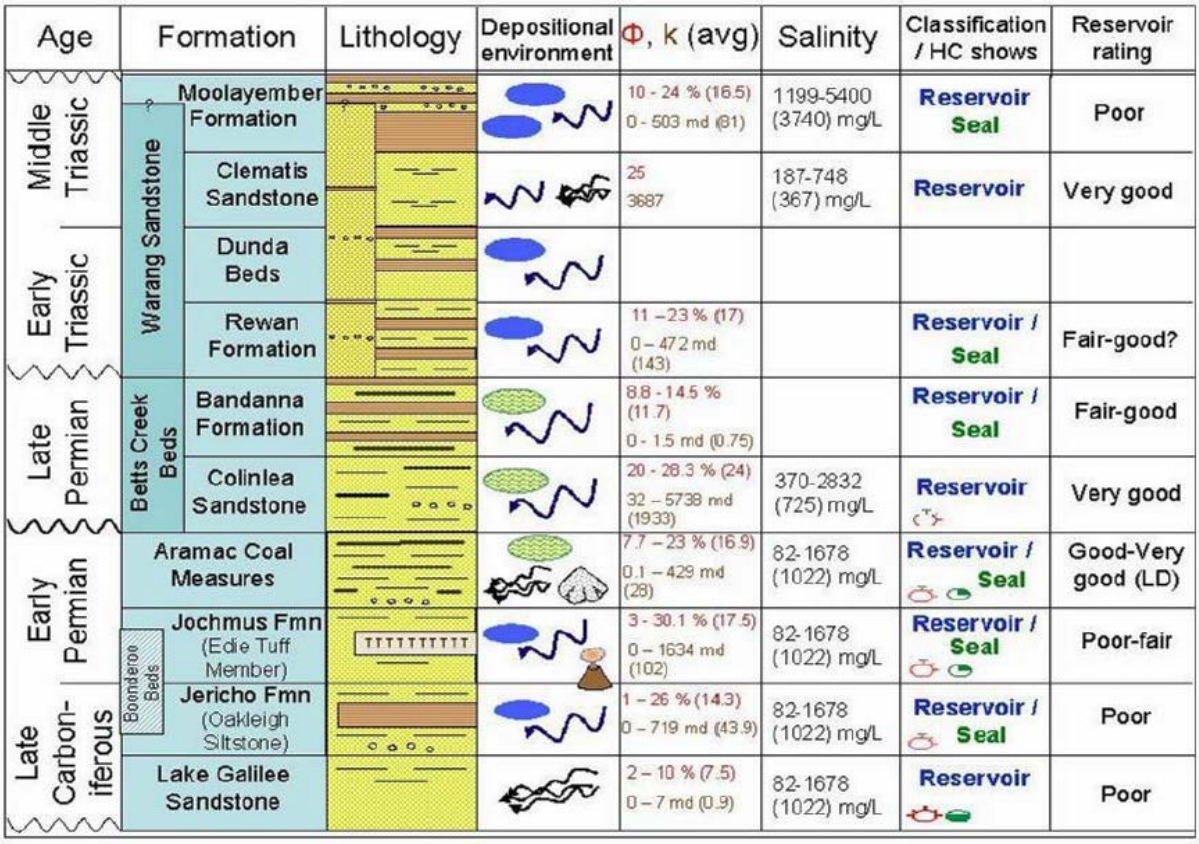

Figure 42 Summary of key properties of formations in the Galilee Basin (© Copyright, Marsh et al. 2008).

A further limitation with the amalgamated Marsh et al. (2008) dataset is that the permeability is not differentiated into horizontal or vertical permeability. The distinction is very important when it comes to determining connectivity in a particular context, such as using the data in a model or some other form of predictive tool. Knowing the method of testing can sometimes help in determining if vertical or horizontal permeability has been tested. However, Rawsthorn et al. (2009) use the Marsh et al. (2008) dataset in building a geological model and they do provide a breakdown of the Marsh et al. (2008) data, including into vertical and horizontal permeability. Plots of vertical versus horizontal permeability are presented in Rawsthorn et al. (2009) based on three divisions: Triassic, Late Permian and Early Permian formations. The Late Permian dataset is provided as an example in Figure 43. Both the Late and Early Permian formations indicate a potential positive linear relationship between horizontal and vertical permeability. The Triassic dataset suggests a 10 to 1 relationship

between horizontal and vertical permeability; however, it is based on only four data points and hence is not a statistically significant or reliable relationship.

The final aspect of the data presented in the Hawkins papers (e.g. Hawkins & Green 1993; Jackson et al. 1981; Hawkins 1978) and Marsh et al. (2008) data of note is that the distribution of testing in various formations is highly skewed with some formations containing very limited data. Based simply on a visual count from Figure 40, (i.e. not from raw data) the number of tests in each formation were estimated (bracketed figures indicate the number of tests):

- Middle Triassic – Moolayember (6), Clematis Sandstone (1), Rewan (3) and Warang Sandstone (57)
- Late Permian – Bandanna Formation (1), Colinlea Sandstone (1) and Betts Creek Beds (40)
- Early Permian – Aramac Coal Measures (31) , Jochmus Formation (44) and Jericho Formation (36) (note that the Jericho Formation also occurs in the Late Carboniferous)
- Late Carboniferous – Lake Galilee Sandstone (9).

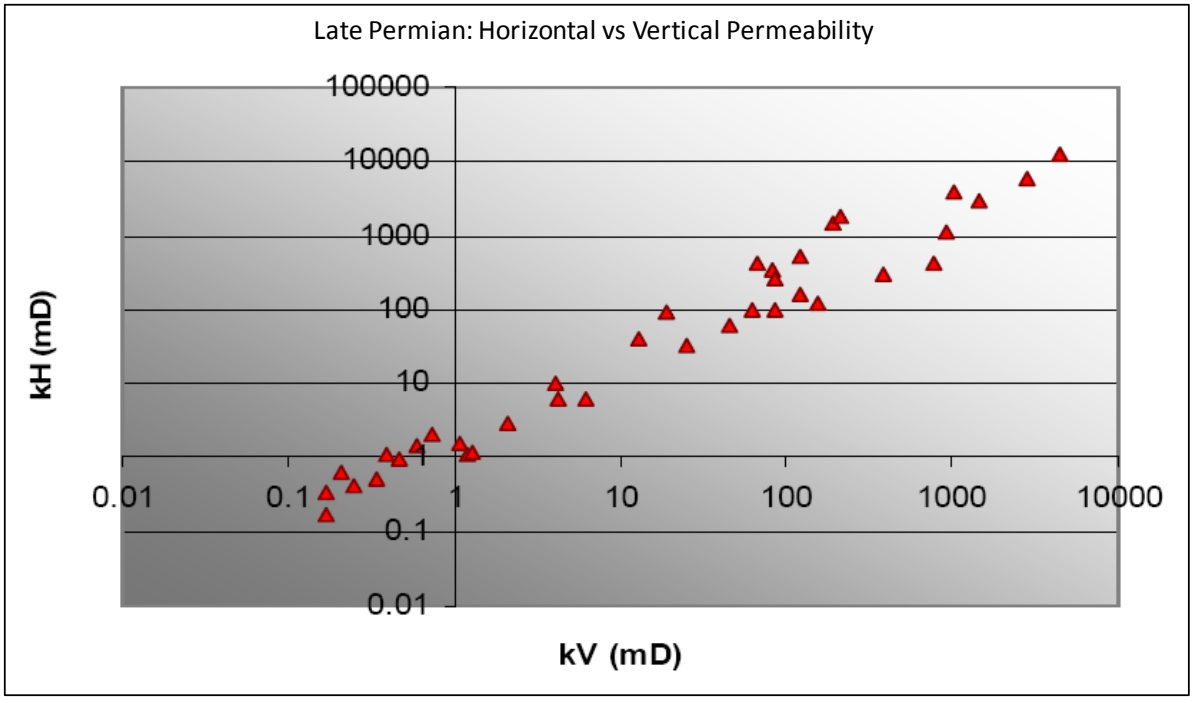

Figure 43 Late Permian horizontal versus vertical permeability (© Copyright, Rawsthorn et al. 2009).

It can be seen that the vast majority of tests have been in the Permian units and many of these in the prospective economic formations (e.g. Aramac Coal Measures, Betts Creek Beds). In contrast, there are very few tests in the formations that overlie these units (e.g. six tests only in the Moolayember Formation and three in the Rewan Formation) – these formations will exert a major control on connectivity between aquifers if the Permian units are depressurised for CSG development.

It should also be noted that the test numbers described are from a limited spatial dataset. Rawsthorn et al. (2009) suggest that the Hawkins data and Marsh et al. (2008) data is based on only 10 wells. This is a significant data gap. In particular, there is paucity of data in the southern part of the Basin, although Marsh et al. (2008) suggest that some permeability data is available in this area but was not collated in their assessment.

8.2.2 Local datasets

8.2.2.1 AGL (2012) underground water impact report

Near the middle of the Galilee Basin (approximately 50 km north-east of Longreach), AGL has operated five pilot CSG production wells since December 2009. The wells target the Betts Creek Beds at depths of 950 to 1000 m below ground level. As part of their assessment of impacts of these pilot activities AGL have simulated the extraction test with a numerical model. The process of calibrating the numerical model provides predictions on hydraulic properties of the formations. The calibration process includes use of an observation bore in the Betts Creek Beds (at two vertical locations) and the (lower) Hutton Sandstone. The model calibrated hydraulic parameters are presented in Table 27. Units above the Hutton Sandstone were not monitored during the test and hence the parameters for those formations can be considered estimates rather than calibration determined parameters.

Table 27 Model calibrated hydraulic parameters for AGL pilot well testing, December 2009 to January 2012 (© Copyright, AGL 2012).

Hydrostatigraphic unit	Horizontal hydraulic conductivity (m/d)	Vertical hydraulic conductivity (m/d)	Specific storage (−/m)	Approximate storativity (-)
Winton/Mackunda Formation	1	0.1	0.000001	Variable
Wallumbilla Formation	0.00003	0.000003	0.000001	Variable
Cadna-owie Formation/Hooray Sandstone	0.5	0.05	0.000001	0.0001
Westbourne/Birkhead Formation	0.00005	0.000005	0.000001	0.0001
Hutton Sandstone	0.5	0.05	0.000001	0.0001
Rewan Formation	0.00005	0.000005	0.000001	Variable
Permian Coal Measures	0.004	0.00005	0.0000006	0.0001

Some depressurisation, in the order of 2 m, was observed in the observation bore in the (lower) Hutton Sandstone during the pilot extraction. AGL (2012) concluded that:

> *'…no conclusive cause for the observed pressure reduction can be identified at this time; although a slight decline in the pressures in the Hutton Sandstone aquifer due to the ongoing depressurisation of the Permian aquifers cannot be ruled out. A pressure decline of this level can be replicated using numerical modelling, however it is also possible that the position of the logger altered during deployment and this could account for part or all of the decline in pressure'.*

Hence while the report concludes that the calibration against the observed drawdown in the Hutton Sandstone can be achieved (within realistic bounds of hydraulic conductivity), it is apparent that the final calibrated parameters as presented in Table 27 are not based on calibration against the Hutton Sandstone bore. At the time of writing, AGL noted that an investigation program was underway to identify the cause of the pressure reduction in the Hutton Sandstone bore.

The vertical hydraulic conductivity of the Rewan Formation used in the modelling (i.e. as shown in Table 27) is approximately four orders of magnitude lower than that indicated by the laboratory test data in Section 8.2 (noting low sample size) and approximately two to three orders of magnitude lower than values identified for the Rewan in other parts of the GAB by Audibert (1976).

8.2.2.2 Alpha Coal project - groundwater investigation for environmental assessment

The Alpha Coal project is located in the south-east of the Galilee Basin, approximately 50 km north of Alpha. As part of the environmental assessment process, the project prepared an investigation summarising the hydrogeology of the area and examined potential impacts on groundwater from mining operations. The Late Permian, coal-bearing strata sub-crop in the area and dip gently (<1°) to the west. Tertiary sediments are present at the site but groundwater occurrence is sporadic in these units (JBT 2010). The Tertiary sediments unconformably overlie the Rewan Formation and Permian sediments. The Rewan Formation occurs only in the far west of the mining lease, where it subcrops under Tertiary cover. Permian units at the site comprise the Bandanna Formation and underlying Colinlea Sandstone (of the Galilee Basin), which contain economic and sub-economic coal seams.

JBT (2010) reports on two investigations, which involved collection of hydraulic parameters:

- Surface water, groundwater and geotechnical investigations by Australian Groundwater Consultants (AGC 1983) for Bridge Oil Limited, during 1982-1983. Hydraulic properties were calculated from pumping tests at four sites ranging from 1 to 4 days in duration. The unit tested is referred to as the D-E Sandstone (which is the Colinlea Sandstone). The average hydraulic conductivity for the unit across the four sites ranged from 0.25 to 1.6 m/day. Average storage coefficients across the four sites ranged from 0.00001 to 0.001.
- Groundwater investigations undertaken by Longworth and McKenzie (1984) for Bridge Oil Limited. A test targeting an interval including the C and D coal seams and interburden yielded an average hydraulic conductivity of 0.14 m/day (S of 0.005) and a test in the Colinlea Sandstone between the D and E coal seams yielded average hydraulic conductivity of 0.26 m/day (S of 0.00003).

JBT (2010) also describe pumping bores which have been installed at three sites (in the D-E sandstone and sub-E sandstone) and refer to the results being presented in a supplementary report, however this report was not able to be obtained.

The report refers to the fact that the lower boundary of the GAB (outcrop of the Rewan Formation) occurs approximately 10-15 km west of the western limit of mining. In order for the Alpha mine to impact on the water resources of the GAB, drawdown from the operation would need to propagate through the Rewan Formation aquitard, which is taken to be approximately 175 m thick in the area to the west of the mining lease application (MLA) and possessing a vertical hydraulic conductivity in the order of 1×10^{-4} to 1×10^{-3} m/day, based

on calibrated values for GAB confining units from an early phase of GAB groundwater modelling (Audibert 1976).

8.2.2.3 South Alpha Coal project area

Waratah Coal Incorporated proposes to establish a new open cut coal mine in the Galilee Basin, in the South Alpha Mine project lease area, which is located west of the Alpha township (and close to but south of the Alpha Coal project described above). The area is characterised by an unconfined shallow porous aquifer zone in the Tertiary and younger alluvial sediments and a deeper multi-layered semi-confined to confined porous/fractured aquifer system in the Permian sediments, between and below the coal seams. The mine lease area is close to the eastern margin and recharge zone of the GAB. SKM (2009) reported on a baseline groundwater study, which was the first phase of a three phase impact assessment.

Unconsolidated sands, silts and clay (Quaternary and Tertiary age) form an extensive blanket over the project area, with thickness of up to 90 m in the eastern and central sections. In the east of the mine project area, these sediments sit directly on the Permian strata. The Alpha coal deposit comprises five Permian seams termed A to E. The overlying Quaternary and Tertiary sediments tend to thin to the west. The Triassic age Rewan Formation lies unconformably over the Permian formations. Where not removed by the Cenozoic sediments, the contact between the Rewan and Permian sits 20 to 40 m above the A seam. Stratigraphic information reported by Australian Mining Engineering Consultants (AMEC 2007) suggests the lower coal seams (C, D, E) at Alpha occur in the Upper to Lower Permian Colinlea Sandstone and correlative Peawaddy Formations, whereas the shallower (A and B) coal seams occur in the Upper Permian Bandanna Formation. AMEC (2007) reported on aquifer parameters for the C to D and D to E sandstone units from Geological Survey of Queensland 1973 Explanatory Notes for the 1:250 000 Jericho geological map (Senior 1972):

- C-D Sandstone: K = 0.5 m/day, S = 0.001
- D-E Sandstone: K = 0.7 m/day, S = 0.00004

SKM (2009) noteed that these figures are considered to be very preliminary and should be used with caution.

8.2.3 Summary

The largest permeability dataset in the Galilee Basin consists of a Northern Galilee dataset compiled by Peter Hawkins and supplemented by Marsh et al. (2008), with some data from the Southern Galilee Basin. The combined dataset is presented in Marsh et al. (2008). It is apparent that most of this data is from laboratory tests (and possibly some from drill stem tests). Given the size of the Gililee Basin, this is a relatively small dataset – spatially some areas are very poorly represented and some key formations have very few tests. In particular, the two key aquitards (the Moolayember and Rewan Formations) have a total of only nine permeability tests between them. Further, there is an absence of any regional assessment of vertical hydraulic conductivity for these units. Marsh et al. (2008) imply that more permeability data in the southern Galilee Basin which exists and could be incorporated into the regional dataset. They also present a map showing where core is available throughout the Gililee Basin, which could potentially be used for additional/new (laboratory) testing (although the core is likely to have dried out, unless it has been stored very carefully).

AGL has commenced pilot testing in their Authority To Prospect (ATP) and calibration of a numerical model against the testing has yielded hydraulic parameters for associated formations in that area. Investigative reports related to environmental impact assessment

and/or mine planning at two coal sites (both near Alpha) referenced pumping tests and related hydraulic parameters from the 1970s and 1980s. This suggests that these types of reports may be more widespread across the Galilee Basin, but as they are held in private company reports they may not be readily available.

8.3 Structural properties

Figure 44 shows two representations of key structural elements of the Galilee Basin. The figure on the left hand side (Marsh et al. 2008) presents more minor structural features than the right hand side (van Heeswijck 2006). Structure of the Galilee Basin is dominated by slightly curvilinear, steeply dipping reverse fault systems. Three regional scale north-west to south-west trending thrusts are present: the Hopkins Thrust System, Bingeringo Thrust System and the Mingobar Structure (van Heeswijck 2006). Current understanding of the Galilee Basin is that it is relatively unstructured, having remained a topographic and structural low over a long period of time (Marsh et al. 2008). As shown in Figure 44, most of the structures in the Galilee Basin are concentrated around the basin margins and are typically caused by reactivation of older basement structures (Hawkins & Green 1993). Most of these basement structures do not penetrate into the Galilee Basin sediments, although the Southern Galilee Basin is more structured than the Northern Galilee Basin (Marsh et al. 2008).

The van Heeswijck doctoral thesis on *The Structure, Sedimentology, Sequence, Stratigraphy and Tectonics of the Northern Drummond and Galilee Basins, Central Queensland, Australia* (van Heeswijck 2006) provides probably the most detailed analysis of the structure of the Northern Galilee Basin to date. This was based on analysis of 750 km of seismic data, sixteen control boreholes and regional magnetic and gravity data. van Heeswijck (2006) divided the northern Galilee Basin into six seismic facies as related to outcrop and borehole data. It is noted that movement along individual thrust planes is not large, with displacement averaging 400 m. There is an apparent discrepancy here between Marsh et al. (2008) and AGL (2012) who describe only minor fault related displacement in the order of tens of metres and van Heeswijck (2006) who describe fault displacement of hundreds of metres. The difference is attributed to the fact that the faults of interest described in van Heeswijck (2006) are regional-scale major structural features, which define key basin architecture. In contrast, the Marsh et al. (2008) and AGL (2012) focus was on faulting at a sub-regional scale. There is much more detail on structural features of the Galilee Basin documented in the van Heeswijck (2006) thesis.

The building of a 3D geological model of the Aramac Trough (the Galilee Aramac Petrel Project; Rawsthorn et al. 2009) involved mapping fault features. Fault surfaces were interpreted where significant vertical offset was observed. The four surfaces modelled were the top of the Triassic, top of Permian (Clematis Sandstone), top of Early Permian and top of Late Permian; even though the final model was constrained to the Triassic Clematis Sandstone, the early part of the geological modelling included older units. The model did not identify and thus represent any faulting in the Triassic surface:

> *'…as it is an unconformable surface which has since only undergone gentle deformation... any faulting which occurred in association with the uplift and erosion event in the Late Triassic to Early Jurassic cannot be detected using this technique.'*
>
>

From the model representations, a significant offset in the lower surfaces (top of Permian, top of Early Permian and top of Late Permian) was deduced, which may be fault related.

These were often coincident with the edge of the Aramac Trough, and the degree/extent of fault offset was noted to decline in younger strata.

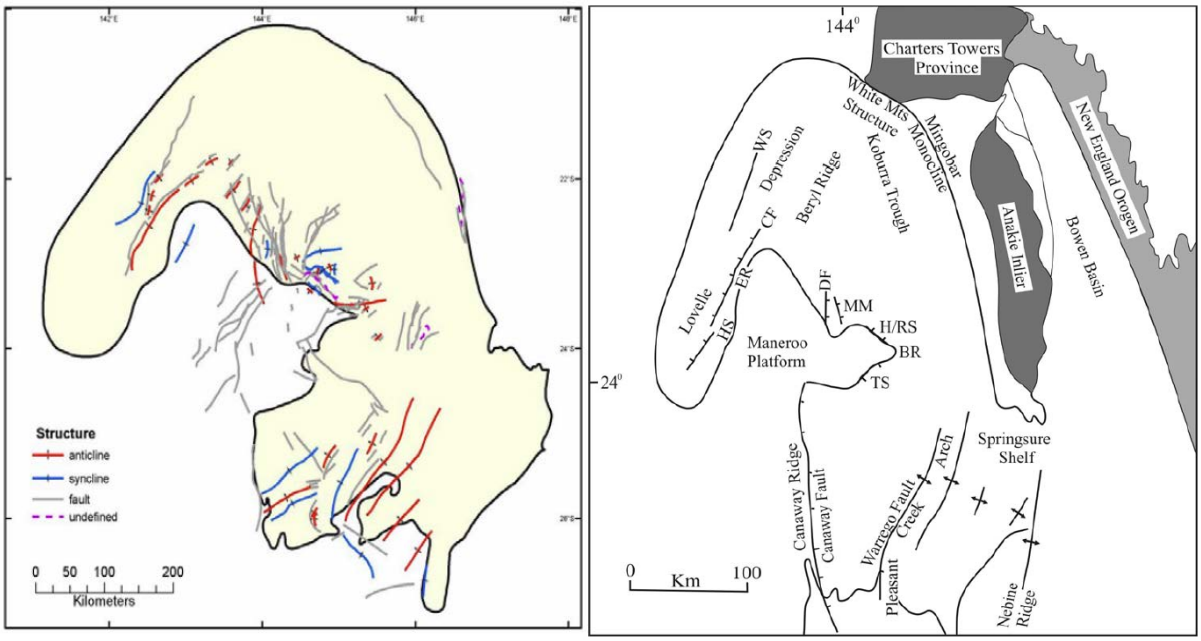

Figure 44 Two representations of key structural features of the Galilee Basin. LHS image was compiled from a number of maps from well completion reports and literature (© Copyright, Marsh et al. 2008); RHS image shows the Mingobar monocline and some structures on the southern margin occurring in outcrop (© Copyright, van Heeswijck 2006); modified from Evans 1980).

Codes: WS – Weatherby Structure, CF – Cork Fault, ER – Elderslie Ridge, HS – Holberton Structure, DF – Dariveen Fault, MM – Marathona Monocline, H/RS – Hutton Rd Structure, BR – Barcaldine Ridge, TS – Tara Structure.

Rawsthorn et al. (2009) suggest the need for further study to investigate faulting within the Late Triassic/Early Jurassic formations. They note that there is evidence of faults penetrating through to land surface (i.e. within these formations), in the form of rivers and creeks which appear to be following lineaments related to faults which predate the Early Permian/Carboniferous.

Most of the knowledge regarding structural features is derived from seismic surveys. Marsh et al. (2008) and Rawsthorn et al. (2009) both note that in spite of a large amount of seismic data collected, there is still an absence of a good regional dataset due to both the quality and variability in spatial coverage of existing data. Due to the format of data preservation, they further note that of the 29 820 kms of seismic line data theoretically available, only approximately 12 500 km of data is actually usable (Rawsthorn et al. 2009).
Marsh et al. (2008) recommended that reprocessing all available data should occur to allow more detailed and accurate interpretation of the subsurface geology of the Galilee Basin.

As exploration and associated activities in the Basin progress, companies are adding to this regional seismic dataset. For example, AGL have conducted seismic surveys within their lease area. Their assessment of the survey results was that structure within the project area is minimal with only minor faulting observed (in the order of 10 m to 15 m of movement) and minimal folding, suggesting that no large structures are present (AGL 2012). They observed

frequent faulting in the Toolebuc and Wallumbilla Formations; however, the faulting dies out at the Cadna-Owie Formation and does not penetrate through to the Jurassic (Hutton Sandstone) aquifers. Significantly, they concluded that (within the vicinity of their current CSG pilot exploration program):

> *'…there are no observed large scale structures that connect the Permian water bearing zones with the shallow beneficial aquifers.'*
>
>

Other companies are also conducting new seismic programs (e.g. Comet Ridge conducted a 200+ km high resolution 2D seismic survey across the southern part of mining lease area, in late 2011), which will add to the regional dataset.

As part of a doctoral thesis Moya (2011) was developing a 3D geological model in the central part of the Galilee Basin. This was using the geological modelling software Gocad, and based on verified lithological and stratigraphic data from exploration wells and groundwater bores and four seismic surfaces (i.e. Basement, P Horizon, C Horizon and Toolebuc). Major faults of potential hydrological significance will be interpreted from the seismic surfaces.

RPS (2012) reports that the springs in the Galilee Basin study area are thought to be associated with shallow occurrences of the host aquifer sediments and not regional faulting, and that this assessment would need to be confirmed with field investigations.

The following key conclusions can be drawn from this section:

- The Galilee Basin is relatively unstructured having remained a topographic and structural low over a long period of time. Most of the structures are concentrated around the Basin margins, and are typically caused by reactivation of older basement structures.
- There is a reasonably large seismic dataset across the Galilee Basin, but this suffers from variable spatial coverage and sometimes poor data quality. Reprocessing of some data would improve and add to the usable regional dataset.
- The Petrel model (Rawsthorn 2009) and interpretation of seismic data by AGL (AGL 2012) note relatively small displacement of identified faults (around 10-15m); the mapping by van Heeswijck (2006) that identified average fault offsets of 400 m is understood to refer to regional scale faults and offsets at depth within basement rock.
- The Petrel model is inconclusive regarding whether faulting in lower formations penetrates through the Late Triassic/Early Jurassic formations. This is an important data gap in that faults represent potential preferred pathways for connection across Permian zones (targeted for CSG development) with shallow aquifers.
- The literature review did not identify any studies in the Galilee Basin which have examined the hydraulic behaviour of faults (e.g. examining whether they enhance or reduce permeability).

8.4 Geomechanical properties

A review of the literature did not identify any significant references regarding geomechanical properties of formations in the Galilee Basin. van Heeswijck (2006) refers briefly to stresses related to formation of the Basin, but not information on current in situ stresses, relative stress magnitudes or stress contrasts within/between units. This review did not include examination of individual well completion or drilling reports which may have captured this

information on a bore-by-bore basis. It is apparent that at least some petroleum/coal companies are collecting geomechanical information; however, these programs are either not complete or the results are not yet published. For example, Exoma refers to commencement of a drilling program (of at least 10 and up to 21 wells) in May 2011, which was to include collecting coal and shale core for a variety of tests, including geomechanical properties (Exoma 2011). Expansion of the 2011 drilling program occurred during 2012.

Geomechanical properties constitute a significant data gap within the Galilee Basin. In the interim, estimates of geomechanical parameters of some formations could be made where the formation is present in adjoining Basins (e.g. Bowen or Surat Basins).

8.5 Geochemistry and isotopes

Marsh et al. (2008) present salinity ranges and averages for various formations in the Galilee Basin (see column 6 in Figure 42). The data is reported to be based on a limited number of samples (e.g. the Moolayember Formation data is from three samples and only the Clematis and Colinlea Formations have more than eight samples in the dataset). Given the size of the Galilee Basin, this indicates that data/knowledge regarding geochemistry of the Basin is a significant data gap. RPS was engaged by a group of operators in the Galilee Basin to develop a baseline understanding of groundwater within the Eromanga and Galilee Basin strata, part of which involved collation of a baseline groundwater quality dataset (RPS 2012). The dataset used in the RPS study included water bores from the Queensland Groundwater Database and exploration bores (Queensland Petroleum Exploration Database[4], CSIRO Pressure Plot[5], QDEX[6] and well completion reports).

In contrast to the RPS study (RPS 2012), the Moya (2011) study involved collection of new data (groundwater chemistry and isotope sampling). Preliminary results from the Moya thesis are presented in Figure 45; these are from Queensland Groundwater Database bores across the Galilee Basin. Figure 45 indicates that in 2012 there were few water chemistry samples for the Permian units of the Galilee Basin available in the Queensland Groundwater Database. Most of the Permian formations have less than five samples available and some important units such as the Aramac Coal Measures do not have any sample records in the database.

The Triassic Clematis Sandstone has a Na-HCO_3 water type, similar to the Jurassic aquifers of the GAB (Moya et al. 2012) and is bounded by two aquitards with Na-Cl water (i.e. Moolayember Formation and Rewan Formation). The salinity of the Moolayember is notable for being significantly higher than all other formations. As described previously in this chapter, the Moolayember Formation is important in that it separates the Clematis Sandstone from the Jurassic aquifers.

---

4 Queensland Petroleum Exploration Database contains general well history, company and Geological Survey of Queensland stratigraphic picks, drill stem tests, hydrocarbon indications, references, wireline log types, downhole temperatures, analytical results (e.g. oil, gas, pyrolysis, petrophysics, thermal maturity), and location information for over 7000 petroleum, coal seam gas and stratigraphic wells.

5 PressurePlot was developed by CSIRO (CSIRO 2007) to query the PressureDB database and visualise its oil and gas data. PressureDB currently contains data for 1853 wells from basins across Australia.

6 The Geological Survey of Queensland manages the collection of company exploration reports using an internet document management system called QDEX (Queensland Digital Exploration Reports system) http://mines.industry.qld.gov.au/geoscience/company-exploration-reports.htm

	TDS (mg/l)	pH	EC (µS/cm)	Na (mg/l)	K (mg/l)	Ca (mg/l)	Mg (mg/l)	HCO3 (mg/l)	CO3 (mg/l)	Cl (mg/l)	SO4 (mg/l)
Winton Fm	3059	7.6	5432	**1120**	7.9	148.8	49.0	258	80	**1853**	213
Mackunda Fm	2795	7.8	3954	**1190**	5.0	107.2	36.3	450	107	**1594**	460
Allaru Md	5883	7.9	8079	**1629**	4.6	207.6	150.6	442	59	**2691**	580
Toolebuc Fm	1145	7.5	1340	**159**	1.1	50.3	**100.0**	**447**	0.9	**216**	32
Walumbilla Fm	692	8.1	1023	**297**	4.6	11.5	2.4	308	27	**301**	17
Cadna-owie Fm	1213	8.4	1732	**486**	2.1	7.7	2.9	**783**	32	308	15
Hooray Sst	815	8.3	1417	**328**	3.7	4.2	1.2	**618**	40	117	25
Westbourne Fm	999	8.3	1664	**3756**	3.1	7.8	7.6	**669**	60	153	37
Adori Sst	483	8.4	812	**183**	1.9	4.2	1.5	**299**	17	95	14
Birkhead Fm	505	8.3	883	**211**	3.9	4.4	1.0	**389**	24	83	16
Hutton Sst	407	8.1	669	**144**	6.4	7.9	3.9	**257**	26	76	17
Boxvale Mbr	221	7.9	397	**80**	11.4	6.4	1.8	**166**	1.5	45	10
Evergreen Fm	442	7.9	727	**155**	18.9	4.0	1.4	**310**	21	63	9
Precipice Sst	258	8.1	434	**90**	7.1	5.5	1.5	**185**	6	42	8
Moolayember Fm	4343	7.3	3091	**1233**	10.4	174.2	110.4	150	49	**2166**	357
Clematis Sst	395	7.9	628	**159**	8.1	3.4	1.8	**264**	44	84	6
Rewan Fm	370	7.3	595	**113**	18.5	7.1	7.1	**138**	0.1	**121**	12
Betts Creek Beds	413	8.0	649	**146**	5.8	5.0	0.6	**299**	6	63	8
Jericho Fm	267	8.1	443	**98**	4.8	2.8	0.2	**205**	1.5	38	0.8
Adavale Basin	930	8.0	1400	**340**	9.0	4.9	0.6	**675**	8	136	18
Granite	923	7.9	1407	**358**	4.0	6.8	0.1	**752**	3	109	41

1 or 2 samples
3 to 5 samples
6 to 10 samples
11 to 30 samples
30 to 60 samples
over 80 samples

Figure 45 Average values/concentrations for chemistry parameters for formations of the Great Artesian Basin and the Galilee Basin. Dominant anions and cations are in bold (© Copyright, Moya et al. 2012).

Evans (1996) examined fluoride concentrations across the Queensland section of the GAB. Flouride acts as a tracer which can provide insight into groundwater flow and aquifer interactions. The Permian aquifers contain the highest concentrations of fluoride (around 7-9 mg/L) while lower concentrations (2-4 mg/L) are present in the Jurassic aquifers. Evans (1996) postulates that the origin of the fluoride is the granitic basement rocks and hence there is suspected upwards flow from the basal Permian aquifers to the intermediate depth Jurassic aquifers. The Maneroo Platform is the primary basement structure that truncates the Galilee Basin sediments and is considered to be responsible for the upward flow characteristics in this area (Evans 1996). Assuming this conceptual model is correct, water extraction associated with CSG would reduce the upward flow from the Permian aquifers to the intermediate depth Jurassic aquifers – whether this reduction is significant in the context of the overall water balance of the Jurassic aquifers needs to be assessed.

In addition to the more regional studies described above, there are local studies associated with individual Authority To Prospect and Mining Lease Applications that have (or will) yield

geochemical data. The two which have published some preliminary results are briefly described below:

- AGL (2012) – as part of the program of works associated with the Underground Water Impact Report (related to five pilot production wells near the middle of the Galilee Basin), AGL conducted some preliminary geochemistry sampling and analysis. Based on results from stable isotope samples it was concluded that the water within the Permian Coal Measures is of meteoric origin (PB 2012b). They note that the isotopic signature of groundwater from the Hutton Sandstone is more enriched than the deeper formations (Betts Creek Beds and Aramac Coal Measures), but still plots on the global meteoric water line, indicating groundwater in this aquifer is also of meteoric origin and younger than the deeper water held in the Permian Coal Measures (PB 2012b). As part of the water monitoring program, water from each well has been sampled and analysed on a quarterly basis since mid 2010. Based on a tri-linear plot of the data, AGL (2012) conclude that there is not a high variation between the Permian coal seam water and that sampled from the Hutton and Hooray Sandstones (i.e. in terms of water type, there are differences in concentrations of dissolved solids). All sampled waters indicate Na(+K)-HCO3, with the Permian aquifers slightly more Na(+K)-HCO3-Cl than the Hutton Sandstone.
- Alpha coal – JBT (2010) conducted groundwater sampling as part of the EIS process for the Alpha Coal project (on the eastern margin of the Galilee Basin), as well as collating groundwater quality data from the Queensland Groundwater Database. There was little analysis of this data beyond comparison with beneficial use guidelines.

The Carbon Storage Initiative (under Queensland Geological Survey) completed a study (Grigorescu 2012) on the mineralogy and petrography of the Southern Galilee Basin, with a focus on the Moolayember Formation and the Clematis Sandstone. While not a hydrogeological investigation, the study further contributes to understanding the properties of these formations.

The following key conclusions can be drawn from this section:

- There is a paucity of hydrochemical data for formations in the Galilee Basin. In particular, there are few water chemistry samples for the Permian units, which generally have less than five samples available and some important units such as the Aramac Coal Measures have no sample records in the Queensland Groundwater Database.
- Hydrochemistry data has not been examined to evaluate connectivity between Permian coal seams and the overlying GAB aquifer formations or hydraulic connection between the Clematis Sandstone (Triassic) and the Jurassic aquifer sequence (the Moya PhD thesis, in progress at time of writing, is the first such study).
- There are local studies starting to be published with new hydrochemical data (including data from the data scarce Permian units).

8.6 Recharge and discharge

8.6.1 Recharge

Marsh et al. (2008) states that groundwater recharge into the Eromanga Basin and Triassic part of the Galilee sequence occurs in the north-east with generally south westerly flow.

Apart from this fleeting reference to recharge, the literature on recharge processes in the Galilee Basin appears to be very limited. Groundwater investigations as part of the Alpha Coal project (on the eastern edge of the Galilee Basin) was the only field study identified in the literature review assessing recharge processes at a local scale in the Galilee Basin. The investigation included installation of eight vibrating wire piezometer sites and two automated rain gauges (in December 2009). A review of hydrographs did not indicate an increase in groundwater levels that could be interpreted as aquifer recharge in response to the (high) wet season rainfall over the 2009/2010 wet season (JBT 2010). The report concluded that groundwater occurs under confined conditions in the western area of the Alpha Coal MLA, potentially becoming unconfined to the east of Lagoon Creek in the outcrop area of the Colinlea Sandstone. Geotechnical drilling and permeability testing in the Colinlea Sandstone at shallow depths (1 and 5 m) were cited as further support of the conclusion that even under above average rainfall conditions infiltration is limited in this area of Colinlea Sandstone outcrop, unless rainfall is sufficient to saturate the rock profile. JBT (2010) discuss a number of recharge mechanisms at the site, including direct recharge to outcrop areas, diffuse recharge along the Great Dividing Range, flood recharge from Lagoon Creek and diffuse recharge through surface Tertiary sediments. In the west of the MLA, the potentiometric surface of the upper Colinlea (C-D sandstone) is higher than the potentiometric surface deeper in the formation, (D-E sandstone) indicating downward flow potential within this formation).

For shallow aquifers at the site, evidence is presented in support of Great Dividing Range diffuse recharge being the most important recharge mechanism and recharge from the area of the Colinlea Sandstone outcrop/subcrop being relatively less regionally significant. However, it is acknowledged that this recharge process may be important for deeper units within the Colinlea Sandstone aquifer. It is apparent from the report that a number of potential recharge mechanisms have been identified but that the relative importance of these requires further data gathering, including additional monitoring sites, but also longer monitoring periods. The Coordinator General review of the Alpha Coal project EIS also put conditions on mining approval related to better characterising recharge at the site (Queensland Government 2012).

Recharge processes are also discussed in relation to EIS studies for the proposed mining operations within the South Alpha MLA, including whether the proposed mining area could physically affect recharge to the GAB. Based on the regional data, the South Alpha MLA is located east of the conventionally considered outermost GAB intake beds (the Jurassic age, GAB intake beds of the Lower Hutton Sandstone, which outcrop west of Jericho) and the Triassic age Clematis Sandstone outcropping along the Great Dividing Range (SKM 2009). Regional terrain suggests that recharge to the MLA entering the Tertiary age aquifers (from wet season precipitation and infiltration from along losing streams) overlying the Permian sandstone aquifers would drain in a northerly direction towards the Belyando River system. However, the underlying Permian stratigraphy and associated aquifers dip conformably towards the west, underlying the younger GAB aquifers.

Piezometric levels in the individual Permian aquifer zones are not known. It is expected, however that within the South Alpha MLA these aquifers are recharged predominantly by vertical leakage from the overlying Tertiary and younger sediments. SKM (2009) postulated that it is unlikely that a pressure gradient exists towards the west in the confined sections of the Permian aquifers. Instead, it is proposed that a gradient in the Permian aquifers to the north, following a similar direction to the groundwater flow in the overlying Tertiary Sediments, is more likely. The assessment concluded that:

> *'…as the mine lease area is located to the east of the recognised GAB recharge zone, a confirmed pressure gradient in the Permian aquifer zones to the west would be required to suggest that the Galilee Basin forms part of the greater recharge zone of the GAB.'*
>
> © Copyright, SKM (2009)

8.6.2 Discharge

There is very limited information in the literature on discharge processes in the Galilee Basin. RPS (2011) noted that the:

> *'…GAB recharge springs in the Galilee Basin occur in association with the intake bed outcrops and sub-crop areas.'*
>
> © Copyright, RPS (2011)

Recharge springs refer to springs that occur in the same outcropping unit that the recharge occurred.

RPS (2011) presented a plot of mapped springs in the Galilee Basin (no source is indicated however). Outflow from springs is commonly associated with geo-structural features, such as faults and shear zones, which allow upward flow of groundwater. The Alpha Coal project (JBT 2010) also reported the presence of (recharge) springs within the wider study area. The dominant groundwater discharge process in the MLA however was considered to be towards Lagoon Creek (and either to wetlands associated with the creek or to the alluvial sediments of the creek). This was similar to the conclusions reached in SKM (2009) for the South Alpha coal MLA (discussed in previous section) where discharge was considered likely to be north towards the Belyando River system. The common theme from these two studies regarding groundwater discharge was that in the far eastern part of the Galilee Basin (where units of the Galilee Basin outcrop/subcrop), relatively local discharge processes appeared to be dominant. This implied a groundwater divide, where some recharge is directed west towards the deeper units in the central parts of the Galilee Basin. Investigations or even discussions of these processes were not identified in the literature.

While there is limited discussion on discharge in the outcrop/subcrop areas, there was no information identified on discharge processes in the main parts of the Galilee Basin (i.e. to the west). Given the submerged nature and geometry of the Galilee Basin, discharge must be some combination of diffuse vertical discharge through confining beds to overlying formations (ultimately to the GAB) and sub-surface discharge to neighbouring sedimentary basins or adjoining basements units. The relative importance and spatial distribution of these processes is unknown.

The key conclusions from this section are:

- Beyond regional studies examining recharge to the GAB (e.g. Kellett et al. 2003) there is very limited information in the literature on recharge processes/areas/rates in the Galilee Basin. The Kellett study focused on the Hooray Sandstone (and equivalents) and to a lesser degree the Hutton and Adori Sandstones. Hence, there is a data gap in terms of recharge (in the outcrop/subcrop areas) to the Triassic (Clematis Sandstone) and Permian age formations (Colinlea Sandstone, Aramac Coal Measures and Betts Creek Beds) of the Galilee Basin. One field study was identified in the eastern edge of the Galilee Basin (associated with the Alpha Coal project), however it is apparent that further data collection and analysis is required to fully understand recharge processes in the

area.

- The Alpha Coal and South Alpha coal assessments both indicated a knowledge gap regarding understanding recharge processes in the outcrop areas in the eastern edge of the Galilee Basin. The studies indicated uncertainty as to whether recharge to the Triassic and Permian aquifer outcrops/subcrops would follow local topographic gradients or if recharge would follow the regional stratigraphic westerly dip of these formations.
- In addition to a lack of understanding recharge in the outcrop areas, there was no information identified in the literature on the significance of vertical leakage as a recharge process to the formations of the Galilee Basin.
- There is some information on discharge mechanisms in the outcrop/subcrop areas of the Basin (e.g. mapping of recharge springs), although it is apparent that processes are still not well understood. There was no information identified on discharge processes in the main part of the Basin (i.e. to the west where the Basin underlies the GAB). Discharge is likely to be a combination of diffuse vertical discharge through confining beds to overlying formations and sub-surface discharge to neighbouring sedimentary basins/adjoining basements units - the relative importance and spatial distribution of these processes is unknown.

8.7 Groundwater level data

As described earlier in this chapter a regional baseline study (RPS 2011) to characterise groundwater within the Eromanga and Galilee Basin strata has recently been completed. Part of this involved collation of a baseline groundwater level dataset. The information used to compile the dataset included water bores from the Queensland Groundwater Database, and exploration bores (Queensland Petroleum Exploration Database, CSIRO Pressure Plot, QDEX well completion reports). RPS (2011) note that the Queensland Groundwater Database yields data for ‘shallow’ water bores, which include Lower Eromanga and upper Galilee aquifers tapped in the east, and Eromanga and surficial aquifers in the west, while the Queensland Petroleum Exploration Database, CSIRO Pressure Plot and QDEX well completion reports yield data for the Permian age aquifers and basement aquifers.

The RPS study includes contoured piezometric surfaces for the Rolling Downs Group, Cadna-owie Formation/Hooray Sandstone Aquifers, and the Hutton Sandstone aquifer.

Key points from the study are listed below (RPS 2012; RPS 2011):

- Groundwater-level data are available for over 4400 Galilee Basin water bores. Groundwater levels were found to be consistent with the GAB in general and ranged from deeper than 300 m bGL to artesian conditions.
- Groundwater level data from the Rolling Downs Group aquifers, Cadna-owie/Hooray Sandstone aquifers and the Hutton Sandstone aquifer was contoured to identify and evaluate changes in the groundwater potentiometric surface. These formations are all within the Eromanga Basin sequence. Groundwater levels for the Galilee Basin aquifers could not be contoured because of the lack of data for any given formation.
- Time-series plots of groundwater level data were produced to identify long-term water level trends. However, the Queensland Groundwater Database contained only 14 water bores with more than 10 measurements.
- Nearly 1100 water bores were compiled with groundwater flow data, including

groundwater discharge, static groundwater level and calculated static groundwater level. The water bore discharge peaked in the early 1900s at over 100 L/s per bore for a small number of bores and declined to about 40 L/s per bore around 1975. Groundwater flow continued to slowly decline to approximately 30 L/s per bore around the year 2000. This decrease in groundwater flow predates any lowering of the water pressure in Permian coals by CSG exploration.

- Most historical deep water bores tap more than one formation, which makes the use of these bores in development of water level surfaces for different formations difficult.
- When detailed bore logs are not available, the interval screened needs to be estimated from the depth of the bore and the interpolation of surface from nearby bores with known lithology/stratigraphy. It is there often difficult to assign an aquifer or group of aquifers to a particular water bore.
- 'Spot' bore dip readings can be meaningless or misinterpreted (e.g. there is low quality control on this data, which is often collected near the time of drilling and hence may not represent a fully stabilised water level).
- There are too few data points for the Permian formations to allow preparation of a piezometric surface.

Given the paucity of time series water level data, RPS (2011) considered options for developing a groundwater level dataset. While there are a large number of existing water bores, the disadvantage of using these is that this will cause a significant bias towards the shallow, dominant Eromanga Basin aquifer (except in the east). Futhermore, data on bore construction and water use history are incomplete, and these bores often tap multiple aquifers and deeper aquifers will be missed. Monitoring groundwater levels and aquifer pressures in exploration wells that have been converted to monitoring wells will provide access to the deeper aquifers, including those closer to the Permian Coal Measures. However, RPS considers that this will be logistically more difficult to do this due to likely artesian pressures. RPS (2011) concluded that monitoring groundwater levels at dedicated wells (i.e. newly installed monitoring wells) will be required in the future where existing water bores or converted exploration wells are absent (or inadequate).

8.8 Groundwater modelling

This review has not identified any regional numerical groundwater modelling work undertaken in the Galilee Basin. The following modelling was undertaken for specific development proposals:

- AGL well field simulation model – as part of assessment of impacts of five pilot wells, AGL simulated the extraction testing with a numerical model. The 10-layer model was developed using the United States Geological Survey (USGS) MODFLOW code and covers the whole of the tenement. The model was completed in March 2012 and is documented in PB (2012a). The objective of the modelling was to support the UWIR in the area of *Part C: Predicted Water Level Declines for Affected Aquifers*. Each of the layers represented key hydrostratigraphic units identified in the Galilee and Eromanga Basins. The model was constructed using available lithological and seismic reflection data. Model calibration was against steady state and transient conditions (including flow rates from the wells and against water levels in observation bores in the Betts Creek Beds and the Hutton Sandstone; AGL 2012).

- Alpha Coal project - JBT (2010) refers to regional 3D groundwater modelling that is being undertaken to provide prediction of the magnitude and extent of groundwater level impacts from the Alpha and Kevin's Corner mines (cumulative impacts). The groundwater numerical modelling report was submitted to the Coordinator General in March 2012 (Queensland Government 2012), which was a more advanced modelling effort, based on prior review of the model by DERM and RPS (this report does not appear to be publically available). The modelling concluded that:

  '…no connection has been identified between the aquifers affected by the mine and the GAB.'

  However, the Coordinator General's review recommended more detailed work be undertaken on groundwater modelling and in particular, on the cumulative impacts of the Galilee mines on groundwater. The evaluation also describe conditions that would accompany approval of the project, including the need for updating the model during mining operations, identifying the source of recharge to groundwater in the area and identifying any impacts on the GAB.

Zhenjiao Jiang commenced work in 2012 on a PhD thesis at Queensland University Technology involving numerical modelling of hydraulic impacts of CSG extraction in the central northern Galilee Basin. The thesis involves determining the hydraulic properties of two key aquitards using geophysical logging data, laboratory testing and cores using synchrotron tomography. These aquitard properties will be used in the model, which will be undertaken using FEFLOW software.

In addition to these groundwater numerical models, two regional geological models were identified:

- *Aramac Trough Petrel model* - the CO2CRC has developed the Aramac Trough Petrel model in the Galilee Basin and is described in Rawsthorn et al. (2009) (note that Petrel is the brand of model used). This is a 3D geological model which encapsulates the geological and structural features of the entire Aramac Trough. The model is focused on the Triassic-aged Clematis Sandstone; however, Permian and Triassic formations are included in the model, with the underlying Carboniferous and overlying Jurassic excluded. In addition to constructing surfaces of various formations (based on well data, seismic data, gravity data, magnetic data and down hole geophysics), the facies model was populated with porosity and permeability data from core measurements, repeat formation tester (which is essentially a form of downhole packer testing) and downhole geophysics data used to predict porosity. The ultimate aim of the model was to use it as the basis for construction of a dynamic model to simulate fluid flow (in this case carbon dioxide into the Clematis Sandstone). Rawsthorn et al. (2009) indicated that simulations will be carred out by other researchers at the CO2CRC by linking the Aramac Trough Petrel model with other programs such as Eclipse Black Oil or the CGM simulation package. Whether this was conducted is not known.
- Claudio Moya (as part of a PhD thesis) at the time of writing was developing a sub-regional basin geological model for the Galilee Basin and the overlying Eromanga Basin, including the GAB Artesian aquifers (Moya 2011). The model domain is to be centred near Longreach and is 300 km by 275 km (west-east and north-south, respectively). The

3D visualisation model (GVS) will incorporate all available data as well as new company generated information. The model is being produced in collaboration with Exoma Energy Ltd. This is not a model for simulating groundwater flow or transport, but could potentially be used to provide the structural information for such groundwater models.

8.9 Aquifer connectivity

There has been relatively little assessment on aquifer connectivity across the Galilee Basin, either in the natural or the developed condition. The focus of investigations in the Galilee Basin to date has been on the geology of the Basin and reservoir characteristics of the Permian units. The hydraulic connectivity of the Permian coal seams and the overlying GAB units has not been studied in any detail. Based on the hydrostratigraphy of the Basin, there are large parts of the Basin where significant thicknesses of (apparently) low permeability formations (the Rewan and Moolayember Formations) separate the Permian Formations targeted for CSG/coal development from overlying aquifers that have high value beneficial uses. Indeed the 'sealing' properties of these formations was one of the reasons why the Galilee Basin was selected as a priority geosequestration target; associated investigations indicated that parts of the Basin were favourable for CO_2 storage and further investigation was recommended (Rawsthorn et al. 2009; Marsh et al. 2008).

The Galilee Basin is understood to be relatively unstructured and the limited number of local assessments to date (e.g. seismic surveys on ATPs) appear to indicate that faults are not continuous across the Permian units and into the Jurassic-Cretaceous formations. Preliminary geochemistry assessment supports the fact that the Permian units (in their natural state) are relatively hydraulically separate from overlying aquifers currently developed. Limited local groundwater modelling to date (one on the eastern edge of the Basin where the Permian units sub/outcrop and one near the centre of the Basin in the Koburra Trough) suggests that the overlying aquitard will limit significant connectivity, although the latter model only examines impacts from pilot production and not full scale CSG production.

However, the above conclusions suggesting limited connectivity between targeted Permian units and overlying aquifers with high value beneficial use need qualification:

- Key confining units are not continuous across the Basin. In particular, the top of the Moolayember Formation is an unconformable surface which was subject to a long period of erosion. Consequently, in parts of the Basin the formation is thin or absent, leaving potential for connection between the Permian coal units and overlying fresh aquifers (e.g. Hutton Sandstone). The potential for this is greatest to the northwest of the Aramac Trough and along the western margin of the southern Galilee Basin (Marsh et al. 2008). Further, Marsh et al. (2008) note that this locally occurs within the Aramac Trough along fault control ridges which may have been exposed during periods of uplift. The Bandanna Formation also becomes very thin at the southern margin of the Aramac Trough, but is still considered likely to be present when underlain by the Colinlea Sandstone (Marsh et al. 2008).
- The Warang Formation (found mainly in the north of the Basin) is comprised mainly of sandstone and interfingers with the entire Triassic sequence. As it is in contact with the Eromanga Basin, this makes the Warang Formation a potential connecting unit between the Permian units and low salinity aquifers.

In summary, there will be areas where the likelihood of significant connectivity is relatively low, but other areas where the risks of connectivity between the Galilee and overlying strata are much higher.

- There is potential for depressurisation in Permian units deeper in the Basin to propagate laterally to eastern parts of the Galilee Basin, where these units outcrop/subcrop. This creates the potential for impact on surface water features in these areas. This process (including assessment of how likely this risk is) does not appear to have been examined in the literature.
- The Southern Galilee Basin has been poorly studied compared with the northern half of the Galilee Basin.
- The permeability of key aquitards in the Galilee Basin is based on a very limited dataset. Information may be available from equivalent units in other parts of the GAB, but this cannot replace local data for modelling and predictive purposes. Examples are noted of local numerical models in the Galilee Basin where there is a significant discrepancy between the vertical hydraulic conductivity values used for key aquitards in the model and vertical hydraulic conductivity values for the same formations from the current available dataset (i.e. the models are using much lower values). It is possible that the model estimates are more realistic than indicated by the very small dataset, but in the absence of such a suitable dataset there remains uncertainty regarding appropriate hydraulic conductivity values to use in these key formations and hence, uncertainty regarding aquifer connectivity.
- Existing permeability datasets in the Galilee Basin to date are virtually all based on small-scale testing (predominantly laboratory tests and some drill stem tests). This is a significant limitation as there is a wide body of literature indicating that permeability increases with increasing scale of measurement (e.g. refer CSIRO-SKM 2012, for a literature review on this topic).
- While local seismic assessments to date indicate that faults are not continuous across the Permian units and into the Jurassic-Cretaceous formations, the Rawsthorn et al. (2009) Aramac Trough geological model investigating a larger area indicated that this aspect was inconclusive in their assessment and was an area requiring further investigation. Further, it is apparent that the hydraulic behaviour of faults has not been studied in the Galilee Basin.
- While two local numerical models identified to date have suggested there is essentially no aquifer connectivity, these are both only focused on individual impacts from one operation. Cumulative impacts across the Galilee Basin may alter potential connectivity compared to developments assessed in isolation.

In summary, it seems that significant parts of the Galilee Basin represent areas of relatively low inter-aquifer (and surface) connectivity, but there are areas where the geology suggests risks are much higher. Further, even in areas where connectivity risks appear low, there are significant data gaps that require filling in order to confirm this conclusion.

8.10 Knowledge gaps

The following key knowledge gaps have been identified in this review:

- The Southern Galilee Basin is relatively less studied compared to the Northern Galilee

Basin in the literature in terms of litho-stratigraphic interpretation and structural analysis.

- There is difficulty correlating parts of the Galilee Basin stratigraphy from the better studied outcrop areas to the central areas of the Basin. In particular, nomenclature problems correlating units of the Clematis and Colinlea Sandstone in the centre of the Basin with formations named in outcrop areas are noted.
- The relationship of the Warang Sandstone and the remaining Triassic sequence is an area poorly understood. Its relatively permeable lithology and inter-fingering with the entire Jurassic sequence creates potential for this unit to 'connect' Permian units and the overlying Eromanga basin under CSG depressurisation or coal dewatering.
- The permeability/hydraulic conductivity dataset (particularly given the size of the Galilee Basin) is small. Spatially some areas are very poorly represented and some key formations have very few tests. In particular, at the time of writing, the two key aquitards (the Moolayember and Rewan Formations) had a combined total of only nine permeability tests.
- There is an absence of any regional scale assessment of vertical hydraulic conductivity for key confining units (the Moolayember and Rewan Formations).
- There is a reasonably large seismic dataset across the Basin, but this suffers from variable spatial coverage and sometimes poor data quality. Reprocessing of some data would improve and add to the usable regional dataset.
- The Aramac Trough geological model is inconclusive regarding whether faulting in lower formations penetrates through the Late Triassic/Early Jurassic formations. This is a data gap in that faults represent potential preferred pathways for connection across Permian zones (targeted for CSG development) with shallow and low salinity aquifers.
- No studies in the Galilee Basin were identified which have examined the hydraulic behaviour of faults (e.g. examining whether they enhance or reduce permeability).
- The review did not identify any references (of significance) regarding geomechanical properties of formations in the Galilee Basin.
- There is a paucity of hydrochemical data for formations in the Galilee Basin. In particular, there are few water chemistry samples for the Permian units, which generally have less than five samples available and some important units such as the Aramac Coal Measures have no sample records in the Queensland Groundwater Database.
- Hydrochemistry data has not been examined to look at the issue of connectivity between Permian coal seams and the overlying GAB aquifer formations, or hydraulic connection between the Clematis Sandstone (Triassic) and the Jurassic aquifer sequence (although there is PhD in progress examining these aspects).
- Beyond regional studies examining recharge to the GAB there is very limited information in the literature on recharge processes/areas/rates in the Galilee Basin. There is a data gap in terms of recharge (in the outcrop/subcrop areas) to the Triassic (Clematis Sandstone) and Permian age formations (Colinlea Sandstone, Aramac Coal Measures and Betts Creek Beds) of the Galilee Basin. There is also uncertainty as to assess whether recharge to the Triassic and Permian aquifer outcrops/subcrops would follow local topographic gradients and discharge to local streams, or whether recharge would follow the regional stratigraphic westerly dip of these formations and provide recharge to

the central areas of the Basin.

- There was no information identified in the literature on the significance of vertical leakage as a recharge process to the formations of the Galilee Basin. There is also an absence of assessment of vertical gradients between units.
- There is some information on discharge mechanisms in the outcrop/subcrop areas of the Basin (e.g. mapping of recharge springs), although it is apparent that processes are still not well understood. There was no information identified on discharge processes in the main part of the Galilee Basin (i.e. to the west where the Basin underlies the GAB). Discharge is likely to be a combination of diffuse vertical discharge through confining beds to overlying formations and sub-surface discharge to neighbouring sedimentary basins/adjoining basements units - the relatively importance and spatial distribution of these processes is unknown.
- There is a paucity of time series groundwater level data, which makes it difficult to evaluate groundwater levels prior to groundwater development. With the exception of the GAB monitoring bores comparatively few groundwater level observations have been collected (at the time of writing, an average of two observations per bore).
- Most historical deep water bores tap more than one formation, which makes the use of these bores in the development of water level surfaces for different formations difficult.
- There are insufficient data points for the Permian formations to allow preparation of a piezometric surface.

9 Knowledge gaps

The previous four chapters (chapters 5 to 8) of this report have concluding sections that are dedicated to knowledge gaps specific to each basin. This chapter synthesises these knowledge gaps into one consolidated list and attempts to distinguish between what are truly gaps in knowledge versus gaps in data that are required to improve current knowledge. By presenting all of the gaps in tabular format (Table 28) it becomes clear that most apply to all four basins reviewed in this report. We also list the relative scale to which these gaps apply and identify a qualitative prioritisation based on collective expert opinion from all authors. Finally, an indicative timeframe required to address the gaps (assuming unlimited availability of scientists with the right capability and sufficient operating budget) and a brief description of the desired outcomes are presented.

Table 28 Knowledge gaps (prefix K) and data gaps (prefix D).

No.	Knowledge or data gap	Scale (local/ regional/ basin)	Priority [high (H), medium (M) or low (L)]	Indicative timeframe required	Outcome if gap was addressed
K1	Cumulative impacts of CSG water extraction	Regional-Basin	H	5 years	Understanding potential environmental and socio-economic impacts
K2	Spatial variability in hydraulic properties (esp. vertical hydraulic conductivity) of aquitards	Regional-Basin	H	5 years	Improved definition of areas with high potential for inter-aquifer leakage
K3	Methods to estimate formation-scale hydraulic conductivity of aquitards	Local-Regional	H	1-3 years	Reduced uncertainty in the prediction of inter-aquifer leakage responses to CSG water extraction
K4	Natural connectivity between Permian coal seam units and Jurassic-Cretaceous GAB units via Triassic sandstone units	Basin (all basins)	M	2-3 years	Baseline assessment of inter-aquifer leakage
K5	Presence and importance of faults in controlling groundwater flow and inter-aquifer leakage	Basin (all basins)	M	3-5 years	Reduced uncertainty in the prediction of inter-aquifer leakage responses to CSG water extraction and re-injection
K6	Importance of considering dual-phase flow for modelling of inter-aquifer leakage	Local	M	1-2 years	Reduced uncertainty in the prediction of inter-aquifer leakage responses to CSG water extraction

No.	Knowledge or data gap	Scale (local/ regional/ basin)	Priority [high (H), medium (M) or low (L)]	Indicative timeframe required	Outcome if gap was addressed
K7	Methods to model groundwater flow accounting for mechanical deformation of aquifers/aquitards	Local-Regional	M	3-5 years	Reduced uncertainty in the prediction of inter-aquifer leakage responses to CSG water extraction and re-injection
K8	Methods to measure inter-aquifer leakage under highly stressed (hydraulic) conditions	Regional	M	2-3 years	Ability to collect independent data to calibrate groundwater models
K9	Presence of major erosion features or pinch outs	Basin (Bowen)	L	2-3 years	Improved definition of areas with high potential for inter-aquifer leakage
D1	Formation-scale vertical hydraulic conductivity	Local-Regional (all basins)	H	3-5 years	Reduced uncertainty in the prediction of inter-aquifer leakage responses to CSG water extraction and re-injection
D2	Consolidated database of corrected hydraulic head data from all States	Basin (all basins)	H	1-3 years	Improved definition of areas with high potential for inter-aquifer leakage
D3	High density measurements of vertical head gradients	Regional (all basins, especially Bowen and Galilee)	H	1-3 years	Improved definition of areas with high potential for interaction
D4	Time-series groundwater level data for individual aquifer formations	Basin (especially Galilee and Bowen)	H	2-3 years	Baseline assessment and long-term monitoring
D5	Systematic mapping of polygonal faulting	Regional (Eromanga Basin)	M	1-3 years	Improved definition of areas with high potential for interaction
D6	Measurements of fault throw magnitudes	Regional (all basins)	M	3-5 years	Improved definition of areas with high potential for interaction
D7	Locations and estimates of inter-aquifer leakage through poorly completed/decommissioned boreholes	Basin (all basins)	M	3-5 years	Improved definition of areas with high potential for interaction

No.	Knowledge or data gap	Scale (local/ regional/ basin)	Priority [high (H), medium (M) or low (L)]	Indicative timeframe required	Outcome if gap was addressed
D8	Hydrochemical data for Permian units and Aramac Coal Measures.	Basin (Galilee)	M	1-3 years	Baseline assessment of inter-aquifer leakage
D9	Changes in hydraulic conductivity with depth	Basin (all basins)	M	3-5 years	Reduced uncertainty in the prediction of inter-aquifer leakage responses to CSG water extraction and re-injection
D10	Stratigraphic interpretation and structural analysis	Basin (especially southern Galilee)	M	1-2 years	Fundamental data for conceptual understanding
D11	Connectivity between northern Bowen Basin aquifers and their equivalents in southern Bowen Basin	Basin (Bowen)	M	1-3 years	Baseline assessment of connectivity
D12	Direction and magnitude of principal stress field	Local-Regional	L	1-2 years	Improved data to predict changes in connectivity due to depressurisation and/or reinjection
D13	Geomechanical properties of aquitards	Regional (all basins)	L	3-5 years	Reduced uncertainty in the prediction of inter-aquifer leakage responses to CSG water extraction and re-injection

10 Conclusions and recommendations

For this review aquifer connectivity is formally defined as the interaction between aquifers separated by aquitards. The degree of connectivity is only partly influenced by the hydraulic properties of the aquitards and the presence of preferential pathways, such as fractures, faults and open boreholes. Major controls on aquifer connectivity are local and regional hydraulic and concentration gradients.

A wide variety of methods exist at different spatial and temporal scales to assess the hydraulic properties of aquifers and aquitards. However, the hydraulic characterisation of natural fracture networks remains a very challenging task.

Mine dewatering, coal seam gas depressurisation and co-produced water reinjection are some examples of man-made changes to the natural hydraulic gradients which will result in changed aquifer connectivity. A better understanding is needed on how aquifer connectivity will be affected by the interplay of changing gradients, in situ stress, mechanical deformation, fluid properties and hydrogeological characteristics.

Despite a long history of water resources development and hydrogeological investigations in the GAB, very few studies have explicitly focused on aquifer connectivity and inter-aquifer leakage. A recent reclassification of the hydrostratigraphy of the GAB (including the Surat Basin) has defined three aquitard types of varying hydraulic conductivity: leaky aquitards, tight aquitards and aquicludes. Anomalous decreases in potentiometric pressure that are coincident with major faults have been observed in the northeast of the Eromanga Basin. Similarly, the Eromanga Depocentre features widespread faulting and vertical displacement of aquifers. Polygonal faulting has been observed in the Rolling Downs Group aquitard throughout the central region of the Eromanga Basin. In summary, significant tectonic disruption of the Eromanga Basin has compromised the sealing capacity of what were traditionally viewed as confining beds in many parts of the Basin. Recent studies of groundwater discharge represent some of the most relevant research relating to aquifer connectivity in the GAB; several studies have identified the role of faults and fractures as preferential pathways for inter-aquifer leakage (Crossey et al. 2012; Gardner et al. 2012; Wolaver 2012), while others have quantified the rate of diffuse vertical leakage from GAB aquifers which, although very low, can occur over broad areas and thereby constitute a significant component of total groundwater discharge (Harrington et al. 2012).

Compared to the GAB, many more studies of aquifer connectivity have been undertaken in the Surat Basin, even though the latter is only one-quarter the size of the GAB. However, there is still large uncertainty around inter-aquifer leakage, particularly between the Hutton Sandstone and Precipice Sandstone via the Evergreen Formation. Analysis of vertical hydraulic gradients in different parts of the Basin provides conflicting evidence, with some data indicating the Evergreen Formation is an effective seal while other data indicates a high degree of hydraulic connection. There is hydraulic and hydrochemical evidence for connectivity between the Walloon Coal Measures and Condamine River Alluvium. Finally, studies of groundwater discharge in the Surat Basin have identified the role of faults and fractures as preferential paths for groundwater flow (Habermehl 1982).

Coal mining has been occurring in the Bowen Basin for over one hundred years. Over the last two decades, there has been a shift from predominantly shallow, open-pit mining operations to deeper, underground mines and large-scale CSG fields. The potential for connectivity between coal seams and overlying aquifers has only been assessed at the local

scale of the mining operation and not at the cumulative basin-scale. In the south of the Bowen Basin, the thick Rewan Group is assumed to be a low-permeability aquitard between the coal seams in the Bandanna Formation and the overlying Clematis Group sandstones; however, there is no field data or measurements to support this assumption. In the north of the Bowen Basin, the connectivity between the coal seams (the Moranbah Coal Measures, Fort Cooper Coal Measures and Rangal Coal Measures) and the overlying alluvial and Tertiary basalt aquifers is poorly understood. No cumulative basin-scale assessment of inter-aquifer connectivity has been conducted. Additionally, the connectivity between the Moolayember Formation, Rewan Group and Clematis Group sandstones in the north of the Basin is unknown.

Previous investigations in the Galilee Basin have focused on the geology of the Basin and reservoir characteristics of the Permian units; there are no detailed studies of aquifer connectivity between the Permian coal seams and the overlying GAB units, particularly in the southern parts of the Basin. Local-scale seismic surveys and preliminary hydrochemical assessment suggest that faults in the Basin are not continuous across the Permian units and into the Jurassic-Cretaceous formations, however this requires further investigation. High inter-aquifer connectivity most likely occurs in parts of the Galilee Basin where either the primary aquitards are not continuous or drawdown in the Permian units propagates laterally to eastern parts of the Basin where these units subcrop beneath alluvial aquifers or outcrop in the surface drainage network.

For all of the Basins studied in this literature review, there is a paucity of data that can be used to infer aquifer connectivity – more specifically inter-aquifer leakage fluxes – at a scale relevant for regional water resource assessment. As a consequence of this data gap, any previous modelling studies that use estimates of aquitard hydraulic conductivity obtained from laboratory testing of core samples or drill stem tests have likely under-estimated the fluxes of inter-aquifer leakage that may result from CSG development or coal mining. More generally, there are limited examples in the international literature to demonstrate changes in aquifer connectivity caused by mechanical deformation. The following components of work would assist in addressing aquifer connectivity knowledge gaps:

- research to develop improved methods for identifying fractures and faults and for determining formation-scale hydraulic conductivity of aquitards
- field data collection from the relevant geological formations to enable determination of effective hydraulic conductivity, which can then be fed into existing and future groundwater models
- development of a consolidated, cross-jurisdictional groundwater database that contains corrected hydraulic head data for assessment of potential areas of preferential inter-aquifer leakage
- research into the interplay between changing hydraulic conditions, in situ stress, mechanical deformation, fluid properties and hydrogeological characteristics and the subsequent implications for changes in aquifer connectivity
- establishing an ambient earthquake baseline, using information from current active faults, to assess new and/or induced seismicity.

11 References

AGC 1983. *Alpha Coal Project (A to P 245C), Surface Water and Groundwater Aspects – Preliminary Evaluations*. Report prepared by Australian Groundwater Consultants (AGC) for Bridge Oil Limited.

AGC 1984. *Olympic Dam Water Supply, Wellfield A Investigation*, report prepared by Australian Groundwater Consultants (AGC) for Roxby Management Services.

AGC - Woodward Clyde 1995. *Ernest Henry Mine dewatering review*, Australian Groundwater Consultants (AGC) Woodward-Clyde report to Ernest Henry Mining, Perth, WA.

AGE 2007. *Report on Groundwater Assessment: Berwyndale and Argyle Gas Fields Surat Basin*, unpublished report prepared by Australasian Groundwater and Environmental (AGE) consultants for Queensland Gas Company Pty Ltd, Brisbane, Qld.

AGE 1999. *Development of a sub-regional groundwater model and predictive modelling, Ernest Henry Mine*, Australasian Groundwater and Environmental (AGE) Consultants report to Ernest Henry Mining, Perth, WA.

AGL 2012. *Draft Underground Water Impact Report (for consultation) ATP529P – Galilee Basin*. AGL, 28 May 2012.

Airey PL, Bentley H, Calf GE, Davis SN, Elmore D, Gove H, Habermehl MA, Phillips F, Smith J and Torgersen T 1983. 'Isotope hydrology of the Great Artesian Basin, Australia', *Papers of the International Conference on Groundwater and Man*, Sydney, 5–9 December 1983, Australian Water Resources Council Conference Series, Australian Government Publishing Service, Canberra, ACT, pp. 1-11.

Airey PL, Calf GE, Campbell BL, Habermehl MA, Hartley PE and Roman D 1979. 'Aspects of the isotope hydrology of the Great Artesian Basin, Australia', in: *International Symposium on Isotope Hydrology*, Atomic Energy Agency and United Nations Educational, Scientific and Cultural Organisation, International Atomic Energy Agency, Vienna, pp. 205–219.

Al-Bazali T, Zhang J, Chenvert ME, Sharma MM 2008. 'Maintaining the stability of deviated and horizontal wells: Effects of mechanical, chemical and thermal phenomena on well designs'. *Geomech Geoeng Int* J 3, pp. 167–178.

Allen J & Fielding C 2007a. 'Sedimentology and stratigraphic architecture of the Late Permian Betts Creek Beds, Queensland, Australia'. *Sedimentary Geology,* 202(1-2), pp. 5-34.

Allen J & Fielding C 2007b. 'Sequence architecture within a low accommodation setting: An example from the Permian of the Galilee and Bowen basins, Queensland, Australia'. *AAPG Bulletin* 91(11), pp. 1503-1539.

AMEC 2007. *Preliminary Investigations of Hydrogeology and Belyando River Water Resources for The Alpha Coal Project*. Unpublished report prepared by: Australian Mining Engineering Consultants, prepared for Waratah Coal Pty Ltd. December 2007.

Anderson M P & Woessner W W 1992. *Applied groundwater modeling; simulation of flow and advective transport*, London, Academic Press Inc.

Aquaterra 2009. 'Hydrogeological assessment', Part 2 in: *Narrabri Coal Mine Stage 2 Longwall Project environmental assessment, Volume 1 - Specialist consultant studies compendium*, Aquaterra on behalf of Narrabri Coal Operations.

Armstrong D & Berry KA 1997. *Olympic Dam Operations recalibration of GAB95 numerical flow model (renamed ODEX1), and updated simulation of borefield B operation, report no. HYD-T069*, WMC Resources Ltd.

Arrow Energy 2011. *Underground water impact report – for authority to prospect 1103* – for consultation.

ASTM 2001. *D 4525 Standard test method for permeability of rocks by flowing air*. American Society for Testing and Materials.

Audibert M 1976. *Progress report on the Great Artesian Basin hydrogeological study 1972-1974*, record 1976/5, Bureau of Mineral Resources, Geology and Geophysics, Canberra, ACT.

APPEA 2013. *Coal seam gas industry data,* Australian Petroleum Production and Exploration Association (APPEA) (http://www.appea.com.au/industry-in-depth/industry-statistics/ [accessed 20 Jan 2014]).

Bakker M 2010. *TTim: A multi-aquifer transient analytic element model version 0.01. Technical report*, Water Resources Section, Civil Engineering and Geosciences Delft University of Technology, Delft, The Netherlands.

Barclay DF 2001. *Great Artesian Basin Bore Audit*, Queensland Department of Natural Resources and Mines internal report, Brisbane, Qld.

Barnett BG & Muller J 2008. *Upper Condamine Groundwater Model Calibration Report*, A report to the Australian Government from the CSIRO Murray-Darling Basin Sustainable Yields Project, CSIRO, Canberra, ACT.

Barnett B, Townley L, Post V, Evans R, Peeters L, Richardson S, Werner A, Knapton A & Boronkay A 2012. *Australian groundwater modelling guidelines*. Waterlines Report Series No. 82. National Water Commission, Canberra.

BC Oil & Gas Commission 2012. In*vestigation of observed seismicity in the Horn River Basin*. BC Oil and Gas Commission.

Bense VF & Person MA 2006. Faults as conduit-barrier systems to fluid flow in siliciclastic sedimentary aquifers. *Water Resources Research*, 42**,** doi:10.1029/2005WR004480.

Bentley HW, Phillips FM, Davis SN, Habermehl MA, Airey PL, Calf GE, Elmore D, Gove HE and Torgersen T 1986. 'Chlorine 36 dating of very old groundwater, The Great Artesian Basin, Australia', *Water Resources Research*, vol. 22, pp.1991–2001.

Berry K 2005. *Olympic Dam Expansion Studies: 2005 interim pre-feasibility study*, Groundwater resource evaluation, Great Artesian Basin numerical flow model ODEX5, BHP Billiton.

Berry KA & Armstrong D 1995. *Hydrogeological investigation and numerical modelling, Lake Eyre region, Great Artesian Basin*, Western Mining Corporation Report, report no. HYD-T044.

Bethke CM, Xiang Z & Torgersen T 1999. 'Groundwater flow and the ^{4}He distribution in the Great Artesian Basin of Australia', *Journal of Geophysical Research*, vol. 104, pp. 12999–13011.

BHP Billiton 2009. 'Stuart Shelf regional groundwater flow model', appendix K6 in: *Olympic Dam expansion draft environmental impact statement 2009*, BHP Billiton.

BMA 2009a. *Daunia EIS: Groundwater impact assessment*. BHP Billiton Mitsubishi Alliance.

BMA 2009b. *Caval Ridge EIS: Groundwater impact assessment*. BHP Billiton Mitsubishi Alliance.

BMA 2008. *BMA Bowen Basin Coal Growth Project. Initial Advice Statement*. BHP Billiton Mitsubishi Alliance.

Bickle MJ 2009. Geological carbon storage. *Nature Geosci*, vol. 2**,** pp. 815-818.

Bilge H 2002. *Lower Gwydir Valley groundwater model: groundwater flow model*, Centre for Natural Resources, Department of Land and Water Conservation, NSW.

Bilge H 2007. *Lower Macquarie groundwater flow model, model calibration and development (draft)*, Water Management Division, Department of Water and Energy, Parramatta, NSW.

Biot MA 1941. General theory of three-dimensional consolidation. *Journal of Applied Physics*, vol. 12**,** pp. 155-164.

Botha JF & Cloot AJ 2004. Deformations and the Karoo aquifers of South Africa. *Advances in Water Resources*, vol. 27**,** pp. 383-398.

Bouzelakos S, Timms W, Rahman P, McGeeney D & Whelan M 2013. 'Geotechnical centrifuge permeameter for characterizing the hydraulic integrity of partially saturated confining strata for CSG operations' in *Reliable Mine Water Technology*, IMWA 2013. Golden Colorado, USA.

Brackel AT, Totterdell JM, Wells AT & Nicoll, MG 2009. *Sequence stratigraphy and fill history of the Bowen Basin, Queensland*. Geoscience Australia.

Bradshaw BE, Spencer LK, Lahtinen AC, Khider K, Ryan DJ, Colwell JB, Chirinos A & Bradshaw J 2009. *Queensland carbon dioxide geological storage atlas*.

Bradshaw BE, Spencer LK, Lahtinen A-L, Khider K, Ryan DJ, Colwell JB, Chirinos A, Bradshaw J, Draper JJ, Hodgkinson J & McKillop M 2010. *An assessment of Queensland's CO_2 geological storage prospectivity: The Queensland CO_2 geological storage atlas*, CO_2 Geological Storage Solutions Pty Ltd, 10p.

Brauchler R, Hu R, Vogt T, Al-Halbouni D, Heinrichs T, Ptak T & Sauter M 2010. 'Cross-well slug interference tests: An effective characterization method for resolving aquifer heterogeneity'. *Journal of Hydrology*, vol. 384**,** pp. 33-45.

Bredehoeft JD, Neuzil CE & Milly PD 1983. *Regional flow in the Dakota Aquifer: A study of the role of confining layers*. USGS Water-Supply Paper 2237. U.S. GPO: Alexandria, Virginia.

Brodie RC 2002. 'Airborne and ground magnetics'. In: PAPP, E. (ed.) *Geophysical and remote sensing methods for regolith exploration*. Cooperative Research Centre for Landscape Environments and Mineral Exploration, Open File Report 144.

Brown BR 1981. 'Warroon Gas Discovery Supports Exploration of Anticlines', *The Australian Petroleum Exploration Association Journal*, vol. 21, pp. 85-90.

Burbey TJ & Zhang M 2010. 'Assessing hydrofracing success from earth tide and barometric response'. *Ground Water*, vol. 48**,** pp. 825-835.

BurVal Working Group 2006. 'Borehole logging in hydrogeology'. In: Kirsch R, Rumpel H, Scheer W & Wiederhold H (eds.) *Groundwater resources in buried valleys*. Hannover: Leidniz Institute for Applied Geosciences.

Butler JJ, Jin W, Mohammed GA & Reboulet EC 2011. 'New insights from well responses to fluctuations in barometric pressure'. *Ground Water*, vol. 49, pp. 525-533.

Cadman SJ, Pain L & Vuckovic V 1998. *Bowen and Surat Basins, Clarence-Moreton Basin, Gunnedah Basin, and other minor onshore basins*, Queensland, NSW and NT. Australian Petroleum Accumulations Report 11, Bureau of Resources Sciences, Canberra.

Caine JS & Forster CB 1999. 'Fault zone architecture and fluid flow: Insights from field data and numerical modeling'. In: W.C. HANEBERG ET AL. (ed.) *Faults and Subsurface Fluid Flow in the Shallow Crust*. Washington, DC: American Geophysical Union.

Caine JS, Evans JP & Forster CB 1996. 'Fault zone architecture and permeability structure'. *Geology*, vol. 24, pp. 1025-1028.

Calf GE & Habermehl MA 1984. 'Isotope hydrology and hydrochemistry of the Great Artesian Basin, Australia', paper for International Atomic Energy Agency (IAEA) & United Nations Educational Scientific and Cultural Organization (UNESCO) *International Symposium on Isotope Hydrology in Water Resources Development*, Vienna, Austria, 12–16 September 1983, in: Isotope Hydrology 1983, IAEA, Vienna, pp.397–413.

Cartwright J 2007. 'The impact of 3D seismic data on the understanding of compaction, fluid flow and diagenesis in sedimentary basins', *Journal of the Geological Society*, vol.164, pp.881-893.

Cartwright J 2011. 'Diagenetically induced shear failure of fine-grained sediments and the development of polygonal fault systems', *Marine and Petroleum Geology*, vol.28, pp.1593-1610.

Celia MA, Nordbotten JM, Court B, Dobossy M & Bachu S 2011. 'Field-scale application of a semi-analytical model for estimation of CO2 and brine leakage along old wells'. *International Journal of Greenhouse Gas Control*, vol. 5, pp. 257-269.

Chen X 2000. *Measurement of streambed hydraulic conductivity and its anisotropy*. Volume 39, Issue 12, pp 1317-1324.

Chen D 2003. *Dumaresq River groundwater model: Border Rivers, model development, calibration and use*, Queensland Department of Natural Resources and Mines report to the Dumaresq-Barwon Border Rivers Commission.

Cherry JA, Parker BL, Bradbury KR, Eaton TT, Gotkowitz MG, Hart DJ & Borchardt MA 2004. *Role of aquitards in the protection of aquifers from contamination: A state of the science report*, AWWA research foundation.

Chopra P, Papp E & Gibson D 2002. 'Geophysical well logging'. In: PAPP, E. (ed.) *Geophysical and remote sensing methods for regolith exploration. Cooperative Research Centre for Landscape Environments and Mineral Exploration*, Open File Report 144.

Cihan A, Zhou Q & Birkholzer JT 2011. 'Analytical solutions for pressure perturbation and fluid leakage through aquitards and wells in multilayered-aquifer systems'. *Water Resources Research*, vol. 47, W10504.

Clark ID & Fritz P 1997. *Environmental isotopes in hydrogeology*, Boca Raton, Lewis Publishers.

Coffey 2012. 'Chapter 14: Groundwater', in: *Arrow Energy, Surat Gas Project Environmental Impact Statement: Volume 3*, (http://www.arrowenergy.com.au/page/Community/Project_Assessment_EIS/Surat_Gas_Project_EIS/ [accessed 10 April 2014]).

Collerson KD, Ullman WJ & Torgerson T 1998. 'Groundwaters with unradiogenic 87Sr/86Sr ratios in the Great Artesian Basin, Australia', *Geology*, vol.16, pp.59-63.

Contreras IA, Grosser PE & ver Strate RH 2007. *The use of the fully-grouted method for piezometer installation*, Boston, MA, ASCE Geotechnical Publication 175.

Cook PG & Böhlke J 2000. 'Determining timescales for groundwater flow and solute transport'. In: Cook, P. G. & Herczeg, A. (eds.) *Environmental tracers in subsurface hydrogeology*. Boston: Kluwer Academic Publishers.

Costanza-Robinson MS, Estabrook BD & Fouhey DF 2011. 'Representative elementary volume estimation for porosity, moisture saturation, and air-water interfacial areas in unsaturated porous media: Data quality implications', *Water Resour. Res.*, vol. 47, W07513- 7

Costelloe JF, Irvine EC, Western AW, Matic V, Walker J & Tyler M 2008. 'Quantifying near-surface diffuse groundwater discharge along the south-west margin of the Great Artesian Basin', in: Lambert M, Daniell TM, Leonard, M (eds), *Proceedings of Water Down Under 2008*, Engineers Australia, Modbury, SA, pp.831-840.

Crossey L, Priestley S, Shand P, Karlstrom K, Love AJ and Keppel M (2012) 'Chapter 2: Source and origin of western Great Artesian Basin spring water', in: Love AJ, Shand P, Crossey L, Harrington GA and Rousseau-Gueutin P (eds) *Allocating Water and Maintaining Springs in the Great Artesian Basin* Vol. 3: Groundwater discharge of the western Great Artesian Basin, Australia in South Australia and the Northern Territory.

CSIRO 2012a. *Water resource assessment for the Carpentaria region*, A report to the Australian Government from the CSIRO Great Artesian Basin Water Resource Assessment, CSIRO Water for a Healthy Country Flagship, Australia.

CSIRO 2012b. *Water resource assessment for the Central Eromanga region*, A report to the Australian Government from the CSIRO Great Artesian Basin Water Resource Assessment, CSIRO Water for a Healthy Country Flagship, Australia.

CSIRO 2012c. *Water resource assessment for the Western Eromanga region*, A report to the Australian Government from the CSIRO Great Artesian Basin Water Resource Assessment, CSIRO Water for a Healthy Country Flagship, Australia.
CSIRO 2008a. *Bowen Basin Structural Geology*, An interpretation based on airborne geophysics and open file exploration data.
CSIRO 2008b. *Water availability in the Condamine-Balonne*, A report to the Australian Government from the CSIRO Murray-Darling Basin Sustainable Yields Project, CSIRO, Canberra, ACT.
CSIRO 2007. *PressurePlot v2.0* (http://www.pressureplot.com/ [accessed 9 April 2014]).
CWI 2013. *Centrifuge Permeameter Facility* [Online]. Connected Waters Initiative, University of New South Wales. Available: http://www.connectedwaters.unsw.edu.au/articles/2013/08/ centrifuge-permeameter-facility
CWIMI 2008. *Scoping study: Groundwater impacts of coal seam gas development – assessment and monitoring*, Prepared by the Centre for Water in the Minerals Industry and the Sustainable Minerals Institute.
Davis GH & Reynolds SJ 1996. *Structural Geology of Rock and Regions*, New York, John Wiley & Sons.
Day RW, Whitaker WG, Murray CG, Wilson IH & Grimes KG 1983. 'Queensland Geology: A companion volume to the 1:2,500,000 scale geological map', *Geological Survey of Queensland*, Publication 383.
de Marsily G 1986. *Quantitative Hydrogeology*, Academic Press, Orlando.
DEEDI 2013. *Code of Practice for Constructing and Abandoning Coal Seam Gas Wells in Queensland*. Queensland Government Department of Employment, Economics Development and Innovation, Brisbane [http://mines.industry.qld.gov.au/assets/petroleum-pdf/code-of-practice-csg-wells-and-bores.pdf (accessed 10 April 2014]].
Delleur JW 2007. *The handbook of groundwater engineering*. CRC Press.
DEHP 2013. *Fraccing*, Queensland Department of Environment and Heritage Protection (http://www.ehp.qld.gov.au/management/non-mining/fraccing.html [accessed 10 April 2014]).
Dent D 2007. 'Environmental geophysics mapping salinity and water resources'. *International Journal of Applied Earth Observation and Geoinformation*, vol. 9, pp. 130-136.
DERM 2011. *Regional Chemistry of the Fitzroy Basin Groundwater*, Queensland Department of Environment and Resource Management, September 2011.
Desaulniers DE, Cherry JA & Fritz P 1981. 'Origin, age and movement of pore water in argillaceous Quaternary deposits at four sites in southwestern Ontario'. *Journal of Hydrology*, vol. 50, pp. 231-257.
DME 1997. *The Surat and Bowen Basins in South-East Queensland, Queensland Minerals and Energy Review Series*. P. Green (editor), Queensland Government Department of Minerals and Energy (DME), CD Reprint 2009.
DNRM 2014a. *Great Artesian Basin Water Resource Plan*, Department of Natural Resources and Mines (DNRM) website, Queensland Government (http://www.dnrm.qld.gov.au/water/catchments-planning/catchments/great-artesian-basin [accessed 9 April 2014]).
DNRM 2014b. *Company exploration reports – QDEX*, Queensland Government Department of Natural Resources and Mines, last updated 7 January 2013 (http://mines.industry.qld.gov.au/geoscience/company-exploration-reports.htm [accessed 9 April 2014]).
DNRM 2014c. *Queensland Petroleum Exploration Database* (QPED) managed by the Geological Survey of Queensland

(http://mines.industry.qld.gov.au/geoscience/company-exploration-reports.htm, and http://mines.industry.qld.gov.au/geoscience/geoscience-wireline-log-data.htm).

DNRM 2005. *Hydrogeological framework report for the Great Artesian Basin Water Resource Plan Area*, Version 1.0. Queensland Government Department of Natural Resources and Mines (DNRM).

Doherty J & Welter D 2010. 'A short exploration of structural noise', *Water Resources Research*, vol. 46, W05525, doi:10.1029/2009WR008377.

Doherty JE, Hunt RJ & Tonkin MJ 2010. *Approaches to highly parameterized inversion: a guide to using PEST for model-parameter and predictive-uncertainty analysis*. US Geological Survey Scientific Investigations Report 2010–5211.

Domenico P & Schwartz F 1990. *Physical and chemical hydrogeology*, Wiley and Sons Inc. New York

Draper J 1985. *Stratigraphy of the Northern Bowen Basin*, The GSA Coal Geology Group, Bowen Basin Coal Symposium, Queensland Department of Mines.

Draper J & Boreham C 2006. 'Geological Controls on Exploitable Coal Seam Gas Distribution in Queensland', *APPEA Journal*, 2006, Vol 46, Part 1.

Drummond B 2002. 'Seismic surveys for imaging the regolith'. In: PAPP, E. (ed.) *Geophysical and remote sensing methods for regolith exploration*. Cooperative Research Centre for Landscape Environments and Mineral Exploration, Open File Report 144.

Dunnivant F, Porro I, Bishop C, Hubbell J, Giles J & Newman M 1997. 'Verifying the Integrity of Annular and Back-Filled Seals for Vadose-Zone Monitoring Wells'. *Ground Water*. Vol 35, No 1. Jan-Feb 1997.

Ellsworth WL, Hickman SH, Lleons AL, McGarr A, Michael AJ & Rubinstein JL 2012. 'Are seismicity rate changes in the midcontinent natural or manmade?' Abstract # 12-137. *Siesmology Society of America 2012 Annual Meeting*. San Diego, CA, 17-19 April.

Ensham 2006. *Ensham Central project EIS: Groundwater impact assessment*. Ensham Resources.

Evans JP 1988. 'Deformation mechanisms in granitic rocks at shallow crustal levels'. *Journal of Structural Geology*, vol. 10, pp. 437-443.

Evans P 1980. *Geology of the Galilee Basin*, ed. by R.A. Henderson & P.J. Stephenson, pp. 299–305. Geological Society of Australia, Brisbane.

Evans PA 1996). 'Fluoride anomalies in aquifers of the Queensland section of the Great Artesian Basin and their significance'. In: *Mesozoic Geology of the Eastern Australia Plate Conference*, Brisbane, 23-26 September, 1996, Geological Society of Australia Extended Abstracts No. 43, pp. 172-178.

Exoma 2011. *Quarterley activities report*, Exoma Energy Limited, ASX Release, March 2011 ((http://www.asx.com.au/asxpdf/20110429/pdf/41ybvksywgxkym.pdf [accessed 10 April 2014]).

Exon NF 1976. *The Geology of the Surat Basin in Queensland*, Bureau of Mineral Resources, Geology and Geophysics, Australian Government Publishing Service, Canberra.

Feinstein DT, Eaton TT, Hart DJ, Krohelski JT & Bradbury KR 2005. *Regional Aquifer Model for Southeastern Wisconsin*. Technical Report 41. Southeastern Wisconsin Regional Planning Commission.

Ferrill DA, Sims DW, Waiting DJ, Morris AP, Franklin NM & Schultz AL 2004. 'Structural framework of the Edwards Aquifer recharge zone in south-central Texas'. *Geological Society of America Bulletin*, vol. 116, pp. 407-418.

Fetter CW 2001. *Applied hydrogeology*. Fourth Edition. Prentice Hall.

Fielding C, Faulkner A, Kassan J & Draper J 1990a. *Permian and Triassic depositional systems in the Bowen Basin*. Bowen Basin Symposium 1990. Geological Society Australia, Qld Division, Proceedings

Fielding C, Gray ARG, Harris GI & Salomon JA 1990b. 'The Bowen Basin and overlying Surat Basin' In: DM Finlayson (ed) *The Eromanga Brisbane Geoscience Transect: A guide to crustal development across Phanerozoic Australia in southern Queensland*, Bureau of Mineral Resoures, Geology and Geophysics, Bulletin 232

Freeze R & Cherry JA 1979. *Groundwater*. Prentice Hall

GABCC 1998. *Great Artesian Basin Resource Study*, Great Artesian Basin Consultative Council (GABCC), November 1998.

Gardner WP, Harrington GA & Smerdon BD 2012. 'Using Excess 4He to Quantify Variability in Aquitard Leakage', *Journal of Hydrology*, vol. 468-469, pp. 63-75.

Geiger S, Schmid KS & Zaretskiy Y 2012. 'Mathematical analysis and numerical simulation of multi-phase multi-component flow in heterogeneous porous media', *Current Opinion in Colloid & Interface Science*, vol. 17, pp. 147-155.

Gelhar LW, Welty C & Rehfeldt KR 1992. 'A critical review of data on field-scale dispersion in aquifers', *Water Resources Research*, vol. 28, pp. 1955-1974.

Geoscience Australia 2008. *Bowen Basin*. (http://www.ga.gov.au/oceans/ea_Browse.jsp [accessed 23 April 2014]).

Gerber R, Boyce J & Howard K 2001. 'Evaluation of heterogeneity and field-scale groundwater flow regime in a leaky till aquitard', *Hydrogeology Journal*, vol. 9, pp. 60-78.

Gidley JL, Holditch SA, Nierode DE & Veatch RW (eds.) 1989. *Recent advances in hydraulic fracturing, Richardson, TX*, Society of Petroleum Engineers.

Gleeson T & Novakowski KS 2009. 'Identifying watershed-scale barriers to groundwater flow: Lineaments in the Canadian Shiled', *Geological Society of America Bulletin*, vol. 121, pp. 333-347.

Goddard JV & Evans JP 1995. 'Chemical changes and fluid-rock interaction in faults of crystalline thrust sheets, northwestern Wyoming, U.S.A', *Journal of Structural Geology*, vol. 17, pp. 533-547.

Golder Associates 2009. 'QGC groundwater study Surat Basin, Queensland', appendix 3.4 in: *QGC, Queensland Curtis LNG Environmental Impact Assessment: Volume 3* (http://qgc.com.au/environment/assessment-process/queensland-curtis-lng-project.aspx [accessed 23 April 2014]).

Gray DH, Fatt I & Bergamini G 1963. 'The effect of stress on permeability of sandstone cores', *Society of Petroleum Engineers Journal*, vol. 3(2), pp.95-100.

Gray I 1987a. 'Reservoir engineering in coal seams: Part 1 - the physical process of gas storage and movement in coal seams. *Society of Petroleum Engineers Reservoir Engineering*, vol. 2, pp. 28-34.

Gray I 1987b. 'Reservoir engineering in coal seams: Part 2 - observations of gas movement in coal seams', *Society of Petroleum Engineers Reservoir Engineering*, vol. 2(1), pp.35-40.

Gray I 2011. 'Stresses in sedimentary strata, including coals, and the effects of fluid withdrawal on effective stress and permeability', *11th Underground Coal Operators' Conference*, University of Wollongong and the Australasian Institute of Mining and Metallurgy 2011, pp.297-306.

Griffin S & Pippett T 2002. 'Ground penetrating radar' In: PAPP, E. (ed.) *Geophysical and remote sensing methods for regolith exploration*. Cooperative Research Centre for Landscape Environments and Mineral Exploration, Open File Report 144.

Grigorescu M 2012. *Mineralogy and petrography of the southern Galilee Basin, Queensland*. Geological Survey of Queensland. Queensland Geological Record 2012/13

Guha SK 2001. *Induced Earthquakes*, Dordrecht, The Netherlands, Klewer Academic Publishers.

Habermehl MA 1980. 'The Great Artesian Basin, Australia', *Bureau of Mineral Resources Journal of Australian Geology and Geophysics*, vol.5, pp.9-38.

Habermehl MA 1982. *Springs in the Great Artesian Basin, Australia: Their origin and nature*, Bureau of Mineral Resources, Canberra, ACT.

Habermehl MA 2002. *Hydrogeology, Hydrochemistry and Isotope Hydrology of the Great Artesian Basin*, Bureau of Rural Sciences, Water Science Program, Canberra, ACT.

Habermehl MA 2009. *Inter-Aquifer Leakage in the Queensland and New South Wales parts of the Great Artesian Basin*, final report for the Australian Government Department of Environment and Water Resources, Heritage and Arts, Bureau of Rural Sciences, Canberra, ACT.

Habermehl MA and Lau JE 1997. *Hydrogeology of the Great Artesian Basin, Australia*, 1: 2,500,000 Map, Australian Geological Survey Organisation, Canberra, ACT.

Hantush MS 1960. 'Modification of the theory of leaky aquifers', *Journal of Geophysical Research*, vol. 65, pp. 3713-3725.

Hantush MS & Jacob CE 1955. 'Nonsteady radial flow in an infinite leaky aquifer, Transactions', *American Geophysical Union* vol. 36, pp. 95-100.

Harrington GA, Gardner WP, Smerdon BD & Hendry MJ 2013. 'Palaeo-hydrogeological insights from natural tracer profiles in aquitard porewater, Great Artesian Basin, Australia', *Water Resources Research*, vol. 49 issue 7.

Harrington GA, Hendry MJ & Robinson NI 2007. 'Impact of permeable conduits on solute transport in aquitards: Mathematical models and their application', *Water Resources Research*, vol. 43, W05441.

Harrington GA, Smerdon BD, Gardner WP, Taylor AR & Hendry J 2012. 'Chapter 8: Diffuse discharge', in: Love AJ, Shand P, Crossey L, Harrington GA & Rousseau-Gueutin P (eds) *Allocating Water and Maintaining Springs in the Great Artesian Basin Vol. 3: Groundwater discharge of the western Great Artesian Basin, Australia in South Australia and the Northern Territory.*

Hart DJ, Bradbury K.R & Feinstein DT 2006. 'The vertical hydraulic conductivity of an aquitard at two spatial scales', *Ground Water*, vol. 44, pp. 201-211.

Hawke AE, James AR & Cox ME 2011. *Surat-Bowen Cumulative Management Area 3D Management Tool*, Groundwater Visualisation System (GVS) 3D model and documentation produced for the Queensland Water Commission, Queensland University of Technology, Brisbane, Qld.

Hawkins P 1978. 'Galilee Basin - Review of Petroleum Prospects', *Queensland Government Mining Journal*, vol. 79 (916), pp. 96-112.

Hawkins P & Green P 1993. 'Exploration results, hydrocarbon potential and future strategies for the northern Galilee Basin', *APEA Journal,* vol. 33, pp. 280-296.

Hayes DJ 2012. *Is the Recent Increase in Felt Earthquakes in the Central US Natural or Manmade?* [Online]. U.S. Department of the Interior. [accessed August 19 2012].

Heidug WK & Wong SW 1996. 'Hydration swelling of water-absorbing rocks: a constitutive model', *Int J Numer Anal Methods Geomech*, vol. 20, pp. 403–430.

Hendry MJ, Barbour SL, Zettl J, Chostner V & Wassenaar LI 2011. 'Controls on the long-term downward transport of δ^2H of water in a regionally extensive, two-layered aquitard system', *Water Resources Research*, vol. 47, W06505.

Hendry MJ, Kelln CJ, Wassenaar LI & Shaw J 2004. 'Characterizing the hydrogeology of a complex clay-rich aquitard system using detailed vertical profiles of the stable isotopes of water', *Journal of Hydrology*, vol. 293, pp. 47-56.

Hendry MJ, Kotzer TG & Solomon DK 2005. 'Sources of radiogenic helium in a clay till aquitard and its use to evaluate the timing of geologic events', *Geochimica et Cosmochimica Acta*, vol. 69, pp. 475-483.

Hendry MJ & Wassenaar LI 1999. 'Implications of the distribution of δD in pore waters for groundwater flow and the timing of geologic events in a thick aquitard system', *Water Resources Research*, vol. 35, pp. 1751-1760.

Hendry MJ & Wassenaar LI 2009. 'Inferring Heterogeneity in Aquitards Using High-Resolution δD and δ18O Profiles', *Ground Water*, vol. 47, pp. 639-645.

Hendry MJ, Wassenaar LI & Kotzer T 2000. 'Chloride and chlorine isotopes (36Cl and δ37Cl) as tracers of solute migration in a thick, clay-rich aquitard system', *Water Resources Research*, vol. 36, pp. 285-296.

Hennig A 2005. *A summary of the Southern Eromanga and Surat Basins of the Great Artesian Basin*. Cooperative Research Centre for Greenhouse Gas Technologies, Publication RPT05-0024.

Hennig A, Underschultz J, Johnson L, Otto C & Trefry C 2006. *Hydrodynamic Characterisation of the Triassic Showgrounds Aquifer at the Wunger Ridge Site in Queensland: Assessing Suitability for CO2 Sequestration*. Appendix 10.6.3 of report no.RPT05-0225. Cooperative Research Centre for Greenhouse Gas Technologies, Canberra. Report Number RPT06-0036.

Herczeg A & Edmunds WM 2000. 'Inorganic Ions as Tracers' In: Cook PG & Herczeg A (eds.) *Environmental Tracers in Subsurface Hydrogeology*. Boston: Kluwer Academic Publishers.

Herczeg AL, Torgersen T, Chivas AR & Habermehl MA 1991. 'Geochemistry of ground waters from the Great Artesian Basin, Australia', *Journal of Hydrology*, vol.126, pp.225-245.

Herczeg A & Love A 2007. *Review of recharge mechanisms for the Great Artesian Basin*. Report to the Great Artesian Basin Coordinating Committee under the auspices of a Consultancy Agreement: Commonwealth Dept of Environment and Water Resources, Canberra.CSIRO Water for a Healthy Country National Research Flagship report. Adelaide: CSIRO

Hillier JR 2010. *Groundwater connections between the Walloon Coal Measures and the Alluvium of the Condamine River*, report for Central Downs Irrigators Ltd, 23p, (http://www.cdil.com.au/documents/JHillierfinaldoc.pdf [accessed 23 April 2014]).

Hillis RR, Enever JR & Reynolds SD 1999. 'In situ stress field of Eastern Australia', *Australian Journal of Earth Sciences*, vol.46, pp.813-825.

Hillis RR, Meyer JJ & Reynolds SD 1998. 'The Australian stress map', *Exploration Geophysics*, vol. 29, pp.420-427. (www.asprg.adelaide.edu.au/asm).

Hillis RR & Reynolds SD 2003. 'Chapter 4: In situ stress field of Australia', in: Hillis & Muller (eds) *Evolution and dynamics of the Australian plate*, Geological Society of Australia Special Publication 22, pp.43-52.

Hitchon B & Hays J 1971. 'Hydrodynamics and hydrocarbon occurrences Surat Basin, Queensland, Australia', *Water Resources Research*, vol.7(3), pp.658-676.

Hodgkinson J 2008. *Queensland coal inventory*. Geological Survey of Queensland.

Hodgkinson J & Grigorescu M 2012. 'Background research for selection of potential geostorage targets - case studies from the Surat Basin, Queensland', *Australian Journal of Earth Sciences*, DOI:10.1080/08120099.2012.662913.

Hodgkinson J, Hortle A & McKillop M 2010. 'The application of hydrodynamic analysis in the assessment of regional aquifers for carbon geostorage: Preliminary results for the Surat Basin, Queensland', *Australian Petroleum Production and Exploration Association Journal*, vol. 50, pp. 445-462.

Hodgkinson J, Preda M, Hortle A, McKillop M, Dixon O & Foster L 2009. *The potential impact of carbon dioxide injection on freshwater aquifers: The Surat and Eromanga Basins in Queensland*, Draper J (ed), report for the Department of Employment, Economic Development and Innovation, Qld, 151p.

Hoffmann K, Totterdell J, Dixon O, Simpson G, Brakel A, Wells A & Mckellar J 2009. 'Sequence stratigraphy of Jurassic strata in the lower Surat Basin succession, Queensland', *Australian Journal of Earth Sciences*, vol.56, pp.461-476.

Holland J, Applegate J & Bocking M 2008. 'Recent coalbed methane exploration in the Galilee Basin, Queensland, Australia', *International coalbed and shale gas symposium 2008*, pp. 1-14.

Hopkins B 1996. *Modelling the impacts of irrigation pumping from the Great Artesian Basin intake beds*, Department of Land and Water Conservation, NSW.

Huysmans M & Dassargues A 2005. 'Review of the use of Peclet numbers to determine the relative importance of advection and diffusion in low permeability environments', *Hydrogeology Journal*, vol. 13, pp. 895-904.

Itasca Denver 2011. *Groundwater flow model update and revised inflow predictions in support of underground mining at Ernest Henry Mine*, Itasca Denver report to Xstrata Copper - Ernest Henry Mining.

Jackson KS, Horvath Z & Hawkins PJ 1981. 'An assessment of the petroleum prospects for the Galilee Basin, Queensland', *The APEA Journal*, vol. 21(1), pp. 172-186.

James AR, Hawke AE & Cox ME 2011. *Arrow Regional Basin Model: 3D Visualisation of Hydrogeology of the Surat-Clarence Moreton System, Stage 2*, Groundwater Visualisation System (GVS) 3D model and documentation produced for Arrow Energy Ltd, Queensland University of Technology, Brisbane, Qld.

Javandel I, Tsang CF, Witherspoon PA & Morganwalp D 1988. 'Hydrologic detection of abandoned wells near proposed injection wells for hazardous waste disposal', *Water Resources Research*, vol. 24, pp. 261-270.

JBT 2010. *Alpha Coal Project – groundwater technical report*. Report prepared by JPT (September 2010) for Hancock Prospecting Pty Ltd as part of Alpha Coal Project Environmental Impact Statement.

Jeffrey RG & Settari A 1995. 'A comparison of hydraulic fracture field experiments, including mineback geometry data, with numerical fracture model simulations, SPE 30508', *SPE Annual Technical Conference & Exhibition*, Dallas TX, 22-25 October 1995, Society of Petroleum Engineers.

Josh M, Esteban L, Delle Piane C, Sarout J, Dewhurst DN & Clennell MB 2012. 'Laboratory characterisation of shale properties', *Journal of Petroleum Science and Engineering*, vol. 88–89, pp. 107-124.

Keller CK, van der Kamp G & Cherry JA 1988. Hydrogeology of two Saskatchewan tills, I. Fractures, bulk permeability, and spatial variability of downward flow. Journal of Hydrology, 101, 97-121.

Keller CK, van der Kamp G & Cherry JA 1989. 'A multiscale study of the permeability of a thick clayey till', *Water Resources Research*, vol. 25, pp. 2299-2317.

Kellett JR, Ransley TR, Coram J, Jaycock J, Barclay DF, McMahon GA, Foster LM & Hillier JR 2003. *Groundwater Recharge in the Great Artesian Basin Intake Beds, Queensland*, final report for the NHT Project #982713 Sustainable Groundwater Use in the GAB Intake Beds, Queensland, Department of Natural Resources and Mines, Qld.

Kenyon B, Kleinberg R, Straley C, Gubelin G & Morriss C 1995. 'Nuclear magnetic resonance imaging - technology for the 21st century', *Oilfield Review*. Schlumberger Ltd.

Klinkenberg LJ 1941. *The permeability of porous media to liquid and gases*. Drilling and Production Practice, American Petroleum Institute, 200-213.

Klohn Crippen Berger 2011. *Injection of coal seam gas water into the Central Condamine Alluvium: Technical feasibility Assessment*, final report for the Healthy HeadWaters Coal Seam Gas Water Feasibility Study, Department of Environment and Resource Management, Qld, 126p.

Korsch RJ, Boreham CJ, Totterdell JM, Shaw RD & Nicoll MG 1998. 'Development and petroleum resource evaluation of the Bowen, Gunnedah and Surat Basins, eastern Australia', *The APPEA Journal*, vol. 38(1), pp. 199-237.

Kresic N 2007. *Hydrogeology and groundwater modeling*, Boca Raton, CRC Press.

Krieg GW 1989. 'Geology', in: Zeidler W and Ponder WF (eds) *Natural History of Dalhousie Springs*, South Australian Museum, Adelaide, SA, pp.19-26.

Krishnamurthy J, Mani A, Jayaraman V & Manivel M 2000. 'Groundwater resources development in hard rock terrain - an approach using remote sensing and GIS techniques', *International Journal of Applied Earth Observation and Geoinformation*, vol. 2, pp. 204-215.

Lackey O, Myers WF, Christopherson TC & Gottula JJ 2009. *Nebraska Grout Task Force In-Situ Study of Grout Material 2001-2006 and 2007 Dye Tests*, University of Nebraska-Lincoln, Institute of Agriculture & Natural Resources, Conservation & Survey Division.

Lacombe S, Sudicky EA, Frape SK & Unger AJA 1995. 'Influence of leaky boreholes on cross-formational groundwater flow and contaminant transport', *Water Resources Research*, vol. 31, pp. 1871-1882.

Leap DI 2007. 'Chapter 2: Geological occurrence of groundwater' In: Delleur JW (Ed.) *Handbook of groundwater engineering*. Second Edition CRC Press, 59

Leith B 2011. *Hydraulic fracturing: the state of the science*. U.S. Department of the Interior, U.S. Geological Survey, (presentation previously available on the USGS website, accessed: 2 July 2012).

Löfgren M, Crawford J & Elert M 2007. *Tracer tests- possibilities and limitations. Experience from SKB fieldwork: 1977-2007.* SKB Report R-07-39. Stockholm.

Longworth & McKenzie 1984. *Report on Geotechnical and Groundwater Investigation (1984) Area 2, ATP245C*, Alpha Queensland for Bridge Oil Limited. Report Reference UGT0115/KDS/ejw.

Love AJ, Herczeg AL, Sampson L, Cresswell RG & Fifield LK 2000. 'Sources of chloride and implications for 36Cl dating of old groundwater, southwestern Great Artesian Basin, Australia', *Water Resources Research*, vol.36, pp.1561-1574.

Love AJ, Shand P, Crossey L, Harrington GA & Roussea-Guetin P (eds) 2012. 'Volume 3: Groundwater discharge of the western Great Artesian Basin, Australia in South Australia and the Northern Territory', from the report for the project *Allocating Water and Maintaining Springs in the Great Artesian Basin*, National Water Commission, Canberra, ACT.

Mahara Y, Habermehl MA, Hasegawa T, Nakata K, Ransley TR, Hatano T, Mizuochi Y, Kobayashi H, Ninomiya A, Senior BR, Yasuda H & Ohta T 2009. 'Groundwater dating by estimation of groundwater flow velocity and dissolved 4He accumulation rate calibrated by 36Cl in the Great Artesian Basin, Australia', *Earth and Planetary Science Letters*, vol. 287, pp. 43-56.

Majer EL, Baria R, Stark M, Oates S, Bommer J, Smith B & Asanuma H 2007. 'Induced seismicity associated with enhanced geothermal systems', *Geothermics*, vol. 36, pp. 185-222.

Mallett CW, Pattison C, McLennan T, Balfe P & Sullivan D 1995. 'Bowen Basin', In *Geology of Australian Coal Basins*, CR Ward, HJ Harrington, CW Mallett & JW Beeston (eds.), Geological Society of Australia Special Publication 1, Sydney, 299-339.

Marler J & Ge S 2003 'The permeability of the Elkhorn fault zone, South Park, Colorado', *Ground Water*, vol. 41, pp. 321-332.

Marsh C, Rawsthorn K, Causebrook R, Kalinowski A & Newlands I 2008. *A geological review of the Galilee Basin, Queensland for possible storage of carbon dioxide*. Cooperative Research Centre for Greenhouse Gas Technologies, Canberra, Australia, CO2CRC Publication Number RPT08-0983. 91pp.

Matthews I 1997. *Hydrogeology of the Great Artesian Basin in the Northern Territory*, report no. 52/96A, Department of Lands, Environment and Planning, Darwin, NT.

MatrixPlus 2009. 'Groundwater (deep aquifer modelling) for Santos Gladstone LNG Environmental Impact Statement', report for the *Gladstone Curtis LNG Environmental Impact Statement*, 145 p.

Mazurek M, Alt-Epping P, Bath A, Gimmi T, Niklaus Waber H, Buschaert S, Cannière PD, Craen MD, Gautschi A, Savoye S, Vinsot A, Wemaere I & Wouters L 2011. 'Natural tracer profiles across argillaceous formations', *Applied Geochemistry*, vol. 26, pp. 1035-1064.

McMahon GA, Ransley T, Barclay DF, Coram J, Foster L, Hillier J & Kellett J 2002. 'Aquifer recharge in the Great Artesian Basin, Queensland', *Proceedings of the International Association of Hydrogeologists International Conference 'Balancing the Groundwater Budget'*, Darwin, NT.

Medeiros WE, Do Nascimento AF, Alves Da Silva FC, Destro N & Demétrio JGA 2010. 'Evidence of hydraulic connectivity across deformation bands from field pumping tests: Two examples from Tucano Basin, NE Brazil', *Journal of Structural Geology*, vol. 32, pp. 1783-1791.

Meizner OE 1928. 'Compressibility and elasticity of artesian aquifers', *Economic Geology*, vol. 23, pp. 263-291.

Merrick NP 2001. *Lower Namoi groundwater flow model: Calibration 1980-1998*, report for Department of Land and Water Conservation NSW, project no. C99/44/001, Insearch Ltd, Sydney, NSW.

Mikkelsen PE & Green GE 2003. *Piezometers in fully grouted boreholes*. Symposium on Field Measurements in Geomechanics, Oslo, Norway, September, 1-10.

Mildren SD, Hillis RR & Kaldi J 2002. 'Calibrating predictions of fault seal reactivation in the Timor Sea', *Australian Petroleum Production and Exploration Association Journal*, vol. 42, pp. 187-202.

Moya C 2011. *Hydrostratigraphic and hydrochemical characterisation of aquifers, aquitards and coal seams in the Galilee and Eromanga basins, Central Queensland, Australia*. Confirmation of Candidature report (including literature review for Doctor of Philosophy).

Moya D, Cox M, Raiber M & Taulis M 2012. *Preliminary Hydrochemical-Geological Assessment of the Galilee and Eromanga Basin Groundwaters, Queensland*. Poster presented at the 34th International Geological Conference, Brisbane, 5-10 August 2012.

Mullen IC, Wilkinson KE, Cresswell RG & Kellett J 2007. 'Three-dimensional mapping of salt stores in the Murray-Darling Basin, Australia: 2. Calculating landscape salt loads from airborne electromagnetic and laboratory data', *International Journal of Applied Earth Observation and Geoinformation*, vol. 9, pp. 103-115.

Müller RD, Dyksterhuis S & Rey P 2012. 'Australian paleo-stress fields and tectonic reactivation over the past 100 Ma', *Australian Journal of Earth Sciences*, vol. 59, pp. 13-28.

Narashimhan TN & Goyal K 1984. *Subsidence due to geothermal fluid withdrawal,* In: Man-Induced Land Subsidence Reviews in Engineering Geology, VI, 35-66

Neuman SP & Witherspoon PA 1969a. 'Applicability of current theories of flow in leaky aquifers', *Water Resources Research*, vol. 5, pp. 817-829.

Neuman SP & Witherspoon PA 1969b. 'Theory of flow in a confined two-aquifer system', *Water Resources Research*, vol. 5, pp. 803-816.

Neuzil CE 1986. 'Groundwater Flow In Low-Permeability Environments', *Water Resources Research*, vol. 22, pp. 1163-1195.

Neuzil CE.1994. 'How Permeable Are Clays And Shales?', *Water Resources Research*, vol. pp. 145-150.

NGWA 2014. *National Groundwater Association* webpage, (http://www.ngwa.org/Fundamentals/use/Pages/Groundwater-facts.aspx [accessed 13 January 2014]).

Nicholson C & Wesson RL 1990. *Earthquake hazard associated with deep well injection,* a report to the U.S. Environmental Protection Agency. U.S. Geological Survey Bulletin 1951. United States Geological Survey.

Nielsen PE & Hanson ME.1987. *Analysis and implications of three fracture treatments in coals at the USX Rock Creek site near Birmingham, Alabama. 1987* Coalbed Methane Symposium, Tuscaloosa, AL (Nov. 16-19, 1987).

Nimmo JR & Mello KA 1991. 'Centrifugal Techniques for Measuring Saturated Hydraulic Conductivity', *Water Resources Research*, vol. 27, pp. 1263-1269.

Nordqvist R, Hjerne C & Andersson P 2012. 'Single-well and large-scale cross-hole tracer experiments in fractured rocks at two sites in Sweden', *Hydrogeology Journal*, vol. 20, pp. 519-531.

Novakowski KS & Sudicky EA 2007. 'Chapter 20: Groundwater flow and solute transport in fractured media' In: Delleur JW (ed.) *The handbook of groundwater engineering*. Second Edition CRC Press, 43.

Novakowski KS, Lapcevic PA & Sudicky EA 2006. 'Groundwater flow And solute transport in fractured media'. In: Delleur JW (ed.) *The handbook of groundwater engineering*. Boca Raton: CRC Press LLC.

Noy DJ, Holloway S, Chadwick RA, Williams JDO, Hannis SA & Lahann RW 2012. 'Modelling large-scale carbon dioxide injection into the Bunter Sandstone in the UK Southern North Sea', *International Journal of Greenhouse Gas Control*, vol. 9, pp. 220-233.

NRC 2010. *Management and effects of coalbed methane produced waters in the western United States, Washington, D.C*, National Research Council of the National Academies.

NRC 2012. *Induced seismicity potential in energy technologies*. Pre-publication version - subject to revision. Washington, D.C.: National Research Council of the National Academies.

Olgers F 1970. *1:250,000 geological series – explanatory notes*, Buchanan, Queensland, Sheet SF/55-6, Bureau of Mineral Resources, Geology and Geophysics, Canberra.

Olson RK & Grigg MW 2008. *Mercury Injection Capillary Pressure (MICP) A Useful Tool for Improved Understanding of Porosity and Matrix Permeability Distributions in Shale Reservoirs*. Search and Discovery Article 40322. October 1, 2008 ed.: American Association of Petroleum Geologists.

Pan Z & Connell LD 2012. 'Modelling permeability for coal reservoirs: A review of analytical models and testing data', *International Journal of Coal Geology*, vol. 92, pp. 1-44.

PB 2012a. *Predicted water level declines for affected aquifers – numerical groundwater flow model of ATP529P at Longreach*, unpublished PB report for AGL Energy Limited.

PB 2012b. *AGL Galilee Project – 'Glenaras' hydrogeochemical and isotope study,* unpublished PB report for AGL Energy Limited.

Phillips FM 2000. 'Chlorine-36', In: Cook PG & Herczeg A (eds.) *Environmental tracers in subsurface hydrogeology*. Boston: Kluwer Academic Publishers.

Piller M, Schena G, Nolich M, Favretto S, Radaelli F & Rossi E 2009. 'Analysis of hydraulic permeability in porous media: from high resolution x-ray tomography to direct numerical simulation', *Transport in Porous Media*, vol. 80, pp. 57-78.

Quarantotto P 1989. *Hydrogeology of the Surat Basin, Queensland*, record no. 1989/26, Geological Survey of Queensland, Brisbane, Qld.

QCGI 2009. *Potential for carbon geostorage in the Taroom Trough, Roma Shelf and the Surat, Eromanga and Galilee Basin*, Preliminary report prepared by Queensland Carbon Geostorage Initiative (QCGI) to Geological Survey of Queensland.

QGC 2009. 'Chapter 10: Groundwater' by Queensland Gas Company Ltd (QGC), in: *Queensland Curtis LNG Environmental Impact Statement: Volume 3*.

Queensland Government 2012. *Alpha Coal Project.* Coordinator-General's Evaluation Report on the environmental impact statement. May 2012.

QWC 2012a. *Draft Underground Water Impact Report: Surat Cumulative Management Area, Consultation Draft*, Queensland Water Commission (QWC), May 2012.

QWC 2012b. *Hydrogeology of the Surat Cumulative Management Area*, Queensland Water Commission (QWC), May 2012.

QWC 2012c. *Surat Cumulative Management Area groundwater model report*, Queensland Water Commission (QWC), May 2012.

QWC 2012d. *Inventory of groundwater monitoring in the Surat Cumulative Management Area*, Queensland Water Commission (QWC), May 2012.

Radke BM, Ferguson J, Cresswell RG, Ransley TR & Habermehl MA 2000. *Hydrochemistry and implied hydrodynamics of the Cadna-Owie- Hooray aquifer, Great Artesian Basin*, Bureau of Rural Sciences, Canberra, ACT.

Rawsthorn K, Marsh C & Causebrook R 2009. *Building a Geological Model of the Triassic Clematis Sandstone of the Aramac Trough in the Galilee Basin, Queensland*. Cooperative Research Centre for Greenhouse Gas Technologies, Canberra, Australia, CO2CRC Publication Number RPT08-0999. 38pp.

Remenda VH, van der Kamp G & Cherry JA 1996. 'Use of vertical profiles of δ18O to constrain estimates of hydraulic conductivity in a thick, unfractured aquitard', *Water Resources Research*, vol. 32, pp. 2979-2987.

Rennard P & Allard D 2011. 'Connectivity metrics for subsurface flow and transport', *Advances in Water Resources*, (in press).

Riese WC, Pelzmann WL & Snyder GT 2005. 'New insights on the hydrocarbon system of the Fruitland Formation coal beds, northern San Juan Basin, Colorado and New Mexico, USA', *GSA Special Papers*, vol. 387, pp. 73-111.

RLMS 2009. *Galilee Basin – historical perspective and future challenges*. Presentation to QLD/NT PESA by Sue Slater, 18 February 2009.

Roshan H & Oeser M 2012. 'A non-isothermal constitutive model for chemically active elastoplastic rocks', *Rock Mechanics and Rock Engineering*, vol. 45, pp. 336-374, doi: 10.1007/s00603-011-0204-z

Ross J 2010. 'The Nebraska Grout Study', *Water Well Journal*, November 2010, pp. 25-31.

RPS 2011. *Galilee Basin - Galilee Basin hydrogeological investigations briefing to RAPAD Longreach*, 16 May 2011.

RPS 2012. *Galilee Basin, Report on the Hydrogeological Investigations*, RPS Australia East Pty Ltd report prepared for RLMS. Under preparation, as at March 2012.

Rust PPK 1994. *Cannington Project regional groundwater investigation for borefield development: Numerical modelling*, Rust PPK report to BHP Billiton, Townsville, Qld.

Rust PPK 1995. 'Groundwater', appendix C in: *Ernest Henry Project impact assessment study, Supplementary, Volume 3*, RUST PPK on behalf of Ernest Henry Mining, Brisbane, Qld.

Santos 2009. *Glandstone LNG Environmental Impact Statement – Shallow Groundwater*. Final Report.

Scott S, Beeston J & Carr A 1995. *Galilee Basin*, (ed.) CR Ward, HJ Harrington, CW Mallet & JW Beeston, pp 341-352. Geological Society of Australia-Coal Geology Group, Brisbane.

Seaton WJ & Burbey TJ 2005.' Influence of ancient thrust faults on the hydrogeology of the Blue Ridge province', *Ground Water*, vol. 43, pp. 301-313.

Seidel GE 1978. *Hydraulic calibration of the GABHYD model of the Great Artesian Basin*, Bureau of Mineral Resources, Geology and Geophysics Record 1978/12, Canberra, ACT.

Senior DA 1972. *Jericho, Queensland, 1:250 000 geological series map*. Sheet SF/55-14, 1st edition., Bureau of Mineral Resources, Australia

Sener E, Davraz A & Ozcelik M 2005. 'An integration of GIS and remote sensing in groundwater investigations: a case study in Burdur, Turkey', *Hydrogeology Journal*, vol. 13, pp. 826-834.

Shaban A, Khawlie M & Abdallah C 2006. 'Use of remote sensing and GIS to determine recharge potential zones: the case of Occidental Lebanon', *Hydrogeology Journal*, vol. 14, pp. 433-443.

Siemon B, Christiansen AV & Auken E 2009. 'A review of helicopter-borne electromagnetic methods for groundwater exploration', *Near Surface Geophysics*, 2009, pp. 629-646.

Siemon B, Steuer A, Ullmann A, Vasterling M & Voß W 2011. 'Application of frequency-domain helicopter-borne electromagnetics for groundwater exploration in urban areas'. *Physics and Chemistry of the Earth*, Parts A/B/C, 36, 1373-1385.

SKM 2009. *Galilee Coal Project Groundwater Impact Assessment - Galilee Basin*, Unpublished report prepared by Sinclair Knight Merz (SKM) for Warratah Coal Inc.

SKM 2010. *Prominent Hill Mine groundwater model update (PH5),* report prepared by Sinclair Knight Merz (SKM) on behalf of OZ Minerals Pty Ltd.

Small M 2004. 'The value of information for conflict resolution', In: Linkov I & Ramadan A (eds.) *Comparative risk assessment and environmental decision making*. Netherlands: Kluwer Academic Publishers

Smerdon BD, Harrington GA, Gardner WP & Smith LA 2012. *Using in-situ pore pressure to constrain the permeability of a major confining layer in the Great Artesian Basin,* IAH 2012 Congress, Niagara Falls, Canada,

Smith AJ & Welsh WD 2011. *Review of groundwater models and modelling methodologies for the Great Artesian Basin: A technical report to the Australian Government from the CSIRO Great Artesian Basin Water Resource Assessment*, CSIRO Water for a Healthy Country Flagship, Canberra, ACT.

SARIG 2014. *South Australian Resources Information Geoserver*, South Australian Department for Manufacturing, Innovation, Trade, Resources and Energy (http://www.minerals.dmitre.sa.gov.au/sarighelp/home [accessed 9 April 2014]).

Spitz K & Moreno J 1996. *A practical guide to groundwater and solute transport modeling*. Wiley. ISBN: 978-0-471-13687-3.

SRK 2008, *Bowen and Surat Basins Regional Structural Framework Study*. SRK Consulting.

Sudicky EA, Unger AJA & Lacombe S 1995. 'A noniterative technique for the direct implementation of well bore boundary conditions in three-dimensional heterogeneous formations', *Water Resources Research*, vol. 31, pp. 411-415.

SWS 2011. 'Groundwater modelling of the Surat Basin', prepared by Schlumberger Water Services (SWS), appendix B in: Coffey 2012. *Appendix G: Arrow Energy Surat gas project groundwater impact assessment report*, in: Arrow Energy, Surat Gas Project Environmental Impact Statement: Volume 3.

SWS 2012. *Namoi catchment water study independent expert final study report*, report for Department of Trade and Investment, Regional Infrastructure and Services, NSW, Schlumberger Water Services (SWS), Perth, WA, 129p. (http://www.namoicatchmentwaterstudy.com.au/client_images/1085523.pdf [accessed 24 April 2014]).

Timms W, Acworth RI, Jankowski J & Lawson S 2000. 'Groundwater quality trends related to aquitard salt storage in the Lower Murrumbidgee alluvium, Australia', In Sililo et al. (eds.) *Groundwater: past achievements and future challenges*, Balkema, Rotterdam, Netherlands, pp. 655-660.

Timms W & Acworth R 2005. 'Propagation of pressure change through thick clay sequences: an example from Liverpool Plains, NSW, Australia', *Hydrogeology Journal*, vol. 13, pp. 858-870.

Timms WA & Hendry MJ 2008. 'Long-term reactive solute transport in an aquitard using a centrifuge model', *Ground Water*, vol. 46, pp. 616-628.

Timms W, Acworth I, Hartland A & Laurence D 2012. 'Leading practices for assessing the integrity of confining strata: application to mining and coal-seam gas extraction' in *International Mine Water Association Conference*, Bunbury, West Australia, 30 September - 4 October 2012

Torgersen T, Habermehl MA, Phillips FM, Elmore D, Kubik P, Jones BG, Hemmick T & Gove HE 1991. 'Chlorine-36 dating of very old groundwater 3: Further studies in the Great Artesian Basin, Australia', *Water Resources Research*, vol. 27, pp. 3201-3213.

Tracy MR & Direen NG 2002. 'Gravity', In: Papp E. (ed.) *Geophysical and remote sensing methods for regolith exploration*. Cooperative Research Centre for Landscape Environments and Mineral Exploration, Open File Report 144.

Ungemach P 1975. *Great Artesian Basin groundwater project - explanatory note on digital model package*, Great Artesian Basin simulation model (GABSIM), Bureau of Mineral Resources, Geology and Geophysics, record 1975/169, Canberra, ACT.

URS 2009a. 'Final report: Gladstone LNG Environmental Impact Statement: Shallow Groundwater', report no. 42626220, in: URS 2009. *Gladstone LNG project: Environmental impact statement,* 148p. + appendices, <http://www.glng.com.au/Content.aspx?p=90>.

URS (2009b) 'Section 6: Coal seam gas field environmental values and management of impacts; Section 6.6: Groundwater', in: URS (2009), Gladstone LNG project: Environmental impact statement, 148p. + appendices.

US DOE undated. *Hydraulic fracturing white paper*. United States Department of Energy (provided as Appendix A in US EPA 2004).

US EPA 2004. *Evaluation of impacts to underground sources of drinking water by hydraulic fracturing of boalbed methane reservoirs*, EPA 816-R-04-003. United States Environmental Protection Agency: Washington, DC.

USQ 2011. *Preliminary assessment of cumulative drawdown impacts in the Surat Basin associated with the coal seam gas industry: Investigation of parameters and featrues for a regional model of Surat Basin coal seam gas developments*, University of Southern Queensland (USQ) (http://eprints.usq.edu.au/19462/1/USQ_SuratBasin_PrelimAssessment_2011_PV.pdf [accessed 24 April 2014]).

Varma S, Hodgkinson J, Langhi L, Ciftci B, Harris B, and Undershultz J (2011) Basin resource management for carbon storage: A literature review, CSIRO Earth Science and Resource Engineering, Kensington, WA, 80p.

van Bergen F, Pagnier H & Krzystolik P 2006. 'Field experiment of enhanced coalbed methane-CO2 in the upper Silesian basin of Poland', *Environmental Geosciences*, vol. 13, pp. 201-224.

van der Kamp G 2001. 'Methods for determining the in situ hydraulic conductivity of shallow aquitards – an overview', *Hydrogeology Journal*, vol. 9, pp. 5-16.

van der Kamp G & Gale JE 1983. 'Theory of Earth tide and barometric effects in porous formations with compressible grains', *Water Resources Research*, vol. 19, pp. 538-544.

van Heeswijck A 2006. *The structure, sedimentology, sequence stratigraphy and tectonics of the northern Drummond and Galilee Basins, Central Queensland, Australia*. PhD thesis, James Cook University. (http://eprints.jcu.edu.au/1557/ [accessed 24 April 2014]).

Wassenaar LI & Hendry MJ 2000. 'Mechanisms controlling the distribution and transport of 14C in a clay-rich till aquitard', *Ground Water*, vol. 38, pp. 343-349.

Watson TL & Bachu S 2009. 'Evaluation of the Potential for Gas and CO2 Leakage Along Wellbores', *SPE Drilling & Completion*, pp. 115-126.

Watterson J, Walsh J, Nicol A, Nell PAR & Bretan PG 2000. 'Geometry and origin of a polygonal fault system', *Journal of the Geological Society*, vol. 157(1), pp. 151-162.

Welsh WD 2000. *GABFLOW: A steady state groundwater flow model of the Great Artesian Basin*, Bureau of Rural Sciences, Canberra, ACT.

Welsh WD 2006. *Great Artesian Basin transient groundwater model*, Bureau of Rural Sciences, Canberra, ACT.

Welsh WD 2008. *Border Rivers groundwater modelling: Dumaresq River*, report to the Australian Government from the CSIRO Murray-Darling Basin Sustainable Yields Project, CSIRO, Australia, 32pp.

Wilford J 2002. 'Airborne gamma-ray spectrometry', In: Papp, E. (ed.) *Geophysical and remote sensing methods for regolith exploration.* Cooperative Research Centre for Landscape Environments and Mineral Exploration, Open File Report 144.

WMC 2010. 'Cannington borefield model update', appendix R, prepared by Water Management Consultants (WMC) in: *Cannington Life Extension Project environmental impact statement: Volume 2*, Water Management Consultants (WMC) on behalf of BHP Billiton.

Wohling DL, Love AJ, Fulton SA, Rousseau-Gueutin P & De Ritter S (eds.) 2012. *Volume 2: Groundwater recharge, hydrodynamics and hydrochemistry of the Western Great Artesian Basin in South Australia and the Northern Territory*, report for the project 'Allocating Water and Maintaining Springs in the Great Artesian Basin', National Water Commission, Canberra, ACT.

Wolaver B 2012. 'Chapter 6: Hydrogeology of Dalhousie Springs', in: Love AJ, Shand P, Crossey L, Harrington GA & Rousseau-Gueutin P (eds.) *Allocating Water and Maintaining Springs in the Great Artesian Basin Vol. 3: Groundwater discharge of the western Great Artesian Basin, Australia in South Australia and the Northern Territory*.

Wolfgang C 2000. *Hydrogeology of the Pilliga Sandstone, Coonamble Embayment and water resources management*. PhD Thesis, Fenner School of Environment, Australian National University

Woods PH 1990. *Evaporative discharge of groundwater from the margin of the Great Artesian Basin, near Lake Eyre, South Australia*, PhD thesis, Flinders University, Bedford Park, SA.

WorleyParsons 2010a. 'Volume 5: Attachment 21: Groundwater technical report: Gas fields', in: *WorleyParsons, Australia Pacific LNG Project Environmental Impact Statement*, (http://www.aplng.com.au/environment/our-environmental-impact-statement [accessed 24 April 2014]).

WorleyParson 2010b. *Spatial Analysis of Coal Seam Water Chemistry: Task 1: Literature Review*, Prepared for Department of Environment and Resource Management, December 2010.

Wright M, Dillon P, Pavelic P, Peter P & Nefiodovas A 2002. 'Measurement of 3-D hydraulic conductivity in aquifer cores at in situ effective stresses', *Ground Water*, vol. 40, pp. 509-517.

Yu S, Unger AJA & Parker B 2009. 'Simulating the fate and transport of TCE from groundwater to indoor air', *Journal of Contaminant Hydrology*, vol. 107, pp. 140-161.

Zarrouk SJ & Moore TA 2009. 'Preliminary reservoir model of enhanced coalbed methane (ECBM) in a subbituminous coal seam, Huntly Coalfield, New Zealand', *International Journal of Coal Geology*, vol. 77, pp. 153-161.

Appendix A - additional reading

Al-Bazali T, Zhang J, Chenvert ME, Sharma MM 2008. 'Maintaining the stability of deviated and horizontal wells: Effects of mechanical, chemical and thermal phenomena on well designs', *Geomech Geoeng Int J,* vol. 3,pp. 167–178.

Bouzelakos S, Timms W, Rahman P, McGeeney D & Whelan M 2013. 'Geotechnical centrifuge permeameter for characterizing the hydraulic integrity of partially saturated confining strata for CSG operations' in *Reliable Mine Water Technology*, IMWA 2013. Golden Colorado, USA.

Bradbury & Muldoon 1990. *Hydraulic conductivity determinations in unlithified glacial and fluvial materials. Groundwater and vadose zone monitoring*. ASTM.STP 1053, American Society for Testing Materials, Philadelphia, pp. 138-151.

Brakel AT, Totterdell JM, Wells AT & Nicoll MG 2009. 'Sequence stratigraphy and fill history of the Bowen Basin, Queensland', *Australian Journal of Earth Sciences: An International Geoscience Journal of the Geological Society of Australi*, vol. 56, pp. 401-432.

Celia MA, Bachu S, Nordbotten JM, Gasda S & Dahle HK 2004. 'Quantitative estimation of CO2 leakage from geological storage: Analytical models, numerical models and data needs', In, *Presentations, IEA Greenhouse Gas Programme*, Cheltenham, UK.

CWI 2013. *Centrifuge Permeameter Facility* [Online]. Connected Waters Initiative, University of New South Wales. (http://www.connectedwaters.unsw.edu.au/articles/2013/08/centrifuge-permeameter-facility [accessed 24 Spril 2014]).

Davies, Mathias, Moss, Hustoft & Newport 2012. 'Hydraulic fractures: How far can they go?', *Marine and Petroleum Geology*, vol. 37(1), pp. 1-6.

Doherty J & Welter D 2010. 'A short exploration of structural noise', *Water Resources Research*, vol. 46(5).'

Heidug WK & Wong SW 1996. 'Hydration swelling of water-absorbing rocks: a constitutive model', *Int J Numer Anal Methods Geomech* vol. 20(6), pp. 403–430.

Kiraly L 1975. 'Rapport sur l'état actuel des connaissances dans le domaine des caractères physiques des roches karstiques [Report on the present knowledge of the physical characters of karstic rocks]', In *Hydrogeology of Karstic Terrains*. (eds. A. Burger, and L. Dubertret), pp. 53-67. International Association of Hydrogeologists, International Union of Geological Sciences, Paris, France.

Lake LW & Srinivasan S 2004. 'Statistical scale-up of reservoir properties: concepts and applications', *Petroleum Science and Engineering*, vol. 44, pp. 27-39.

Moore C & Doherty J 2012. 'Upscaling hydraulic processes and properties to assess impacts on groundwater from coal seam gas abstractions', in *Hydrology and Water Resources Symposium 2012*, Sydney, 19-22 November 2012.

Nimmo JR & Mello KA 1991. 'Centrifugal Techniques for Measuring Saturated Hydraulic Conductivity', *Water Resources Research*, vol. 27, pp. 1263-1269.

Ontario MoE 1996. *Guidance on Sampling and Analytical Methods for Use at Contaminated Sites in Ontario*, Ontario Ministry of Environment and Energy Standards Development Branch.

Osborn SG, Vengosh A, Warner NR & Jackson RB 2011. 'Methane contamination of drinking water accompanying gas-well drilling and hydraulic fracturing', *PNAS Early Edition,* vol. 108(37), pp. E665-E666.

Pells SE & Pells PJN 2012a. 'Impacts of longwall mining and coal seam gas extraction on groundwater regimes in the Sydney Basin Part 1 – theory', *Australian Geomechanics Journal*, vol. 47(3), pp. 36-51,

(http://www.pellsconsulting.com.au/selectedPapers/coalSeamGasCSG/ [accessed 24 April 2014]).

Pells & Pells 2012b. 'Impacts of longwall mining and coal seam gas extraction on groundwater regimes in the Sydney Basin Part 2 - practical applications', *Australian Geomechanics Journal,* vol. 47(3), pp. 53-68, (http://www.pellsconsulting.com.au/selectedPapers/coalSeamGasCSG/ [accessed 24 April 2014]).

Pinto MJ & Wagner BJ 2002. 'Designing groundwater monitoring networks for regional-scale water quality assessment: a bayesian approach', *American Geophysical Union, Fall Meeting 2002*, abstract #H51C-08.

Rau GC 2011. *Experimental Analysis of Heat as a Tracer for the Quantification of Thermal Dispersion and Water Flow in Sand*, PhD thesis, 235 pp, University of New South Wales, Sydney.

Rau GC, Anderson MS & Acworth RI 2012a. 'Experimental investigation of the thermal time-series method for surface water-groundwater interactions', *Water Resources Research*, Vol. 48, doi:10.1029/2011WR011560.

Rau GC, Anderson MS & Acworth RI 2012b. 'Experimental investigation of the thermal dispersivity term and its significance in the heat transport equation for flow in sediments', *Water Resources Research*, vol. 48, doi:10.1029/2011WR011038.

Roshan H & Oeser M 2011. 'A non-isothermal constitutive model for chemically active elastoplastic rocks', *Rock Mechanics and Rock Engineering*, vol. 45(3), pp. 361-374.

Rubin ES, Keith DW & Gilboy CF (eds.) 2004. 'Volume 1: Peer-Reviewed Papers and Plenary', *Proceedings of 7th International Conference on Greenhouse Gas Control Technologies*, 5 September 2004, Vancouver Canada.

Smerdon BD, Marston FM & Ransley TR 2012. *Water resource assessment for the Great Artesian Basin*. Synthesis of a report to the Australian Government from the CSIRO Great Artesian Basin Water Resource Assessment.Timms W, Acworth I, Hartland A & Laurence D 2012. 'Leading practices for assessing the integrity of confining strata: application to mining and coal-seam gas extraction' in *International Mine Water Association Conference*, Bunbury, West Australia, 30 September - 4 October 2012.

US EPA 2002. *Guidance on choosing a sampling design for environmental data collection,* for use in developing a Quality Assurance Project Plan. United States Environmental Protection Agency (US EPA), Washington DC, December 2002 (http://www.epa.gov/quality/qs-docs/g5s-final.pdf [accessed 24 April 2014]).

USGS 2013. *Glossary of hydrologic terms*, US Department of the Interior, US Geological Survey (http://or.water.usgs.gov/projs_dir/willgw/glossary.html [accessed 24 April 2014]).

Zhang C 2007. *Fundamentals of environmental sampling and analysis*, John Wiley and Sons Inc.